The International Celestial Reference System, Maintenance and Future Realizations

Proceedings of IAU General Assembly XXV,
Joint Discussion 16
Sydney, Australia, 22 July 2003

Edited by
Ralph Gaume,
Dennis McCarthy,
Jean Souchay

IAUXXV
General Assembly
Sydney 13-26 July 2003

Table of Contents

Summary of IAU Joint Discussion 16, "The International Celestial Reference System, Maintenance and Future Realizations

Ralph A. Gaume, Dennis D. McCarthy

U.S. Naval Observatory, Washington, DC 20392, USA

Jean Souchay

Observatoire de Paris, DANOF, 61, avenue de l'observatoire, 75014 Paris, France

1.   Introduction

The International Astronomical Union (IAU) Joint Discussion 16 (JD16) was held in connection with the XXVth General Assembly of the IAU in Sydney, Australia in July 2003. The title of the meeting was "The International Celestial Reference System, Maintenance and Future Realizations." The International Celestial Reference System (ICRS) has recently been redefined with the adoption of an International Celestial Reference Frame (ICRF) and revised concepts and models to access the system. The ICRF is a radio reference frame and the current realization in optical wavelengths is the Hipparcos Catalogue. Maintenance and improvement of the ICRF requires continuing, coordinated observations.

Extension and densification of the system to other wavelengths remains as a work to be accomplished. It is also necessary at this time to anticipate the maintenance and extension of the ICRF to meet future needs. The models currently used in the definition of the system also require maintenance to ensure that they are able to meet improving observational accuracy in all wavelengths. The potential significant improvement of reference frames from the results of future space astrometry missions requires planning for the long-term realization of the ICRS. These topics were addressed by a series of invited and contributed presentations

2.   Oral Presentations

JD 16 oral contributions were presented in four sessions, followed by a general discussion led by K. Seidelmann.

Session 1: The International Celestial Reference Frame

A. Fey, "Status of the International Celestial Reference Frame."
C. Ma, "Potential Refinement of the ICRF."
O. Titov, "ICRF Solution by the Geoscience Australian IVS Analysis Center."
A.M Gontier, "Contribution of Stable Radio Sources to ICRF Improvements."

M. Hosokowa, "Astrometric Microlensing and Degradation of Reference Frames."

Session 2: Extension of the International Celestial Reference Frame

C. Jacobs, "Extending the ICRF to Higher Radio Frequencies: 24 & 43 GHz."
S. Urban, "Densification of the ICRF/HCRF in Visible Wavelengths."
N. Zacharias, "Extending the ICRF into the Infrared: 2MASS-UCAC Astrometry."
C. Pinigin, "About Progress of the Link Between Optical and Radio Systems."
P. Charlot, "Source Structure."

Session 3: Models

V. Dehant, "Geophysical Nutation Model."
P. Wallace, "Practical Consequences of the Improved Precession-Nutation Model."
D. McCarthy, "IERS Conventions."
T. Fukushima, "New Determination of Precession Formulas."
M. Soffel, "ICRS, ITRS and the IAU Resolutions Concerning Relativity.'
J. Vondrak, "Earth Orientation Catalog- An Improved Reference Frame."

Session 4: Space-Based Astrometry and Dynamical Reference Frames

I. Platais, "Astrometry with Large Un-Astrometric Telescopes."
R. Gaume, "Status of Space-Based Astrometric Missions."
F. Mignard, "Future Space-Based Celestial Reference Frames."
W. Zharov, "Astrometric Goals of the Radioastron Mission."
J. Kovalevsky, "Misleading Proper Motions of Galactic Objects at the Microarcsecond Level."
M. Standish, "Relating the Dynamical Frame and the Ephemerides to the ICRF."

3.   Posters

The work of JD16 was enhanced by a large number of poster contributions. These are listed below.

Wang Wen-Jun, "Celestial three-pole rotations of the Earth."
Hu Hui, "Optical positions of 55 radio stars."
W. Dick, "The ICRS and the IERS information system."
V. Martin, "Ground-based astrometry: optical-radio connection."
P.C. Rocha Poppe, "Relativistic reference systems transformations."
E. Khrutskaya, "Pul-3 catalog of 58483 stars on the Tycho-2 system."
I. Kumkova, "ICRS-ITRS connection consistent with IAU(2000) resolutions."
E. Pitjeva, "The planetary ephemerides EPM and their orientation to ICRF."
M. Stavinschi, "Report of the WG: Future development of ground-based astrometry."
B. Bucciarelli, "Astrometric measurements of radio-stars optical counterparts."
M. Stavinschi, "Reference frames and ground-based astrometry."

S. Lambert, "Coupling between the Earth's rotation rate and nutation."
G. Bourda, "Temporal gravity field and modelisation of Earth rotation."
G. Damljanovic, "ICRF densification via Hipparcos-2MASS cross identification."
F. Mitsumi, "On the construction of radio reference frame using VERA."
A. Fey, "Extending the ICRF to higher frequencies: imaging results."
P. Fedorov, "The star positions and proper motions of stars around ERS."
T. Yano, "Japanese astrometry satellite mission - JASMINE project."
M. Zacharias, "The USNO extragalactic reference frame link program."
A. Kahrin, "An-all wave classification and principle astrometry problem."
D. Boboltz, "Testing the Hipparcos/ICRF link using radio-stars."
J. Souchay, "Numerical approach to the free rotation of celestial bodies."
G. Kaplan, "Another look at non-rotating origins."
O. Roopesh, "IDV sources as ICRF sources: viability and benefits."
O. Roopesh, "USNO/ATNF astrometry and imaging of southern ICRF sources."
F. Bustos, "CDD-based astrometric measurements of photographic plates."
M. Crosta, "Relativistic satellite attitude in the realization of space-borne astrometric catalogues."

Status of the International Celestial Reference Frame

Alan L. Fey

U.S. Naval Observatory, 3450 Massachusetts Avenue NW, Washington DC, 20392-5420, USA

Jean Souchay

Observatoire de Paris, DANOF, 61, avenue de l'observatoire, 75014 Paris, France

Abstract.
 We present a brief report on the status of the International Celestial Reference Frame. There have been two extensions (updates) of the ICRF since its initial definition in 1998. The primary objectives of extending the ICRF were to provide positions for the 109 extragalactic radio sources observed since the definition of the ICRF and to refine the positions of candidate and other sources using additional observations. A secondary objective was to monitor sources to ascertain whether they continue to be suitable for use in the ICRF. Positions of the ICRF defining sources have remained unchanged. Improved positions and errors for the candidate and other sources were estimated and reflect the changes in the data set and the analysis. The 109 new sources were added with ICRF coordinates. We also discuss current efforts toward ICRF maintenance and the International Celestial Reference System Product Center.

1.   Introduction

At the XXIII General Assembly of the International Astronomical Union (IAU) held on 20 August 1997 in Kyoto, Japan, the International Celestial Reference Frame (ICRF) (Ma *et al.* 1998) was adopted as the fundamental celestial reference frame. As a consequence, the definitions of the axes of the celestial reference system are no longer related to the equator or the ecliptic but have been superseded by the defining coordinates of the ICRF. The ICRF is currently defined by the radio positions of 212 extragalactic objects obtained using the technique of Very Long Baseline Interferometry (VLBI) at frequencies of 2.3 and 8.4 GHz over the past 20+ years. The ICRF has now replaced the FK5 optical catalog as the fundamental frame and is the realization of the International Celestial Reference System (ICRS) (Arias *et al.* 1995) at radio wavelengths. The HIPPARCOS catalog (Perryman *et al.* 1997) is the realization of the ICRS at optical wavelengths (Kovalevsky *et al.* 1997).

In this paper, we discuss the current status of the ICRF. There have been two extensions/updates (Fey *et al.* 2004) of the ICRF since its initial definition in 1998 (Ma *et al.* 1998).

We also briefly discuss current observing programs and plans for maintenance of the ICRF. Finally, we describe the tasks of the ICRS Product Center,

Figure 1. Distribution of the 608 ICRF sources on an Aitoff equal-area projection of the celestial sphere. The dotted line represents the Galactic equator.

which was established specifically for the purpose of overseeing ICRF maintenance.

2. A Brief ICRF Timeline

- 1988: The IAU sets up working groups to establish a new reference frame.

- 1991: The IAU establishes the theoretical basis for a new reference frame.

- 1994: The IAU defines the ensemble of fiducial points for a new reference frame as extragalactic objects.

- 1995: A sub-group of the IAU Working Group on Reference Frames is tasked to construct a new reference frame based on VLBI observations of quasars.

- 1997: The IAU establishes the ICRS and adopts the ICRF.

- 1998: On January 1st, the ICRF replaces the FK5 optical catalog as the fundamental celestial reference frame.

- 1999: The first extension of the ICRF, ICRF Ext.1, is completed adding 59 new radio sources with ICRF coordinates.

- 2001: The ICRS Product Center is formed and tasked with overseeing the maintenance of the ICRF.

- 2002: The second extension of the ICRF, ICRF Ext.2, is completed adding 50 new radio sources with ICRF coordinates.

Figure 2.   Distribution of the 212 ICRF Defining sources on an Aitoff equal-area projection of the celestial sphere. The dotted line represents the Galactic equator.

3.   The ICRF

The ICRF is currently defined by the radio positions of 212 extragalactic objects. The radio positions are based upon a general solution for all applicable dual frequency 2.3 GHz and 8.4 GHz Mark III VLBI data available through the middle of 1995 consisting of 1.6 million pairs of group delay and phase delay rate observations. The positional accuracy of the ICRF sources is better than about 1 mas in both coordinates. The ICRF "defining" sources set the direction of the ICRS axes and were chosen based on their observing histories and the stability and accuracy of their position estimates. In addition to the 212 defining sources, positions for 294 less observed "candidate" sources along with 102 less suitable "other" sources were also given by Ma *et al.* (1998) to densify the frame. The final orientation of the frame axes was obtained by a rotation of the positions into the system of the International Celestial Reference System (ICRS) (Arias *et al.* 1995) and is consistent with the FK5 J2000.0 optical system, within the limits of the latter system accuracy. The sky distribution of the 608 ICRF sources is shown in Figure 1. The sky distribution of the ICRF Defining sources is shown in Figure 2.

4.   ICRF Ext.1

The primary objectives of extending the ICRF were to provide positions for extragalactic radio sources observed since the definition of the ICRF and to refine the positions of candidate and other sources using additional observations. A secondary objective was to monitor sources to ascertain whether they continue to be suitable for use in the ICRF.

The data added to the ICRF in ICRF Ext.1 (Fey *et al.* 2004) spanned December 1994 through April 1999 and were obtained from both geodetic and
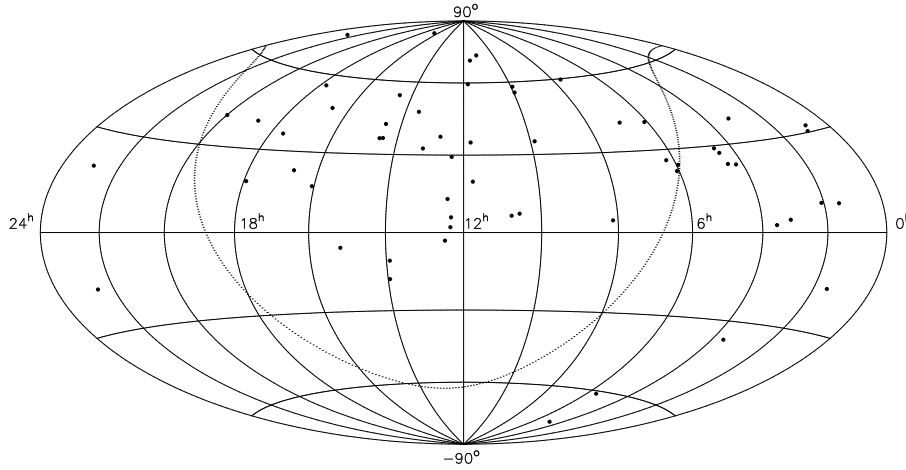
Figure 3.   Distribution of 59 new sources in ICRF Ext.1 on an Aitoff equal-area projection of the celestial sphere. The dotted line represents the Galactic equator.

astrometric observing programs. Approximately 0.6 million new observations from 461 sessions were added. There were 59 new sources. The positions and errors for the defining sources were unchanged from the ICRF. Improved positions and errors for the candidate and other sources were estimated and reflect the changes in the data set and the analysis. (While the coordinates of individual sources may change to better match the available observations, the IAU recommendation adopting the ICRF states that any updates of the ICRF will keep the same coordinate axes by means of a statistical no-net-rotation condition.) The 59 new sources were added with ICRF coordinates. The distribution on the sky of the new sources is shown in Figure 3.

5.   ICRF Ext.2

The data added to the ICRF in ICRF Ext.2 (Fey *et al.* 2004) spanned May 1999 through May 2002 and were obtained from both geodetic and astrometric observing programs. Approximately 1.2 million new observations from approximately 400 sessions were added. There were 50 new sources. The positions and errors for the defining sources were unchanged from the ICRF. Improved positions and errors for the candidate and other sources were estimated and reflect the changes in the data set and the analysis. The 50 new sources were added with ICRF coordinates. The distribution on the sky of the new sources is shown in Figure 4.

ICRF Ext.2 marks a milestone in that it utilizes all available Very Long Baseline Array (VLBA) RDV data. The VLBA RDV data is obtained through a collaborative program of geodetic and astrometric research between the U.S. Naval Observatory (USNO), the Goddard Space Flight Center (GSFC) and the National Radio Astronomy Observatory (NRAO). A total of over 652 000 de-
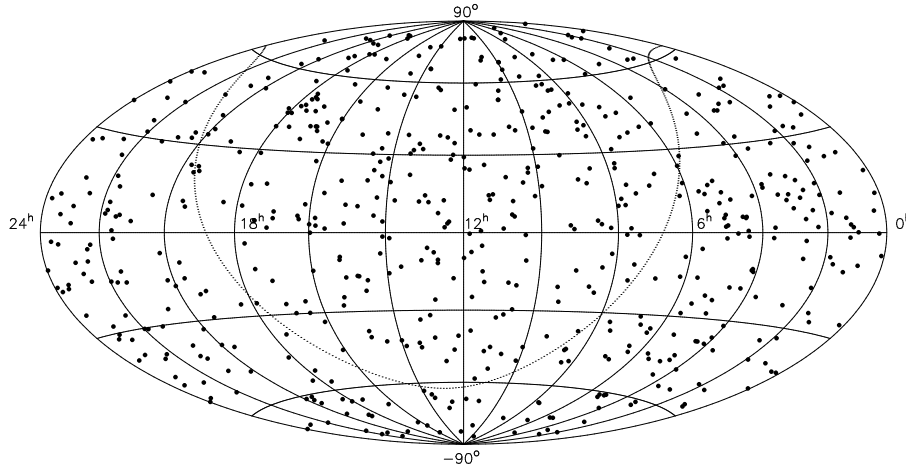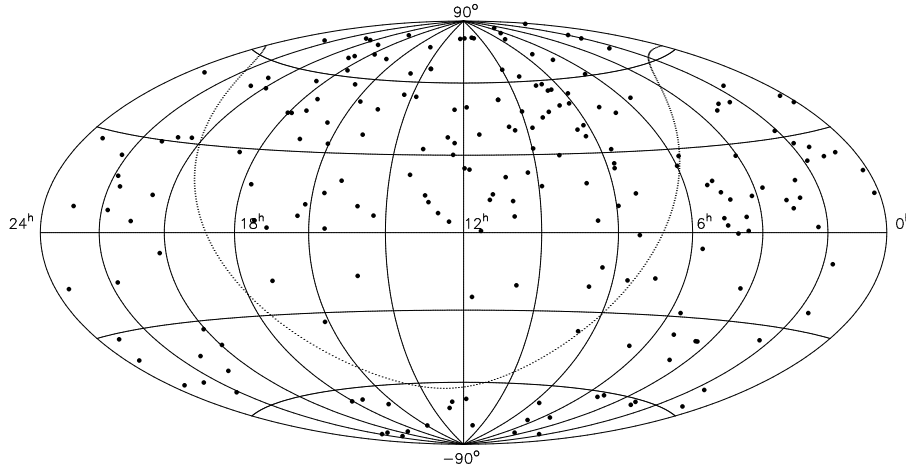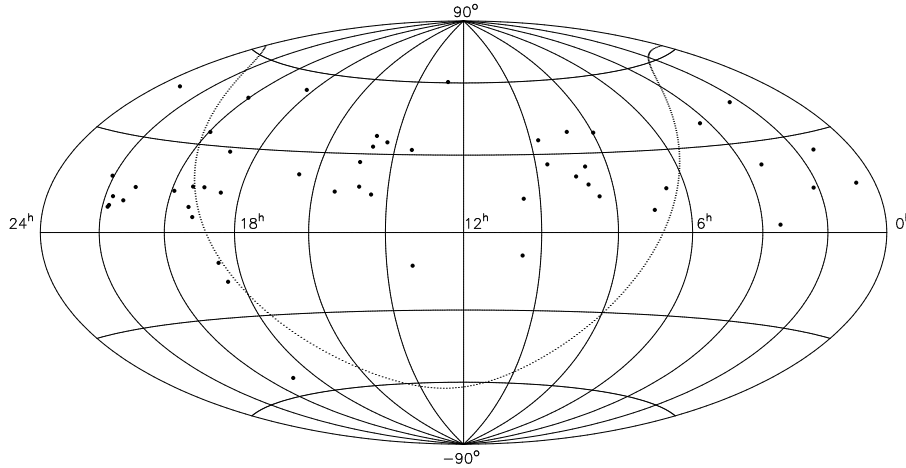
Figure 4.   Distribution of 50 new sources in ICRF Ext.2 on an Aitoff equal-area projection of the celestial sphere. The dotted line represents the Galactic equator.

lay observations (almost 20% of all available observations!) from 30 VLBA geodesy/astrometry sessions were included in the ICRF Ext.2 solution.

6.   ICRF Maintenance

The IAU has charged the International Earth Rotation and Reference Systems Service (IERS) with the maintenance of the ICRF. Maintenance activities are run jointly by the IERS ICRS Product Center and the International VLBI Service (IVS).

The IERS ICRS Product Center is directly responsible for the maintenance of the ICRS and ICRF. The Center is run jointly by the Observatoire de Paris and the USNO and is discussed in more detail in the next section. More information can also be obtained from the ICRS Product Center Web page at `http://www.iers.org/iers/pc/icrs/`.

The IVS is an international collaboration of organizations which operate or support VLBI. The IVS provides a service which supports geodetic and astrometric work on reference systems, Earth science research, and operational activities. Many of the observing programs for maintenance of the ICRF are coordinated by the IVS. More information about the IVS can be obtained from the IVS Web page at `http://ivscc.gsfc.nasa.gov/`.

6.1.   Observing Programs for ICRF Maintenance

The following observing programs are among those that contribute astrometric data for maintenance of the ICRF.

- **IVS CRF Experiments:** These 24^{hr} duration VLBI experiments, co-ordinated by the IVS, concentrate primarily on observation of southern

hemisphere ICRF sources for monitoring and to increase the sky density of ICRF defining sources.

- **VLBA RDV Experiments:** These 24^{hr} duration VLBI experiments are part of a collaborative program of geodetic and astrometric research between the USNO, GSFC and NRAO. VLBA RDV experiments concentrate primarily on observation of northern hemisphere ICRF sources ($\delta > -30°$). Intrinsic source structure information is also obtained from these experiments.

- **IVS Geodetic/Astrometric Experiments:** These 24^{hr} duration VLBI experiments, coordinated by the IVS, concentrate primarily on observation of sources for geodetic purposes and for Earth Orientation Parameter estimation but are also useful for astrometric purposes.

- **VLBA Calibrator Surveys:** These 24^{hr} duration VLBI experiments are part of a joint NRAO/GSFC program to expand both the list of high quality geodetic sources and the list of phase reference calibrators for imaging.

- **EVN Experiments:** These 24^{hr} duration VLBI experiments are part of a Bordeaux Observatory program to expand the list of ICRF defining sources in the northern hemisphere using the European VLBI Network (EVN).

- **LBA:** These 24^{hr} duration VLBI experiments are part of a joint USNO/ATNF program to expand the list of ICRF defining sources in the southern hemisphere using the Australia Telescope National Facility (ATNF) Long Baseline Array (LBA). Intrinsic source structure information is also obtained from these experiments.

7. The ICRS Product Center

The IERS ICRS Product Center is responsible for the maintenance of the ICRS and ICRF. The Center is run jointly by the Observatoire de Paris and the USNO. Product Center tasks are as follows:

- Maintenance and extension of the ICRF.

- Investigation of future realizations of the ICRS.

- Monitor intrinsic source structure to assess astrometric quality.

- Maintenance of the time stability of the ICRF.

- Maintenance of the link to the Hipparcos Catalog.

- Linking the ICRF to frames at other wavelengths.

- Linking the ICRF to the dynamical reference frame.

In order to get details concerning the objectives of these various tasks and their realizations, we can refer to the Reports of the IERS published annually (cf. IERS Annual Report 2001). Among them, specific comparisons are done on a yearly basis between the ICRF and celestial catalogs produced as results of all the observations obtained during one year. Rotation angles (A_1,A_2,A_3) and rates are obtained by means of least-squares analysis.

Moreover, effects of the selection of defining sources on the realization of the ICRF axes are investigated (Arias & Bouquillon 2003) as well as improvements of the quality of the ICRF by a suitable selection of positionally stable sources (Feissel-Vernier 2003). A Technical Note produced by the IERS Product Center is scheduled in the near future in order to describe exhaustively the recent investigations concerning the tasks above.

More information can also be obtained from the ICRS Product Center Web page at `http://www.iers.org/iers/pc/icrs/`.

References

Arias, E. F., Charlot, P., Feissel, M., & Lestrade, J. –F. 1995, A&A, 303, 604

Arias, E.F. & Bouquillon, S. 2003, A&A, in press

Feissel-Vernier, M. 2003, A&A, 403, 105

Fey, A. L., Ma, C., Arias, E. F., Charlot, P., Feissel-Vernier, M., Gontier, A. -M., Jacobs, C. S., Li, J., & MacMillan, D. S. 2004, AJ, submitted

IERS Annual Report 2001 (Verlag des Bundesamts für Kartographie und Geodesie, Frankfurt am Main 2002)

Kovalevsky, J., Lindegren, L., Perryman, M. A. C., Hemenway, P. D., Johnston, K. J., Kislyuk, V. S., Lestrade, J. F., Morrison, L. V., Platais, I., Röser, S., Schilbach, E., Tucholke, H.-J., de Vegt, C., Vondrak, J., Arias, F., Gontier, A. -M., Arenou, F., Brosche, P., Florkowski, D. R., Garrington, S. T., Kozhurina-Platais, V., Preston, R. A., Ron, C., Rybka, S. P., Scholz, R.-D., Zacharias, N. 1997, A&A, 323, 620

Ma, C., Arias, E. F., Eubanks, T. M., Fey, A. L., Gontier, A.-M., Jacobs, C. S., Sovers, O. J., Archinal, B. A., Charlot, P. 1998, AJ, 116, 516

Perryman, M. A. C., Lindegren, L., Kovalevsky, J., Høg, E., Bastian, U., Bernacca, P. L., Crézé , M., Donati, F., Grenon, M., van Leeuwen, F., van der Marel, H., Mignard, F., Murray, C. A., Le Poole, R. S., Schrijver, H., Turon, C., Arenou, F., Froeschlé , M., Petersen, C. S. 1997, A&A, 323, 49

Potential Refinement of the ICRF

Chopo Ma

NASA Goddard Space Flight Center, Code 926, Greenbelt, MD 20771,
USA

Abstract. The ICRF analysis and data represented the state of the art in global, extragalactic, X/S band microwave astrometry in 1995. Similar analysis has been used to extend the ICRF with subsequent data consistent with the original catalog. Since 1995 there have been considerable advances in the geodetic/astrometric VLBI data set and analysis that would significantly improve the systematic errors, stability, and density of the next realization of the ICRS when the decision is made to take this step. In particular, data acquired since 1990, including extensive use of the VLBA, are of higher quality and astrometric utility because of changes in instrumentation, schedule design, and networks as well as specifically astrometric intent. The IVS (International VLBI Service for Geodesy and Astrometry) continues a systematic extension of the astrometric data set. Sufficient data distribution exists to select a better set of defining sources. Improvements in troposphere modeling will minimize known systematic astrometric errors while accurate modeling and estimation of station effects from loading and nonlinear motions should permit the reintegration of the celestial and terrestrial reference frames with Earth orientation parameters though a single VLBI solution.

1. Introduction

The ICRF (International Celestial Reference Frame) is the first realization of the ICRS (International Celestial Reference System) at radio frequencies and consists of 212 defining sources whose positions are independent of the equator, equinox, ecliptic and epoch but consistent with the previous stellar and dynamical realizations within their respective errors. The accuracy of individual positions has a floor of 0.25 milliarcseconds based on an extensive error analysis while the orientation stability of the axes is ∼20 microarcseconds. Initially the ICRF positions of 608 sources were estimated (Ma *et al.* 1998). While the ICRF did not come into official use until 1 January 1998, the catalog positions were used before that date to orient and stabilize the HIPPARCOS catalog, the ICRS realization at optical frequencies. Since then the radio positions have been improved for non-defining sources and the catalog of objects with ICRF positions has been extended by 109 sources in ICRF-Ext.1 and ICRF-Ext.2 (Fey *et al.* 2004) using newer data from conventional geodetic/astrometric sessions along with ∼1200 sources from a series of VLBA sessions devoted to the VLBA Calibrator Survey (Beaseley *et al.* 2002).

2.   Considerations for generating the next ICRF

The process for introducing and adopting the ICRF was detailed and lengthy. A firm theoretical framework, sufficient observational data, established VLBI analysis, an expectation of order of magnitude improvement over the stellar celestial reference frame, and preparation of the astronomical community were all important in a smooth transition from FK5 to ICRF. The rationales for the next radio realization are rather different and the process may be less formally structured.

One rationale and a prerequisite is useful improvement in the intrinsic quality of a new realization. The limitations of the ICRF are the error floor (related to modeling, estimation, and data imperfections), the defining sources (too sparse, unevenly distributed spatially, insufficiently stable in retrospect), and data distribution (overall sparseness of sources and particular deficiency in the southern hemisphere). Each of these weaknesses can be significantly ameliorated by developments since 1995 and expected changes in analysis and CRF observing in the next few years.

There are two areas that would directly benefit by a more accurate and stable realization. Spacecraft navigation using differential VLBI relative to a nearby ICRF object is now a standard technique in the NASA solar system exploration program and is also planned for the Japanese and Chinese lunar probes. This measurement type is dependent on the accuracy of ICRF positions as well as ICRF objects in the relevant parts of the sky. The second area is VLBI monitoring of Earth orientation parameters (EOP), particularly precession/nutation and UT1. These measurements will continue to be the unique domain of VLBI. Enhanced stability and accuracy are needed to detect the small, variable effects of deep structures of the Earth.

A prospective development in optical astrometry, the GAIA mission, may prove to be the most stringent requirement for the radio realization. Expected to be launched within a decade, GAIA is projected to achieve 10 microarcsecond precision for brighter quasars. To achieve the best optical-radio registration and to ensure the highest accuracy for the transfer from radio to optical realizations, the radio CRF must be pushed to the limit. A particular VLBI observing effort may be needed for the common sources since the current ICRF sources are generally weaker than desirable in the optical band.

The process for adopting the ICRF was quite formal, including a succession of IAU working groups to establish the theoretical framework for an extragalactic frame, to identify potential fiducial objects and to derive the final ICRF catalog and culminated in an IAU resolution at the IAU General Assembly at Kyoto in 1997. Since then the responsibility for the maintenance of the ICRS has been given to the IERS (International Earth Rotation and Reference Systems Service) while the IVS has operational responsibility for the VLBI realization. The IAG (International Association of Geodesy) is forming a working group in Subcommission 1.4 Interaction of Celestial and Terrestrial Reference Frames to investigate the systematic errors in the ICRF because of the impact on EOP and indirectly on the satellite celestial reference frames. While the work for the ICRF was accomplished within an IAU working group, the work for the next VLBI realization may be more loosely coordinated or placed under a different organization. The process for preparing the astronomical community and for formal adoption remains to be decided.

3. Areas of refinement

There are four main areas in which the VLBI realization of the ICRS can be improved: analysis, data, defining sources, and observing programs.

Since 1995 considerable progress has occurred in VLBI modeling and estimation. New analysis software has been developed (Titov *et al.* 2004; Tesmer *et al.* 2004). The largest source of errors is probably the troposphere, so that improved troposphere mapping functions that use weather model information such as the IMF (Isobaric Mapping Function) (Niell 2002) and the VMF (Vienna Mapping Function) (Boehm and Schuh 2004) and better gradient estimation should reduce systematic errors and temporal noise. Refined loading models for ocean, atmosphere and hydrology effects should permit the unified solution for CRF, TRF and EOP to exploit the unique capability of VLBI. In constrast, the ICRF analysis estimated station positions for each session to reduce contamination from the TRF. However, analysis methods to model nonlinear station motions as well as apparent sources motions and other instabilities need to be tested and compared. Treating unstable sources as arc parameters as was done for the ICRF may unnecessarily weaken the results. It should be noted that the ICRF-Ext.1 and ICRF-Ext.2 analysis were consistent with the analysis for the ICRF.

The ICRF used all available geodetic/astrometric VLBI data from 1979 to 1995.6. The sources observed, the number of sources and observations in each session, the network sizes and geometries, and the sensitivity of the VLBI equipment evolved over the period and have continued to improve since then. Instead of ∼15 sources with a network of 3-4 stations producing several hundred observations in the earliest years, the most extensive modern sessions use 20 stations and up to 80 sources resulting in several tens of thousands of observations. In addition, Gontier *et al.* (2001) showed that the stability of the CRF improved noticeably around 1990. Consequently the next realization probably will discard early sessions as well as those unsuitable for astrometry. It will remain true, however, that the bulk of the data will come from geodetic sessions, ∼200 "geodetic" sources most frequently observed, and the northern hemisphere. Sessions using the VLBA together with up to ten other stations will contribute a significant fraction of the total observations.

The positions of the 212 defining sources are the formal realization of the ICRS called the ICRF. These sources were chosen with the best information available in 1995 based largely on number of observations and position stability. However, the distribution of the data over sources and over the sky was extremely nonuniform with most of the observations from fewer than 100 "geodetic" sources in the northern hemisphere used in the regularly schedule geodetic sessions. In order to have over two hundred defining sources with somewhat more extensive and uniform sky distribution, the selection criteria could not be too severe. Even so, less than 30% of the defining sources are in the south. On the other hand, some frequently observed sources were not selected as defining sources because they had sufficient data to detect anomalous behavior. Recent analysis by Feissel-Vernier (2003) looking at annual VLBI source position time series from 1990 to 2002 and using very different criteria from the ICRF identified a different set of sufficiently observed sources with stable positions. A number of ICRF defining sources failed to meet these stability criteria. It is clear that the next realization

should reexamine the defining sources and that the data set is robust enough to make a new selection.

While the analysis done by Feissel-Vernier (2003) showed that better defining sources can now be found, the number and distribution of such sources still leaves something to be desired. In the planned IVS observing program the vast majority of the sessions are primarily geodetic in nature. The VLBA sessions contribute to both geodesy and astrometry by design. Recognizing the data deficiencies, the IVS astrometric sessions will concentrate on the southern hemisphere, particularly to provide sufficient temporal coverage to identify stable sources. In addition, a small fraction of each geodetic session will be allocated to observing stable and potentially stable sources to accumulate data more rapidly for time series analysis and estimation of apparent proper motion. Potentially stable sources are those whose current time series have insufficient data to establish stability but do not show disqualifying motions or scatter. Over the next few years these observing efforts should significantly augment the potential defining sources for the next realization.

4.   Summary

The next VLBI realization of the ICRS, perhaps to be designated ICRF-200x, will differ significantly from the ICRF. It will utilize the state of the art VLBI analysis available at the end epoch 200x, correcting known systematic errors in the ICRF and reunifying the CRF, TRF and EOP. The data set will most likely include only astrometrically relevant data from 1990 to 200x. The defining sources will be more extensive and uniformly distributed than those of the ICRF, relying on the geodetic data augmented by recent directed astrometric observations for stable sources and the southern hemisphere.

References

Beasley, A. J., Gordon, D., Peck, A. B., Petrov, L., MacMillan, D. S., Fomalont, E. B., Ma, C. 2002, ApJS, 141, 13

Boehm, J. & Schuh, H. 2004, in IVS 2004 General Meeting Proc., ed. N. Vandenberg & K. Baver (Greenbelt, NASA)

Fey, A. L., Ma, C., Arias, E. F., Charlot, P., Feissel-Vernier, M., Gontier, A.-M., Jacobs, C. S., Li, J., MacMillan, D. S. 2004, AJ, 127, 3587

Gontier, A.-M., Le Bail, K., & Feissel, M. 2001, A&A, 375, 661

Feissel-Vernier, M. 2003, A&A, 403, 105

Ma, C., Arias, E. F., Eubanks, T. M., Fey, A. L., Gontier, A.-M., Jacobs, C. S., Sovers, O. J., Archinal, B. A., Charlot, P. 1998, AJ, 116, 516

Niell, A.E. 2000, Earth Planets & Space, 52, 699

Tesmer, V., Kutterer, H., & Drewes, H. 2004, in IVS 2004 General Meeting Proc., ed. N. Vandenberg & K. Baver (Greenbelt, NASA)

Titov, O., Tesmer, V., & Boehm, J. 2004, in IVS 2004 General Meeting Proc., ed. N. Vandenberg & K. Baver (Greenbelt, NASA)

THE CRF SOLUTION BY THE GEOSCIENCE AUSTRALIA IVS ANALYSIS CENTER

Oleg Titov

GPO Box 378, Canberra, ACT, 2601, AUSTRALIA

Abstract.
    The Geoscience Australia IVS Analysis Center is working for improvement of the ICRF. The catalogue of 659 radiosource positions estimated from the 23-year set of VLBI data (1980-2003) in one global solution (TRF, CRF, EOP) has been obtained using the OCCAM software. Statistical analysis of the results shows that the median accuracy of the source positions is about 0.2 mas in both coordinates. A limitation on the accuracy improvement can be caused by different factors, for example, instability of the quasar positions on different time scales. The long-term apparent motions of 0923+392 (4C39.25) and 2145+067 are analysed to evaluate the instability effects for the two frequently observed objects.

1.   Introduction

The current ICRF realization adopted by the IAU (1998) was made from the VLBI solution by the Goddard Space Flight Center group in 1996 and was extended a few years later. About 2.2 million group delays in S/X bands have been used in the extended solution. The full list of sources contains 608 objects. Due to the varying quality of the estimated positions, all sources were originally separated into three categories: 212 defining sources, mainly from the northern hemisphere; 294 candidate sources and 102 "other" sources with large position variation (Ma *et al.* 1998). Later 59 new sources were added to the list as an extension if the ICRF (Ma 2001).

    Many of the sources are known to have jets that change their position relative to other parts of the quasar structure as well as total radio flux. That causes an apparent motion in estimated quasar coordinates. For example, scientists reported a linear trend (Shaffer *et al.* 1987) and, a few years later, a quadratic trend in the time series for the right ascension of the quasar 0923+392 (Alberdi *et al.*, 1993). Fey *et al.* (1997) estimated an apparent motion of 59.8 μas/year as well as a rate of 13.6 μas/year^{-2} since 1986. On the map the quasar image consists of four components, one of them being a superluminal component. The observed effect is explained by deceleration of the superluminal motion, as calculated, being rejected from the core at an epoch close to 1980 (Fey *et al.*, 1997). Additional astrophysical discussion is presented by Alberdi *et al.*, (2000). The facts encourage scientists to fix a list of the sources appropriate for the CRF determination and, from on the other hand, to learn more about the quasar apparent motions. Recently, Feissel-Vernier (2003) has proposed a list of 199 'stable' radiosources from analysis of the time series of 707 radiosource coordinates by Fey (USNO). Alternatively, a systematic pattern in the observed

proper motion vector field of quasar global set has been detected at GSFC by McMillan (2003). He found significant harmonics using the expansion of spherical harmonics for the proper motion vector field on the celestial sphere.

2.   Geoscience Australia CRF Solution and Discussion of Results

The Geoscience Australia IVS Analysis Center is working to improve and densify the International Celestial Reference Frame (ICRF). The OCCAM software (Titov, *et al.*, 2001) has been updated to produce a global solution from VLBI data by the least squares collocation method. The coordinates of all radiosources were treated as global parameters, *i.e.* constant for the whole period of the observations. Five EOPs, station coordinates and clock rates as daily parameters, clock offsets, wet delays and wet troposphere gradients - as stochastic parameters were also determined. Indeed, the strategy is not optimal because many sources are not stable, so it causes a loss of accuracy in global positions of the sources. Nonetheless, the approach provides a first step to the more optimal strategy.

An individual CRF catalogue can be constructed as described above. The aus2003a.crf solution was obtained from a 23-year set of the VLBI data (April, 1980 - May, 2003) using 2925 daily sessions (more than 2.6 million time delays) by 55 VLBI stations. The catalogue of 659 radiosource coordinates is available currently through the IVS Website. The weigthed rms of the solution is about 0.67 cm (22 ps). Median accuracy of the source positions is 0.2 mas in both coordinates (Fig.1).
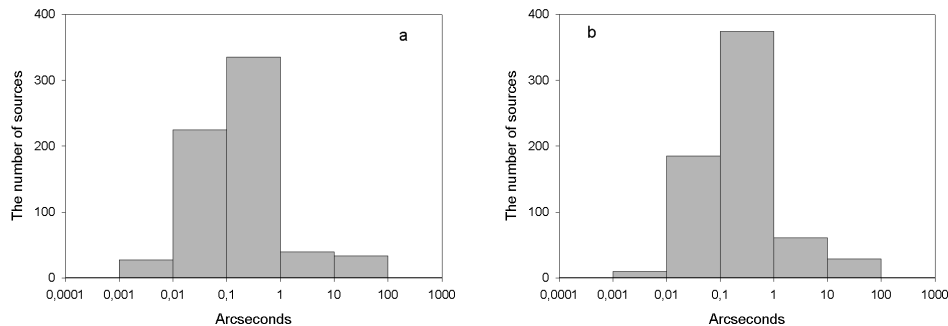
Figure 1.   The histogram of the formal error distribution in right ascenssion (left) and declination (right)

Additional research has been done to analyze the individual motions of the selected quasars (0923+392 and 2145+067). Coordinates of each quasar have been treated as daily parameters keeping coordinates of all other quasars fixed. Fig. 2a shows the right ascension variations of 0923+392 from 1986 till 2003 after elimination of the quadratic trend, estimated as -2.5+/-0.4 μas/year^{-2}. The time series consists of 792 individual daily estimates. The power spectral density (PSD) is shown in Fig. 2b. The wide peak detects a quasi-periodic signal with a period 5.6 years and an amplitude of 65+/-11 μas. The estimated signal is also shown in Fig. 2a. The trend parameters for the quasar is about 64+/-2

μas/year for the linear component, and that is in good agreement with that obtained by Fey *et al.*, (1997). The deceleration rate estimate is significantly less.
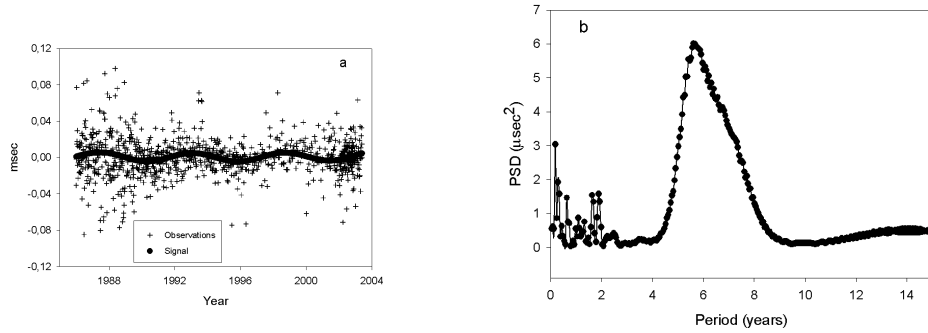
Figure 2.   Variations of the 0923+392 quasar right ascension daily positions after trend removal during 1986-2003 and approximation by signal with period 5.6 years (left). PSD of the values (right)
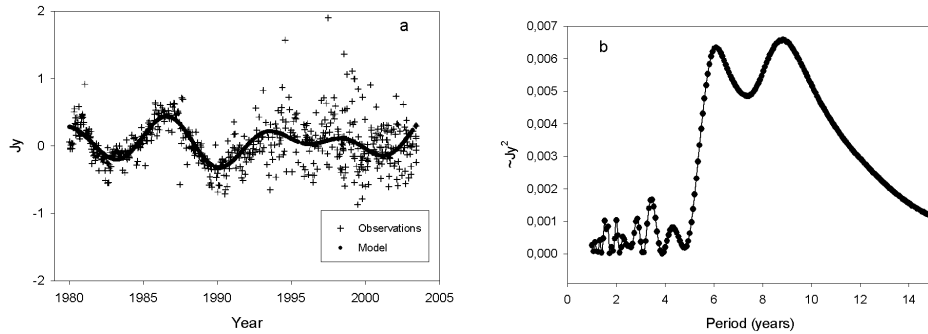
Figure 3.   Variations of the 0923+392 flux density at 8.4 GHz after trend removal during 1980-2003 and approximation by two signals with periods 6 and 9 years (left). PSD of the values (right)

Total flux density can provide independent information about physical processes inside the quasar. The University of Michigan database contains important information about the radio flux density in the same bands. Fig. 3a demonstrates the variations of the flux density for the quasar 0923+392 in X-band in 1980-2003 after removal of a trend, and Fig. 3b, the PSD of the residual time series. Two components (periods 6 and 9 years) appear in the signal. The model reaches maxima in 1986-1987, 1993-1994 and 1998-1999. The presense of a signal with a period of about 6 years in the astrophysical data confirms that the quasi-periodic variarions in right ascension are caused by some physical processes rather than shortcomings of the adjustment procedure.

Another radiosource 2145+067 also demonstrates quasi-periodic variations in its right ascension time series from 428 daily estimates between 1993 and 2003 (Fig. 4a). Fig. 4b shows the PSD of the time series. The signal is so strong that it appears without removing the trend as shown on the plot. The linear trend estimate is -59+/-5 μas/year, whereas the amplitude of the signal with period

about 4.8 years is extremely high (207+/-18 μas). The alternative estimate of the linear trend only without the signal is about -5+/-14 μas/year, *i.e.* one order less (Feissel, 2003). That underlines the importance of the quasi-periodic variations of the quasar apparent motion study. Fig. 5a,b show the variations of the flux density at the X and S bands, correspondingly, from the Michigan database. The variations in both bands are essentially irregular but do not show periodical character. Nonetheless, the time range between the maxima for the X-band curve (1994 and 2000) is about 6 years. That is comparable to the period of signal in the astrometrical time series.
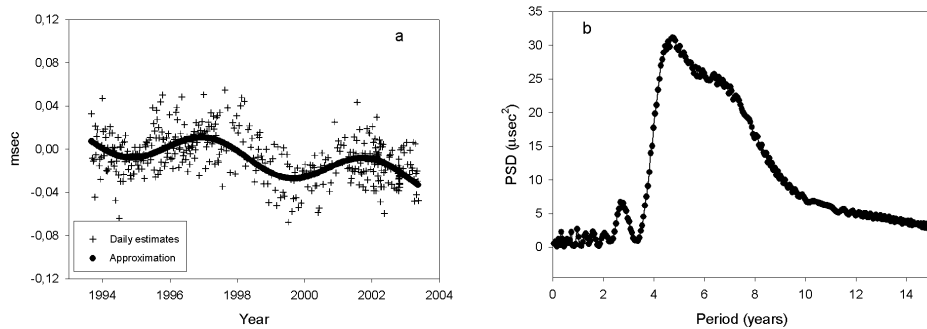
Figure 4.   Variations of the 2145+067 quasar right ascension daily positions during 1993-2003 and the linear model and signal with a period of 4.8 years (left) and the PSD of the values (right)
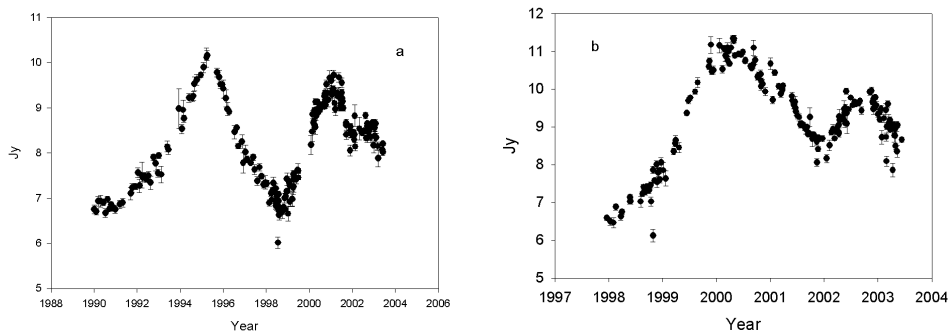
Figure 5.   Variations of the 2145+067 quasar flux density at the 8.4 GHz band during 1990-2003 (left) and 14GHz band during 1997-2003 (right)

3.   Conclusion

The Geoscience Australia celestial reference frame solution has good accuracy and can be used for compilation of the next ICRF as an independent catalogue. However, some problems concerning optimization of the analysis strategy have to be solved. The selection procedure of a set of truly stable quasars is becoming a task as crucial as the estimation of their positions. Some radio sources show so significant apparent linear motions and quasi-periodic variations (on the level 50-

200 μas) that are comparable to the current accuracy of the individual solutions (200-300 μas) and, consequently, can limit the accuracy of a future realization of the ICRF. Maintenance of the ICRF requires the measure and the elimination of the significant trends and signals from the observed time series of quasar positions to improve the astrometric solutions. The analysis of all observed quasars is essential to improve the ICRF accuracy in a global sense.

References

Alberdi, A., Marcaide, J. M., Marscher, A. P., Zhang, Y. F., Elosegui, P., Gomez, J. L., Shaffer, D., 1993, ApJ, 402, 160

Alberdi, A., Gomez, J. L., Marcaide, J. M., Marscher, A. P., Prez-Torres, M. A., 2000, A&A, 361, 529

Feissel-Vernier, M., 2003, A&A, 403, 105

Fey, A., Eubanks, T., Kingham, K., 1997, AJ, 114, 2284

Ma, C., Arias, E. F., Eubanks, T. M., Fey, A. L., Gontier, A.-M., Jacobs, C. S., Sovers, O. J., Archinal, B. A., Charlot, P., 1998, AJ, 116, 516

Ma, C., 2001, in Proc. of the 15th Working Meeting on European VLBI for Geodesy and Astrometry, ed. by D.Behrend and A.Rius, 187.

McMillan, D. 2003, astro-ph/0309826.

Shaffer, D.B., Marscher, A.P., Marcaide, J., & Romney, J.D., 1997, ApJ, 314, L1

Titov, O., Tesmer, V., Boehm, J., 2001, OCCAM Users Guide, AUSLIG Technical Notes, 7

Contribution of stable sources to ICRF improvements

A.-M. Gontier & Martine Feissel-Vernier

Observatoire de Paris, SYRTE, 61, avenue de l'observatoire, 75 014
Paris France

Abstract. A set of stable compact radio sources is proposed for the future maintenance of the ICRF axes, based on time series analysis of VLBI-derived coordinates of extragalactic radio sources. The selection scheme makes use of combined statistical and deterministic tests. It identifies 199 stable sources, to be compared to the current 212 defining sources. Their consideration for the maintenance of the frame axes is expected to improve the frame stability by a factor of five, reaching the level of less than 10 microarcseconds in the medium term. The improved stability and internal consistency of the frame also enhances the quality of the Earth orientation determinations.

1. Introduction

At its XXIIIrd General Assembly, in 1997, the IAU adopted the ICRF (International Celestial Reference Frame), based on extragalactic radio sources as the conventional reference frame realizing the International Celestial Reference System (ICRS). It also decided that a new realization be introduced only when justified by the availability of improved models or improved observations. The adopted positions of the defining sources may then be re-estimated, but the direction of the coordinate axes will be maintained by implementing the statistical condition that the new set of coordinates of selected sources show no global rotation with respect to the old set. It was also foreseen that some sources may be deleted or new ones could be added in the future. This would be done by adhering strictly to the above procedure.

The study of long time series of radio sources coordinates makes it possible to detect unstable sources that are not suitable for the maintenance of the frame. We present hereafter such a selection and its impact on various applications of the celestial reference frame, including comparison and validation of celestial reference frames, and use in the determination of the Earth Orientation Parameters: polar motion, universal time, and precession and nutation angles.

2. The Set of Stable Sources

Gontier *et al.* (2001) studied several statistical tests to select stable defining sources. They showed that starting around 1990, the noise in individual time series of source coordinates becomes much lower, explained by improvements in VLBI technology, observing networks and scheduling of observations.
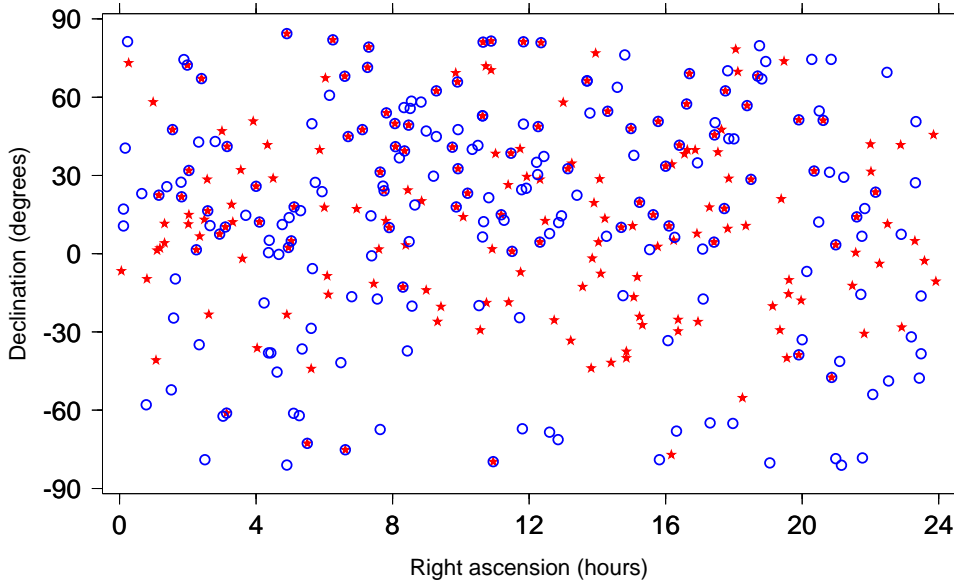
Figure 1.   Sky distribution of the 199 stable sources (stars) and the 212 ICRF defining sources (circles).

Analysing 3.4 millions observations in 3338 VLBI observing sessions from 1980 to May 2002, Fey (2002) derived the source coordinates by session for 721 sources, resulting in time series of 110, 111 individual positions. Using these time series over 1989.5-2002.3, Feissel-Vernier (2003) defined source stability indices and proposed a list of 199 stable sources that could replace the current set of defining sources in a future improved ICRF. After selecting the 362 best observed sources, *i.e.* those for which quasi-continuous series of yearly average coordinates could be derived, a selection scheme based on the detection of drifts and stability evaluation by the Allan variance test (Allan 1966) detects 199 stable sources and 163 unstable sources. The other 359 sources were too sparsely observed to allow the implementation of the selection scheme. They constitute a small proportion (less than 10%) of the total observational data.

3.   Stable Sources vs ICRF Qualifiers

In 1998, the ICRF authors (Ma *et al.* 1998) set up three categories of sources using qualitative and quantitative criteria such as apparent drift, formal uncertainty of the global coordinates over 1980-1995, and source structure indices, which were available at that time only for a small number of sources. For the definition of the ICRF axes only the 212 sources considered as the most reliable ones were used and named "defining sources". A second set of 396 apparently reliable sources that had not been observed enough in 1995 were considered as "candidates". The last category of sources called "other" was for the 102 sources considered not suitable for the maintenance of the frame axes. In addition, a source structure index (Fey & Charlot 2000) qualifies the level of position distur-

bance expected as a result of the the source structure (1 for the least disturbed, 4 for the most disturbed).

The sky distribution of the ICRF defining sources and that of the stable sources are shown in Figure 1. Note the deficiency of stable sources south of declination -30°with respect to the defining sources. This is an effect of the relatively sparse observation history of these sources due to a weaker observing network. In the initial ICRF the criteria to select defining sources were relaxed in the southern hemisphere in order to compensate for this observational bias.

Table 1 shows the relationship of the Feissel-Vernier stability index with two ICRF qualifiers: the source status and the structure index. The unstable sources are mostly those having a linear drift ≥ 50 μas/year over 1989.5-2002.3 in one of the two coordinates. For completeness, the correspondence is also shown for the sources that could not be submitted to the statistical stability screening because of an observation history that was too sparse.

Table 1.   Relationship between ICRF source qualification and the stability index.

	Defining	Candidate	Other	index:	1-2	3-4
Stable	81	68	49		73	26
Unstable	60	62	38		34	19
Sparse	71	164	15		15	26

We notice that there is no clear relationship between the two selections. While the proposed scheme rescues a number of sources that may be useful for the maintenance of the axes, a number of defining sources are found to be unstable or drifting. Similarly, there is no particular correlation of the instantaneous structure indices with the time stability ones. More investigations, such as studying the time evolution of the structure index for each source, are needed to explained this poor correlation.

4.   Comparison and Validation of Celestial Reference Frames

To compare the respective efficiency of the defining sources and of the stable sources for maintaining the direction axes of the celestial reference frame that they realize, we consider 19 yearly differential reference frames (at epochs 1984.0 through 2002.0) that are formed by the coordinates of the defining (stable) sources observed in each year. The frames are differential in the sense that each series of sources coordinates is brought to zero in the average over its observation span. The yearly differential rotation angles $A_1(y)$, $A_2(y)$, $A_3(y)$ around the axes of the equatorial coordinate system for year y are then computed for each of the 19 years. Figure 2 shows the time variation of these angles using either the defining sources or the stable sources. The already-mentioned stabilization of the frame axes starting at 1990.0 is obvious, in particular when using the stable sources. Note that although the starting sets of sources are comparable in size (212 defining sources and 199 stable ones), the numbers of sources effectively observed each year are higher for the stable sources, reflecting the fact that the first selection criterion was a dense observational history. Gontier *et al.* (2001)
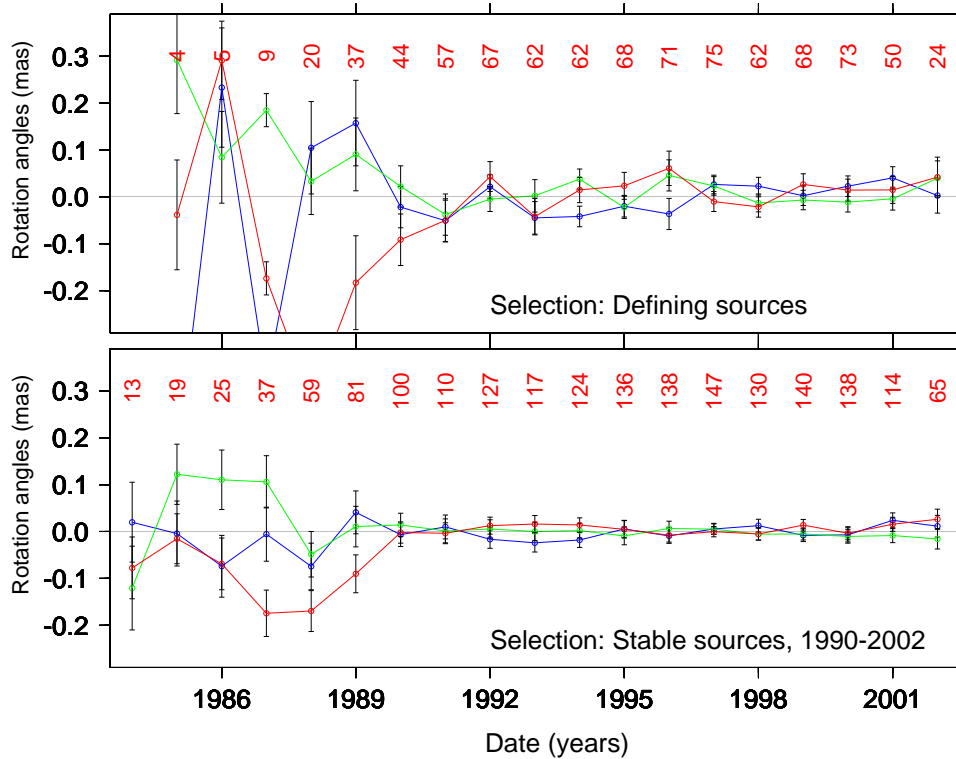
Figure 2.   Yearly differential rotation angles using the defining sources or the stable sources A_1 is shown in blue (dark), A_2 in green (dashed), and A_3 in red (light). The numbers of sources with observed coordinates are shown above the respective graphs.

showed that the much lower noise for the stable sources solution is not only an effect of the number of sources but that it also results from better statistical properties. Table 2 gives two types of statistics on the time variations of the differential rotation angles: the usual standard deviation that characterizes the scattering of the sets of rotation angles, and their Allan standard deviation for one-year and four-year sampling times, that characterize their stability in time. Note that if the time series of the rotation angles have white noise, the four-year Allan standard deviation will be equal to half (square root of one fourth in sampling times) the one-year one. In the case of flicker noise, both values will be equal. The set of 199 selected stable sources lowers the medium-term instability of the celestial reference frame from 28 to 6 μas. In addition, the original flicker noise error spectrum of the axes directions is replaced by white noise.

    As a check of external consistency, Arias and Bouquillon (2004) compared two independant celestial reference frames, RSC(BKGI) 02 R 01 and RSC(IAA) 02 R 03, that were submitted to the IERS/ICRS Product Center for the 2002 IERS Annual Report (IERS 2003). They evaluate the rotation and deformation parameters using either the ICRF defining sources or the set of stable sources. They conclude that the set of stable sources defines the axes of ICRF better than the defining ones ($\pm$ 0.11 mas vs $\pm$ 0.23 mas). For both frames the directions of

Table 2.   Stability of yearly celestial reference frames

Source selection scheme	Nb of sources kept	Std dev. μas	Allan Std dev. 1 year μas	4 years μas
ICRF Defining	212	25.6	26.0	27.6
Stable	199	10.8	9.4	5.9

the axes are found to be closer to those of ICRF when using the stable sources. The weighted post-fit mean residuals for both comparisons indicate that the quality of the fit is better by a factor of two for the stable sources (0.13 mas vs 0.22 in α cosδ, 0.14 vs 0.30 in δ).

5.   Improved EOP Determination

The Earth Orientation Parameters (EOP) are the five angles traditionally used for describing the Earth's rotation irregularities. They include the coordinates of the moving rotation pole in an Earth-fixed reference system, two parameters linked to the orientation of the axis of figure in space (precession and nutation angles), and universal time, directly dependent on the sidereal rotation of the planet. The EOP are determined from every 24-hour VLBI session taking into consideration all sources observed.

The stability of time series of EOP of various origins can be compared using the Allan variance. The Allan variance of a time series x_i with N items and sampling time τ is defined as:

$$\sigma_A^2(\tau) = \frac{1}{2N} \sum_i (x_{i+1} - x_i)^2.$$

The Allan variance analysis allows one to characterize the power spectrum of the variability in time series, for sampling times ranging from the initial interval of the series to about 1/3 of the data span, in our case one year through four years. This method allows one to identify white noise (spectral density S independent of frequency f), flicker noise (S proportional to f^{-1}), and random walk (S proportional to f^{-2}). Note that one can simulate flicker noise in a time series by introducing steps of random amplitudes at random dates. When several series of measurements of the same phenomenon are available, it is possible not only to derive the level of measurement noise, but also its spectrum by the three-corner-hat method (Barnes 1967), assuming that their measurement errors are independent. The slope of the graph giving the Allan variance as a function of sampling time, both in logarithmic scale, points to white noise (slope = -1), flicker noise (slope = 0), or random walk noise (slope = +1).

Figure 3 shows stability graphs for polar motion and Universal Time determinations over 1990-2002 based on either all sources or on the stable sources only. The results shown here involve both GPS and VLBI for polar motion, and only VLBI solutions for Universal Time. The set of VLBI solutions con-
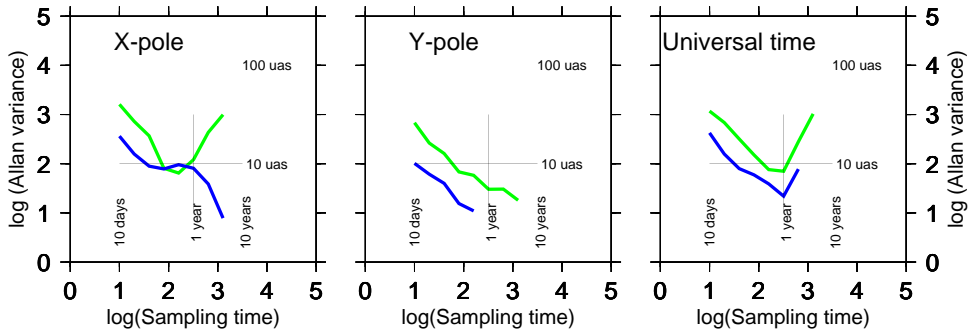
Figure 3. Stability of pole coordinates and Universal Time measurements over 1990-2002 according to source selection. All sources: light; stable sources only: dark.

sidered is based on seven different source selections, considering various sources characteristics, *e.g.* defining, stable, unstable, *etc.* (Ma 2003).

In addition to the fact that the Allan variance is always lower when using the stable sources only, a striking feature for x-pole is that the use of the stable sources cancels the random walk signature appearing beyond one-year sampling time when using all sources. The reference to the stable sources ensures or strengthens white noise in the long term for the measurement of polar motion. The measurement of Universal Time involves the stability of both the terrestrial and the celestial reference frames. The possible influence of the terrestrial frame on the remaining random walk signature beyond one year should be investigated.

Nutation is the motion of the Earth's figure axis in space in response to the torque exerted by the Moon, Sun and planets. The state of the art model recommended by the IAU in 2000 (Mathews, *et al.* 2002), is based on *i*) the modelling of the astronomical external torque at the 0.1 μas accuracy level (Souchay and Kinoshita 1996, 1997), *ii*) the modelling of the response of the non rigid Earth to this external torque, and *iii*) the VLBI observations relative to extragalactic directions realized by the quasars. When observed at the current level of precision (a fraction of a milliarcsecond), no object is really pointlike. Apparent motions, if existing, may be related to the existence of jets originating in the sources. Such motions may give rise to time varying inhomogeneities in the celestial reference frame that, in turn, could mimic nutation signals.

Studying the influence on nutation of the variable torque exerted by the atmosphere and the ocean, Dehant *et al.* (2003) showed that apparent variability in the celestial frame can lead to changes in estimates of precession or long-period nutations coefficients at a level comparable to that of the variable nutation excited by the Earth's fluid layers (a few tens of μas). Figure 4 shows the celestial frame effect on precession and obliquity rate and on the 18.6 year nutation term. Depending on the selection osf sources in the analysis, the precession and obliquity rates may change by 20 μas/year and the 18.6 year prograde component by 30 μas.
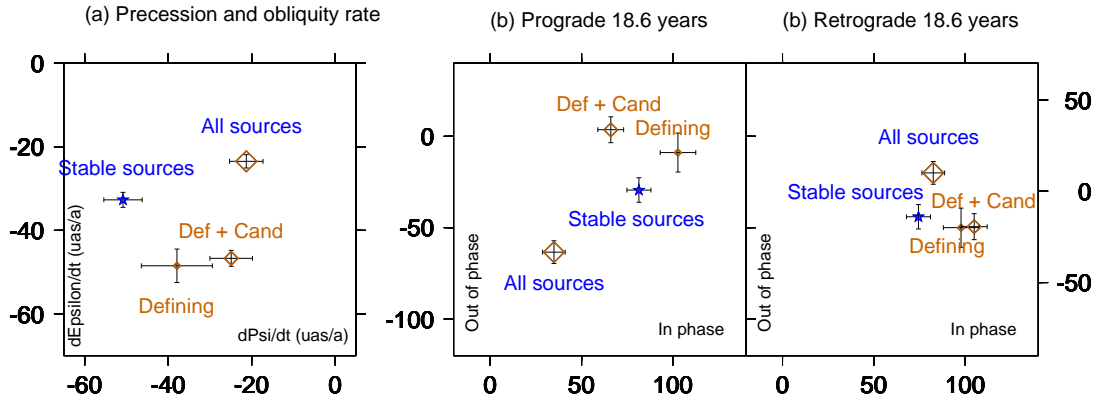
Figure 4.   Precession and obliquity rate corrections (left graph) and pro-
grade and retrograde corrections to the 18.6 year nutation term in μas (right
graph) for various source selections.

6.   Conclusion

Feissel-Vernier (2003) proposed a source selection scheme based on time series
analysis of source coordinates that makes it possible to detect unstable sources.
The consideration of the stable sources strengthens the no-net-rotation condi-
tion of the celestial reference frame axes. It improves the internal consistency of
the frame, as shown by the improvements of yearly differential rotation angles,
but also the external consistency showed by the convergence of independent
realizations of celestial reference frame. It impacts positively the determina-
tion of Earth orientation parameters. The poor correlation between the sources
structure indices and the new selection needs further investigation.

We recommend that this new source classification be considered by the
International VLBI Service (IVS) in the future scheduling of VLBI observing
sessions. For the next generation of ICRF, this type of selection scheme could
be applied on extended time series in order to find the set of the most stable
sources to be used for the maintenance of ICRS axes.

References

Allan, D.W. 1966, Proc. IEEE 54, 221.

Arias, F., and Bouquillon S. 2004, A&A, in press.

Barnes, J.A. 1967, NBS Report 9284.

Dehant, V., Feissel-Vernier, M., de Viron, O., Ma, C., Yseboodt, M., and Bizouard, C.
        2003, JGR, 108 B5, 2275.

Feissel-Vernier, M. 2003, A&A, 403, 105.

Fey, A.L. 2002, Private communication.

Fey, A.L., and Charlot, P. 2000, ApJS, 128, 17

Gontier, A.-M., Le Bail, K., Feissel, M., and Eubanks, T.M. 2001, A&A, 375, 661.

IERS 2003, International Earth Rotation and Reference Systems Service Annual Report
        2002, (Frankfurt am Main: BKG), 56.

Ma, C., Arias, E.F., Eubanks, T.M., Fey, A.L., Gontier, A.-M., Jacobs, C.S., Sovers, O.J., Archinal, B.A., and Charlot, P. 1998, AJ, 116, 516.

Ma, C. 2003, Private communication.

Mathews, P.M., Herring, T.A., & Buffett, B.A. 2002, JGR, 107, 1029.

Souchay, J., and Kinoshita, H. 1996, A&A, 312, 1017.

Souchay, J., and Kinoshita, H. 1997, A&A, 318, 639.

Astrometric Microlensing and Degradation of Reference Frames

Mizuhiko Hosokawa

Communications Research Laboratory, Tokyo, 184-8795, Japan

Kouji Ohnishi

Nagano National College of Technology, Nagano, 381-8550, Japan

Toshio Fukushima

National Astronomical Observatory, Mitaka, Tokyo, 181-8588, Japan

Abstract. In a previous paper we have already pointed out that the positions of extragalactic radio sources fluctuate on the order of micro arcseconds (μas) because of the astrometric microlensing by stars and MACHOs in our galaxy (Hosokawa *et al.* 1997). This means that the kinematical reference frames based on the positions of extragalactic radio sources are degraded by these kind of fluctuations. Recently, we have shown that in the case of the extragalactic sources in the direction close to the Galactic Center, the optical depth for a lensing event of 10 μas fluctuation is about 0.25 when we adopt the standard model of our galaxy (Hosokawa *et al.* 2002). Further, macro scale astrometric gravitational lensing by the collective mass of the Galactic Center appears in a different manner. In this paper we discuss the type, the magnitude and the time scale of the degradation of reference frames due to astrometric gravitational lensing. For an astrometric gravitational lensing event of a few μas caused by each star, the event duration is expected to be several years. On the other hand, the induced motion due to macro scale astrometric gravitational lensing is practically regarded as secular.

1. Introduction

When we observe the positions of compact sources with accuracies of 10 μas or better, we have to be careful of the gravitational deflection of the sources due to the foreground stars. It has been pointed out that in the case where the lens star is within 100 pc of an appropriate background source within a separation of 1 arcsecond, the mass of the lens star can be measured by observing the variation of the gravitational deflection with an accuracy on the order of 10 μas (Hosokawa *et al.* 1993). After the discovery of photometric microlensing (Alcock *et al.* 1993; Aubourg *et al.* 1993), the complementariness of the astrometric observation to the photometric observation for solving the degeneracy of the lensing parameters was already pointed out (Hosokawa *et al.* 1995; Høg *et al.* 1995).

Now the celestial reference frame ICRF is determined by the position of extragalactic objects (Arias *et al.* 1995; Ma *et al.* 1998). When we measure the position of extragalactic objects to construct the celestial reference frame with
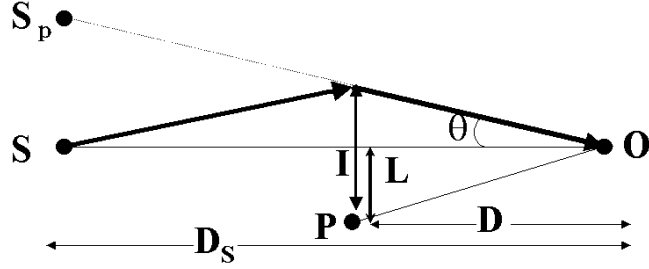
Figure 1.   Configuration of gravitational lensing

the accuracy better than 10 μas, we have to be careful of the positional shift of the extragalactic objects due to gravitational lensing by stars in our galaxy. Such a shift would be a very serious problem when we aim to construct the celestial reference frame with an accuracy of the order of μas (Hosokawa *et al.* 1997a, 1997b; Sazhin *et al.* 1998). Recently, it is also pointed out that for the QSOs close to the direction of the Galactic Center, this fluctuation can be larger than 10 μas (Hosokawa *et al.* 2002). In these discussions, the compact objects such as disk stars, bulge stars or MACHOs themselves are considered as the deflectors. The total mass in the Galactic Center, however, is the order of $10^{10} M_\odot$ and we have to consider the macro lens effect, the collective gravitational deflection by the core and the bulge of the Galaxy (Ohnishi *et al.* 2003).

Astrometric gravitational lensing by each kind of source will cause the degradation of reference frames with different magnitudes and timescales. In this paper, we will review the astrometric gravitational lensing by all sources in our galaxy and discuss the degradation of reference frames due to them. Since most of the formulae needed for the discussion have been derived in (Hosokawa *et al.* 1997b) and (Hosokawa *et al.* 2002), hereafter we will cite them as Paper I and Paper II, respectively.

2.   Description of Weak Gravitational Deflection

2.1.   The Case of Point Lens Source

Let us begin by reviewing the gravitational deflection by a point mass. The typical configuration is shown in Fig.1.

Here O is the observer, P is the deflector, and S is the source. The distances from the observer to the deflector and the source are denoted by D and D_S, respectively. The apparent angular shift of the source is denoted by θ. The distance between P and the straight line OS is denoted by L. The impact parameter, i.e. the distance between P and the lensed ray, is denoted by I.

Here I is obtained by solving the equation

$$I = L + \frac{2r_g D}{I} \ , \tag{1}$$

where $r_g = 2GM/c^2$ is the Schwarzschild radius of the deflector, and M is the mass of the deflector.
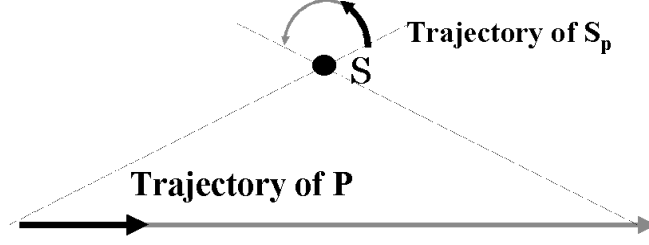
Figure 2.   Induced proper motion due to gravitational lensing

Assume that S is an extragalactic source and P is a star in the Galaxy near the line of sight to S. Hence $D_S \gg D$. Since we consider the case of weak lensing, here we take $I \sim L$ and $L/D \gg \theta$.

When we discuss the statistical nature of weak lensing, the physical key quantities are the optical depth $\tau(\theta)$ and the event rate $\Gamma(\theta)$. The optical depth is the probability that the positional shift is larger than the given observational threshold θ, and the event rate is the number of events of the positional shift greater than the observational threshold θ per year. Their mathematical formulae are

$$\tau(\theta) \equiv \left(\frac{L(\theta)}{L_1}\right)^2 \quad , \Gamma(\theta) \equiv \frac{2L(\theta)v}{\pi L_1^2} \quad , \tag{2}$$

respectively, where $L(\theta)$ is the distance between the deflector and the line of sight when the positional shift is θ, L_1 is the mean radius of what we called the active cylinder in Paper I and v is the speed of the lens star relative to the Sun. The former is derived in Paper I and the latter in Paper II. The following expressions for $\tau(\theta)$ and $\Gamma(\theta)$ are also shown in Paper II.

$$\tau(\theta) = 9.8 \times 10^{-3} \left(\frac{M}{0.2\ M_\odot}\right) \left(\frac{\Sigma}{10^3\ M_\odot/\mathrm{pc}^2}\right) \left(\frac{\theta}{10\ \mu\mathrm{as}}\right)^{-2} , \tag{3}$$

$$\Gamma(\theta) = 8.1 \times 10^{-4} \left(\frac{\Sigma}{10^3\ M_\odot/\mathrm{pc}^2}\right) \left(\frac{\theta}{10\ \mu\mathrm{as}}\right)^{-1} \left(\frac{v}{100\ \mathrm{km/s}}\right) \ [\mathrm{yr}^{-1}], \tag{4}$$

where Σ is the column density along the line of sight, $\Sigma \equiv \int \rho \mathrm{d}D$.

The average values of time between events Δt and the duration of an event t_e are directly related to the optical depth and the event rate by the following formulae.

$$\langle \Delta t \rangle \equiv \Gamma(\theta)^{-1}, \quad \langle t_e \rangle \equiv \frac{\tau(\theta)}{\Gamma(\theta)}. \tag{5}$$

By using these formulae, we evaluate the average event duration as

$$\langle t_e \rangle = 12.1 \left(\frac{M}{0.2\ M_\odot}\right) \left(\frac{\theta}{10\ \mu\mathrm{as}}\right)^{-1} \left(\frac{v}{100\ \mathrm{km/s}}\right)^{-1} \ [\mathrm{yr}]. \tag{6}$$
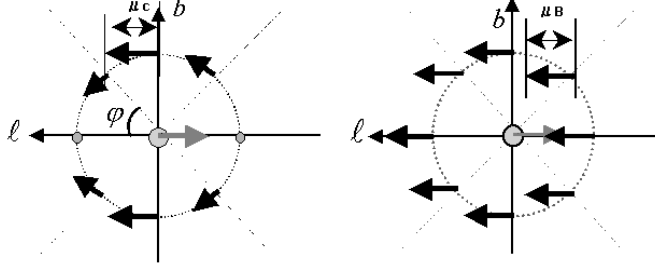
Figure 3.   Effect of core motion (left) and bulge motion (right)

2.2.   The Case of Collective Gravitational Lensing

In the case of the collective gravitational lensing, we have to consider the mass distribution of the lens stars. We assumed that the mass distribution near the Galactic Center is almost spherically symmetric with respect to the Galactic Center. Thus the column density $\Sigma(L)$ is axisymmetric with respect to the direction to the Galactic Center, where L is the distance between the Galactic Center and the line of sight to the QSO. In this case, the total deflection due to the distributed mass is obtained by considering that the total mass is concentrated in the central axis. The total column mass of the stars in a cylinder of the radius L from the Galactic Center, $m(L)$ is expressed as

$$m(L) = \int_0^L \Sigma(L')2\pi L' \mathrm{d}L'. \tag{7}$$

Then, the total gravitational deflection of the images of the referenced QSOs by the stars in the Galaxy is approximated as $\theta = m(L)/L$. Though it amounts to the order of an arcsecond if $L < 100$pc, this deflection itself is not observable. Rather the time variation due to the galactic rotation is measurable:

$$\mathrm{d}\theta = \left(2\pi\Sigma(L) - \frac{1}{L^2}\int_0^L \Sigma(L')2\pi L' \mathrm{d}L'\right)\mathrm{d}L. \tag{8}$$

For instance, let us evaluate the gravitational deflection caused by approximately a constant column density sheet, $\Sigma = \Sigma_0$ around a center. In this case, the column mass within the centered cylinder $m(L) = \pi L^2 \Sigma_0$ leads to the deflection angle $\theta = \pi L \Sigma_0$. Thus an apparent proper motion $\mu = \mathrm{d}\theta/\mathrm{d}t$ is constant when its amplitude is of the order of sub-μas/yr. Therefore we should note that the lensing by constant mass distribution is quite different from the case caused by a point mass.

3.   Model of the Mass Distribution and Estimates

3.1.   4-components Model

Since the formulae of the astrometric lensing quantities are obtained as functions of the distribution of mass and velocity of the deflectors, we should consider

the model of those in our galaxy. Here we adopt the 3-components model of Alexander & Sternberg (Kent 1992; Genzel *et al.* 1996; Alexander & Sternberg 1999); the core, the bulge, and the disk. Their mass density distribution are given as

$$\rho_{core}(r) = \frac{\rho_c}{1 + 3\left(\frac{r}{r_c}\right)^2}, \ \rho_{bulge}(r) = \rho_b K_0\left(\frac{r}{r_b}\right), \ \rho_{disk}(r) = \rho_d \exp\left(-\frac{r}{r_d}\right), \ (9)$$

where $K_0(x)$ is a modified Bessel function. The numerical values of the parameters are $\rho_c = 4 \times 10^6 \ M_\odot \text{pc}^{-3}$, $r_c = 0.38$ pc (Genzel *et al.* 1996), $\rho_b = 3.53 \ M_\odot \text{pc}^{-3}$, $r_b = 667$ pc, $\rho_d = 3 \ M_\odot \text{pc}^{-3}$, and $r_d = 3001$ pc (Kent 1992). In the actual calculation, we took into account the contribution of the disk only for $r > 1$ kpc. As for the velocity distribution, the main source is the uniform galactic rotation. Since the gravitational lensing depends on the relative velocity to the observer, we must split the disk into two components: the near side and the far side ones. So here we consider the 4-components model that consists of the core, the bulge and the two disk components. As for the relative speed to the Sun, we adopt the following values; $v_{core} = v_{bulge} = 220$ km/s, $v_{disk(farside)} = 440$ km/s, $v_{disk(nearside)} = 30$ km/s. Here we considere the effect of a random velocity field for the near side disk component.

For simplicity, we assume that the mass of the deflectors are the same and equal to 0.2 $M_\odot$ (Salpeter 1955). Recent observations (Ghez *et al.* 1998) suggest that the ratio of the heavier stars in the core might be larger than expected from the Salpeter function. In such a case, the optical depth of the lensing becomes larger. The case of 1 $M_\odot$ deflectors is also shown in Paper I and II.

3.2. Estimates

By using the above formulae and parameters, we can estimate the column density Σ, optical depth τ, and the event rate Γ for each component as a function of the direction from the Galactic Center, as well as the apparent motion caused by the collective lensing of the Galactic Center.

On the collective lensing, the effects of the core and the bulge are calculated separately. Before going further, we remark that the impact parameter L is much smaller than the scale length of the bulge $r_{\rm b}$. Then we treat the bulge as a thick sheet of constant column density, while the size of the core $r_{\rm c}$ is much smaller than L. Therefore we have to consider the radial density distribution carefully.

The details of the results caused by the compact objects are shown in Paper I and Paper II. The outlines of the two main components together with the result caused by the collective lensing are shown in Table 1. Here we evaluate the magnitude of the positional shift in the case the optical depth is 0.1. As for the direction, the quantities in Table 1 are estimated for the case each component is most dense. The terms on the nearside disk component and the core component are omitted since the contribution of the former is negligible and that of the latter is effective for only a very narrow area near the Galactic Center, say, within one degree. In Paper I, it is also shown that the contribution of MACHOs, if they exist, is also negligible.

It should be noted that the positional shift by individual star should be analyzed statistically since it is very hard to identify any lens star. The lensing

Table 1.   Summary of lensing

	Mass $M/M_\odot$	Proper Motion mas/y	$\theta(\tau = 0.1)$ μas	Δt y	t_e y	Induced Motion μas/y
Disk (far)	0.2	12	8	40	4	2
Bulge star	0.2	~6	8	80	8	1
Bulge	10^{10}	6	2×10^6	2×10^8	10^7	0.2

due to the collective mass of the bulge is, however, definite, same as is the case of solar gravitational lensing. On this collective lensing, we evaluate the effects of the core and the bulge separately. The disk contribution is negligible due to the symmetrical distribution with respect to the axis of galactic rotation.

Using the adopted model, the apparent proper motion by the core is,

$$(\mu_\ell, \mu_b) = (\mu_{\mathrm{core}}(1 - \cos 2\varphi) \ , \ -\mu_{\mathrm{core}} \ \sin 2\varphi) \ , \tag{10}$$

where μ_ℓ and μ_b are respectively the proper motion in galactic longitude and in galactic latitude, and

$$\mu_{\mathrm{core}} = 0.2\mu\mathrm{as/yr} \left(\frac{L}{100\mathrm{pc}}\right) \left(\frac{\rho_\mathrm{c}}{4 \times 10^6 m_\odot/\mathrm{pc}^3}\right) \left(\frac{r_\mathrm{c}}{0.38\mathrm{pc}}\right)^2 \left(\frac{v}{220\mathrm{km/s}}\right). \tag{11}$$

The angle φ is the latitude measured from the galactic plane. Note that the direction of apparent shift is opposite to the direction of the motion of the core relative to the observer. The shift reduces to zero when the QSO is on the galactic plane. The maximum is around 0.4 μas/yr and is reached on the galactic meridian.

On the other hand, the effect of the bulge is almost constant everywhere within a few degrees from Galactic Center;

$$(\mu_\ell, \mu_b) = (\mu_{\mathrm{bulge}}, \ 0) \ ; \ \mu_{\mathrm{bulge}} = 0.2\mu\mathrm{as/yr} \left(\frac{\Sigma(100\mathrm{pc})}{6 \times 10^6 m_\odot/\mathrm{pc}^2}\right) \left(\frac{v}{220\mathrm{km/s}}\right). \tag{12}$$

This time, the direction of apparent shift is opposite to the direction of the motion of the bulge. Note that μ_{bulge} and μ_{core} are almost the same. The total motion, depending on the direction with respect to the Galactic Center, is expected to be of the order of 0.2 μas/yr, as is also shown in Table 1.

4.   Discussion

When we evaluate the degradation of the position of a source, we have to consider θ together with t_e in Table 1. For example, if we care about a 8 μas or less uncertainty in the position of a reference source in the Galactic Disk, the astrometric gravitational lensing might cause the same order positional fluctuation. Continuous checking of its position in the period much longer than t_e, however, should enable us to eliminate the lensing event. Apparent motion of
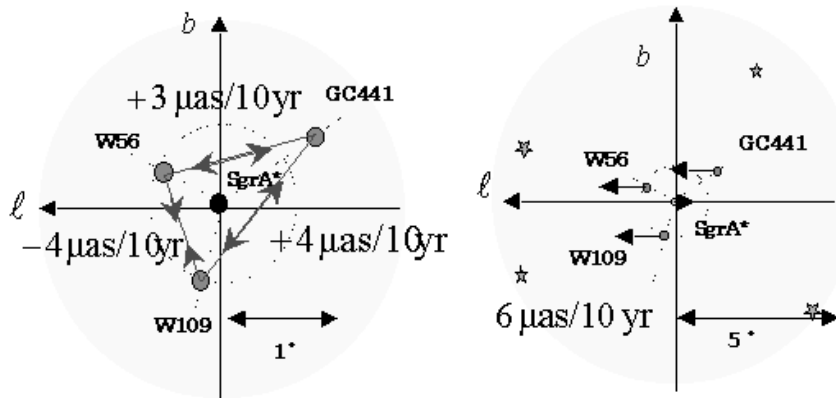
Figure 4.   Internal motion (left) and Collective Motion (right) of QSOs

the lensing event caused by the individual star has a trend shown in Fig. 2, and when the event is finished, the apparent position of the star returns to the original position. So the positional fluctuation can be corrected by the continuous observations, or smoothed out by the averaging in terms much longer than t_e.

The power-law dependencies of the optical depth and other lensing quantities on M, Σ and θ are shown in Eqs.(3), (4), (6), (11) and (12). They are useful to estimate the various cases concerning the parameters of lensing stars. For example, the power-law for θ shows that, even in the case of the positional shift of 25 μas, a 4% probability of such a deflection still remains with an event duration of about 2.2 years (Paper II).

The case of collective lensing can be compared to the lensing induced by solar gravity. The difference, however, concerns the periods. The sun goes around the celestial sphere in one year. On the contrary, the Galactic Center accomplishes its apparent revolution in about two hundred million years and the event duration is of the order of ten million years. This duration is practically considered as secular. It is interesting to notice that the maximum deflections are of the order of 1 arcsecond in both cases. In the case of solar gravitational deflection, we have already taken it into account and corrected the effect when we construct the celestial reference frame with an accuracy of the order of 1 mas. Similarly, we should correct the gravitational lensing by the Galactic Center when constructing it with an accuracy of the order of 1 μas. It is well known that there are three QSOs within 1 degree of the Galactic Center, named W56, W109 and GC441. Their position relative to the Galactic Center are measured precisely to investigate the galactic rotation and the motion of the Galactic Center (Backer & Sramek 1999; Reid *et al.* 1999). When the positioning accuracy reaches a few μas with several years of continuous observations, relative expansion or contraction of the distances among the three objects above should be taken into account. These secular motions are illustrated in Fig.4 (Ohnishi *et al.* 2003).

To summarize, there are several kinds of deflectors in our galaxy that cause the positional shift of the extragalactic sources of the order of μas in a few years.

Therefore, we have to take them into account and make corrections when we construct the extragalactic reference frame with accuracy of μas order.

References

Alcock, C., Akerloff, C. W., Allsman, R. A., Axelrod, T. S., Bennett, D. P., Chan, S., Cook, C. H., Freeman, K. C., Griest, K., Marshall, S. L., Park, H. S., Perlmutter, S., Peterson, B. A., Pratt, M. R., Quinn, P. J., Rodgers, A. W., Stubbs, C. W., Sutherland, W. 1993, Nature 365, 621

Alexander, T., Sternberg, A. 1999, ApJ, 520, 137

Arias, E. F., Charlot, P., Feissel, M., Lestrade, J.-F. 1995 A&A303,604

Aubourg, E., Bareyre, P., Brehin, S., Gros, M., Lachieze-Rey, M., Laurent, B., Lesquoy, E., Magneville, C., Milsztajn, A., Moscoso, L., Queinnec, F., Rich, J., Spiro, M., Vigroux, L., Zylberajch, S., Ansari, R., Cavalier, F., Moniez, M., Beaulieu, J. P., Ferlet, R., Grison, P., Madjar, A. Vidal, Guibert, J., Moreau, O., Tajahmady, F., Maurice, E., Prevot, L., Gry, C. 1993, Nature, 365, 623

Backer, D. C., & Sramek, R. A. 1999, ApJ, 524, 805

Genzel, R., Thatte, N., Krabbe, A., Kroker, H., & Tacconi-Garman, L. E. 1996, ApJ, 472,153

Ghez, M., Klein,L., Morris, M., Becklin, E. 1998, ApJ, 509, 678

Høg, E., Novikov, I. D., Polnarev, A. G. 1995, A&A, 294, 287

Hosokawa, M., Ohnishi, K., Fukushima, T., Takeuti, M. 1993, A&A, 278, L27

Hosokawa, M., Ohnishi, K., Fukushima, T., Takeuti, M. 1995 in *Astronomical and astrophysical objectives of sub-milliarcsecond optical astrometry* proceedings of the 166th Symposium of the IAU, ed. E. Høg, P. Kenneth Seidelmann, p.305

Hosokawa, M., Ohnishi, K., & Fukushima, T. 1997a, in Proc. of Technical Work Shop on APT and APSG 1996, (Kashima: Kashima Space Research Center), 70

Hosokawa, M., Ohnishi, K., & Fukushima, T. 1997b, AJ, 114, 1508

Hosokawa, M., Jauncey, D., Reynolds, J., Tzioumis, A., Ohnishi, K., & Fukushima, T. 2002, ApJ, 580, L43

Kent, S. 1992, ApJ, 387,181

Ma, C., Arias, E. F., Eubanks, T. M., Fey, A. L., Gontier, A.-M., Jacobs, C. S., Sovers, O. J., Archinal, B. A., Charlot, P. 1998, AJ,116 516

Ohnishi, K., Hosokawa, M, Fukushima, T. 2003 in ASP Conference Series, Vol.289, *IAU 8th Asian-Pacific Regional Meeting*, ed. S. Ikeuchi, J. Hearnshaw, and T. Hanawa, 461

Reid, M.J., Readhead, A.C.S., Vermeulen, R.C., & Treuhaft, R.N. 1999, ApJ, 524, 816

Salpeter, E. 1955, ApJ,121,161

Sazhin, M.V., Zharov, V.E., Volynkin, A.V., Kalinina, T.A. 1998, MNRAS, 300, 287

Schneider, P., Ehlers, J., Falco, E. E. 1992, Gravitational Lenses (Springer, Berlin)

Extending the ICRF to Higher Radio Frequencies: Initial Global Astrometric Results

C.S. Jacobs, G. E. Lanyi, C. J. Naudet, O. J. Sovers, and L. D. Zhang

Jet Propulsion Laboratory, 4800 Oak Grove Dr., Pasadena CA 91109

P. Charlot

Observatoire de Bordeaux, BP 89, 33270 Floirac, France

D. Gordon & C. Ma

Goddard Space Flight Center, Code 926, Greenbelt MD, 20771

and the KQ VLBI Survey Collaboration

Abstract. We have constructed an initial set of celestial reference frames at K-band (24 GHz) and Q-band (43 GHz) based on VLBI astrometric survey observations of active galactic nuclei. Three VLBA observing sessions covered the full 24 hours of right ascension and declinations down to $-30°$. Our catalog of 108 sources has K-band median formal position uncertainties of ≈ 250 μas; Q-band uncertainties are ≈ 1.5 times larger. Weighted RMS (WRMS) residuals were 32 ps and 70 fs/s in delay and rate, respectively. Comparison of the K-band frame to the S/X-band ICRF shows agreement at the sub-milliarcsecond level.

The motivations for extending the ICRF to higher frequencies are to use more compact sources to construct a more stable frame, to provide calibrators for phase referencing, and to support spacecraft navigation at higher frequencies.

1. Introduction

Early in the development of the Very Long Baseline Interferometry (VLBI) technique, it was appreciated that VLBI observations of distant active galactic nuclei (AGNs) had the potential to form the basis of a quasi-inertial celestial reference frame with milli-arcsecond (mas) or better accuracy. In the 1990s the IAU working group on reference frames brought together workers from astrometric groups from around the world to produce a standard celestial reference frame that became known as the International Celestial Reference Frame (ICRF,*cf.* Ma *et al.* (1998)). This foundational work was done at S/X-band (2.3/8.4 GHz) with a parallel realization of the frame at optical frequencies based on HIPPARCOS satellite data. It was appreciated by many specialists that the extension of the ICRF to additional frequencies would further enhance the value of the work already done.

A number of developments have now converged to make the first decade of the new millenium an opportune time to pursue the extension of the ICRF to radio frequencies in the 24–43 GHz range. First, the S-band environment is

increasingly cluttered by radio frequency interference making continued observations at S/X ever more difficult. Second, high frequency radio amplifiers at K (24 GHz), Ka (32 GHz), and Q-band(43 GHz) are now available for use by the VLBI technique. Evidence, based on the same data used for this paper, suggests that sources are more compact—and therefore more astrometrically stable—at these frequencies than at X-band (*see* Fey *et al*, this volume). Thus there is potential for constructing a new frame that is superior to the current S/X-based ICRF. Such a new frame would provide calibrators permitting narrow field phase referencing work at these higher frequencies. Third, radio systems for planetary probes are moving to Ka-band and are expected to require sub-mas tracking accuracy. Interpolating the K and Q-band results will provide initial constraints on astrometric suitability of sources at Ka-band thereby allowing one to build a roadmap for high accuracy spacecraft navigation at 32 GHz.

Our long term goal is to move from simultaneous dual frequency S/X-band to X/Ka-band. Ka-band will allow for higher telemetry rates to deep space probes and will reduce plasma related errors by roughly a factor of 16 compared to X-band. Ka-band (32 GHz) is preferred because it is not as close to the 22 GHz H_2O line as is K-band (24 GHz); similarly, Ka-band is preferred because it is not as close to the 60 GHz O_2 line as is Q-band (43 GHz). Thus the choice of the 32 GHz frequency is an attempt to optimize atmospheric transparency. Over the next year or two, X/Ka long baseline systems are scheduled to come on line.[1] We envision gradually moving our focus away from single band K or Q-band work to simultaneous X/Ka-band work. In the meantime, we must rely on the K and Q-band results.

Thus this paper will describe the initial results of our efforts to extend realizations of the ICRF to those bands. The presentation is organized as follows: Section 2 will review the observations that have been collected at the present time. Section 3 will present the results obtained from our first three observing sessions. Section 4 will present frame comparisons which will provide both internal (K vs. Q-band) and external (K vs. S/X-band) tests of our frame's accuracy. Section 5 will show evidence for systematic zonal errors at the level of 100s of μas. Section 6 will present the conclusions of this paper.

2. Observations

The results presented here show the progress made based on the first three VLBA sessions: 15 May 2002, 25 August 2002, and 26 December 2002. The first two sessions observed the same set of 65 sources which was selected for expected compactness and strong flux (typically > 0.7 Jy). The third session extended observations to weaker sources. Each source was observed with 3–5 snapshots, each of which used the entire array for 2 minutes at K-band and then 2 minutes at Q-band. This strategy was chosen to allow adequate *uv* coverage for simultaneous imaging while still permitting sub-mas global astrometry based on group delays over a 400 MHz spanned bandwidth. Recorded bandwidth was

---

[1]Goldstone CA in 2001, Madrid Spain in late 2003, and Canberra, Australia in 2005

128 Mbps. There were 22,215 usable pairs of delays and rates which were fit with 728 degrees of freedom.

The VLBA is limited to U.S. territory by design. The longer baselines contribute proportionally more to the astrometric solution. The longest baseline is from Mauna Kea, Hawaii to St. Croix, U.S. Virgin Islands. These two stations also represent the extremes of one of the leading systematic errors in VLBI: the troposphere. The Mauna Kea station is at such a high altitude that it is above a considerable portion of the atmosphere. St. Croix on the other hand is nearly at sea level. Its proximity to the ocean makes it susceptible to unmodelled fluctuations in water vapor refractivity. The array has a greater East-West extent compared to its North-South extent. As a result, the VLBA produces better precision in right ascensions than declinations by a factor of ≈ 1.5.

3. Results

Data from the first three sessions yield a global reference frame of right ascensions and declinations for 108 sources. The distribution of sources is illustrated in Fig. 1. Note that:

1) Observations covered only down to $\delta \approx -30°$.

2) Declination uncertainty systematically increases as one moves south. This may be seen from the symbol coding which indicates σ_δ.

3) The dashed line indicates the galactic plane.

4) The dotted line indicates the ecliptic plane.

Q-band results are similar but with $\sigma_\delta \approx 1.5$ times larger than at K-band due to fewer measurements and lower SNR.

When the minimal 3 coordinates are held fixed in order to set the frame orientation, the solution for the right ascensions and declinations yields median formal K-band position uncertainties of 212 and 273 μas in $\alpha \cos(\delta)$ and δ, respectively. For Q-band the corresponding results were 309 and 427 μas in $\alpha \cos(\delta)$ and δ, respectively. The solution used 3 hour troposphere breaks and yielded WRMS residuals of 32 ps and 70 fs/s, respectively.

Because these sources are at extreme extra-galactic distances (median redshift $z \approx 1$), we have assumed that proper motions and parallaxes are negligible. Exploratory S/X fits estimate apparent proper motions that are well below 100 μas/yr thus supporting our decision to neglect proper motion parameters.

4. Internal and External Catalog Comparisons

Our past experience with analysis of S/X data suggests that formal uncertainties often underestimate the true errors (*e.g.* Jacobs *et al.* (1998), Ma *et al.* (1998)). In order to gain a more realistic estimate of the true accuracy of our reference frame, we made two comparisons. First, we compared the K frame to an external standard, the S/X frame. Next, we examined the internal consistency of our data and analysis by comparing K and Q-band results against each other.

The external standard of comparison was a recent JPL S/X solution labelled DDOR_2002 which included nearly 3 million group delay measurements acquired from 1978 to 2002. This S/X frame is an unpublished extension of the ICRF

extension-1 frame and was verified to be consistent with that frame at the 100 μas (WRMS) level. The MODEST software (Sovers, *et al.* (1998)) was used both for the physical modelling and parameter estimation used to build this frame.

Figs. 2a. and 2b. show the K minus S/X differences for $\alpha \cos \delta$ and δ, respectively (3 coordinates fixed in each frame). The histogram of $\Delta \alpha \cos(\delta)$ shows a median difference of -42 μas and a WRMS about the mean of 294 μas. Both these values are too large to be explained by the modelled formal uncertainties and thus indicate the presence of unmodelled systematic errors. Declinations are somewhat worse. The histogram of $\Delta \delta$ shows a median difference of 242 μas and a WRMS about the mean of 574 μas thus indicating the presence of systematic errors in the declinations.

While these comparisons do not determine to what extent the systematic errors are in the K vs. the S/X frame, the latter's vastly larger data set and more carefully scrutinized analyses lends more weight to the S/X results. Thus, our working hypothesis is that K-band systematic errors dominate the comparison.

Having compared to an external standard, let us now check the internal consistency of our two high frequency frames. Figs. 3a. and b. show histograms of K minus Q-band differences, $\Delta \alpha \cos \delta$ and $\Delta \delta$, respectively. These differences are consistent with the formal uncertainties as shown by the median normalized differences $\Delta \alpha$ and $\Delta \delta$ being 0.8 and 1.0, respectively. Note that since K and Q-band data formal uncertainties are statistically independent, the formal uncertainty of each difference is the root sum square of the individual K and Q uncertainties. Given that the plasma-induced delays of solar plasma and the Earth's ionosphere are the most obvious frequency dependent effects, we take the K-Q normalized differences to be an indication that plasma effects are not yet dominating our error budget. Thermal noise is still an issue. As further data are added, formal uncertainties will be reduced thereby increasing sensitivity to K vs. Q-band systematic errors. Thus we are considering various strategies for quantifying plasma systematic effects which are expected to arise in future analyses. While the WRMS scatter about the mean is roughly consistent with the formal errors, the same cannot be said of the mean differences which, respectively, are $< \Delta \alpha \cos \delta > = 159 \pm 32$ μas and $< \Delta \delta >= 142 \pm 52$ μas. Thus we are detecting systematic errors.

5.   Zonal Errors

Given evidence from both external and internal comparisons for the presence of unmodelled systematic errors, we will now take a closer look at the distribution of the differences. A plot of $\alpha \cos \delta$ differences vs. δ shows evidence of zonal errors.

Figs. 4a. and b. plot $\Delta \alpha \cos(\delta)$ vs. δ for two cases. On the left, Fig. 4a. reflects a K-band solution with the minimal 3 coordinate parameters fixed. On the right, Fig. 4b. reflects a solution with 8 coordinates (from 4 well spread sources) constrained to the S/X solution. The formal 1σ (diagonal) uncertainties are indicated as error bars. Note that while inter-source correlations are not graphically indicated, they are significant especially in the first case—a point that we will return to in a moment. In Fig. 4a. the $\Delta \alpha \cos \delta$ vs. δ trend is significant (-7.5 ± 0.9 μas/deg). Removing this trend reduces the WRMS scatter

from 296 to 225 μas. In Fig 4b. the additional source constraints have effectively constrained the $\Delta\alpha\cos\delta$ vs. δ zonal error. In this second case, removing a trend results in almost no improvement in WRMS scatter—which remained very close to 210 μas. Note that the geometric strength introduced by the extra source position constraints is reflected in the smaller errors bars in Fig. 4b.

Examining declination differences (not plotted) shows a similar story. With 1.5 sources fixed, the WRMS scatter of $\Delta\delta$ is 511 μas. Removing a $\Delta\delta$ vs. δ trend reduces the scatter to 466 μas. With 4 sources fixed the WRMS scatter of $\Delta\delta$ is 408 μas and removing a trend vs. δ reduces that only slightly to 393 μas.

While some small residual zonal trends are still present, the basic picture is that there are large zonal errors in both α and δ vs. δ that are effectively constrained by fixing a small number (4) of well spread sources. It is clear that a stronger declination measuring geometry (*i.e.* North-South baselines) will be needed to solidify our frame. We hope to add a Tidbinbilla, Australia station to future sessions to do just that.

5.1. Right ascension inter-source correlations

In searching for the underlying cause of the right ascension systematic differences, we discovered that the right ascension parameters themselves are not yet well separated by the data in hand.

Figs. 5a. and b. show the right ascension inter-source correlations vs. the arclength between a given pair of sources. On the left, Fig. 5a. reflects the solution with 3 coordinates fixed whereas Fig. 5b., on the right, reflects 8 coordinates held fixed. The most obvious and important change between the two figures is that the addition of 5 more constraints to the solution leads to large reductions in inter-source correlations. From this we conclude that, with our current data set, *a minimally constrained solution is not able to separate adequately the right ascension parameters.*

This deficiency appears to worsen as one moves further south in declination, presumably because the northern based VLBA's observing geometry is systematically weakened as one observes further south. Also note in Fig. 5a. the "knee" at about 25° arclength. For arclengths shorter than this, right ascensions are almost all positively correlated and thus may tend towards systematic offsets also known as zonal errors. Thus both low declinations and short arcs especially reveal the geometric weakness of our current database of observations.

6. Conclusions

We have presented the motivation for and initial results from our program to develop global celestial reference frames at K and Q-bands. A total of 108 sources have been observed with K-band formal position uncertainties of ≈ 250 μas and Q-band uncertainties which were ≈ 1.5 times larger. The true accuracy of our results has been estimated from both internal and external comparisons. K and Q-band solutions showed internal agreement at ≈ 300 and ≈ 500 μas in $\alpha\cos\delta$ and δ, respectively. Comparison with the independent and more strongly established S/X frame gave agreement at approximately the same level.

Examination of zonal errors vs. declination and inter-source correlations shows that after 3 sessions we have not yet separated well the estimated position

parameters. Perhaps this should not be a surprise given that the S/X work took two decades to get to its present level. However, we will likely need more than just repetition of our current observing strategy; we will need a stronger North-South geometry in order to create a more rigid frame that can stand independently of the S/X frame. Thus our work must be continued and refined before any high frequency frame can surpass the S/X frame.

Having acknowledged these issues, we would like to end on a positive note. Before we undertook the work described in this paper, there was very little global astrometric data available at frequencies above X-band (8.4 GHz). There were uncertainties as to whether reference frames at K, Q, and Ka-bands were even feasible. In particular, we did not know if there were sufficient well-spaced sources to track spacecraft with differential VLBI at Ka-band. We were uncertain as to how well K, Q, and Ka-band positions would agree with the S/X frame.

The results presented in this paper have answered these questions well enough that we are now optimistic about the future of high frequency radio frames both for general astrometry and for spacecraft tracking. We have a reasonably large catalog of reasonably strong sources detected at both K-band (24 GHz) and Q-band (43 GHz) and assuming that we may interpolate to Ka-band (32 GHz), we now have a sufficiently large and sufficiently accurate catalog to begin supporting demonstrations of spacecraft measurements in 2005. In conclusion, this work is a major step forward for both the astrometry and spacecraft navigation communities.

References

Ma, C., E.F. Arias, T.M. Eubanks, A.L. Fey, A.-M. Gontier, C.S. Jacobs, O.J. Sovers, B.A. Archinal, and P. Charlot 1998, 'The ICRF as Realized by VLBI', AJ, 116, 1, 516-546

Fey, A. L., D. A. Boboltz, P. Charlot, E .B. Fomalont, G. E. Lanyi, L. D. Zhang, and the K-Q VLBI Survey Collaboration, 'Extending the ICRF to Higher Radio Frequencies—First Imaging Results', this volume.

Jacobs, C.S., O.J. Sovers, C.J. Naudet, R.F. Coker, and R.P. Branson 1998, 'The JPL Extragalactic Radio Reference Frame: Astrometric Results of 1978-96 Deep Space Network VLBI', NASA JPL TDA Progress Reports, vol. 133, 1-55

Sovers, O.J., J.L. Fanselow, & C.S. Jacobs 1998, 'Astrometry & Geodesy with Radio Interferometry: Experiments, Models, Results', Rev Mod Phys, 70, 4
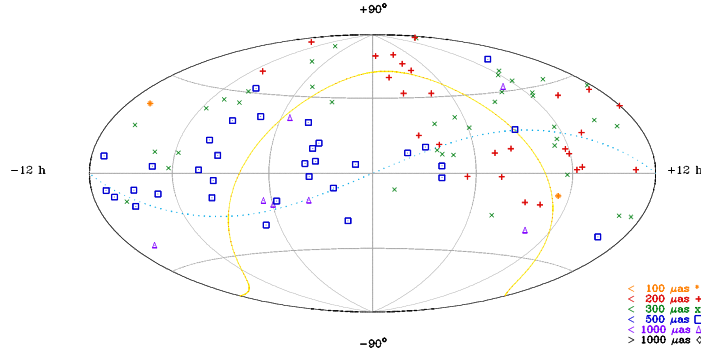
Figure 1.   Distribution of 108 K-band sources. Symbols indicate σ_δ.
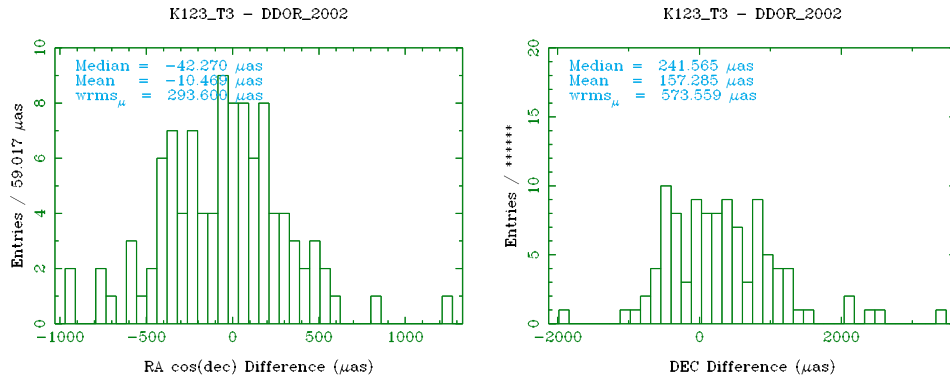
Figure 2. $K - S/X$: $\alpha \cos \delta$ differences are shown on the left. δ differences are shown on the right.
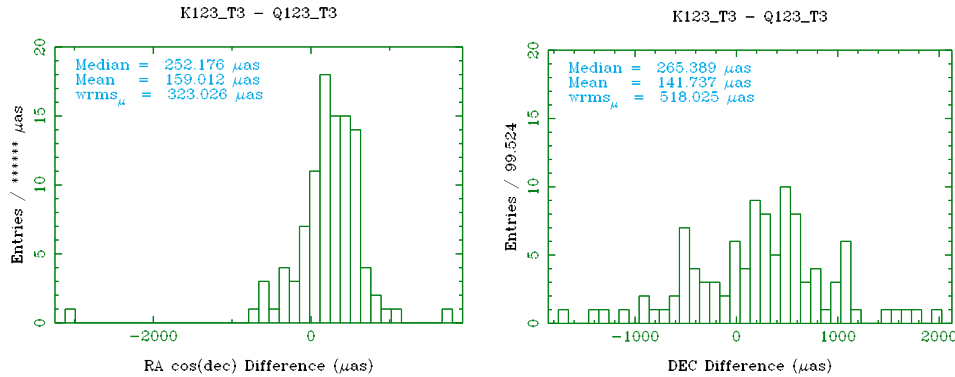
Figure 3. $K - Q$-band differences. Median differences in $\alpha \cos \delta$ and δ are 252 and 265 μas wrms, respectively. WRMS differences are 323 and 518 μas, respectively. The labels K123 and Q123 indicate catalogs combining data from sessions 1,2 and 3.
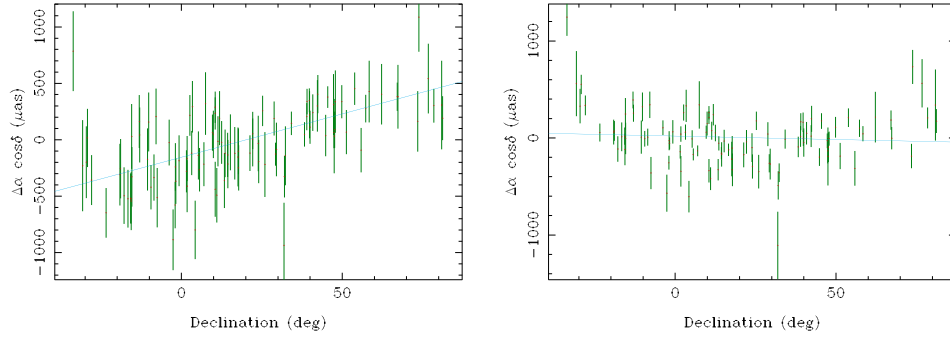
Figure 4. K minus S/X-band differences: $\Delta\alpha\cos\delta$ vs. δ. Fig. 4a. (left) reflects the minimal 3 coordinate constraint whereas fig. 4b (right) reflects fixing 8 coordinates to their S/X catalog values. Note how the additional constraints control the zonal error vs. δ.
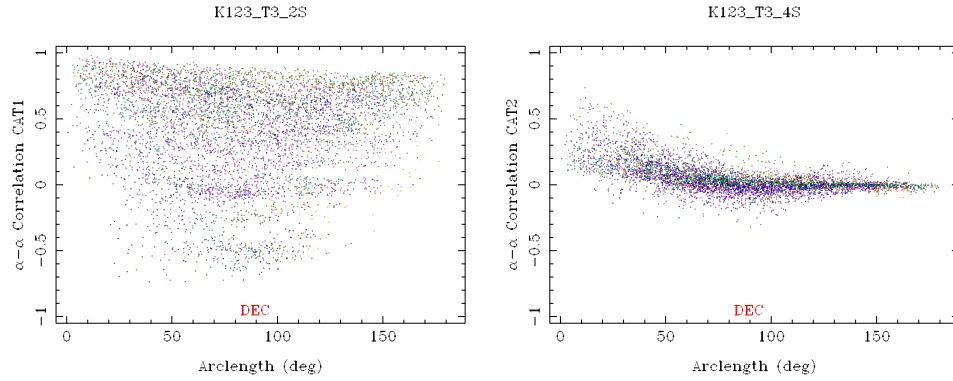
Figure 5. K-band right ascension inter-source correlations: Fig 5a. (left) reflects a minimally constrained solution; Fig 5b. (right) reflects 8 total coordinates fixed to the S/X solution.

Densification of the ICRF/HCRF in Visible Wavelengths

Sean E. Urban

U.S. Naval Observatory, 3450 Massachusetts Ave. NW, Washington DC, 20392-5420

Abstract. With the release of the Hipparcos Catalogue and the IAU resolution designating its ≈100,000 star subset as the HCRF, the optical reference frame increased 20-fold in the number of stars over the FK5. For many applications, even these 100,000 stars are inadequate in spatial density and limiting magnitude. However, Hipparcos is dense enough and deep enough to reduce many astrometric catalogs directly; the resulting data can be used to densify the HCRF and extend its magnitude limit. The initial major densification efforts of the HCRF utilized the Tycho data, culminating in the Tycho-2 Catalogue of 2.5 million stars. Over the last few years, several groups have been working toward even greater densification. Some resulting catalogs, such as the CMC 13, M2000, and SPM 2.0 are zonal, covering selected areas of the sky. Others, such as UCAC, USNO-B, and GSC 2.3 aim at global coverage but with varying degrees of accuracy and magnitude regimes. Others, namely DENIS and 2MASS, are extending the HCRF into the near-IR realm. The current state of many of these projects, and what is expected in the next few years in terms of densification of the optical frame, is presented.

1. Introduction

With the exception of determining Earth orientation parameters and observations made in the radio frequencies, the 608 objects that make up the International Celestial Reference Frame (ICRF; Ma *et al.* 1998) are useless to most astronomers' applications. In order for a reference frame to be useful, its fiducials need to be observable, their spatial density needs to be high, and the astrometry needs to be systematically consistent. As for observability, the optical counterparts to the ICRF objects are difficult (at best) to observe because of their faint visual magnitudes (typically 17-21). As for frame density, 608 objects translates into one every 67 square degrees. This is seven times less dense than the FK5 and its extension (Fricke *et al.* 1988, 1991), and the FK5's ability to be used for direct reduction of observational data was often lacking due to its relatively low spatial density. As for systematic consistency, the ICRF is the standard which other frames try to attain.

Most professional astronomers know and use the International Celestial Reference System (ICRS) not by the 608 frame objects, but by the optical star catalogs that are adjusted to the ICRS. These catalogs can contain millions of stars including the brightest, and hence are much more useful to many astronomers than the ICRF objects themselves. In general, these are densifications of the Hipparcos Catalogue (ESA 1997), which contains 118,000 objects. The Hipparcos Catalogue includes all stars to V≈7.2, contains roughly three stars

per square degree, and is systematically consistent to 0.25 mas/yr (Kovalevsky *et al.* 1997). Its accuracies for individual stars of ≈ 1 mas in position and parallax and ≈ 1 mas/yr for proper motions provide such a good reference frame that at the beginning of 1998, the IAU adopted the Hipparcos Catalogue as "the primary realisation of the ICRS at optical wavelengths" (IAU 1997). In 2000 this was modified slightly to exclude the $\approx$20,000 stars marked with a Double or Multiplicity Code flag. The remaining $\approx$100,000 stars were officially designated the Hipparcos Celestial Reference Frame (HCRF; IAU 2000).

Although a tremendous data source in its own right, the Hipparcos data can be utilized to reduce other deeper, denser positional catalogs to the HCRF. Staff at the United States Naval Observatory (USNO) in 1998 and 1999 reduced a series of 150 ground-based catalogs to minimize systematic errors by position, magnitude, and color. At the same time, staff at the Copenhagen University Observatory were re-reducing the Tycho observations extracting 2.5 million positions from the star mapper experiment that flew on the Hipparcos satellite. The two data sets were combined and released as the Tycho-2 Catalogue in 2000 (Høg *et al.* 2000). Being nearly complete down to V=11.0, Tycho-2 has been used to put deeper observations on the HCRF. The density of Tycho-2 has been especially important as telescopes transition from very wide field detectors (photographic plates) to smaller ones (CCDs).

There are a few observatories around the world that continue to reach fainter and denser astrometric catalogs; many of these projects will reach conclusion in this triennium. There are also plans for new telescopes and detectors that will be able to observe the ICRF objects simultaneously with the bright stars, therefore removing the rather cumbersome "linking" processes that must currently be employed due the the finite dynamic range of the detectors and the faint magnitudes of the ICRF objects themselves. This paper will discuss some of the current work being done in densifying the optical reference frame, briefly discuss some future projects, and plead that the IAU continues to be the organizational outlet for these programs.

2. IAU Organization

The optical realization of the ICRS is currently the Hipparcos Celestial Reference Frame (HCRF), and although more than 150 times the density of the ICRF it still is not useful for many applications. The IAU has recognized this and since 1997 has had a group of astronomers working toward greater densification. This group is organized under the ICRS Working Group sponsored directly by Division I. Table 1 shows a list of the current members. A web page devoted to densification in the optical (and infrared, to some extent), is maintained by the chairman, currently S. Urban, at "http://ad.usno.navy.mil/dens_wg/dens.html".

Since the 2000 IAU General Assembly, much work has taken part in this area. At that time, Hipparcos was the primary source for bright star astrometry; the Tycho-2 Catalogue was the first de-facto standard when the Hipparcos Catalogue was either not dense or deep enough for applications; and the USNO-A catalog with 526 million stars, although without proper motions, was typically used when neither Hipparcos nor Tycho-2 were appropriate. Over the past three

Table 1.   Members of the IAU Densification sub-group

Member	Country	Member	Country
W. van Altena	USA	I. Kumkova	Russia
B. Bucciarelli	Italy	B. Mason	USA
N. Capitaine	France	F. Mignard	France
T. Corbin	USA	D. Monet	USA
D. Evans	UK	I. Platais	USA
G. Gontcharov	Russia	T. Rafferty	USA
C. Jacobs	USA	J. Souchay	France
K. Johnston	USA	S. Urban (chair)	USA
V. Kislyuk	Ukraine	N. Zacharias	USA

years, several projects have matured to the point where large areas of the sky are covered by precise astrometry, going fainter and denser than Tycho-2.

3.   Deep Zonal Catalogs

3.1.   Meridien 2000

Between 1996 and 2000, the Bordeaux Observatory has been engaged in observing the zone from $+11°$ to $+16°$ using a 20-cm transit circle fitted with a CCD; see Fig. 1. The coverage is complete from V=9.5 to V=15.4, and includes stars as faint as V=16.3. The first version of the catalog, called Meridien 2000 (M2000; Rapaport *et al.* 2001), was released in 2001. On average, each star has been observed seven times and the positional errors at mean epoch are believed to be about 35 mas for the better stars and degrade to near 80 mas at the faint end. Although currently without proper motions, the Bordeaux Observatory has a unique data set to exploit. The area observed was chosen to be coincident with the area that Bordeaux photographed as part of the Carte du Ciel (CdC) program. The 511 plates covering this region that were observed in the early 20th century have been digitized on the Automatic Plate Measuring machine run by the Institute of Astronomy at Cambridge, England. The plan is to utilize these data down to the CdC limiting magnitude of about 14.5, and use measures of Northern and Southern Proper Motions plates (Klemola *et al.* 1987; Platais *et al.* 1998) – measured on the Precision Measuring Machine (PMM; Monet and Levine 2001) – for the fainter stars. A new catalog complete with proper motions is expected near the end of 2003.

3.2.   Carlsberg Meridian Circle Program

The Carlsberg Meridian Circle program – a joint project between the Institute of Astronomy (Cambridge), the Copenhagen University Observatory, and the Real Instituto y Observatorio de la Armada en San Fernando – has recently released its thirteenth catalog aptly named CMC 13 (ftp://ftp.ast.cam.ac.uk/pub/cmc13/). The telescope, robotically operated since 1984, is a 17.8-cm transit circle fitted in 1997 with a CCD and operating in drift-scanning mode (Evans 2001). The catalog contains 36 million stars from declinations $-3°$ to $+30°$ with a magnitude range of 9 to 17 in the Sloan r′ band; see Fig. 1. Positional errors are
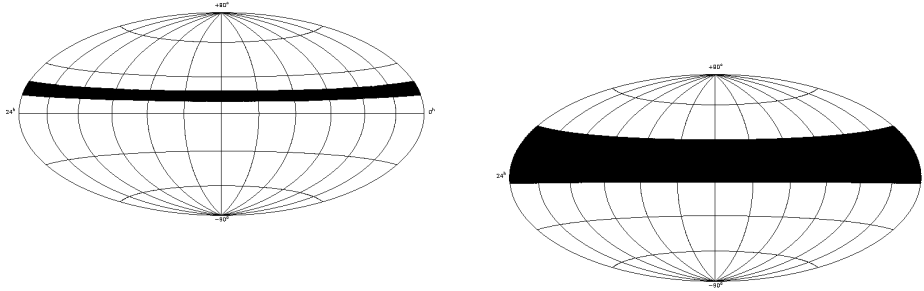
Figure 1. Sky coverage of M2000 (left) and CMC 13 (right)

magnitude dependent; they are estimated to be 40 mas at r$'$ = 14 and $\approx$ 100 for the faint end. There are no proper motions and no plans to provide them for this data set as funding for this program runs out in mid-2004. It is expected that observations from declinations $-15°$ to $+50°$ will be completed, reduced, and published in 2004.

3.3. Southern Proper Motions Program

The Southern Proper Motions Program (SPM) is an ongoing observational program run by Yale University and the National Observatory of San Juan, Argentina. The telescope, a 50-cm double astrograph, is located at Cesco Observatory, El Leoncito, Argentina. For the latest two catalogs, the SPM 2.0 and SPM 3.1 (Platais *et al.* 1998), photographic plates were used but currently the telescope is being fitted with a CCD camera. The SPM 2.0 and 3.1 cover the same area of sky, that is non-galactic plane regions between declinations $-40°$ and $-25°$ as shown in Fig. 2. However the SPM 2.0 has higher precision but fewer stars than SPM 3.1. The SPM 2.0 contains 320,000 stars measured on a high precision PDS machine. The SPM 3.1, utilizing the same photographic plates, contains about 11 million stars measured on the PMM. Both contain proper motions through use of two sets of plates taken with the same instrument. Accuracies for SPM 2.0 are believed to be about 20 mas at mean epoch with proper motions about 2 mas/yr. For SPM 3.1, the accuracies are estimated to be roughly twice as high as SPM 2.0.

4. Deep Full-sky Catalogs

4.1. USNO CCD Astrograph Catalog Program

The US Naval Observatory CCD Astrograph Catalog program (UCAC) is an ongoing project designed to give full sky astrometry in the magnitude range from about R=8.0 to R=16.0. As its name implies, it is run by the USNO and uses an 8-inch twin astrograph with a 4k x 4k CCD behind a five-element lens; the system yields about a one square degree field of view. All observations are guided in a stare mode using feedback from the second tube which is fitted with an autoguider. Observations are made in semi-automatic mode. The observing
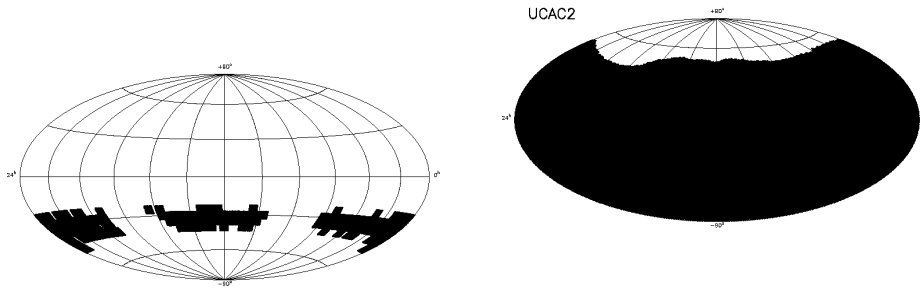
Figure 2.   Sky coverage of SPM 2.0 and 3.1 (left) and UCAC2 (right)

program began in 1998 at Cerro Tololo Inter-American Observatory. Following three years of observations, the telescope was moved to the U.S. Naval Observatory Flagstaff Station where it continues observing today. It is anticipated that all observations will be finished by mid-2004 with a final catalog released in 2005. There have been two interim data releases, UCAC1 (Zacharias *et al.* 2000) and UCAC2. The UCAC2 was recently completed and distributed at this IAU GA; it is available on a three CD set (Zacharias *et al.* 2004) and completely supersedes UCAC1. UCAC2 contains 48 million stars covering over 86% of the sky; its coverage is shown in Fig. 2. Positional accuracies are from about 20 mas for the well-exposed stars and deteriorate to 70 mas for the faintest and brightest ones. All stars contain proper motions that range in accuracy from about 1 to 3 mas/yr for well-observed stars up to about V=12, to 6 mas/yr for stars fainter. The proper motions were derived using the same data set and software as for the Tycho-2 motions, but also include data from the NPM and SPM programs for the faint stars and new measures of the AGK2 plates for brighter stars in the north. Additional information can be found in N. Zacharias's paper in these Proceedings.

4.2.   Guide Star Catalogue Program

The Guide Star Catalogue program, a joint venture between Space Telescope Science Institute (USA) and Torino Observatory (Italy), uses plates taken with the Palomar and UK Schmidt telescopes measured on a PDS microdensitometer as data for its all-sky catalogs (http://www-gsss.stsci.edu/gsc/gsc2/GSC2home.htm). The latest release, GSC2.2 contains 455 million objects and is believed complete down to photographic J magnitude 19.5. Positional accuracies are around 300 mas and have much lower systematic errors than previous GSC releases due to refined reduction algorithms (Morrison *et al.* 2001). There are no proper motions at this time, but plans are made to release GSC 2.3 that would contain about 1 billion stars with proper motions. No schedule for the release of GSC 2.3 has been given.

4.3.   USNO-B Program

The USNO-B catalog has been released by the U.S. Naval Observatory and supersedes the USNO-A series (Monet *et al.* 2003). Like the USNO-A, USNO-

B's data are taken from Palomar, UK, and ESO Schmidt plates measured on the Precision Measuring Machine (Monet and Levine 2001). The catalog contains slightly over 1 billion objects and is believed complete down to V=21. The catalog contains proper motions; accuracies of the objects are estimated to be $\approx$200 mas in position at mean epoch and 8 to 10 mas/yr for the motions. The catalog is 80 Gbytes, so is not widely distributed; however, segments of it can be downloaded at http://www.nofs.navy.mil/projects/pmm/. A future release is planned near the beginning of 2004 that will include UCAC and 2MASS data to improve the astrometric accuracy and extend the photometry to the near IR.

5.   Future work

5.1.   Catalog consolidation

As shown in the above summaries, many of the projects under way are not yet complete but will be within the next three years. As these projects come to fruition, the astrometric community faces the prospect of having several products that the wider astronomical community can use. Choices can be good but confusing if one does not have intimate knowledge of the particular data sets; it is likely that users will not "choose" the best catalog for the job but instead select one that comes up first on a web search. The IAU has recognized this and has set up a web site for survey information; see http://www.skysurveys.org. It is the author's opinion that several of these catalogs should be combined, producing fewer but better catalogs.

This type of situation took place a few years ago following the release of the Tycho Catalogue (ESA 1997). At that time, Tycho's proper motion accuracies were a poor 25 mas/yr due to the short observational span of the program. Within 2 months of the Tycho release, the USNO released the ACT Reference Catalog (ACT; Urban *et al.* 1998) with improved proper motions of about 3 mas/yr. The following year, the Tycho group released the Tycho Reference Catalogue (TRC; Høg *et al.* 1998) with similar characteristics as the ACT. For a few years, many astronomers were unsure if they should use Tycho, ACT, or TRC. This situation improved when Høg and Urban agreed to pool their resources and jointly produce Tycho-2 (Urban and Høg 1998). The astronomical community benefitted from this consolidation by having the best product that could be produced and by having a clear identification of what data set should be used.

5.2.   Direct links to the ICRF

The densification projects mentioned above (with the exception of SPM 2.0) all utilize the Tycho-2 Catalogue as representative of the HCRF. The HCRF, in turn, is representative of the ICRF. This multi-step approach to link the optical catalogs to the ICRS is unfortunate because systematic errors, mostly in the Tycho-2 data set (Urban *et al.* 2000), can propagate into the final catalogs. However, it has been necessary due to the inherent dynamic range limitations of photographic plates and CCDs; this makes it almost impossible to observe both the brighter stars and the optical counterparts of the ICRF sources on the same program. This may be changing with the advent of large dynamic range

technologies such as CMOS detectors. Telescopes and detector systems can be designed to observe both the Hipparcos stars and the faint ICRF objects simultaneously and with the same instrument. USNO has plans for such an instrument, called "URAT" (for USNO Robotic Astrometric Telescope) that will eliminate the need for multi-step HCRF/ICRF linking (de Vegt *et al.* 2003). With observations of both HCRF and ICRF objects, traditional reduction methods on individual frames (requiring a dense reference frame) and block-adjustment methods on the entire sky (requiring only a handful of objects) can both be employed. At that time, a direct densification of the ICRF can be made.

Within a decade, it is very likely that a new astrometric satellite mission will be in operation, as described by Gaume in these Proceedings. Depending on which of the instruments are launched, the ICRF in its present state may be superseded by optical data. At that point, the astrometric community will need to reconsider what is the "standard" reference frame. If GAIA is successful, then the densification of that frame will require large, sophisticated instruments to attain high accuracies at magnitudes in the V=20 to 25 range.

6.   Summary

There are several astrometric projects that have progressed over the last few years and will shortly come to conclusion. This paper gives the current state of some of the projects that aim to densify and extend the optical reference frame beyond the Tycho-2 limits for large areas of the sky. Much of this work has taken place between members of the IAU sub-group on Densification of the Optical Reference Frame. During the XXV IAU General Assembly, there was much consideration given to the reorganization of Division I and the breakup of the ICRS Working Group; it is the author's hope that this group remains intact to move the densification issues forward.

References

de Vegt, C., Laux, U., and Zacharias, N. 2003, A dedicated 1-meter telescope for high precision astrometric sky mapping of faint stars, in "Small Telescopes in the New Millennium II. The Telescopes We Use." ed. T. Oswalt, Dordrecht: Kluwer Acad. Publ, p. 255

ESA 1997, SP-1200

Evans, D. W. 2001, Astronomische Nachrichten, 322, 347

Fricke, W., Schwan, H., Lederle, T., Bastian, U., Bien, R., Burkhardt, G., Du Mont, B., Hering, R., Jährling, R., Jahreiß, H., Röser, S., Schwerdtfeger, H.-M., and Walter, H. G. 1988, Fifth Fundamental Catalogue (FK5). Part 1: The Basic Fundamental Stars, Karlsruhe: Verlag Braun

Fricke, W., Schwan, H., Corbin, T., Bastian, U., Bien, R., Cole, C., Jackson, E., Jährling, R., Jahreiß, H., Lederle, T., and Röser, S. 1991, Fifth Fundamental Catalogue. Part 2: The FK5 Extension, Karlsruhe: Verlag Braun

Høg, E., Fabricius, C., Makarov, V. V., Urban, S., Corbin, T., Wycoff, G., Bastian, U., Schwekendiek, P., and Wicenec, A. 2000, A&A, 335, L27

Høg, E. Kuzmin, A., Bastian, U. Fabricius, C., Kuimov, K., Lindegren, L., Makarov, V.V., and Röser, S. 1998, A&A, 355, L65

IAU 1997 in Proceedings of the Twenty-third General Assembly – Kyoto 1997, Resolution B2, 39

IAU 2000 in Proceedings of the Twenty-fourth General Assembly – Manchester 2000, Resolution B1.2, 36

Klemola, A., Jones, B. and Hanson, R. 1987, AJ, 94, 501

Kovalevsky, J., Lindegren, L., Perryman, M. A. C., Hemenway, P. D., Johnston, K. J., Kislyuk, V. S., Lestrade, J. F., Morrison, L. V., Platais, I., Rser, S., Schilbach, E., Tucholke, H.-J., de Vegt, C., Vondrak, J., Arias, F., Gontier, A. M., Arenou, F., Brosche, P., Florkowski, D. R., Garrington, S. T., Kozhurina-Platais, V., Preston, R. A., Ron, C., Rybka, S. P., Scholz, R.-D., Zacharias, N., 1997,A&A, 323, 620

Ma, C., Arias, E. F., Eubanks, T. M., Fey, A. L., Gontier, A.-M., Jacobs, C. S., Sovers, O. J., Archinal, B. A., and Charlot, P. 1998, AJ, 116, 516

Monet, D. G., and Levine, S. E. 2001, ASP Conference Series, 232, 284

Monet, D. G., Levine, S. E., Canzian, B., Ables, H. D., Bird, A. R., Dahn, C. C., Guetter, H. H., Harris, H. C., Henden, A. A., Leggett, S. K., Levison, H. F., Luginbuhl, C. B., Martini, J., Monet, A. K. B., Munn, J. A., Pier, J. R., Rhodes, A. R., Riepe, B., Sell, S., Stone, R. C., Vrba, F. J., Walker, R. L., Westerhout, G., Brucato, R. J., Reid, I. N., Schoening, W., Hartley, M., Read, M. A., Tritton, S. B., 2003 AJ, 125, 984

Morrison, J., Röser, S., McLean, B., Bucciarelli, B., and Lasker, B. 2001, AJ, 121, 1752

Platais, I., Girard, T. M., Kozhurina-Platais, V., van Altena, W. F., Lpez, C. E., Mndez, R. A., Ma, W.-Z., Yang, T.-G., MacGillivray, H. T., Yentis, D. J., 1998 aj, 116, 2556

Rapaport, M., Le Campion, J.-F., Soubiran, C., Daigne, G., Pri, J.-P., Bosq, F., Colin, J., Desbats, J.-M., Ducourant, C., Mazurier, J.-M., Montignac, G., Ralite, N., Rquime, Y., Viateau, B., 2001,A&A, 367, 325

Urban, S., Corbin, T., and Wycoff, G. 1998, AJ, 115, 2161

Urban, S. and Høg, E. 1998, private communications

Urban, S., Wycoff, G., and Makarov, V. V. 2000, AJ, 120, 501

Zacharias, N., Urban, S. E., Zacharias, M. I., Hall, D. M., Wycoff, G. L., Rafferty, T. J., Germain, M. E., Holdenried, E. R., Pohlman, J. W., Gauss, F. S., Monet, D. G., Winter, L., 2000,AJ, 120, 2131

Zacharias, N., Urban, S. E., Zacharias, M. I., et al. 2004, in preparation

Extending the ICRF into the Infrared: 2MASS–UCAC Astrometry

Norbert Zacharias

U.S. Naval Observatory, 3450 Massachusetts Ave. NW, Washington DC, 20392-5420

Howard L. McCallon, Eugene Kopan & Roc M. Cutri

IPAC, Caltech, MS 100-22, 770 S. Wilson Ave., Pasadena, CA 91125

Abstract.

An external comparison between the infrared 2MASS and the optical UCAC positions was performed, both being on the same system, the ICRS. About 48 million sources in common were identified. Random errors of the 2MASS catalog positions are about 60 to 70 mas per coordinate for the $K_S = 4$ to 14 range, increasing to about 100 to 150 mas for saturated and very faint stars. Systematic position differences between the 2 catalogs are very small, about 5 to 10 mas as a function of magnitude and color, with somewhat larger errors as a function of right ascension and declination. The extension of the ICRF into the infrared has become a reality.

1. Introduction

The International Celestial Reference Frame (ICRF) is defined by a few hundred radio sources (Ma & Feissel 1997). The optical representation of the ICRF is the Hipparcos Celestial Reference Frame (HCRF) of about 100 thousand stars. The optical system has been densified by the Tycho-2 Catalogue, and recently by the USNO CCD Astrograph Catalog (UCAC) (Zacharias *et al.* 2000, 2004). The Two-Micron All Sky Survey (2MASS) (Skrutskie *et al.* 1997; Cutri *et al.* 2003) is primarily a highly accurate short-wave infrared (IR) photometric catalog. It also provides accurate positions at its observational epoch (1997 to 2001) for over 470 million sources, most of them stellar. The 2MASS represents the best extension of the ICRF into the IR currently available. Here we investigate the astrometric performance of the 2MASS catalog by comparing it with UCAC2 (Zacharias *et al.* 2004).

Contrary to the defining, extragalactic sources, stars move significantly. No proper motions are available from 2MASS, so this astrometric coordinate system at IR wavelengths is currently limited to positions only. However, it is closely tied to the optical system, thus "inheriting" proper motions from optical data, as far as they are available. As with the current optical system, the 2MASS IR system is not directly linked to the defining sources. It depends on a link *via* moving stars, affected by the same potential problems of possible deviations from an inertial system. However, these deviations are expected to be well below 1 mas/yr in rotation, with the zero point of the coordinate systems coinciding to within about 3 mas at current epochs. This is smaller than the systematic errors seen in the 2MASS to UCAC comparison as a function of various parameters. We must assume the optical and IR centroids of the matched sources coincide.

There is no reason to believe otherwise on the mas level, since most sources are stars. A random scatter is introduced by unresolved double stars, where the centroid location can be a function of the bandpass.

Table 1.   2MASS observational details.

2 telescopes	Mt. Hopkins, Cerro Tololo
observing epochs	1997 Jun − 2000 Dec (North)
	1998 Mar − 2001 Feb (South)
aperture	1.3 meter
J (1.24 μm), H (1.66 μm), K_S (2.16 μm) simultaneously	
survey tiles	8.5' by 6 degree (RA by Dec)
6 x 1.3 sec samples	each point on the sky
raw data volume	24.5 TB
all-sky release data volume	50 GB compressed
all-sky release date	March 2003
number of point sources	470,992,970
other data	atlas images, extended sources

Table 2.   UCAC2 observational details.

1 telescope	USNO Twin astrograph
observing epochs	1998 Feb − 2001 Sep (CTIO)
	2001 Nov − 2004 May (NOFS)
aperture	0.2 meter
detector	4k x 4k CCD (0.9"/px, 9 μm, 61' FOV)
2 exposures / field	2–fold overlap of fields
single bandpass	579−642 nm
positional errors	30 mas for r = 8 .. 10
	20 mas for r = 10 .. 14.5
	70 mas for r = 16

2.   Observations

Both 2MASS and UCAC2 positions are on the same system, the ICRS, due to the use of Tycho-2 (Høg *et al.* 2000) reference stars. This also means that 2MASS and UCAC2 positions are highly correlated for stars in the r ≈ 8 to 12 mag range (= Tycho2 stars). Some observational details of the 2 surveys are summarized in Table 1 and 2. 2MASS covers the entire sky, while UCAC2 covers 86% of the sky (90° ≤ δ ≤ ≈ +45°). More details are given at the respective home pages *ad.usno.navy.mil/ucac* and *www.ipac.caltech.edu/2mass/releases/allsky/*.

UCAC2 and 2MASS positions were cross-correlated using a match radius of 0.5 arcsec. There are 47,958,962 common sources found, which represent 99.23% of all UCAC2 sources. The UCAC2 proper motions were applied to bring the UCAC2 positions to the observational epoch of individual 2MASS sources. Errors from proper motions are negligible here because of the small epoch difference between UCAC2 and 2MASS (≈ 1 to 2 years). The positional errors of UCAC2 are negligible in this comparison for stars in the R= 10 to 14.5
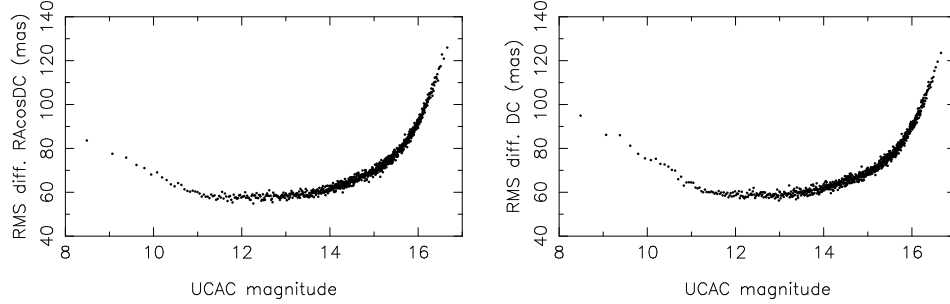
Figure 1.   RMS 2MASS−UCAC2 position differences as a function of magnitude for declination zone −40° to −30°, right ascension on the left, declination on the right. Other areas in the sky look very similar.
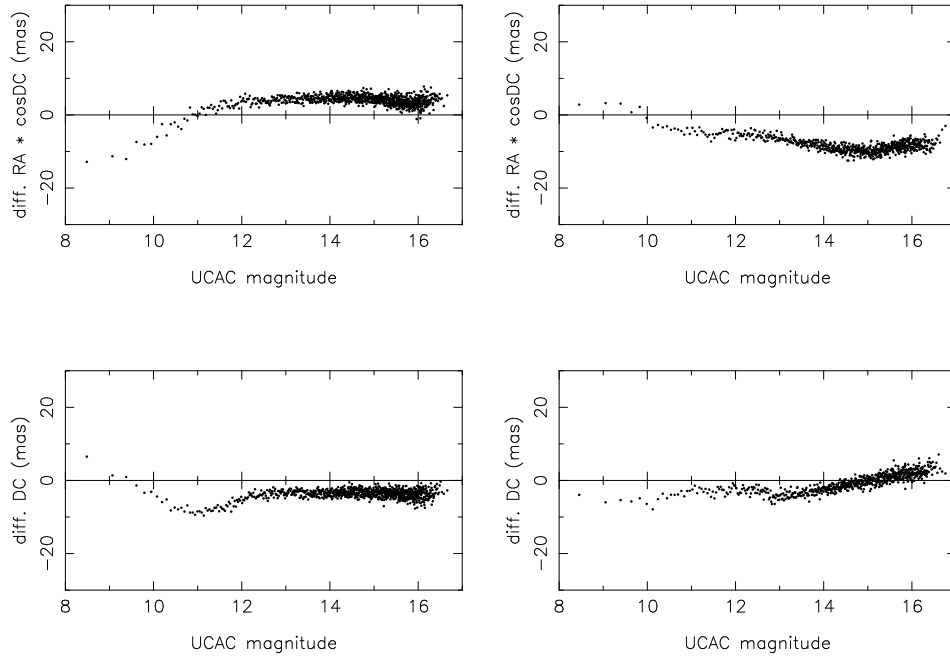
Figure 2.   2MASS−UCAC2 position differences as a function of magnitude for declination zones −40° to −30°, and +30° to +40°, on the left and right, respectively, Right Ascension on top, Declination below.

magnitude range (see Table 2). From internal estimates and comparisons with other catalogs, the expected positional errors in the 2MASS data is about 70 mas for $K_S = 4$ to 14.5, with larger errors for saturated and faint stars.

3. Results

3.1. Random Errors

Figure 1 shows the root-mean-square (RMS) differences between the 2MASS and UCAC2 positions. This and all following similar figures show binned data with one plotted point representing the mean over 5000 stars. This confirms the 2MASS average random position errors to be about 60 to 70 mas for the mid-magnitude range, independent of location in the sky. The increased scatter beyond R=15 is due to the decreasing signal-to-noise ratio of the UCAC2 data, conforming to 70 mas external errors per coordinate at R=16. The increased scatter at the bright end is caused by larger errors in both catalogs as compared to the mid-magnitude range. For these bright stars the error contributions from each catalog individually can not be separated without additional external data or assumptions.

3.2. Systematic Errors

Figure 2 shows the 2MASS−UCAC2 position differences as a function of UCAC magnitude (between V and R) for the same declination zones as Fig. 1. The results are similar for other areas in the sky, showing different patterns. Systematic differences are only on the 5 to 10 mas level and shows the high astrometric quality of both data sets. In particular, there is no significant (linear) magnitude equation between the 2 catalogs.

Figure 3 shows the position differences as a function of 2MASS J magnitude. The transition between the patterns for bright and faint stars ($\Delta\alpha$) is more pronounced for the J magnitude than the UCAC magnitude. The slight discontinuity is related to the 2MASS observations (see section 3.3).

Figure 4 shows the systematic differences as a function of color (UCAC2 r − 2MASS J), which are also in the 5 to 10 mas range. The slope (linear color equation) is generally less than 2.5 mas/mag, almost insignificant. The average offset of the $\Delta\alpha$ plot for the $-40°$ to $-30°$ zone (left hand side) is caused by the magnitude equation (see Fig. 3); it is not an effect of color.

Figure 5 shows the systematic position differences as a function of right ascension for the same declination zones as before. Using the same binning (5000) as before the larger scatter is obvious here. Similarly, Figure 6 shows the position differences as a function of declination, here for 2 slices along right ascension, 3 to 4 hours and 15 to 16 hours, respectively. The increased scatter near 8h and 16h in the $-30°$ to $-40°$ plots and near 6h and 20h in the $+30°$ to $+40°$ deg plots in Figure 5 is likely the result of increasing confusion in the Galactic Plane.

3.3. Read1 Errors

The 2MASS measurements of bright stars were derived from short 51 ms exposures (Read1), while those of fainter stars were derived from longer 1.3 sec
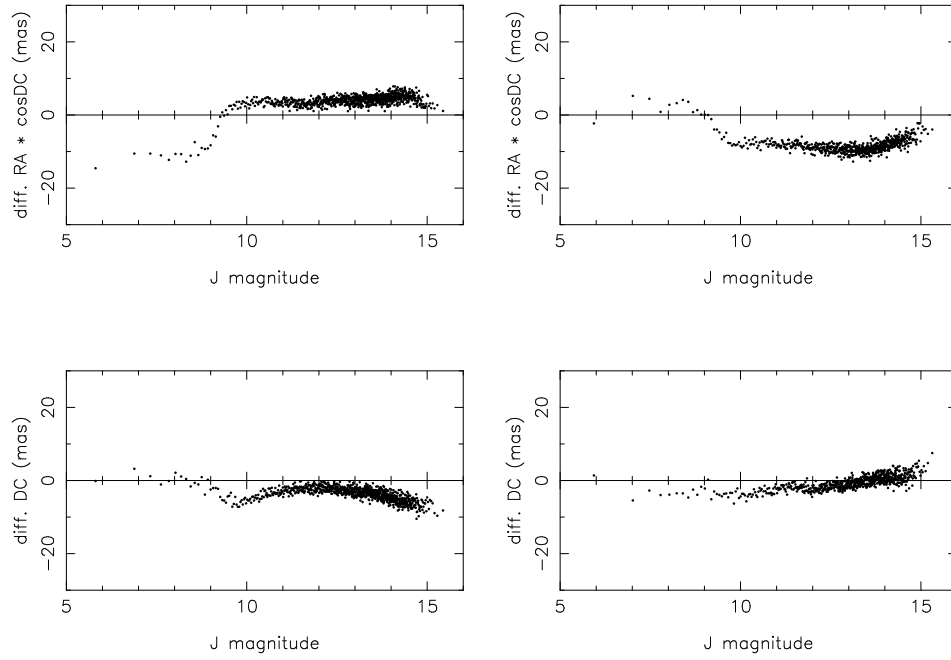
Figure 3.   2MASS−UCAC2 position differences as a function of 2MASS J magnitude for the same declination zones as before.
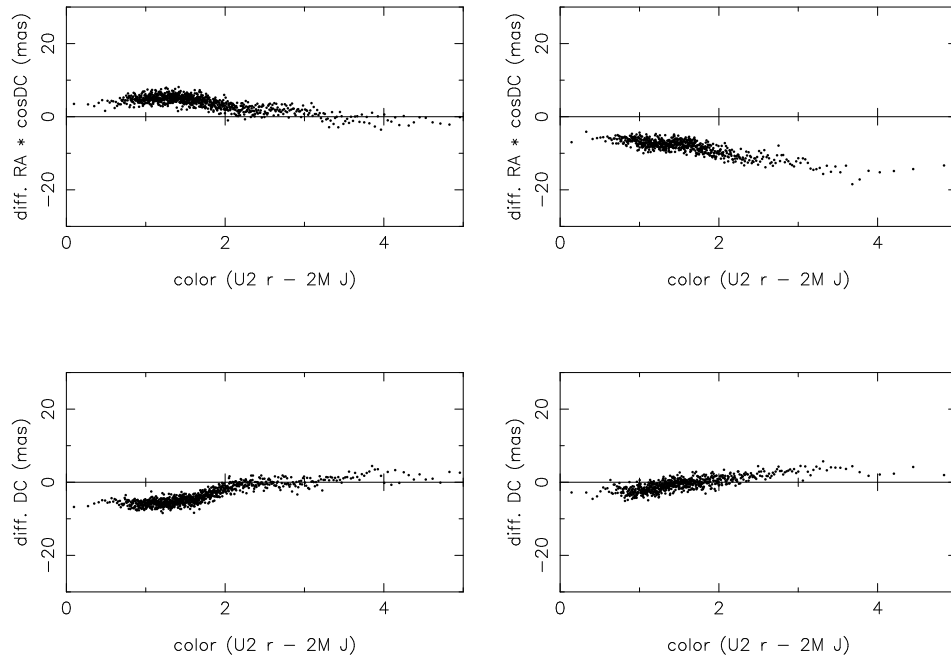
Figure 4.   2MASS−UCAC2 position differences as a function of color (UCAC r - 2MASS J) for the same declination zones as before.
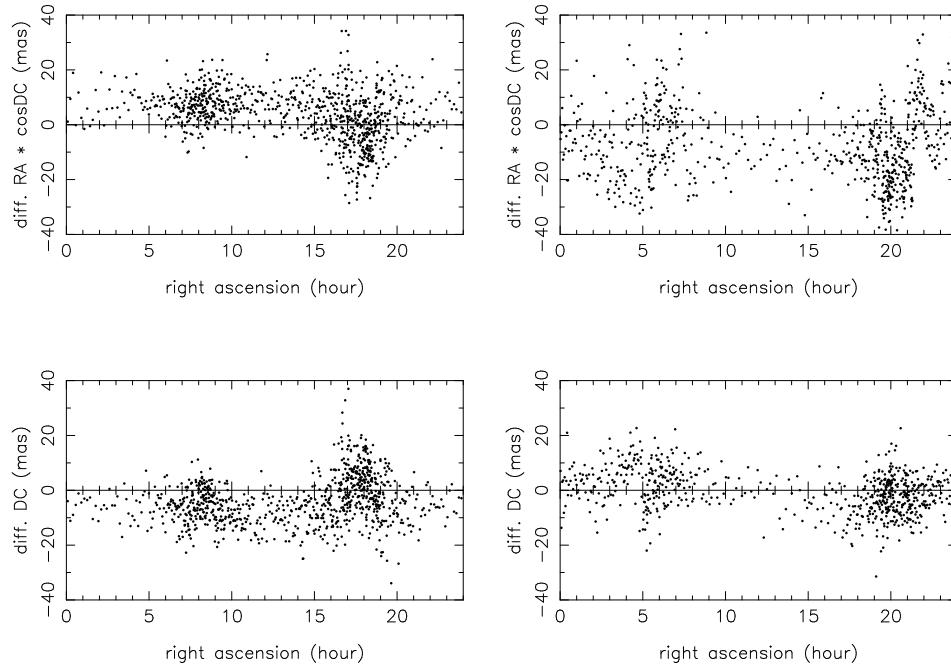
Figure 5.   2MASS−UCAC2 position differences as a function of right ascension for the same declination zones as before.
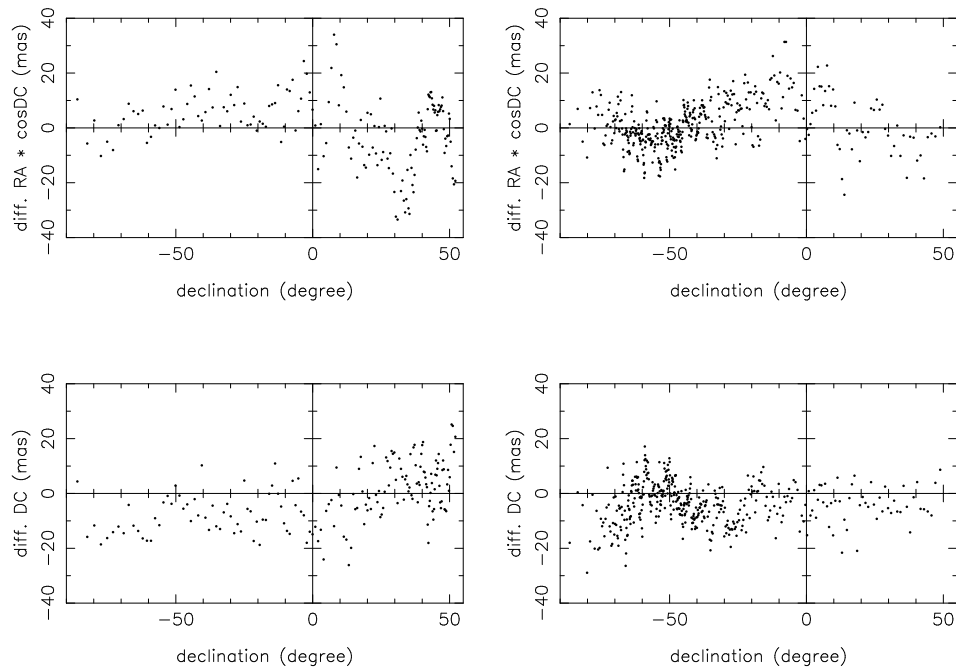
Figure 6.   2MASS−UCAC2 position differences as a function of declination for the Right Ascension = 3 to 4 h (left) and 15 to 16 h (right) slice.
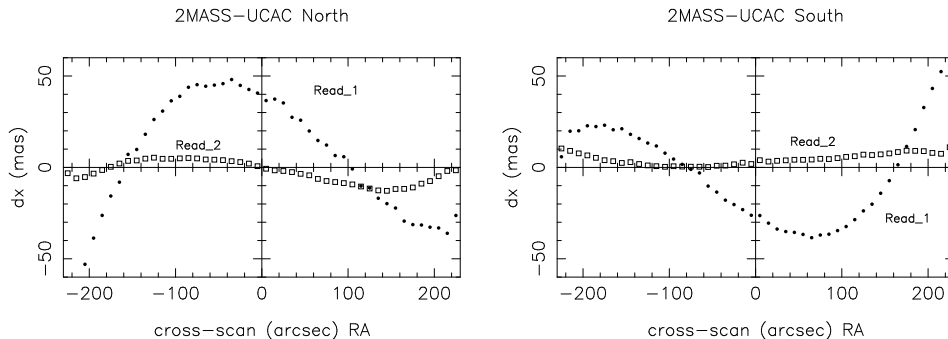
Figure 7.   Systematic errors of 2MASS positions as a function of cross-scan coordinate (RA) for "Read1" of bright stars. The "Read2" (long exposures) for most of the stars show small errors.

exposures (Read2). A field distortion effect was inadvertantly left uncorrected in the position reconstruction of the Read1 detections, resulting in a systematic error of about $\pm$ 50 mas for the x-coordinate (RA) as a function of cross-scan (RA) position, with a repeatable pattern for about every 500 arcsec. This is the single, largest systematic error contribution found in the 2MASS data.

4.   ICRF−2MASS Comparison

Out of the 708 ICRF plus extension 1 sources, 391 could be identified with 2MASS sources. These counterparts are generally very faint and the mean expected random error of the 2MASS positions is over 100 mas. Nevertheless this test provides a valuable system check at the faint end of 2MASS with a direct comparison to the ICRF. Table 3 gives the results. The mean offsets in the (ICRF−2MASS) position differences are small. For a 400 mas cut (of outliers), the standard error of the mean is 6.4 mas. Thus even the offset in RA (-9.1 mas) is only at the 1.5 sigma level, and not significant. A plot of these differences as a function of declination or magnitude does not reveal any systematic trends.

Table 3.   ICRF−2MASS position differences (mas).[a]

limit(mas)	ns	meanx	sigx	meany	sigy
200	302	-3.7	86	-0.7	87
300	350	-5.5	104	0.1	109
400	375	-9.1	124	0.2	124
500	391	-15.4	145	-2.5	139

[a] Results vary slightly as a function of the cut-off limit for outliers. ns gives the number of sources, mean and sig give the average position offset and scatter over all sources in the sample, for the x and y coordinate (RA, Dec), respectively. Unit is mas.

5. Conclusions and Summary

The 2MASS positions (at current epoch) are as precise as the UCAC2 positions at its faint end (r $\approx$ 16), which is about 70 mas per coordinate. For saturated and very faint 2MASS images the positional errors are about 100 to 150 mas. The 2MASS positions are more precise than the USNO A or B positions, which were derived from Schmidt plate scans, thus even benefiting optical astrometry, providing a dense (470 million stars), all sky net of reference stars. For stars in the r = 10 to 15 mag range, the UCAC is more accurate than the 2MASS by a factor of about 3.

Compared to UCAC2 the 2MASS positions show small systematic differences (5 to 10 mas) as a function of magnitude and color, with larger scatter as a function of RA and Dec. Either one of the catalogs might have true systematic errors on this level. The largest systematic error of about 50 mas is a function of cross-scan (RA) for bright images, which were observed with the "Read1" short exposures.

The 2MASS catalog is on the ICRF, with no significant offsets in its coordinates. It is also on the Tycho-2 system, consistent with the HCRF for bright stars. Systematic errors of 2MASS positions with respect to Hipparcos stars have not been investigated here. The strength of 2MASS astrometry (applications) will be at fainter than Hipparcos magnitudes. The extension of the ICRF into the infrared has become a reality!

References

Cutri, R.M, Skrutskie, M.F., Van Dyk, S, Beichman, C.A., Carpenter, J.M., Chester, T., Cambresy, L., Evans, T., Fowler, J., Gizis, J., Howard, E., Huchra, J., Jarrett, T., Kopan, E.L., Kirkpatrick, J.D., Light, R.M, Marsh, K.A., McCallon, H., Schneider, S., Stiening, R., Sykes, M., Weinberg, M., Wheaton, W.A., Wheelock, S., Zacharias, N.,2003, *Expl. Suppl. to the 2MASS All Sky Data Release*, http://www.ipac.caltech.edu/2mass/releases/allsky/doc/explsup.html

Høg, E., Fabricius, C., Makarov, V. V., Urban, S., Corbin, T., Wycoff, G., Bastian, U., Schwekendiek, P., Wicenec, A., 2000, A&A, 355, L27

Ma,C. & Feissel,M. (eds.) 1997, IERS Tech.Note 23, Paris

Skrutskie, M. F., Schneider, S. E., Stiening, R., Strom, S. E., Weinberg, M. D., Beichman, C., Chester, T., Cutri, R., Lonsdale, C., Elias, J., Elston, R., Capps, R., Carpenter, J., Huchra, J., Liebert, J., Monet, D., Price, S., Seitzer, P., 1997, in *The Impact of Large Scale Near-IR Sky Surveys*, Garzon, F., Epchtein, N., Omont, A., Burton, B., Persi, P., eds., Kluwer, p.25

Zacharias, N., Urban, S. E., Zacharias, M. I., Hall, D. M., Wycoff, G. L., Rafferty, T. J., Germain, M. E., Holdenried, E. R., Pohlman, J. W., Gauss, F. S., Monet, D. G., Winter, L., 2000, AJ, 120, 2131

Zacharias,N. et al. 2004, in preparation for AJ

Progress on Linking Optical-Radio Reference Frames Using CCD Ground-Based Telescopes

N.Maigurova, G.Pinigin, Yu.Protsyuk

Nikolaev Astronomical Observatory, Observatorna 1, Nikolaev, 54030 UKRAINE

R.Gumerov

Kazan State University, Kremlevskaya 18, Kazan, 420008 RUSSIA

Z.Aslan & I.Khamitov

Turkish National Observatory TUG, Antalya, 07058 TURKEY

W.Jin, Z.Tang, S.Wang

Shanghai Astronomical Observatory, Nandan Road 80, Shanghai, 200030 CHINA

Abstract.
Results of the Joint Project between observatories from China, Russia, Turkey and Ukraine on improvement of linking optical and radio reference frames are discussed. The 300 extragalactic radio sources (ERS) observation program is extended to $-40°$ declination. At present observations of more than 150 ERS were used. The intermediate internal estimation of the link between optical and radio reference frames showed rotation angles near zero within an accuracy of about 6 mas by using secondary reference stars from UCAC2. A comparison of results with other investigations was made.

1. Introduction

The link between optical (Hipparcos) and radio (ICRF) reference frames was realised in position within ±0.6 mas at the mean epoch 1991.25 and in rotation within 0.25 mas per year (Kovalevsky 1997). However, the accuracy of the Hipparcos-ICRF link degrades over time owing to the error in the Hipparcos proper motions. This is a reason for verification and refinement of the frame's link using different methods and telescopes (Zacharias *et al.* 1999; Stavinschi 2003).

The task of the Joint Project (JP) between astronomical observatories from China, Turkey, Russia and Ukraine is the refinement of optical / radio links with collaborating CCD telescopes (Tang *et al.* 2000, Pinigin *et al.* 2000). This paper describes briefly observation and reduction procedures, intermediate results and discusses linking parameters obtained by using of UCAC2 and USNO-B1.0 catalogs.
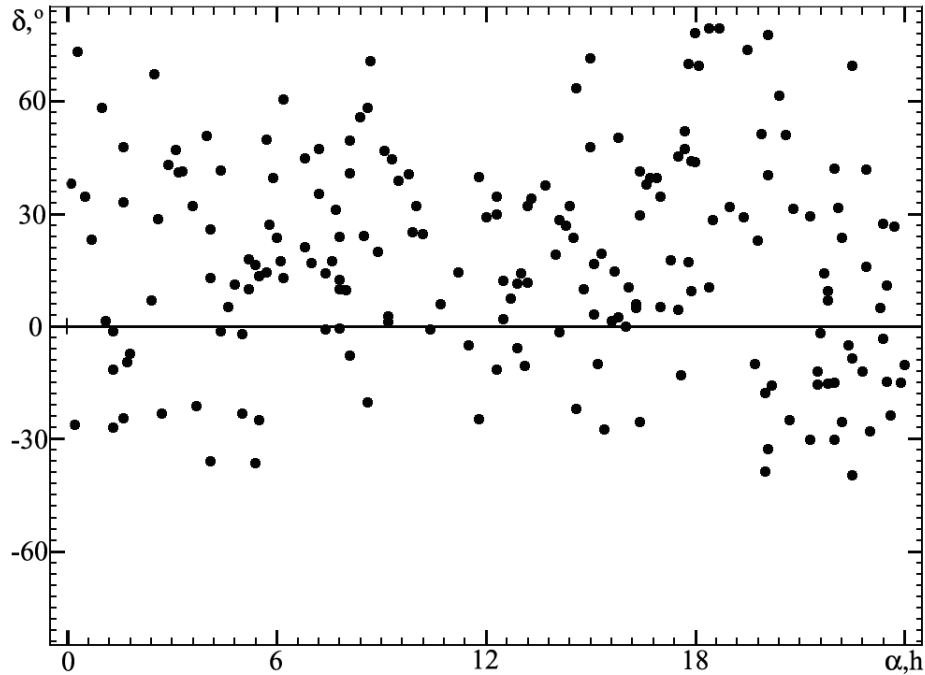
Figure 1.   Distribution of the ERS fields in right ascension and declination.

2.   Program and Instrumentation

The final co-operative program list includes about 300 ERS in the selected fields of the celestial sphere in the declination zone from $-40°$ to $+80°$ (Figure 1). There are about 200 ERS optical counterparts in the northern sky and 100 ERS in the southern sky. Several CCD telescopes of collaborating observatories taking part in the Joint Project are shown in Table l.

3.   Observation and Reduction

3.1.   Observation

Observations in China of 22 ERS in the Southern Hemisphere and optical positions determination relative to the UCAC1 were carried out. (Tang *et al.* 2000) Additionally, coordinates of 24 ERS observed in Yunnan observatory were obtained with internal accuracy of about 30 mas in both coordinates (Table 1).

Observations of 70 ERS with the RTT150 in Antalia and optical position determinations relative to the USNO-B1.0 were carried out with internal accuracy of 30 mas in right ascension and declination. Also, reductions of 14 ERS observed with a 2K×2K CCD were made using UCAC2 (Table 1).

3.2.   Reduction Methods and Results

Processing of the CCD images including dark, flat, and defect fields corrections, digital image filtration, identification of objects, and determination of coordinates for star-like objects (see Protsyuk 2000). To reduce measured CCD coordinates (X,Y) to tangential coordinates a process involving 6 constants was adopted.

Positions of about 150 ERS optical counterparts were obtained by CCD direct imaging mainly using the 1.0m Yunnan and RTT150 telescopes, with secondary reference stars of mainly magnitudes 14-18. More than 2000 CCD frames during 2000-2003 were treated. Every ERS field was observed an average of 6 times.

Table 1.   Collaborated CCD telescopes.

$Telescope$	ZA (Nikolaev, Ukraine)	AZT-8 (Kharkov, Ukraine)	1.0m Yunnan (Shanghai, China)	RTT150 (Antalia, Turkey)	
ϕ	$+47°$	$+50°$	$+31°$	$+36°$	
$Type$	refractor	reflector	reflector	reflector	
$D(mm)$	160	700	1000	1500	
$f(mm)$	2044	2819	13000	11700	
$CCD:$	ISD017A	ST-6	TI	ST-8[a]	Andor DW436
— $size, pixels$	$1040{\times}1160$	$375{\times}241$	$1024{\times}1024$	$1530{\times}1020$	$2K{\times}2K$
— $pixel, \mu m$	$16{\times}16$	$23{\times}27$	$24{\times}24$	$9{\times}9$	$13.5{\times}13.5$
— FOV/pix	$1''6$	$1''8{\times}2''1$	$0''37$	$0''16$	$0''24$
— FOV	$28'$x $31'$	$8'$x $10'$	$6'.5$ x $6'.5$	$4'$x $3'$	$8'$x $8'$
$Mode$ [b]	1,2	1	1	1	1,2
$Magnitude$	12^m - 15^m	15^m - 17^m	17^m-19^m	19^m-21^m	19^m-22^m
n_1 [c]	10	65	100	150	17
n_2 [d]			46	21	14
n_3 [e]			-	70	-

[a] Observed with two CCD readout
[b] Mode 1 - stare, Mode 2 - drift scan
[c] Number of observed ERS
[d] Number of ERS used in rotation angle calculation with respect to UCAC2
[e] Number of ERS used in rotation angle calculation with respect to USNO-B1.0

Differences $\Delta\alpha_{O-R}\cos\delta = (\alpha_O - \alpha_R)\cos\delta$ and $\Delta\delta_{O-R} = \delta_O - \delta_R$ are made from ERS optical and radio coordinates, respectively and their distributions are shown in Figure 2.
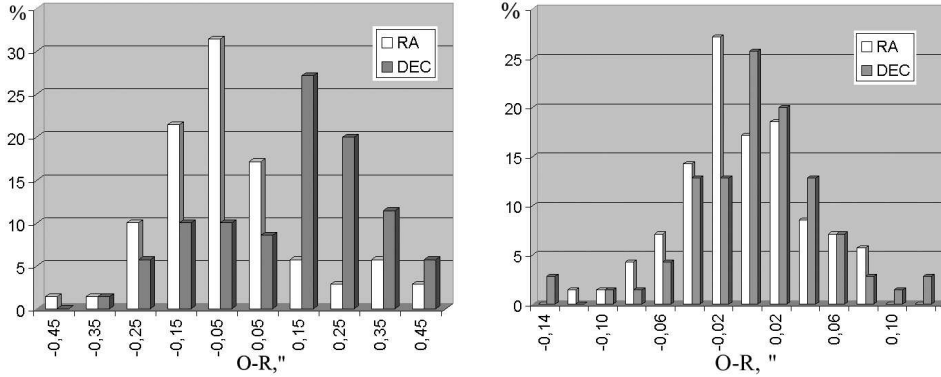
Figure 2. Distribution of differences between ERS coordinates in optical and radio ($\Delta\alpha_{O-R}\cos\delta$ (light) and $\Delta\delta_{O-R}$ (dark)) using USNO-B1.0 catalogue (left) and UCAC2 catalogue (right).

4. Determination of Preliminary Angles between Optical and Radio References Frames

Values of the angles between optical and radio reference frames corresponding with available observation were calculated by the formulas:

$$
\begin{aligned}
\Delta\alpha_{O-R}\cos\delta &= \omega_x \sin\delta\cos\alpha + \omega_y \sin\delta\sin\alpha - \omega_z \cos\delta, \qquad (1)\\
\Delta\delta_{O-R} &= -\omega_x \sin\alpha + \omega_y \cos\alpha,
\end{aligned}
$$

where: $\Delta\alpha_{O-R} = \alpha_O - \alpha_R$ and $\Delta\delta_{O-R} = \delta_O - \delta_R$ are differences in the coordinates of ERS in optical and radio reference frames; $\omega_x, \omega_y, \omega_z$ - rotation angles about the x, y, z axes, respectively.

Taking into account the small field size of the CCD frames of collaborating telescopes (Table 1) the first processing approach was made using the most numerous catalogue USNO-B1.0 (Monet *et al.* 2003). Some differences in positions between USNO-B1.0 and ICRF are possibly due to systematic errors including: position errors depending on star brightness, declination and regional differences in positions between ICRF and USNO-B1.0. Some other errors may be due to individual CCD frame reduction and possible structure problems of some ERS.

On the other hand, we used secondary reference stars of similar magnitudes (16 m-18 m) in comparison with selected ERS optical counterparts (Figure 3). So, corrections for brightness equation in $\Delta\alpha_{O-R}$ and $\Delta\delta_{O-R}$ are expected to be negligible.

For the first analysis the free term in declination was determined in two equations (1) for consideration of differences between USNO-B1.0 and ICRF. However the results of analysis show that the free term has obtained unreliable values and still remain unclear, as discussed also in Assafin *et al.* 2001 and Dario *et al.* 2000 for USNO-A2.0.

After taking into account all remarks, the values of the rotation angles were determined with accuracies of about 29 mas by using secondary reference stars from USNO-B1.0.
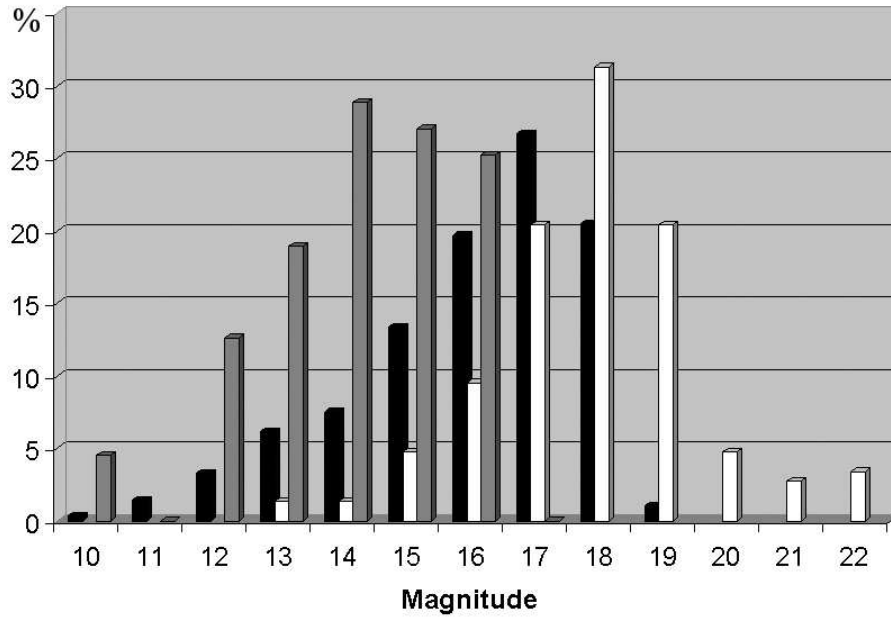
Figure 3.   Distribution of secondary reference stars from USNO-B1.0 (dark), UCAC2 (grey) and selected ERS (light) with magnitude.

Very promising results, which were determined recently with the new catalog UCAC2, are shown in Table 2. UCAC2 has the best accuracy in position nearly 20 mas for 10m to 14m and nearly 70 mas at 16m; in proper motion $1 - 3$ mas/yr to 12 m and $4 - 7$ mas/yr to 16m; it consists of about 48 millions stars in declination range from $-90°$ to $+52°$ (Zacharias 2003).

Very interesting results were determined by using UCAC2 and USNO-B1.0 for combined reduction of CCD frames with large $(8' \times 8')$ and small $(4' \times 3')$ size fields (see Table 2). For comparison in Table 2 the angles determined by different authors are given (Stone 1997; Stone 1998; Kumkova *et al.* 1995; Zacharias *et al.* 1999) It is to be noted on the basis of Table 2 that results obtained with UCAC2 are similar to the best. They have better than about 6 mas accuracy due to good secondary reference star positions of the UCAC2.

USNO-B1.0 is convenient and suitable for the reduction of CCD frames with small fields. By processing of available observations using of USNO-B1.0 complete investigations should be necessary. First estimation of rotational parameters by combined reduction showed accuracy of about 12 mas.

5.   Conclusions

1. At present observations of about 200 ERS made by collaborating Joint Project telescopes are available for reduction.
2. The best rotational parameters have been obtained in the system of more precise catalogs like the UCAC2 with an accuracy level of 6 mas.
3. Using small size CCD frames to determine precise linking parameters is

Table 2.   Optical-radio rotational parameters.

Source	Cat[a]	ω_x[b]	ω_y[b]	ω_z[b]	N[c]	σ_1[d]
Kumkova *et al.* (1995)	FK5	38±18	22±16	-17±16	78	-
Stone (1997)	FK5	3±5	25±5	16±4	689[e]	104
Stone (1998)	HC	-2.2±3.3	-2.2±3.4	3.3±2.9	689[e]	-
Zacharias *et al.* (1999)	ERL	-0.2±3.9	-5.4±3.9	-2.5±3.9	318	58
JP 2003	UCAC2	-13.1±6.1	2.7±6.2	6.7±4.9	81	39
JP 2003	UCAC2 + USNO-B1.0	-24±12	13±13	27±11	151	116

[a] Catalogue used as reference

[b] Rotation angles with their standard errors (in mas)

[c] Number of ERS sources in the solution

[d] Error of unit weight (in mas)

[e] Number of FK5 or HC stars, determined in the ICRF from CCD observations with the FASTT

possible by combining CCD observations with secondary reference stars from UCAC2 and USNO-B1.0 catalogs.

References

Assafin, M., Andrei, A., Vieira Martins, R., da Silva Neto, D., Camargo, J., Teixeira, R., Benevides-Soares, P., 2001, ApJ, 552, 380

Dario, N. Da Silva Neto, A., Andrei, A. et al, 2000, AJ, 119, 1470

Kumkova, I. I., Tel'Nyuk-Adamchuk, V. V., Babenko, Yu. G., Vertypolokh, O. A., 1995, in IAU Symposium. No 166 *Astronomical And Astrophysical Objectives of Sub-Milliarcsecond Optical Astrometry*, eds E.Hog, P.K.Seidelmann,383

Kovalevsky, J., 1997, Proceedings of the ESA Symposium 'Hipparcos-Venice 97', 13-16 May, Venice, Italy; ESA, SP-402 (July 1997)

Monet, D. Bird A., Canzian, B., Dahn, C., Guetter, H., Harris, H., Henden, A., Levine, S., Luginbuhl, C., Monet, A. K. B., Rhodes, A., Riepe, B., Sell, S., Stone, R., Vrba, F., Walker, R., 1998, USNO-A2.0 Catalog (Flagstaff: US Naval Observatory)

Monet, David G., Levine, Stephen E., Canzian, Blaise, Ables, Harold D., Bird, Alan R., Dahn, Conard C., Guetter, Harry H., Harris, Hugh C., Henden, Arne A., Leggett, Sandy K., Levison, Harold F., Luginbuhl, Christian B., Martini, Joan, Monet, Alice K. B., Munn, Jeffrey A., Pier, Jeffrey R., Rhodes, Albert R., Riepe, Betty, Sell, Stephen, Stone, Ronald C., Vrba, Frederick J., Walker, Richard L., Westerhout, Gart, Brucato, Robert J., Reid, I. Neill, Schoening, William, Hartley, M., Read, M. A., Tritton, S. B. 2003, USNO-B Catalog, AJ, 125, 984

Pinigin, G., Shulga, A., Maigurova, N., Protsyuk, Yu., Velichko, F., Fedorov, P. Jin, W., Tang, Z., Wang, S., Gumerov R., Bikmaev, I. 2000, in: "Kinematics and Physics

of Celestial Bodies, Suppl. Ser.", N3, Y.Yatskiv(ed.), Kiev, 59

Protsyuk, Y. 2000, Baltic Astronomy, 9, 554

Stavinschi, M. 2001, in: *"Extension and Connection of Reference Frames using CCD Ground-Based Technique"*, G.Pinigin (ed.), Atoll, Nikolaev, 29

Stone, R., 1997, AJ, 114, N2, 850.

Stone, R., 1998, ApJ, 506, 93

Tang, Z., Jin, W., Wang, S., Pinigin, G., Shulga, A., Maigurova, N., Protsyuk, Yu. 2000, In: IAU Colloquium 180, USNO, 57

Tang, Z., Wang, S., Jin W. 2002, AJ, 123, 125

Zacharias, N., Zacharias, M., Hall, D., Johnston, K., de Vegt, C., Winter, L., 1999, AJ, 118, 2511

Zacharias, N. 2003, UCAC2 (available on CD-ROM)

Extended emission structure in extragalactic sources

Patrick Charlot

Observatoire Aquitain des Sciences de l'Univers–CNRS/UMR 5804,
BP 89, 33270 Floirac, France

Abstract. The compact extragalactic radio-emitting objects used to define the International Celestial Reference Frame (ICRF) are only imperfect fiducial points in the sky on milliarcsecond scales. Many sources show frequency- and time-dependent extended emission structures with varied morphologies that are understood in the framework of unified theories of active galactic nuclei. Such theories are useful to make predictions about the expected source morphology at optical and infrared wavelengths. In the radio band, large imaging surveys conducted with Very Long Baseline Interferometry (VLBI) arrays are now available to evaluate the astrometric suitability of the sources on a statistical basis. Additionally, exploratory work is being carried out to correct for the effect of source structure in actual VLBI astrometric analyses by using hundreds of source maps obtained from VLBI structure monitoring. Recent progress in these areas are reviewed in the framework of future possible ICRF realizations.

1. Standard theories of active galactic nuclei

The International Celestial Reference Frame (ICRF) is defined based on positions of active galactic nuclei (AGN), a class of extragalactic objects located at the center of active galaxies and characterized by extremely compact and bright emission on milliarcsecond (mas) scales. These objects show various observational properties over the whole electromagnetic spectrum, ranging from radio to γ-ray energies, most of which are explained by unified theories of active galactic nuclei. According to the standard representation (Urry and Padovani 1995), illustrated in Fig. 1, the key elements of an active galactic nucleus are: a central supermassive black hole, an accretion disk, a broad-line region (fast-moving gas clouds) surrounded by a dusty torus region, an extended narrow-line region (slow-moving gas clouds), and, at least for radio-loud AGN, a pair of relativistically out-flowing jets which originate within a few tens of Schwarzschild radii from the black hole and eventually decelerate on larger scales. About 10% of AGN, the "radio-loud" objects, show strong radio emission, while the other 90% of AGN, the "radio-quiet" objects, show only weak or no radio emission.

Powerful relativistic jets emitting synchrotron radiation are a distinguishing feature of radio-loud objects although weaker or perhaps sub-relativistic jets may also exist in radio-quiet objects. The inner compact radio structure (usually defined as the source core) detected by Very Long Baseline Interferometry (VLBI) arrays, originates at the base of the jet where the optical depth is approximately unity. Depending on the jet power, outer radio emission may be observed at very large distances from the core (up to several megaparsecs for the
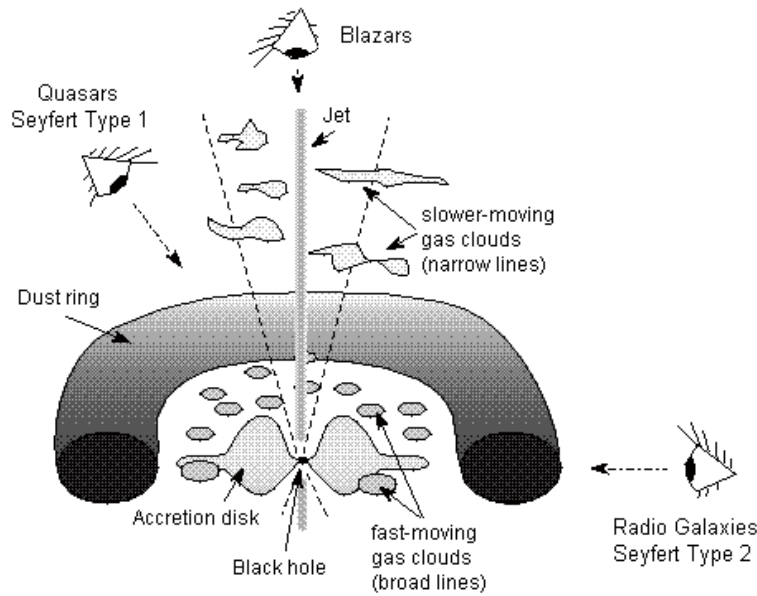
Figure 1.   Schematic drawing of the key elements of an active galactic nucleus with indication of AGN types according to viewing angle.

largest objects), although generally with a more diffuse appearance. Orientation has a major influence on observed properties of radio-loud AGN since relativistic beaming strongly amplifies kinematics and brightness for jets that are pointed towards us while it attenuates these for jets that are pointed away from us. As a result, most sources show a one-sided morphology with a dominant core component on VLBI scales due to sensitivity limitations and selection effects. AGN with jets viewed end-on are classified as blazars (either BL Lac objects or Optically Violently Variable quasars), while ordinary quasars are viewed at larger angles from the jet axis, and radio galaxies have jets more nearly in the plane of the sky (see Fig. 1). Blazars are characterized by strong variability, superluminal motions (observed apparent angular velocities up to ~ 1 mas/yr) and a one-sided morphology, whereas objects nearly in the plane of the sky have stable flux, subluminal motions, and a double or triple morphology. VLBI images of two such typical objects are shown in Fig. 2. Further VLBI images for other ICRF sources reveal a wealth of morphologies (Fey *et al.* 1996; Fey and Charlot 1997, 2000).

Thermal emission from the hot material in the accretion disk is observed at optical, ultraviolet and X-ray wavelengths. This radiation heats the dusty torus region which then re-radiates the absorbed energy in the infrared band. Orientation also largely affects source properties at these wavelengths. For transverse lines of sight, the absorbing material from the torus may obscure the inner parts of the system (accretion disk, broad-line region), thus leading to objects with extinguished nuclear continuum and only narrow lines (case of Seyfert Type 2 galaxies). Conversely, the full AGN system, including broad lines and bright nuclear continuum, may be observed at intermediate lines of sight (case of Seyfert Type 1 galaxies). Simulations are being carried out to predict the source ap-
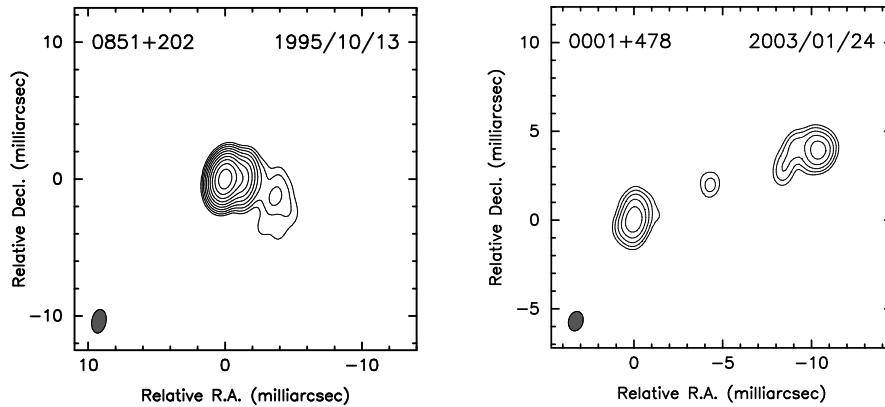
Figure 2. VLBI maps at 8 GHz of two typical active galactic nuclei with different morphology. *Left:* a one-sided core-jet structure oriented close to the line of sight in the BL Lac object 0851+202 (Fey and Charlot 1997). *Right:* a triple structure nearly in the plane of the sky in the compact symmetric object 0001+478 (Charlot *et al.* 2003).

pearance at these wavelengths depending on various parameters like the viewing angle of the disk/torus system or the relative disk-jet luminosity (Woillez and Sol 2003). Actual source structures, not yet detected because of insufficient resolution and sensitivity of existing telescopes, should be revealed in the near future by optical interferometers like the Very Large Telescope Interferometer (VLTI) and the Optical Hawaïan Array for Nanoradian Astronomy (OHANA). Just recently, initial mid-infrared VLTI measurements have succeeded for the first time in resolving the dusty torus of the AGN prototype NGC 1068 (ESO 2003). These indicate the existence of structures of approximately 30 mas in size, in agreement with the standard AGN model described above.

2.   Astrometric suitability of ICRF sources

As stated previously, active galactic nuclei show various morphologies on VLBI scales. For astrometry, the most suitable sources are those that are most compact on such scales, since extended emission introduces structural contributions in the measured VLBI group-delay quantities which degrade the position accuracy (Charlot 1990). By using 8 GHz and 2 GHz VLBI maps from the Radio Reference Frame Image Data Base (RRFID), Fey and Charlot (1997, 2000) investigated the astrometric suitability of a sample of 388 ICRF sources. They derived the average structural VLBI group-delay effect on Earth-bound baselines for each source and introduced a "Structure Index" as an indicator of the source quality. Values of the structure index range from 1 to 4 with increasing values indicating increasing average structural VLBI group-delay corrections on an approximately logarithmic scale. Structure index values of 1 and 2 point to excellent and good astrometric suitability, respectively, while values of 3 and 4 point to poor suitability (a given source may have differing structure index at 8 GHz and 2 GHz depending on the source structure at each frequency band).
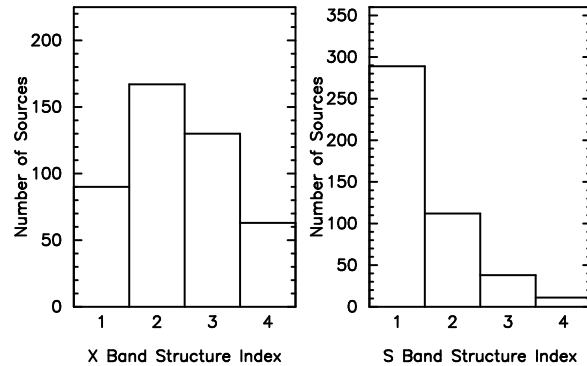
Figure 3.   The structure index distribution at 8 GHz (X band) and 2 GHz (S band) for 450 ICRF sources.

Based on this indicator, correlations between the observed radio structure and the astrometric position accuracy and stability of the sources were found. These correlations indicate that the more extended sources have larger position uncertainties and are less positionally stable than the more compact sources (Fey and Charlot 2000).

The current structure index distribution at 8 GHz and 2 GHz, now covering 450 ICRF sources (about 75% of the total number of ICRF sources), is shown in Fig. 3. Overall, 57% of the sources for which a structure index is available, have a value of either 1 or 2 at 8 GHz, indicating compact or very compact structure for these sources. At 2 GHz, intrinsic structural effects are found to be less significant (89% of the sources have a value of either 1 or 2), a consequence of the fact that the 2 GHz structure corrections are scaled down as a result of the dual-frequency group-delay calibration applied to eliminate propagation effects introduced by the ionosphere. As already pointed out by Fey and Charlot (2000), this analysis also reveals that, despite the stringency of the initial selection criteria, about one-third of the ICRF defining sources have a structure index of either 3 or 4, indicating that they are somewhat spatially-extended and thus may not be appropriate for defining the celestial frame with the highest level of accuracy. This suggests that revision of source categories would be mandatory for realization of a new ICRF.

The astrometric suitability of the sources may also be investigated for higher VLBI observing frequencies. On average, active galactic nuclei are expected to be more compact at higher radio frequencies since extended jet emission has a steep spectrum and thus usually weakens (with regard to the core brightness) as observing frequency increases. Regular VLBI astrometric and imaging observations at K band (24 GHz) and Q band (43 GHz) have been conducted since May 2002 by the VLBA K/Q Survey collaboration (Jacobs *et al.* 2003). These are dedicated to extend the ICRF in the 24–43 GHz range – a requirement for future deep space navigation – and to enlarge the list of VLBI calibrators available for phase-referencing at high-frequency. Based on the data acquired so far, a total of 108 sources have been successfully imaged at both 24 GHz and 43 GHz (Fey *et al.* 2003). This provides a reasonable source sample to evaluate astrometric suitability at these frequencies and to compare with corresponding
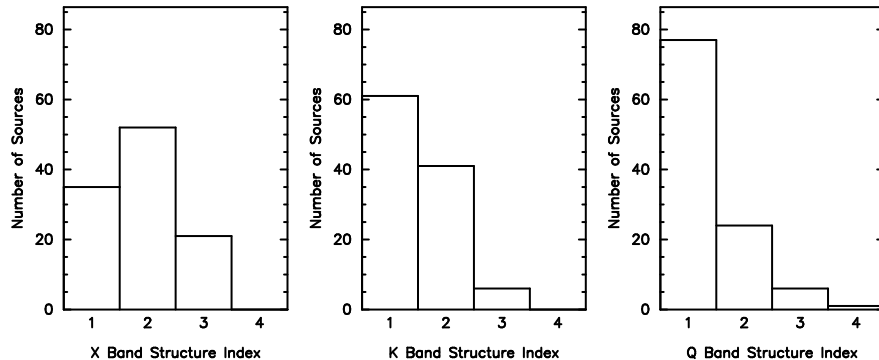
Figure 4.   The structure index distribution at 8 GHz (X band), 24 GHz (K band) and 43 GHz (Q band) for 108 ICRF sources.

source quality at 8 GHz. As shown in Fig. 4, the comparison of the structure index distribution for the three frequencies is striking, indicating a larger proportion of structure index values of 1 as observing frequency increases (32% at 8 GHz, 56% at 24 GHz, and 71% at 43 GHz). Hence, these initial results already suggest that the astrometric suitability of the sources is significantly better at 24 GHz and 43 GHz than at the standard 8 GHz geodetic observing frequency.

3.   Modeling source structure in VLBI analysis

While evaluation of source quality via the structure index indicator is useful for planning experiments and estimating the extra noise caused by extended emission structure in existing data, another approach is to model structural delays directly in actual VLBI observations. This requires identification of a truly kinematically-stable morphological feature for each source and calculation of corrections derived from structure maps for the measured VLBI group-delay quantities (Charlot 1990). Initial exploratory studies in this area showed that such modeling significantly improves the source positional stability and reduces the rms delay residuals for specifically-selected extended sources (see Charlot [2002] for a review of these results).

More recently, such exploratory studies have been extended to a much larger scale with a data set including 155 sources observed over up to 10 epochs spanning 1.5 year and a total of 800 RRFID maps to correct for source structure (Sovers *et al.* 2003). Table 1 shows the delay residual improvement as a function of structure index, indicating larger improvements for increased values of the structure index. These range from a few picoseconds (ps) for structure index 1 values to about 20 ps for structure index 4 values. For some sources with extended or fast-varying structures, improvements were as large as 40 ps. Overall, the weighted rms delay residuals were found to decrease by 8 ps in quadrature upon introducing source maps to model the structure delays. The angular equivalent of this improvement is approximately 0.1 mas for typical VLBI baselines and amounts to a significant fraction of the 0.25 mas systematic error of the ICRF, thus confirming that source structure does affect VLBI analysis even though it is not currently the dominant error.

Table 1.   Delay residual improvement ΔD (root-squared difference) versus X- and S-band structure index (XSI and SSI) from the analysis of Sovers *et al.* (2003).

XSI	N_{src}[†]	N_{obs}[‡]	ΔD (ps)	SSI	N_{src}[†]	N_{obs}[‡]	ΔD (ps)
1	35	72512	1.8	1	110	166509	3.8
2	66	92984	3.0	2	36	37281	7.0
3	35	31103	11.1	3	6	2564	18.5
4	16	9755	18.2	4	0	0	−
−	3	383	2.6	−	3	383	2.6
All	155	206737	4.5	All	155	206737	4.5

[†]Number of sources in each structure index category.
[‡]Number of observations for each structure index category.

The most notable success in application of structure modeling in the analysis of Sovers *et al.* (2003) was for the source 2200+420. This source was undergoing substantial changes at the time of the observations, which were captured in the ten successive maps (Fig. 5). The changes are mostly apparent at 8 GHz where the emission structure consists of two major components, whose relative position and strength varied significantly over the 1.5 yr span of the observations. Application of structure modeling based on these maps was found to dramatically improve the source positional stability, especially in declination where the RMS scatter was reduced by a factor of almost 3 (see Fig. 6). The source 2200+420 was also used as a test case to illustrate the crucial importance of the choice of the reference point in such studies (Charlot 2002). Most notably, it was found that the improvement in positional stability for 2200+420 can vary significantly depending on whether the position of the peak flux, centroid of emission, or northern structural component is used as reference point.

4.   Conclusion

Active galactic nuclei show complex radio morphologies which vary according to the jet power and the viewing angle of the emission structure. Although only a small portion is truly unresolved on milliarcsecond scales, about half of the ICRF sources that have been mapped so far are found to have relatively compact structure with good or excellent astrometric suitability. Imaging of the most southern ICRF sources is in progress (Ojha *et al.* 2003), so that individual source quality should be available for the entire ICRF in the near future.

Although it is not predominant for most of the sources, the effect of source structure is detectable from the data and may be modeled based on dual-frequency VLBI maps. The results of the first massive analysis incorporating such modeling show a slight improvement in the delay residuals as well as in source position stability. Detailed studies of time sequence of maps are important to locate invariant fiducial points within individual sources and further improve modeling. Future work should be targeted at lengthening the time base, which was limited to 1.5 yr in the analysis of Sovers *et al.* (2003), in order to investigate source structure errors on longer time scales.
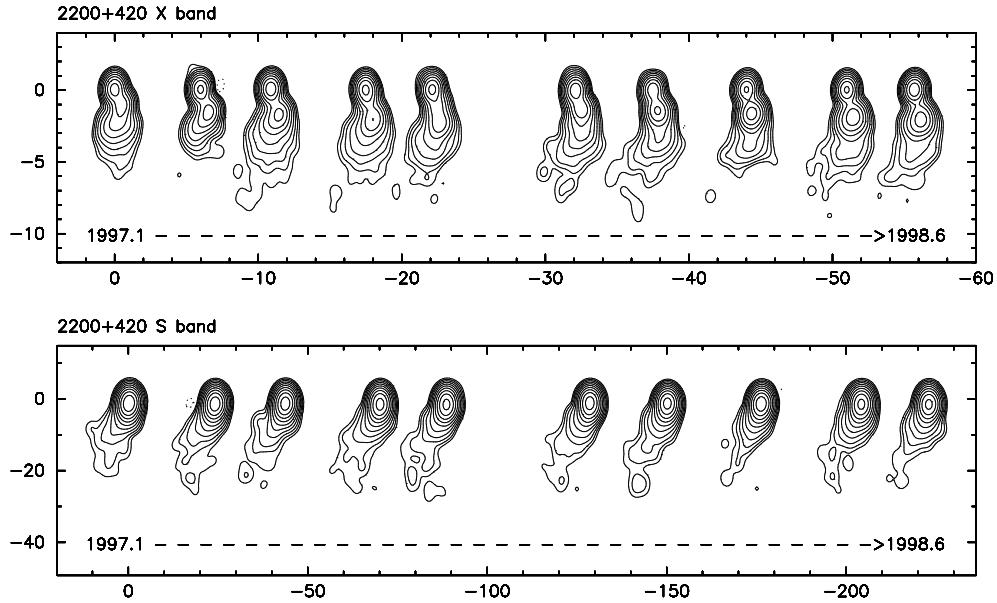
Figure 5.   RRFID VLBI images of 2200+420 at 8 GHz (upper panel) and 2 GHz (lower panel) for 10 successive epochs spanning the period 1997.1–1998.6. The maps are aligned horizontally according to the northern structural component (scale in milliarcseconds) and are spaced linearly according to their observing epochs.

In the coming years, the advent of large optical interferometers should reveal the morphology of extragalactic objects at optical wavelengths with similar resolution as that currently obtained in the radio band with VLBI measurements. Evaluation of the astrometric suitability of the sources in this range will be especially important in the framework of future space missions like GAIA which plan to measure the positions of extragalactic objects ultra-accurately, but will not be able to image the sources. Comparison of source structure at the two wavelengths will also be useful to determine whether the radio or optical band is best to define the most-stable fiducial reference directions for astrometry.
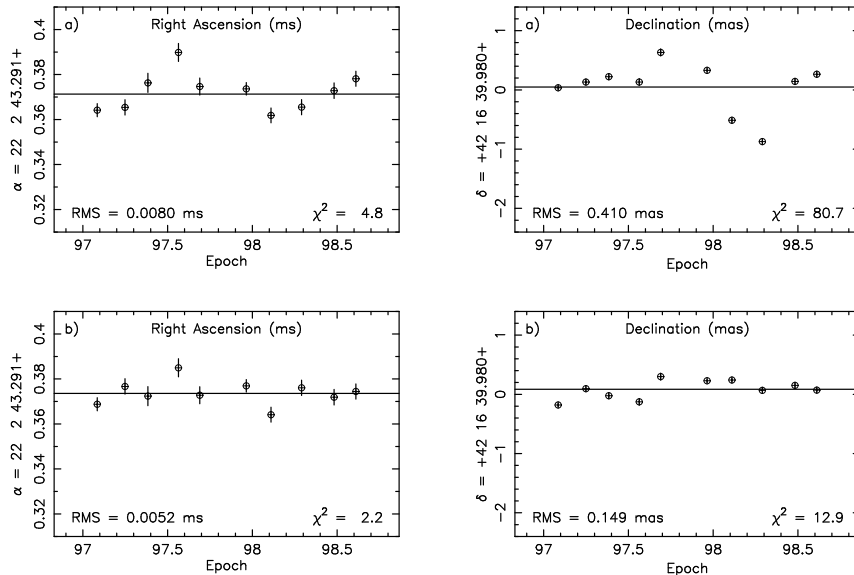
Figure 6.   Estimated right ascension and declination coordinates of 2200+420 for 10 successive epochs spanning the period 1997.1–1998.6: *a*) no source structure modeling; *b*) with source structure modeled. See Charlot (2002) for further details.

References

Charlot, P. 1990, AJ, 99, 1309

Charlot, P. 2002, in *International VLBI Service for Geodesy and Astrometry 2002 General Meeting Proceedings*, N. R. Vandenberg and K. D. Baver, NASA/CP-2002-210002, p. 233.

Charlot, P., Pradel, N., Lestrade, J.-F. 2003, in *Future Directions in High Resolution Astronomy: The 10th Anniversary of the VLBA*, eds. J. D. Romney & M. J. Reid, ASP Conf. Ser. (in press)

ESO 2003, ESO Press Release 17/03, 19 June 2003

Fey, A. L., Clegg, A. W., Fomalont, E. B. 1996, ApJS, 105, 299

Fey, A. L., Charlot, P. 1997, ApJS, 111, 95

Fey, A. L., Charlot, P. 2000, ApJS, 128, 17

Fey, A. L., Boboltz, D., Charlot, P., Fomalont, E. B., Lanyi, G. E., Zhang, L. D., KQ VLBI Survey collaboration 2003, this volume

Jacobs, C. S., Charlot, P., Gordon, D., Lanyi, G. E., Ma, C., Naudet, C. J., Sovers, O. J., Zhang, L. D., KQ VLBI Survey collaboration 2003, this volume

Ojha, R., Fey, A. L., Jauncey, D. L., Johnston, K. J., Dodson, R., Ellingsen, S. J., Nicolson, G. D., Quick, J., Reynolds, J. E., Tzioumis, A. 2003, this volume

Sovers, O. J., Charlot, P., Fey, A. L., Gordon, D. 2003, The Interplanetary Network Progress Report (in preparation)

Urry, C. M., Padovani, P. 1995, PASP, 107, 803

Woillez, J., Sol, H. 2003, A&A (in preparation)

Geophysical nutation model

Véronique Dehant

Royal Observatory of Belgium

Abstract. The nutation model that has been adopted by the IAU in 2000 is the semi-analytical model MHB2000 of Mathews et al. (2002, JGR 107(B4), DOI: 10.1028/ 2001JB000390). We show how robust this model is and examine the information about the interior of the Earth that has been derived. The observations used to derived the parameters of MHB2000 as well as the amplitude of the Earth Free Core Nutation (FCN) are examined in terms of their stability and precision. Additional contributions from the external geophysical fluids (atmosphere, ocean) are also studied and shown to be non-negligible.

Introduction

The nutation modeling has been improved during the last two decades. In particular, a new model based on a very precise rigid Earth nutation theory and a very efficient transfer function for the Earth has replaced the model that had been adopted by the IAU in 1980. The new model is explained in Section 1; in this section, we show that this model is very robust concerning the values of the geophysical parameters used. The robustness of the interpretation of the Very Long Baseline Interferometry (VLBI) data in terms of physics of the Earth's interior is studied in Section 2. The residuals between the recently adopted model and the new data have been analyzed and discussed in Section 3. Note that the present precision of nutation observation by VLBI is at the level of ten microarcsecond (μas) in the frequency domain and the milliarcsecond (mas) in the time domain (Herring *et al.*, 2002).

1. New adopted nutation model: IAU2000

The new model that has been adopted by the IAU, the IAU2000 model, is the model MHB2000 of Mathews *et al.* (2002). In order to reach the observed VLBI precision, as shown in Dehant *et al.* (1999), the rigid Earth nutation model must be very precise and the non-rigid Earth transfer function needs to include an accurate evaluation of very complex effects from the Earth's interior; in addition, the atmosphere and ocean effects should be considered. The rigid Earth nutation model considered for MHB2000 is based on the REN2000 model published by Souchay and Kinoshita (1996, 1997) and Souchay *et al.* (1999). But the other recent rigid Earth nutation models (Bretagnon *et al.*, 1997, 1998, Roosbeek and Dehant, 1998) also have a precision consistent with the observational precision; REN2000 has been considered for historical reasons. The transfer function for MHB2000 is computed from a semi-analytical approach in

which several geophysical parameters are fitted to the observations. It considers the resonances at four normal modes: (1) the Chandler Wobble (CW), (2) the Free Core Nutation (FCN), and the two additional modes due to the inner core: (3) the Free Inner Core Nutation (FICN) and (4) the Inner Core Wobble (see Mathews *et al.*, 1991, de Vries and Wahr, 1991, Dehant *et al.*, 1993, Legros *et al.*, 1993). The theory accounts also for the non-hydrostatic contributions to the global Earth dynamical flattening and to the core-mantle boundary flattening as done in Dehant and Defraigne (1997). Dissipation mechanisms are also considered in MHB2000, such as mantle inelasticity, and electromagnetic coupling at the core-mantle boundary and at the inner core boundary. Getino and Ferrandiz (1996) have used a generalized Hamiltonian approach to express the non-rigid Earth nutations. Their parameters are different with respect to those of MHB2000, but the idea of solving the problem globally is very valuable. The ocean tide effects on nutation are considered in MHB2000 as computed by Chao *et al.* (1996) at different retrograde diurnal frequencies. A scaling factor with respect to Chao *et al.* (1996) has been determined to be 0.97 by a least-squares fit. A seasonal effect, attributed to the combined effect of atmosphere and ocean, has also been determined by least squares fit. The obtained value is consistent with the value obtained from the atmospheric model (see Bizouard *et al.*, 1998).

The MHB2000 model has been constructed from fitting VLBI observations. However, as shown in Feissel-Vernier (2003), the radio-sources may not be as stable as was believed. These authors have found a better choice for the radio-sources considered to compute nutation and have shown that the amplitudes of the nutation may change at the level of a couple of tens of μas. As shown in de Viron *et al.* (1999), in de Viron and Dehant (2000, 2003), and in Yseboodt *et al.* (2002), the atmosphere may also play a role at frequencies other than the prograde annual frequency at the level of a few tens of μas. Even the effect of the atmosphere on the ocean might be important at retrograde diurnal frequencies (see de Viron *et al.*, 2001).

As shown in Dehant *et al.* (2002), even if there are uncertainties in the data (and we have taken 40 μas in agreement with the values given in the above paragraph), the parameters are rather well constrained within the limitations of the model. In particular, the FCN period can only change within half a day, and the FICN is in a range from 830 days to 1300 days. The Q factors are rather well constrained as well: between 19000 and 21500 for the FCN Q and between 520 and 1020 for the FICN Q.

2.   Analysis of the residuals

It is well known that the FCN free mode is excited at an observable level. There exist also contributions from the atmosphere at the prograde semi-annual (induced by the annual modulation of the S1 wave), and at the retrograde semi-annual (induced by the semi-annual modulation of the S1 wave and the resonance due to the proximity of the FCN).

Considering the strategy for taking the best sources into account in the computation of nutation, we have performed a comparison between the IAU2000 model and the new observations. The residuals have been analyzed using wavelet transformations and the results will be published (Dehant *et al.*, 2003). The

role of the atmosphere has particularly been emphasized in the frequency band corresponding to periods between the FCN period and very long periods, in both the retrograde and prograde parts of the spectrum. A 500-day peak has been observed in the VLBI residuals and has been related to the atmosphere. Energy found around 850 days has been particularly analyzed. The spectrum of the atmosphere is particularly flat in that frequency band. So, it is believed that this residual peak in VLBI data could be due to the excitation of the FICN as a free mode.

3. Conclusion and discussion

MHB2000 as adopted by the IAU in 2000 is very robust, in the sense that even if there are uncertainties in the observations or in the model considered, the physical parameters cannot be changed without introducing large deviations between the model and the observation.

Considering the above analysis, it is easy to derive some perspectives for research in nutation: (1) the atmospheric excitation should be considered not only at the prograde annual nutation but at all the frequencies relevant for atmospheric excitation; (2) the non-tidal oceanic excitation should be considered (the response of the ocean to the atmosphere), and (3) additional new coupling mechanisms (viscosity and topography) at CMB and ICB should be considered.

Residuals at the level of 20 μas have been interpreted (and may be interpreted) when the radio-sources are chosen according to a well-defined and well-studied strategy; in particular, we think that we have observed, in addition to the FCN free excitation, atmospheric contributions, and possibly the FICN free excitation.

References

Bizouard C., Brzezinski A., and Petrov S., 1998, Diurnal atmospheric forcing and temporal variations of the nutation amplitudes. *J. Geodesy*, 72, pp 561-577.

Bretagnon P., Rocher P., and Simon J.L., 1997, Theory of the rotation of the rigid Earth. *Astron. Astrophys.*, 319, pp 305-317.

Bretagnon P., Francou G., Rocher P., and Simon J.-L., 1998, SMART97: a new solution for the rotation of the rigid Earth. *Astron. Astrophys.*, 329, pp 329- 338.

Chao B.F., Ray R.D., Gipson J.M., Egbert G.D. , 1996, Ma C., Diurnal/semidiurnal polar motion excited by oceanic tidal angular momentum. *J. Geophys. Res.*, 101, pp 20151-20163.

Dehant V., Hinderer J., Legros H., and Lefftz M., 1993, Analytical approach to the computation of the Earth, the outer core and the inner core rotational motions. *Phys. Earth planet. Inter.*, 76, pp 259-282.

Dehant V. and Defraigne P., 1997, New transfer functions formulations of a non- rigid Earth. *J. Geophys. Res.*, 102, pp 27,659-27,688.

Dehant V., Arias F., Brzezinski A., Buffett B., Capitaine N., Carter W., Defraigne P., Dickey J., Eubanks M., Feissel M., Fliegel H., Fukushima T., Forte A., Gross R., Hartmann T., Herring T., Kinoshita H., Mathews P.M., McCarthy D., Melbourne J., Molodensky S., Roosbeek F., Salstein D., Sasao T., Soffel M., Souchay J., Vondrak J., Wahr J., Williams J., Yatskiv Y., and Zhu S.Y., 1999, Considera-

tions concerning the non-rigid Earth nutation theory. *Celest. Mech. Dynamical Astron.*, 72(4), pp 245-310.

Dehant V., Feissel-Vernier M., de Viron O., Ma C., Yseboodt M., and Bizouard C., 2002, Remaining error sources in the nutation at the sub-milliarcsecond level. *J. Geophys. Res.*, 108(B5), 10.1029/2002JB001763.

Dehant V., de Viron O., Feissel-Vernier M., Ma C., and Rivoldini A., 2003, A new free mode observed in Earth roation. in preparation.

de Viron O., Bizouard Ch., Salstein D., and Dehant V., 1999, Atmospheric torque on the Earth rotation and comparison with atmospheric angular momentum variations. *J. Geophys. Res.*, 104, B3, pp. 4861-4875.

de Viron O. and Dehant V., 2000, Earth's rotation and high frequency equatorial angular momentum budget of the atmosphere. *Survey Geophys.*, 20, 6, pp. 441-462.

de Viron O., Ponte R.M., and Dehant V., 2001, Indirect effect of the atmosphere through the oceans on the Earth's nutation by the torque approach. *J. Geophys. Res.*, 106(B5), pp 8841-8851.

de Viron O. and Dehant V., 2003, 2002, Test on the validity of the Atmospheric Torques on Earth computed from model outputs. *J. Geophys. Res.*, 108(B2), 10.1029/2001JB001196.

de Vries D. and Wahr J.M., 1991, The effects of the solid inner core and nonhydrostatic structure on the Earth's forced nutations and Earth tides. *J. Geophys. Res.*, 96, B5, pp 8275-8293.

Feissel-Vernier M., 2003, Selecting stable extragalactic compact radio sources from the permanent astrogeodetic VLBI program. *Astron. Astrophys.*, 403, pp 105-110.

Getino J. and Ferrandiz, J.M., 1996, Canonical treatment of dissipative forces between Earth core and mantle. In: *Proc. IAU Symposium No 172, Paris, France, 'Dynamics, Ephemeris and Astrometry of the Solar System'*, eds. Ferraz-Mello, Sylvio, Morando, Bruno, Arlot, Jean-Eudes, pp 233-238.

Herring T.A., Mathews P.M., and Buffett B., 2002, Modeling of nutation-precession of a non-rigid Earth with ocean and atmosphere. *J. Geophys. Res.*, 107(B4), DOI: 10.1029/2001JB000165.

Legros H., Hinderer J., Lefftz M. and Dehant V., 1993, The influence of the solid inner core on gravity changes and spatial nutations induced by luni-solar tides and surface loading. *Phys. Earth planet. Inter.*, 76, pp 283-315.

Mathews P.M., Buffett B.A., Herring T.A. and Shapiro I.I., 1991, Forced nutations of the Earth: Influence of inner core Dynamics. I. Theory. *J. Geophys. Res.*, 96, B5, pp 8219-8242.

Mathews P.M., Herring T.A., and Buffett B.A., 2002, Modeling of nutation and precession: new nutation series for nonrigid Earth and insights into the Earth's interior. *J. Geophys. Res.*, 107(B4), DOI:10.1029/2001JB000390.

Roosbeek F. and Dehant V., 1998, RDAN97: an analytical development of rigid Earth nutation series using the torque approach. *Celest. Mech. Dynamical Astron.*, 70, pp 215-253.

Souchay J. and Kinoshita H., 1996, Corrections and new developments in rigid Earth nutation theory: I. Lunisolar influence including indirect planetary effects. *Astron. Astrophys.*, 312, pp 1017-1030.

Souchay J. and Kinoshita H., 1997, Corrections and new developments in rigid Earth nutation theory: II. Influence of second-order geopotential and direct planetary effect. *Astron. Astrophys.*, 318, pp 639-652.

Souchay J., Loysel B., Kinoshita H., and Folgueira M., 1999, Corrections and new developments in rigid Earth nutation theory: III. Final tables 'REN-2000 including crossed-nutation and spin-orbit coupling effects. *Astron. Astrophys.*, 318, pp 639-652.

Yseboodt M., de Viron O., Chin T.M., and Dehant V., 2002, Atmospheric excitation of the Earth nutation: Comparison of different atmospheric models. *J. Geophys. Res.*, 107(B2), 10.1029/2000JB000042.

IAU-IUGG Working Group on Non-rigid Earth Nutation Theory

Véronique Dehant

Royal Observatory of Belgium

Aleksander Brzeziński

Space Research Centre of the Polish Academy of Sciences

Abstract. The International Astronomical Union (IAU) and the International Union of Geodesy and Geophysics (IUGG) created the IAU-IUGG Working Group on Non-rigid Earth Nutation Theory. This group recommended a replacement model for the IAU 1980 Nutation Model that is consistenet with observations and geophysical theory. Its contributions are discussed, and areas for future research are outlined.

1. Introduction

The model adopted by the IAU in 2000 for nutation concerns the long-period motion (longer than two days) of a conventional pole in space. This model provides part of the set of Earth orientation parameters (EOP) used to relate a terrestrial reference frame to a celestial reference frame (and conversely). These EOPs include polar motion (PM), precession-nutation (PN), and the rotation angle related to the the Earth's rotation (see IERS Conventions 2003, McCarthy and Petit 2003). As recommended by the IAU 2000 resolutions, PM is the motion of the Celestial Intermediate Pole in a terrestrial frame, at all frequencies except the retrograde diurnal (which corresponds to the long-period nutations in space). Precession and nutation are long-periodic motions of the Celestial Intermediate Pole in space, restricted to periods above two days. The Celestial Intermediate Pole (CIP) defines the direction of a conceptual axis describing the same motion as the Earth's z-axis in space for long periods (more than two days), and the same motion as the space-fixed Z-axis inside the Earth except for the retrograde motion of quasi-diurnal periods. The adopted nutation model is very accurate and close to Very Long Baseline Interferometry (VLBI) observations. Although we know that there are uncertainties at the level of a few tens of microarcseconds, the geophysical parameters on which this model is based are very robust within the frame of the model considered (see Dehant *et al.*, 2002). For more details see the paper of Dehant (2003) in this volume.

2. Background

The IAU-IUGG Working Group on Non-rigid Earth Nutation Theory (WG) was in charge of transforming the classical expressions of precession and nutation in longitude and in obliquity into the motion (the X- and Y-coordinates) of the CIP in space, as well as of considering the concept of Non-Rotating Origin and the associated corrections (the s-term) in agreement with the IAU 2000 resolutions. This has been done by Capitaine *et al.* (2003a, 2003b, and 2003c).

The WG also evaluated the contributions to polar motion forced by the gravitational attraction of the Moon and the Sun on the Earth. The classical nutation computation is related to the gravitational coupling between the Earth and the Moon or the Sun; this involves the degree 2-order 0 Earth mass distribution (the J_2 term) and the degree 2-order 1 luni-solar gravitational potential (tidal potential). If this gravitational coupling is generalized, all the coupling between all the coefficients of the Earth mass distribution, expressed in terms of the Earth gravitational potential (the Stokes coefficients C_{nm}, S_{nm}), and all the degrees and orders of the luni-solar tidal potential (degree ℓ, order k) should be included. In Table 1, we have summarized the coupling considered (column 1 is for the geopotential coefficients, and column 2, for the tidal potential coefficients), and the related periods in space (column 3, entitled "precession nutation") and in a terrestrial frame (column 4, entitled "polar motion"), as well as the maximum amplitudes of polar motion (column 5). Note that in the conventional representation each component shown in Table 1 can be equivalently treated either as nutation or as polar motion. We marked by the asterisks the choice demanded by the recently adopted definition of the CIP.

Table 1.   Perturbations in the equatorial component of Earth rotation due to gravitational coupling on the Earth.

geo-potential	tidal potential	precession nutation	polar motion	amplitude (μas)
$C_{\ell 0}\ \ell \geq 2$	$V_{\ell 1}$	long period*	retrograde diurnal	$> 10^7$
C_{31}, S_{31}	V_{30}	prograde diurnal	long period*	91
C_{41}, S_{41}	V_{40}	prograde diurnal	trend*	6 μas/yr
C_{22}, S_{22}	V_{21}	prograde semidiurnal	prograde diurnal*	52
C_{32}, S_{32}	V_{31}	prograde semidiurnal	prograde diurnal*	0.2
C_{33}, S_{33}	V_{32}	prograde terdiurnal	prograde semidiurnal*	0.1
C_{31}, S_{31}	V_{32}	retrograde diurnal	retrograde semidiurnal*	0.8
C_{32}, S_{32}	V_{33}	retrograde semidiurnal	retrograde terdiurnal*	0.1

*From this table, it can be seen that there are additional terms to be considered in the long period polar motion (second and third lines of the table, after the classical long-period nutation), and that the triaxiality of the Earth should be considered (fourth line of the table). Both effects are at the level of a few tens of μas (microarcseconds). The other contributions are below one μas.

A few works have already considered triaxiality. Kinoshita (1977) has established that the triaxiality of the Earth gives rise to a semi-diurnal nutation, but he decided that it was too small at the level of precision considered at that time. Chao *et al.* (1991) considered triaxiality of the Earth as well, and have added the non-rigidity of the Earth. They called this effect the "prograde diurnal libration" contributing to polar motion. But, they did not consider terms in lunisolar forcing with $\ell > 2$ because this forcing is proportional to $(1/60)^\ell$ for the Moon and $(1/2500)^\ell$ for the Sun, which was then too small. However, it appears that when computing the corresponding effect in polar motion this decrease of the forcing is compensated by the CW resonance.

In the rigid Earth nutation theory SMART97 (Bretagnon *et al.*, 1997, 1998), REN2000 (Souchay and Kinoshita, 1996, 1997, Souchay *et al.*, 1999), and RDAN97 (Roosbeek and Dehant, 1998), the complete spectrum of subdiurnal nutations was estimated. Brzeziński (2001) and Brzeziński and Capitaine (2002) have then considered the Liouville equation with the assumption that the liquid core is not coupled to the mantle, while accounting for the observed CW period and quality factor. Mathews and Bretagnon (2003) have considered the Liouville equation for an ellipsoidal Earth with a liquid core (the approach of Sasao *et al.*, 1981) and with a frequency dependent mantle rheology. Previously, Getino *et al.* (2001), Escapa *et al.* (2002a) and Escapa *et al.* (2002b) had considered the effect of the triaxiality in the Hamiltonian approach, both for rigid and non–rigid models. Van Hoolst and Dehant (2002) have considered all second order effects in the small quantities and have included triaxiality in the Liouville equations for computing the effects of triaxiality on the normal modes and the transfer function for PM and nutation in the case of an ellipsoidal Earth with a liquid outer. Finally, Brzeziński and Mathews (2002) have published the model that was adopted in the IERS Conventions 2003 (McCarthy and Petit 2003).

3. Future

The perspectives for future research in this frame have been identified:

1. The atmosphere and related ocean effects should be better taken into account; they should be considered either as time varying contributions to some of the nutation periods or in the time domain;

2. The strategy foreseen by Feissel-Vernier (2003) for VLBI data based on more stable radio-sources should be considered;

3. New coupling mechanisms at the core boundaries should be considered, such as viscous coupling;

4. The coupling between the three components of the Earth rotation should be considered (effect of the LOD variations on the nutations, see Souchay and Folgueira 1999);

5. The free mode excitations by the atmosphere, the ocean or any other phenomena should be considered (this is particularly the case for the FCN and the FICN, which are important for nutation).

The excitation of the free modes by the atmosphere (or any other geophysical cause) is important for nutation. The adopted model considers the FCN free mode amplitude and phase (see Herring *et al.*, 2002). Recent developments (Dehant *et al.*, 2003) have shown that the FICN free mode could be a possible explanation for the residuals between the observation and the adopted model. These free modes cannot yet be predicted.

The WG considered that the influence of core triaxiality on the forced solution could be important and consequently wanted to compute the effects on the prograde diurnal polar motion. However, there is no commonly accepted value for the equatorial flattening of the core, nor for its effects on the nutations (2.5 μas according to Escapa *et al.* (2002) versus 1 μas according to Mathews and Bretagnon (2003)). The WG decided to disregard these core-flattening corrections (already small) for the IERS Conventions, leaving it for further research. Rotational symmetry of the core is thus assumed for the nutation and polar motion contributions considered because the models of topography at the CMB derived from seismology or from mantle dynamics are not precise enough, and because the contribution of the core triaxiality is very small.

The relative amplitudes of the atmosphere, ocean, and these coupling terms for the prograde diurnal components are compared in Table 2, where the largest contributions (greater than 10 μas) are shown in bold. For simplicity we give in this table only the coefficients of sin(arg) and cos(arg) of the x-component of polar motion, designated x_s, x_c, respectively. For the prograde harmonic terms shown in Table 2, the corresponding coefficients for the y-component can be computed as $y_s = -x_c, y_c = x_s$.

Table 2.   Amplitudes of the different effects on prograde diurnal polar motion.

Tides	Ocean tide contribution in μas		Atmospheric contribution in μas		Tidal gravitation in μas	
	x_s	x_c	x_s	x_c	x_s	x_c
Q_1	6.2	**26.3**			−2.3	1.3
O_1	**48.8**	**132.9**			−11.4	6.5
P_1	**26.1**	**51.2**	−0.6	1.2	−4.8	2.7
S_1	−0.6	−1.2	5.2	−4.9		
K_1	**−77.5**	**−151.7**	−1.4	−0.7	**14.3**	−8.2
ψ_1	−0.6	−1.2	0.5	−0.5		

4.   Conclusion

In conclusion, we can summarize the work, the conclusions, and the results of the WG with the following:

- The IAU2000 (MHB2000, Mathews *et al.*, 2002) is very robust within the frame of the model considered;

- The conversion of the $\Delta\psi$ and $\Delta\epsilon$ (using the non-rotating origin formalism) in terms of (X, Y) has been computed;

- Improvements are still necessary in the computation of the atmosphere and (non-tidal) ocean effects on nutation;

- In the future, it will be necessary to account for the differential rotation of the inner core, liquid core and mantle, and to account for other coupling at the core-mantle boundary and at the inner core boundary, such as the viscous coupling;

- The FCN and FICN free modes cannot be predicted, and therefore need to be observed;

- The model of polar motion equivalent to diurnal and subdiurnal nutations has been computed;

- Long period polar motion (due to the coupling between C_{31}, S_{31} and V_{30} and to the coupling between C_{41}, S_{41} and V_{40}) and prograde diurnal polar motion (due to triaxiality) are important and should be considered when the precision is below 10 μas.

References

Bretagnon P., Rocher P., and Simon J.L., 1997, Theory of the rotation of the rigid Earth. *Astron. Astrophys.*, 319, pp 305-317.

Bretagnon P., Francou G., Rocher P., and Simon J.-L., 1998, SMART97: a new solution for the rotation of the rigid Earth. *Astron. Astrophys.*, 329, pp 329- 338.

Brzeziński A., 2001, Diurnal and subdiurnal terms of nutation: a simple theoretical model for a nonrigid Earth. In: *Proc. Journées Systèmes de Référence Spatio-temporels 2000*, ed. N. Capitaine, Paris Observatory, pp 243-251.

Brzeziński A. and Capitaine C., 2002, Lunisolar perturbations in Earth rotation due to the triaxial figure of the Earth: geophysical aspects. In: *Proc. Journées Systèmes de Référence Spatio-temporels 2001*, ed. N. Capitaine, Paris Observatory, pp 51-58.

Brzeziński A. and Mathews P.M., 2002, Recent advances in modeling the lunisolar perturbation in polar motion corresponding to high frequency nutation: Report on the discussion of the IAU Commission 19 WG on Nutation. In: *Proc. Journées Systèmes de Référence Spatio-temporels 2002*, eds. N. Capitaine and M. Stavinschi, Ars Docendi, Paris, pp 101-108.

Capitaine, N., Chapront, J., Lambert, S., and Wallace, P., 2003a, Expressions for the Celestial Intermediate Pole and Celestial Ephemeris Origin consistent with the IAU 2000A precession- nutation model. *Astron. Astrophys.*, 400, pp 1145- 1154.

Capitaine, N., Wallace, P. T., and McCarthy, D. D., 2003b, Expressions to implement the IAU 2000 definition of UT1. *Astron. Astrophys.*, 406, pp 1135- 1149.

Capitaine, N., Wallace, P. T., and Chapront, J., and 2003c, Expressions for IAU 2000 precession quantities. *Astron. Astrophys.*, in press.

Chao B.F., Dong D.N., Liu H.S., and Herring T.A., 1991, Libration in the Earth's rotation. *Geophys. Res. Letters*, 18(11), pp 2007-2010.

Dehant V., Feissel-Vernier M., de Viron O., Ma C., Yseboodt M., and Bizouard C., 2002, Remaining error sources in the nutation at the sub-milliarcsecond level. *J. Geophys. Res (Solid Earth)*, 108(B5), 10.1029/2002JB001763.

Dehant V., de Viron O., Feissel-Vernier M., Ma C., and Rivoldini A., 2003, A new free mode observed in Earth roation. in preparation.

Escapa A., Getino J., and Ferrandiz J.M., 2002a, Indirect effect of the triaxiality in the Hamiltonian theory for the rigid Earth nutations. *Astron. Astrophys.*, 389, pp 1047-1054

Escapa A., Getino J., and Ferrandiz J.M., 2002b, Influence of the triaxiality of the non–rigid Earth on the J_2 forced nutations. In: *Proc. Journées Systèmes de Référence Spatio-temporels 2001*, ed. N. Capitaine, Paris Observatory, pp 275-280.

Feissel-Vernier M., 2003, Selecting stable extragalactic compact radio sources from the permanent astrogeodetic VLBI program. *Astron. Astrophys.*, 403, pp 105- 110.

Getino J., Ferrandiz J.M., Escapa A., 2001, Hamiltonian theory for the non-rigid Earth: Semidiurnal terms. *Astron. Astrophys.*, 370, pp 330-341.

Herring T.A., Mathews P.M., and Buffett B., 2002, Modeling of nutation-precession of a non-rigid Earth with ocean and atmosphere. *J. Geophys. Res.*, 107(B4), DOI: 10.1029/2001JB000165.

Kinoshita H., 1977, Theory of the rotation of the rigid Earth. *Celest. Mech.*, 15, pp 277-326.

Mathews P.M., Herring T.A., and Buffett B.A., 2002, Modeling of nutation and precession: new nutation series for nonrigid Earth and insights into the Earth's interior. *J. Geophys. Res.*, 107(B4), DOI:10.1029/2001JB000390.

Mathews P.M. and Bretagnon P., 2003, Polar motions equivalent to high frequency nutations for a nonrigid Earth with anelastic mantle. *Astron. Astrophys.*, 400, pp 1113-1128

McCarthy D. and Petit, G. (eds.), 2003, IERS Conventions 2003, *IERS Technical Note*, in press; also available at `http://maia.usno.navy.mil/`.

Roosbeek F. and Dehant V., 1998, "RDAN97: an analytical development of rigid Earth nutation series using the torque approach.", *Celest. Mech. Dynamical Astron.* 70, pp 215-253.

Sasao T., Okubo S., and Saito M., 1980, A simple theory on the dynamical effects of a stratified fluid core upon nutational motion of the Earth. In: *Proc. IAU Symposium No. 78*, eds. E.P. Federov, M.L. Smith, and P.L. Bender, D. Reidel, Norwell, Mass., pp 165-183.

Souchay J. and Kinoshita H., 1996, Corrections and new developments in rigid Earth nutation theory: I. Lunisolar influence including indirect planetary effects. *Astron. Astrophys.*, 312, pp 1017-1030.

Souchay J. and Kinoshita H., 1997, Corrections and new developments in rigid Earth nutation theory: II. Influence of second-order geopotential and direct planetary effect. *Astron. Astrophys.*, 318, pp 639-652.

Souchay J., Loysel B., Kinoshita H., and Folgueira M., 1999, Corrections and new developments in rigid Earth nutation theory: III. Final tables 'REN-20004 including crossed-nutation and spin-orbit coupling effects. *Astron. Astrophys.*, 318, pp 639-652.

Souchay J. and Folgueira M., 1999, The effect of zonal tides on the dynamical ellipticity of the Earth and its influence on the nutation. *Earth Moon Planets*, 81, pp 201-216.

Van Hoolst T., Dehant V., 2002, Influence of triaxiality and second-order terms in flattenings on the rotation of terrestrial planets: I. Formalism and rotational normal modes. *Phys. Earth planet. Inter.*, 134, pp 17-33.

Practical Consequences of the Improved Precession-Nutation Models

Patrick T. Wallace

Space Science & Technology Dept., CLRC / Rutherford Appleton
Laboratory, Chilton, Didcot, OX14 4HH, United Kingdom

Abstract. The IAU 2000 precession-nutation models are classical in form, unlike the associated Earth rotation model. The counterpart of GST in the new system is "Earth Rotation Angle", which is directly proportional to UT1 and is reckoned with respect to a kinematically-defined "non-rotating origin", the CEO. Though essential for interpreting Earth-rotation at VLBI accuracies and simplifying the computation of (h, δ), the introduction of the CEO has aroused considerable controversy. The new models came into use for VLBI analysis at 2003 January 1, and subsequent IERS Bulletins provide $(\delta X, \delta Y)$ relative to the IAU 2000 celestial pole in addition to the existing $(\delta\Delta\psi, \delta\Delta\epsilon)$ corrections to IAU1976/80. The almanac offices face interesting choices of how to present the new quantities and which, if any, of the existing tabulations can be omitted. Most astronomers will, however, be little affected. In parallel with developing the new canonical models, considerable efforts have been made also to provide classical equivalents of similar accuracy, to give users a choice of when (or whether) to adopt the new methods. The models, both new and classical, have been implemented as Fortran subroutines and published through the IERS website. An extended set of routines has been released through the IAU SOFA initiative.

1. The IAU 2000 Precession-Nutation Models

1.1. The Celestial Pole

New precession-nutation models were adopted by the IAU in 2000 (Resolution B1.6). The models are classical in form, comprising a $(\Delta\psi, \Delta\epsilon)$ nutation series and corrections to the precession rates in longitude and obliquity with respect to the IAU 1976 precession. The pole to which they refer is the Celestial Intermediate Pole (CIP), defined such that the models contain no terms of period less than two days. In addition to the precession rate adjustments and the classical nutation series, the models include a fixed offset of about 18 mas with respect to the ICRS pole, the "frame bias". The IAU 1980 obliquity is retained.

The full precession-nutation model, designated IAU 2000A, contains a nutation series of almost 1400 terms. An abridged version, designated IAU 2000B, has fewer than 80 nutation terms (McCarthy and Luzum 2003). The accuracy of the models is limited by free core nutation (FCN) effects: these cannot be predicted long in advance and set a natural "noise floor". FCN apart, 2000A delivers accuracy below the VLBI uncertainties, currently about 200 μas; the much shorter 2000B model delivers 1 mas accuracy.

The definitive form of the IAU 2000A precession-nutation model is the Fortran code MHB2000 (Mathews et al. 2002). The International Earth Rotation and Reference Systems Service (IERS) also provides, as a derived product, series that generate the (X, Y) coordinates of the CIP directly, with frame bias, precession and nutation all taken into account (Capitaine *et al.* 2003a).

1.2.   Earth Rotation and the Origin of Right Ascension

Though classical in form, the IAU 2000 precession-nutation model does not include a corresponding expression for Greenwich Sidereal Time. Earth rotation is instead provided for by the adoption of a linear formula that links Universal Time (UT1) to the "Earth Rotation Angle" (ERA). This is complemented by a new zero-point for stellar longitudes called the Celestial Ephemeris Origin (CEO). The CEO is kinematically defined, and in the "new paradigm" there is no ecliptic or equinox.

To many astronomers, the introduction of the CEO, a "non-rotating origin" (Guinot 1979), is the most controversial aspect of the new paradigm. Because the equinox is *geometrically* defined, how it is located on the sky is easy to grasp. It seems perfectly natural to draw the equator and ecliptic on a diagram of the celestial sphere and to use their intersection to define the zero point of right ascension.[1] The CEO, on the other hand, is defined kinematically, and a diagram of the celestial sphere shows only the equator and a point on it: the CEO is defined in terms of how it moves from moment to moment, and its initial placement is essentially arbitrary. Most astronomers find this concept difficult at first.

A related difficulty is that agreement on nomenclature for CEO-based stellar longitudes has yet to be reached. Some authors insist that the term "right ascension" be reserved for cases where the zero-point is an equinox, which is not the case for the new paradigm, while others feel that as the longitude zero point in ICRS coordinates is not an equinox and yet the term "ICRS right ascension" is well-established, it is natural to call CEO-based longitudes "right ascensions".

2.   Implementing the IAU 2000 Models

The definitions adopted by the IAU in 2000 were only a starting point, and a number of choices and ambiguities had to be resolved before astronomers could be provided with a suite of practical implementations. For full details see Capitaine *et al.* (2003a, 2003b, 2003c).

2.1.   Pole

The MHB 2000 algorithm implements the frame bias and precession-rate adjustments as nutation terms, fixed and linearly growing respectively, with respect

---

[1]However, defining *precisely* what is meant by the equator and equinox is not so easy. In particular, there are two slightly different definitions of the ecliptic. One is based on the slowly changing direction of the orbital angular momentum vector of the Earth-Moon barycenter (EMB) in inertial space, while the other is based on the slowly tilting plane of the EMB orbit around the Sun. See Standish (1981).

to the Lieske *et al.* (1977) precession. This is a straightforward and practical approach, allowing the new models to be applied easily to existing procedures. However, it is not rigorously correct, because the frame bias and precession are applied in mean coordinates of date when they should be applied in J2000 coordinates.[2] Furthermore, the IAU resolutions do not stipulate which of the Lieske *et al.* precession angles to use. The familiar ζ, z, θ formulation is not the only choice, and the limited resolutions of the polynomial coefficients means that the different choices lead to significantly different answers. Finally, the IAU 2000 definitions do not specify the third frame bias angle, namely the ICRS longitude of the J2000 mean equinox. In order to define IERS implementations, Capitaine *et al.* (2003a) made the following choices:

- The frame bias and precession-rate adjustments are not implemented as nutation terms. Instead, the classical form of the transformation from celestial coordinates to mean coordinates of date is written as the product of the three individual rotation matrices for frame bias, precession and nutation respectively.

- Using lunar laser ranging results, an estimate was made of the third frame bias angle, and a conventional value of $\delta\alpha_0 = -14.6$ mas was adopted. (This equinox offset has only a second-order effect on the final transformation between celestial and terrestrial coordinates, and is canceled by a corresponding fixed term in the new Greenwich Sidereal Time expression.)

- In order that the MHB 2000 precession-rate adjustments could be applied directly to specific Lieske *et al.* (1977) angles, a four-rotation precession formulation, using the angles ϵ_0, ψ_A, ω_A and χ_A, was adopted.

Note that the introduction of a frame bias stage, the appearance of a constant term in the GMST expression and the use of the 4-angle precession formula are all new.

2.2. Rotation

The IAU resolutions adopted a conventional formula linking Earth Rotation Angle and Universal Time and stipulated that there be no jump in UT1 at the beginning of 2003, when the new paradigm was to come into operation. These constraints had the unexpected result of fixing the CEO at J2000, removing any need to debate the relative merits of different starting-points. Similar considerations allowed a new expression linking UT1 and Greenwich Mean Sidereal Time to be developed unambiguously. The new formula for GMST uses the ERA as a basis, a function of UT1 alone, with additional terms that come from precession and hence are functions of TDB (or TT, near enough).

2.3. The CEO

The most obvious departure in the new paradigm is the elimination of the ecliptic and hence the equinox, and the introduction of a new zero-point for "right

---

[2]The rate adjustment is itself a compromise, since it leads to a precession theory which is not dynamically consistent (see Capitaine *et al.* 2003c).

ascension". This was necessary in order to decouple precession-nutation of the pole from Earth rotation, facilitating studies of each phenomenon by simplifying the theory and by eliminating (or at least greatly reducing) crosstalk effects. The purity of the ERA formula in comparison with the GST expression is perhaps the most conspicuous sign that the new paradigm does represent a simplification.

3.   Practical Consequences

The advantanges of the new paradigm are not compelling for the majority of existing astronomers, who would like access to the improved accuracy but without the need to change their existing practices. It should also be borne in mind that all existing text-books use the classical approach, and a considerable re-education program would be needed to effect a complete changeover.

It was consequently essential to provide parallel support for both the classical paradigm and the new paradigm, with equivalent accuracy in both cases. Given that these tools now exist, whether the classical system eventually dies out becomes a matter of secondary importance, and the transition, if it occurs, will take many years.

Of course, having two systems in operation brings its own dangers. For example, ERA and Sidereal Time may be confused, so that a classical right ascension is inadvertently used in conjunction with ERA, or a CEO-based right ascension is used in conjunction with a Sidereal Time. A partial solution to this is to limit the use of CEO-based celestial coordinates, keeping them out of sight as an intermediate stage in transforming between terrestrial and celestial coordinates. Just as mean places are already in decline, with stellar positions now given exclusively as ICRS coordinates, perhaps we will see apparent places (e.g. for planets) replaced by astrometric places.

3.1.   IERS Products

The new models came into official use for VLBI analysis at 0h TT on 2003 January 1. Careful preparations (see Capitaine *et al.* 2003b) meant that at this instant the old and new determinations of UT1 agreed precisely.

A new variant of IERS Bulletin B provides CIP offsets $(\delta X, \delta Y)$ with respect to the IAU 2000A pole. The old Bulletin B, which provides offsets in $(\Delta \psi, \Delta \epsilon)$ with respect to the IAU 1976/80 pole, will continue until at least the end of 2004, and for a subsequent period that depends on demand.

3.2.   The Astronomical Almanac

The groups producing astronomical almanacs are faced with a number of tasks in order to introduce the IAU 2000 changes:

- The new classical models have to be implemented and their effects propagated throughout the publications.

- The precision improvements that are a benefit of the new models call for increased numbers of digits in some of the tabulations, affecting layout.

- Numerical examples and explanatory material have to be modified or rewritten. This is made more difficult by the uncertainties and controversies surround nomenclature for the new concepts.

- There are new quantities to be tabulated (such as ERA) and choices to be made (Should s be tabulated? Would ICRS right ascension of the CEO be useful?).

The costs of the exercise are considerable, consuming a significant fraction of the available effort over several years.

3.3. Consequences for Astronomers

Many astronomers will see the changes simply in the form of slight differences in almanac numbers. Others will require new tools, especially software, so that they can adopt the IAU 2000 changes in their own applications. This has happened in the past as models were improved; what sets the IAU 2000 resolutions apart is that some of them amount to a change of paradigm, as we have already seen. Can astronomers be persuaded that the changes are beneficial, or at least harmless?

The first requirement was to provide software (and algorithms) to support the old and new approaches in parallel. The new, CEO-based, algorithms are definitive, but classical equivalents of equal accuracy for all practical purposes have been developed from them.

The second requirement has been to make the improved classical software compatible with previous software, ideally so that the user simply has to change the name of the subroutine being called. There are unfortunately a number of unavoidable exceptions to this:

- The frame bias is a new step in the precession-nutation transformation. It can of course be neglected if ~ 20 mas accuracy is good enough, much as zonal distortions in star catalogs were often neglected in the past.[3]

- The s' component at the "polar motion" stage is new. However, this can be neglected for all but the most demanding applications.

- The need to supply TT as well as UT1 to the GMST expression changes the subroutine call (though UT1 can simply be supplied twice if the resulting 100 μas errors can be tolerated).

Perhaps the key element in bringing the improved algorithms to classical users painlessly is to remove any need to understand the new paradigm in order to benefit from the improved accuracy. To a large extent this is a matter of considerate subroutine interface design.

---

[3]It might be thought that the extra step could be absorbed into the usual ζ, z, θ precession algorithm, but this turns out not to be so. For previous precession models, those angles tended to zero close to epoch, but in the new model they undergo rapid changes; this makes a polynomial representation impractical.

4.   Software Implementations

The algorithms that realize the IAU 2000 resolutions are set out in the IERS Conventions 2000. Associated software implementations are provided through the IERS website, derived from products developed for the IAU SOFA initiative. Additionally the NOVAS software (Kaplan 1989) now uses IAU 2000 models.

   SOFA (Standards Of Fundamental Astronomy), is an IAU initiative to provide authoritative implementations of standard algorithms for fundamental astronomy (Wallace, 2002). Under the supervision of an international panel called the SOFA Review Board, the initiative has developed a library of Fortran subroutines. The SOFA library at present comprises 69 astronomy routines supported by 52 vector/matrix routines. IAU 2000 precession-nutation and Earth rotation accounts for nearly a third of the 121 routines. The classical (equinox-based) and new (CEO-based) approaches are both supported, and the design of the library offers great flexibility, from single-call end-to-end transformations to low-level building-blocks.

   The IERS Conventions 2000 website provides 15 Fortran subroutines supporting the IAU 2000 resolutions. Two of these are the canonical IAU 2000A and 2000B precession-nutation codes, while the remaining 13 routines provide the definitive models for X, Y, s, s', ERA, GST (GMST and the Equation of the Equinoxes), the 2000A and 2000B nutation models and a selection of useful rotation matrices. As for SOFA, the routines cater for users of both both the classical paradigm and the new paradigm.

   The IERS routines are self-contained as far as their fundamental-astronomy algorithms are concerned, but call vector/matrix utility functions from the SOFA library. The IERS routines were released at a time when the SOFA routines were awaiting formal ratification by the Review Board, but are in essence identical; users are recommended to migrate to the equivalent SOFA routines in due course.

5.   The Old and New Paradigms Compared

One way to compare the old and new paradigms is to consider the transformation from a star's ICRS catalog coordinates to Greenwich hour angle and declination using both methods. This is shown schematically in Figure 1.

   For both the old and the new methods, the first steps are the same, namely taking the catalog data for the star—the ICRS position (α, δ) and proper motion (μ_α, μ_δ), the parallax and the radial velocity—and, knowing the barycentric position and velocity of the observer, predicting the line of sight to star in the Geocentric Celestial Reference System (GCRS). At this stage, either the classical, equinox-based, transformation (left-hand stream) or the new, CEO-based, transformation (right-hand stream) can be used to rotate the coordinate axes into (GHA, δ).

   The classical method involves more steps, which to anyone implementing the transformation from scratch means more opportunity for errors of order and omission. Frame bias, precession and nutation must be applied in that order to obtain true (α, δ); the final z-rotation to (h, δ) requires GST, the sum of GMST (strictly a function of both UT1 and TDB) and the Equation of the Equinoxes (a function of TDB).
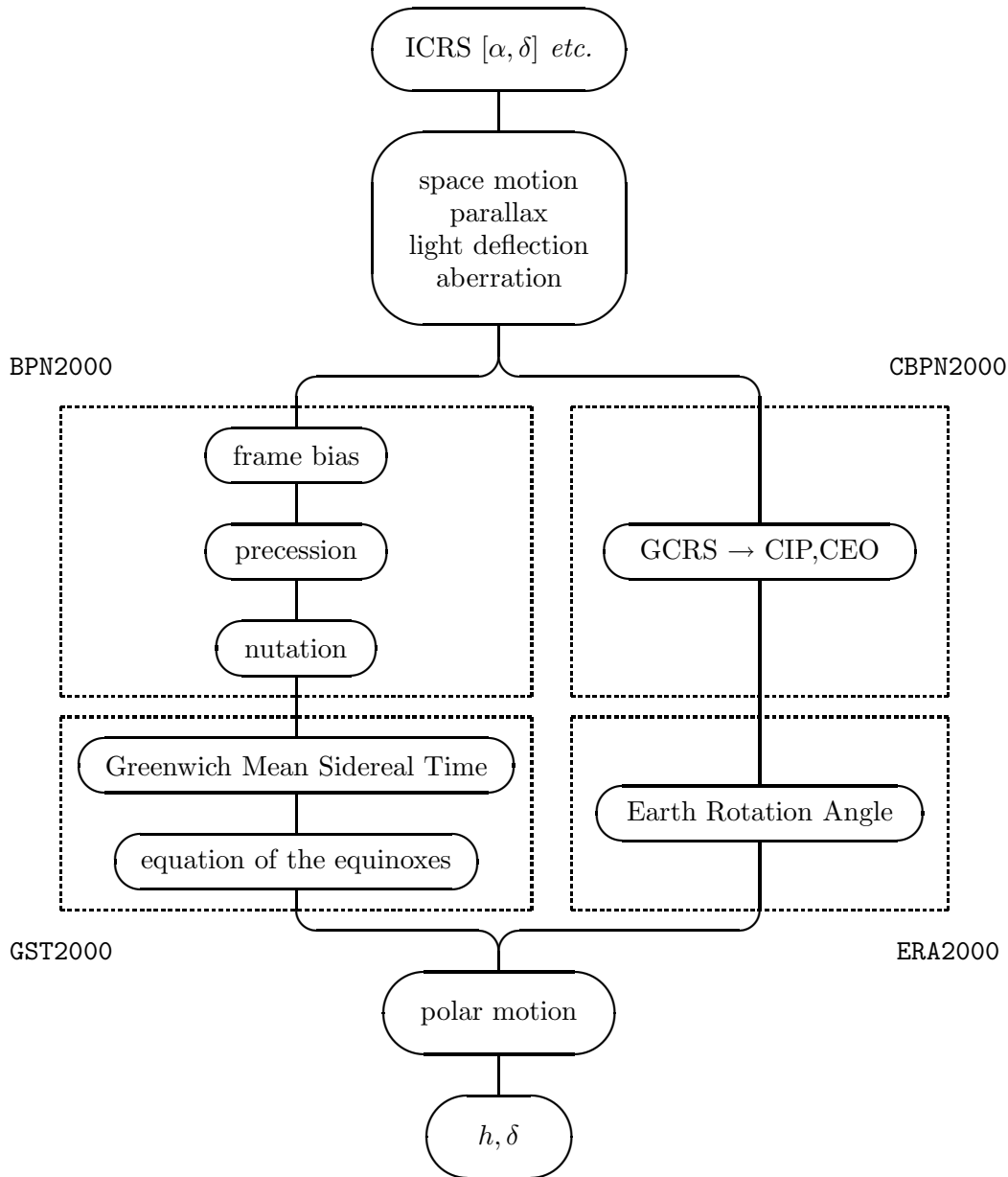
Figure 1.   The transformation from star catalog coordinates to (Greenwich) hour angle and declination. The left and right streams are the alternative ways of performing the transformation, the classical paradigm on the left and the new paradigm on the right. The four dotted boxes identify four of the Fortran subroutines available on the IERS website.

The new paradigm involves only two steps. First the GCRS-to-intermediate rotation matrix is applied; its elements are simple functions of the $X(t), Y(t)$ coordinates of the CIP and the quantity $s(t)$, for which direct series expansions are available. Then a z-rotation is applied, using the Earth Rotation Angle θ, which is a linear function of UT1.

However, if the user is prepared to use "black box" routines, for example the four IERS subroutines marked on Figure 1, the complications can be hidden. Moreover, the total amount of computation turns out to be very similar for the two streams. (In fact using current models for s, the classical method requires fractionally fewer terms to be computed than the new paradigm, though in both cases the computation is dominated by the nutation series. For applications such as telescope pointing where 0.1 arcsecond accuracy is good enough, the convenient approximation $s = 0$ can be used, so that the new paradigm is both simpler and faster than traditional methods.)

Using either the SOFA or IERS Fortran routines, the two streams deliver the same (h, δ) to microarcsecond accuracy. This is a reflection of the great care that went into providing classical equivalents of the new IAU methods.

References

Capitaine, N., Chapront J., Lambert, S. & Wallace, P.T., 2003a, A&A, 400, 1145

Capitaine, N., Wallace P.T. & McCarthy, D.D., 2003b, A&A, 406, 1135

Capitaine, N., Wallace, P.T. & Chapront J., 2003c, A&A, submitted

Guinot, B., 1979, in "Time and the Earth's Rotation", McCarthy, D.D. and Pilkington, J.D. (eds), D. Reidel Publishing Company, 7

IAU, 2000, Transactions of the International Astronomical Union, Vol. XXIVB; Proceedings of the Twenty-Fourth General Assembly; Manchester, UK

IERS Conventions 2000, http://www.usno.navy.mil/conv2000.html, draft

Kaplan, G.H., Hughes, J.A., Seidelmann, P.K., Smith, C.A. & Yallop, B.D., 1989, AJ, 97, 1197.

Lieske, J.H., Lederle, T., Fricke, W. & Morando, B., 1977, A&A, 58, 1

McCarthy, D.D. and Luzum, B.J., 2003, An Abridged Model of the Motion of the Celestial Pole, Celes. Mech. & Dyn. Astron., 85, 37

Mathews, P.M., Herring, T.A. & Buffett B.A., 2002, J. Geophys. R., 107, B4, 10.1029/2001JB000165

Standish, E.M., 1981, A&A, 101, L17

Wallace, P.T, 2002, in: Highlights of Astronomy, Vol. 12, as presented at the XXIVth General Assembly of the IAU – 2000. Edited by H. Rickman. San Francisco, CA: Astronomical Society of the Pacific, ISBN 1-58381-086-2, 128

IERS CONVENTIONS

Dennis D. McCarthy

U.S. Naval Observatory, 3450 Massachusetts Ave. NW, Washington
DC, 20392-5420

Gerard Petit

Bureau International des Poids et Mesures, Paris, France

Abstract.
     The International Celestial Reference Frame (ICRF) is currently a radio reference frame accessed through Very long Baseline Interferometry (VLBI) and refined with technique-dependent improvements described in this Joint Discussion. An important component of the International Celestial Reference System (ICRS) that is the basis for this frame is the set of conventional models and procedures that are used to define the system. The International Earth Rotation and Reference System Service (IERS) Conventions Center, provided jointly by the U.S. Naval Observatory (USNO) and the Bureau International des Poids et Mesures (BIPM), produces the IERS Conventions that contain the models and procedures needed to realize and access the ICRS. The key elements of the Conventions related to the ICRS are outlined, and recent improvements are highlighted. Improvements in the IERS Conventions (models and procedures) should play a role by globally improving IERS products.

1.   Introduction

The realization of the International Celestial Reference System (ICRS) requires a set of conventional models and procedures to be used in the analyses of the observational data. The International Earth Rotation and Reference System Service (IERS) provides these in the IERS Conventions, which contain the recommended procedures not only to define the ICRS but also to derive and interpret the other products of the IERS, such as the International Terrestrial Reference Frame, and the Earth Orientation Parameters.

     The IERS Conventions is a publication that is produced by the IERS Conventions Product Center provided jointly by the U.S. Naval Observatory (USNO) and the Bureau International des Poids et Mesures (BIPM). The Product Center provides a web site
http://maia.usno.navy.mil/conv2003.html containing the IERS Conventions (2003). This site is to be updated as warranted at approximately annual intervals. In addition the Center produces the material for the IERS Technical Notes that document major changes, and it is expected that this document might be provided at approximately 5-year intervals.

     The IERS Conventions (2003) is a continuation of the series of documents begun with the Project MERIT Standards (Melbourne *et al*, 1983) and con-

tinued with the IERS Standards (McCarthy, 1989; McCarthy, 1992) and IERS Conventions (McCarthy, 1996). The current issue of the IERS Conventions is called the IERS Conventions (2003). When referenced in recommendations and articles published in past years, this document may have been referred to as the IERS Conventions (2000).

The celestial system described in the IERS Conventions (2003) is based on IAU (International Astronomical Union) Resolution A4 (1991). It was further refined by IAU Resolution B1 (2000). The definition of time coordinates and time transformations, the models for light propagation and the motion of massive bodies are based on IAU Resolution A4 (1991), further defined by IAU Resolution B1 (2000). In some cases, the procedures used by the IERS, and the resulting conventional frames produced by the IERS, do not completely follow these resolutions. These cases are identified in the document, and procedures to obtain results consistent with the resolutions are shown.

2.   Components

The IERS Conventions contain descriptions of units, models, software and procedures to be used in deriving and understanding the IERS products. These products assume the use of SI units (Le Système International d'Unitès (SI), 1998) and are generally consistent with the use of Geocentric Coordinate Time TCG as the time coordinate for the geocentric system, and Barycentric Coordinate Time TCB for the barycentric system.

The Conventions describe the conventional concepts that underlie the definition of modern high-precision Celestial and Terrestrial Reference Systems. These have little relationship to the precision of the products but they are likely to affect the accuracy as well as the users interpretation.

Models are provided to describe various physical effects. These are often developed to provide a conventional representation of a phenomenon that reduces the size of the internal error as measured by internal residuals. Consequently they generally affect precision but might have only a minimal affect on the accuracy. Included also are constants, the numerical values of parameters of common interest. Perhaps the most important is the software that provides practical numerical implementation of the concepts and models.

Finally, the Conventions publication outlines procedures to implement all of the above. The IERS Conventions (2003) does not go so far as to describe standard procedures for data analyses, such as details regarding solution constraints and appropriate spans of data, but future versions may get to that point. These choices affect precision but have little effect on accuracy.

3.   Concepts

The IERS utilizes data provided by a variety of observational techniques. The analysis centers for each technique would normally establish the technique-specific conventions that are required for the analyses of their observations. The IERS Conventions concern those phenomena that affect more than one technique. The Product Center seeks to determine the effect of conventional mod-

els, software, and procedures on the data contributed to the IERS. The Center expects to work closely with the IERS Analysis Coordinator in this process.

4. Contents

The Contents of the Conventions publication are outlined by the Table of Contents:

Procedure to be used for the transformation consistent with IAU 2000 Resolutions

Expression of Greenwich Sidereal Time using the CEO

The Fundamental Arguments of Nutation Theory

The multipliers of the fundamental arguments of nutation theory

Development of the arguments of lunisolar nutation

Development of the arguments for the planetary nutation

Prograde and Retrograde Nutation Amplitudes

Procedures and IERS Routines for Transformations from ITRS to GCRS

Notes on the new procedure to transform from ICRS to ITRS

6. GEOPOTENTIAL

Effect of Solid Earth Tides

Solid Earth Pole Tide

Treatment of the Permanent Tide

Effect of the Ocean Tides

Conversion of tidal amplitudes defined according to different conventions

7. DISPLACEMENT OF REFERENCE POINTS

Displacement of Reference Markers on the Crust

Local Site Displacement due to Ocean Loading

Effects of the Solid Earth Tides

Rotational Deformation due to Polar Motion

Atmospheric Loading

Displacement of Reference Points of Instruments

VLBI Antenna Thermal Deformation

8. TIDAL VARIATIONS IN THE EARTH'S ROTATION

9. TROPOSPHERIC MODEL

Optical Techniques

Radio Techniques

10. GENERAL RELATIVISTIC MODELS FOR SPACE-TIME COORDINATES AND EQUATIONS OF MOTION

Time Coordinates

11. GENERAL RELATIVISTIC MODELS FOR PROPAGATION

VLBI Time Delay

Background

The VLBI delay model

Laser Ranging

Appendix — IAU Resolutions Adopted at the XXIVth General Assembly

Glossary

The contents of the IERS Conventions (2003) available at http://maia.usno.navy.mil/conv2003.html are presented below in outline form.

Introduction

Chapter 1 - Numerical Standards

Chapter 2 - Conventional Celestial Reference System and Frame

Chapter 3 - Conventional Dynamical Realization of the ICRS

Read me file for DE405 - Provides information concerning the retrieval and use of the DE405.

Chapter 4 - Conventional Terrestrial Reference System and Frame
ITRF2000 - Information on ITRF2000
GCONV subroutine - Transforms geocentric coordinates to geodetic coordinates. Provided by T. Fukushima
ABSMO Nuvel subroutine - Computes the new site position at time t from the old site position at time t0 using the recommended plate motion model. Originally provided by J. B. Minster.

Chapter 5 - Transformation Between the Celestial and Terrestrial Systems
Chapter 5 Tables - Electronic versions of the tables for Chapter 5
Chapter 5 Subroutines - Electronic versions of the subroutines for Chapter 5

Chapter 6 - Geopotential

Chapter 7 - Site Displacement
Angular Argument subroutine - A FORTRAN subroutine to return the proper angular argument to be used with the Schwiderski phases
Mean Pole Positions - mean pole positions provided by the IERS Earth Orientation Centre (D. Gambis).
Atmospheric Regresssion Coefficients - site displacements due to atomspheric loading at specific sites; provided by T. vanDam.

Chapter 8 - Tidal Variations in the Earth's Rotation
ortho eop subroutine - Subdiurnal/Diurnal Subroutine

Chapter 9 - Tropospheric Model

Chapter 10 - General Relativistic Models for Time, Coordinates and Equations of Motion
Fairhead-Bretagnon Model - Computes the periodic terms of TT. Provided by A. Irwin.
Xhf2002.f routine - Computes TCB-TCG as a function of TT. Provided by W. Harada and T. Fukushima.
HF2002.dat - Parameter file read by Xhf2002.f. Provided by W. Harada and T. Fukushima.
xhf2002.out - Output file of the test driver. Provided by W. Harada and T. Fukushima.

Chapter 11 - General Relativistic Models for Propagation

Appendix - Resolutions from the 24th IAU General Assembly

Glossary - List of acronyms used in the Conventions

In comparison with previous versions the latest version has undergone significant changes. These are outlined below by chapter. The principal contributors are also listed for each chapter.

Chapter 1-General Definitions and Numerical Standards
The chapter has been updated for consistency of notation and concepts with other sections according to IAG (International Association of Geodesy) and IAU working groups. It provides general definitions for topics in other chapters and

also the values of numerical standards that are used in the document. It incorporates the previous Chapter 4, which was updated to provide consistent notation and to comply with the recommendations of the most recent reports of the appropriate working groups of the International Association of Geodesy (IAG) and the IAU. It was prepared principally by D. McCarthy and G. Petit with major contributions from M. Burra, N. Capitaine, T. Fukushima, E. Groten, P. M. Mathews, P. K. Seidelmann, E. M. Standish, and P. Wolf.

Chapter 2-Conventional Celestial Reference System and Frame

The chapter, which appeared as Chapter 1 in previous editions has been updated to incorporate the effects of the IAU 2000 24th General Assembly by E. F. Arias with contributions from J. Kovalevsky, C. Ma, F. Mignard, and A. Steppe.

Chapter 3-Conventional Dynamical Reference Frame

Chapter 3 (previously Chapter 2), has been updated to be consistent with notation and concepts of other sections. The conventional solar system ephemeris has been changed to the Jet Propulsion Laboratory (JPL) DE405. It was prepared by E. M. Standish with contributions from F. Mignard and P. Willis.

Chapter 4-Conventional Terrestrial Reference System

Chapter 4 (previously Chapter 3) was rewritten by Z. Altamimi,, C. Boucher, and P. Sillard with contributions from J. Kouba, G. Petit, and J. Ray. It incorporates the new Terrestrial Reference Frame of the IERS (ITRF2000), which was introduced in 2001.

Chapter 5-Transformation Between the Celestial and Terrestrial Systems

The chapter was modified to be consistent with resolutions adopted at the 24th IAU General Assembly and the 2002 IERS Workshop. It was updated principally by N. Capitaine, with major contributions from P. M. Mathews and P. Wallace to comply with the recommendations of the IAU 2000 24th General Assembly. Significant contributions from P. Bretagnon, R. Gross, T. Herring, G. Kaplan, D. McCarthy, Burghard Richter and P. Simon were also incorporated.

Chapter 6-Geopotential

Chapter 6 was updated to include the EGM96 conventional geopotential model and the treatment of tides. V. Dehant, P. M. Mathews, and E. Pavlis were responsible for the revision. Major contributions were also made by P. Defraigne, S. Desai, F. Lemoine, R. Noomen, R. Ray, F. Roosbeek, and H. Schuh.

Chapter 7-Site Displacement

This chapter was updated to be consistent with the geopotential model recommended in Chapter 6. It was prepared principally by V. Dehant, P. M. Mathews, and H.-G. Scherneck. Major contributions were also made by Z. Altamimi, S. Desai, S. Dickman, R. Haas, R. Langley, R. Ray, M. Rothacher, H. Schuh, and T. VanDam. A model for post-glacial rebound is no longer recommended and a new ocean-loading model is suggested. The VLBI antenna

deformation has been enhanced.

Chapter 8-Tidal Variations in the Earths Rotation

Changes were made to be consistent with the nutation model adopted at the 24th IAU General Assembly. The model of the diurnal/semidiurnal variations has been enhanced to include more tidal constituents. The principal authors of Chapter 8 were Ch. Bizouard, R. Eanes, and R. Ray. P. Brosche, P. Defraigne, S. Dickman, D. Gambis, and R. Gross also made significant contributions.

Chapter 9-Tropospheric Model

This chapter has been changed to recommend an updated model. It is based on the work of C. Ma, E. Pavlis, M. Rothacher, and O. Sovers, with contributions from C. Jacobs, R. Langley, V. Mendes, A. Niell, T. Otsubo, and A. Steppe.

Chapter 10-General Relativistic Models for Time, Coordinates and Equations of Motion

The chapter has been updated for consistency of notation and concepts with other sections. New software for the TCB-TCG transformation, developed by Harada and Fukushima, has been checked against existing programs and added to the list of such standards. Previously appearing as Chapter 11, it has been updated to be in compliance with the IAU resolutions and the notation they imply. It was prepared principally by T. Fukushima and G. Petit with major contributions from P. Bretagnon, A. Irwin, G. Kaplan, S. Klioner, T. Otsubo, J. Ries, M. Soffel, and P. Wolf.

Chapter 11-General Relativistic Models for Propagation

This chapter (previously Chapter 12), has been updated for consistency of notation and concepts with other sections. It was updated to comply with the IAU resolutions and the notation they imply. It is based on the work of T. M. Eubanks and J. Ries. Significant contributions from S. Kopeikin, G. Petit, L. Petrov, A. Steppe, O. Sovers, and P. Wolf were incorporated.

5.   Future

The IERS Conventions Center intends to provide updated versions of the Conventions on the web site. These editions will be clearly marked regarding the date of their electronic publication. In addition, the Center will provide printed versions of the Conventions at less frequent intervals when major changes are introduced.

The BIPM has provided for a visiting scientist to investigate the effects of selected models on the products of the IERS Analysis Centers. This is being done in collaboration with the IERS Analysis Coordinator and different Product and Analysis centers. The Product Center will continue to determine the most important directions to improve the consistency of IERS combined solutions and how to implement new conventional models and procedures. Important topics for the future include geocenter motion, impact of using global as opposed to local loading models, and network effects in the solutions of different techniques.

6.   Conclusion

The IERS Conventions are the product of the IERS Conventions Product Center. However, this work would not be possible without the contributions acknowledged above. In addition, we would also like to acknowledge the comments and contributions of S. Allen, Y. Bar-Sever, A. Brzeziński, M. S. Carter, P. Cook, H. Fliegel, M. Folgueira, J. Gipson, S. Howard, T. Johnson, M. King, S. Kudryavtsev, Z. Malkin, S. Pagiatakis, S. Pogorelc, J. Ray, S. Riepl, C. Ron, and T. Springer in the compilation of the work.

References

Le Système International d'Unitès (SI), 1998, Bureau International des Poids et Mesures, Sèvres, France.

McCarthy, D. D. (ed.), 1989, *IERS Standards*, IERS Technical Note 3, Observatoire de Paris, Paris.

McCarthy, D. D. (ed.), 1992, *IERS Standards*, IERS Technical Note 13, Observatoire de Paris, Paris.

McCarthy, D. D. (ed.), 1996, *IERS Conventions*, IERS Technical Note 21, Observatoire de Paris, Paris.

Melbourne, W., Anderle, R., Feissel, M., King, R., McCarthy, D., Smith, D., Tapley, B., Vicente, R., 1983, Project MERIT Standards, *U.S. Naval Observatory Circular No. 167.*

New Precession Formula

Toshio Fukushima

NAO Japan, 2-21-1, Ohsawa, Mitaka, Tokyo, 181-8588, Japan

Abstract.   We adapted J.G. Williams' expression of the precession and nutation using the 3-1-3-1 rotation (Williams 1994) to an arbitrary inertial frame of reference. The modified formulation avoids a singularity caused by finite pole offsets near the epoch. By adopting the planetary precession formula numerically determined from DE405 (Harada and Fukushima 2003) and by using a recent theory of the forced nutation of the non-rigid Earth, SF2001 (Shirai and Fukushima 2001), we analyzed the celestial pole offsets observed by VLBI for 1979-2000 (McCarthy 2000, private communication) and determined the best-fit polynomials of the luni-solar precession angles. Then we translated the results into the classic precession quantities and evaluated the difference in them due to the difference in the ecliptic definition. The combination of these formulas and the periodic part of SF2001 serves as a good approximation of the precession-nutation matrix in the ICRF.

1. Introduction

It is well known that the combination of the IAU 1976 precession formulas (Lieske *et al.* 1977) and the IAU 1980 nutation theory (Seidelmann 1982) is incorrect at the level of 10 mas when referred to the International Celestial Reference Frame (ICRF). See Figure 1. There are secular departures partly due to the difference between the ICRF and the reference frame referred to the mean equator and equinox of the epoch, J2000.0, and partly due to the error of the adopted polynomial coefficients of the IAU precession formula.

Although there have been many studies on the revision of nutation theories treating the revision of precession in the form of linear correction terms such as IAU2000A (Mathews *et al.* 2002), such a remedy is unsatisfactory and the replacement of the IAU 1976 precession formulas as a whole is required. To do this, we presented a lengthy article recently (Fukushima 2003). This report is its concise summary.

The task to be done is split into three different parts. The first part involves an update of the theory on the motion of the ecliptic pole, namely the formula of planetary precession. The second part is an improvement in the theory on the secular motion of the equatorial pole, *i.e.* the luni-solar precession formula. And the last part is a re-consideration of the general relativistic effects named the geodesic precession.

As for the first part, Harada and Fukushima (2003) numerically extracted the secular motion of the instantaneous orbital plane of the Earth-Moon barycenter around the Sun in the latest planetary/lunar ephemerides DE405. On the other hand, all the recent estimates of the third effect is summarized and a best

Observed Nutation Correction
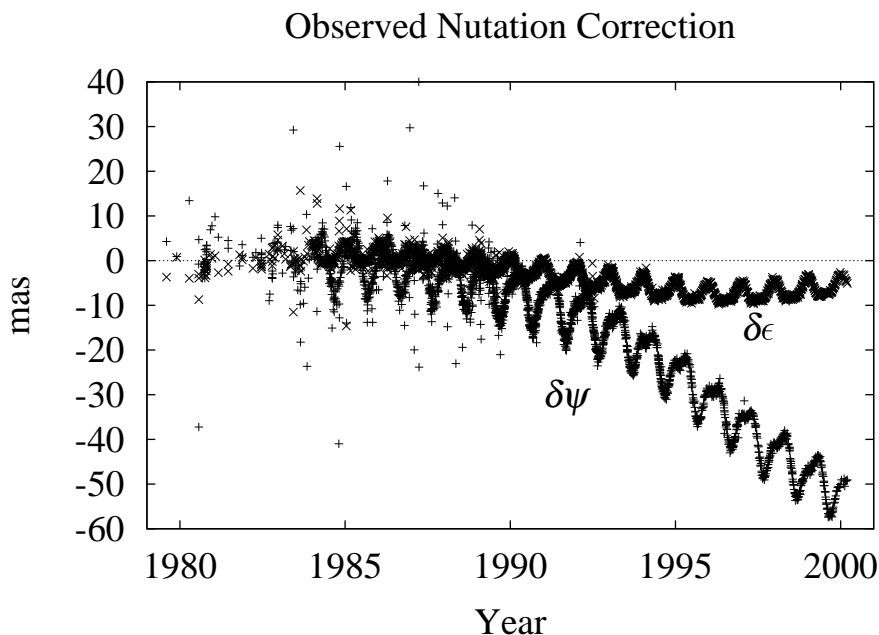
Figure 1.   Celestial Pole Offsets observed by VLBI

estimate is obtained so as to cover all of them within a one-sigma range. The estimate obtained is

$$p_g = (1.9196 \pm 0.0003)''/\text{cy.} \tag{1}$$

¿From an observational point of view, it is difficult to discriminate the luni-solar and geodesic precessions. Then we will call the summed effect loosely the luni-solar precession and determine suitable formulas specifying the luni-solar precession in this report. In actuality, we corrected the quadratic polynomials of the formulas of Williams (1994). This is because his estimate of the rate of variation in the obliquity was so accurate that it was confirmed by the recent determinations using VLBI and LLR observations and partly because the article provided a concise formulation to realize the precession and the precession-nutation matrices based on the 3-1-3-1 rotation.

In performing the adjustment, we used the VLBI pole offset observations mentioned above after reducing their short periodic variations with the aid of the SF2001 nutation theory (Shirai and Fukushima 2001). We adopted the latest determination of planetary precession (Harada and Fukushima 2003), and we considered the difference between the inertial and rotational meanings. We note that the main improvements concern the contributions of the frame biases between the ICRF and the frame referred to the mean equator and equinox at J2000.0 and the corrections to the IAU precession rates in both longitude and obliquity.

2. Modification of Williams' Formulation

In 1994, J.G. Williams presented an important paper on precession (Williams 1994). The main purpose of this paper was to demonstrate some effects due to a tilt of the Moon's orbital plane from the ecliptic, which had not been considered in the theories of precession and nutation. The correction in the obliquity rate, $-0.024''$/century, is so precise and sufficient that it has been confirmed by VLBI/LLR observations.

At the same time, he introduced a new formulation to express the precession and the nutation in a unified manner by using the 3-1-3-1 rotation operation. See Section 9 and Eq.(37) of Williams (1994). Since two angles are necessary to specify the direction of a pole in the given reference frame, this approach needs four rotational operations in total. Since Williams' original formula are referred to the mean equator and equinox at the epoch, we modified it so as to be based on the ICRF. Thus we express the precession and the precession-nutation matrices as

$$\mathcal{P} \equiv \mathcal{R}_1\left(-\bar{\epsilon}\right)\mathcal{R}_3\left(-\bar{\psi}\right)\mathcal{R}_1(\bar{\varphi})\mathcal{R}_3(\bar{\gamma}), \tag{2}$$

$$(\mathcal{NP}) \equiv \mathcal{R}_1(-\epsilon)\mathcal{R}_3(-\psi)\mathcal{R}_1(\bar{\varphi})\mathcal{R}_3(\bar{\gamma}), \tag{3}$$

where

$$\psi \equiv \bar{\psi} + \Delta\psi, \quad \epsilon \equiv \bar{\epsilon} + \Delta\epsilon$$

and $\Delta\psi$ and $\Delta\epsilon$ are the usual nutation. See the new polar and equinox diagrams, Figures 2 and 3.

3. Determination

As for the planetary precession, Harada and Fukushima (2003) obtained the latest formula based on DE405 as

$$\bar{\gamma}_{\text{DE405}} = -(0.021\ 09 \pm 0.000\ 14) + (10.542\ 27 \pm 0.000\ 11)\ t$$

$$+(0.486\ 09 \pm 0.000\ 04)\ t^2, \tag{4}$$

$$\bar{\varphi}_{\text{DE405}} = (84\ 381.405\ 78 \pm 0.00006) - (46.819\ 71 \pm 0.00004)\ t$$

$$+(0.048\ 17 \pm 0.000\ 02)\ t^2, \tag{5}$$

where the units are arcseconds. The comparison of Fourier terms detected by the analysis of DE405 with the similar harmonic decomposition of DE102 by Standish (1982) revealed that the former lacks a Very Long Periodic (VLP) term with a period of around 883 years. By correcting its effect, we obtained the final results as

$$\bar{\gamma} = -(0.052\ 40 \pm 0.000\ 14) + (10.553\ 18 \pm 0.000\ 11)\ t$$

$$+(0.493\ 18 \pm 0.000\ 02)\ t^2, \tag{6}$$

$$\bar{\varphi} = (84\ 381.411\ 27 \pm 0.000\ 06) - (46.812\ 65 \pm 0.000\ 04)\ t$$

$$+(0.048\ 43 \pm 0.000\ 02)\ t^2. \tag{7}$$

New Precession Angles and Nutation Angles
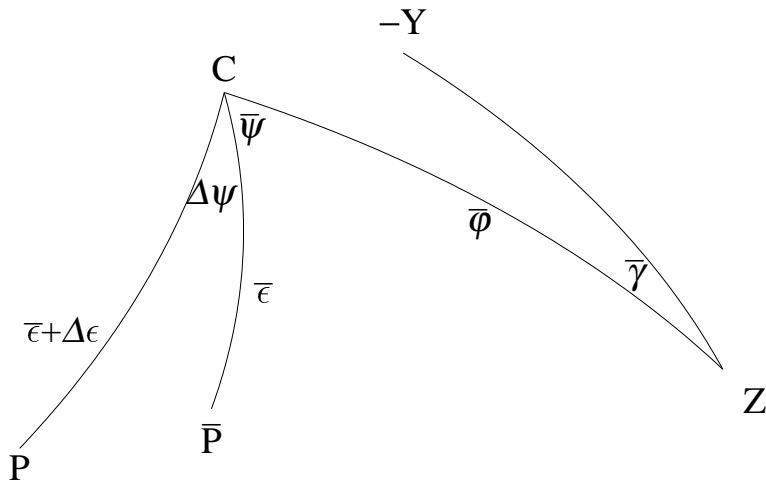
Figure 2.   Polar diagram of new precession angles: Illustrated are the geometrical definitions of the new precession angles in the polar region; $\bar{\gamma}$, $\bar{\varphi}$, $\bar{\psi}$, and $\bar{\epsilon}$. Their definitions are $\bar{\gamma} \equiv 180° - \angle\mathrm{YZC}$, $\bar{\varphi} \equiv \overline{\mathrm{ZC}}$, $\bar{\psi} \equiv \angle\bar{\mathrm{P}}\mathrm{CZ}$, and $\bar{\epsilon} \equiv \overline{\mathrm{C}\bar{\mathrm{P}}}$. Also shown are their relations with the nutation angles $\Delta\psi$ and $\Delta\epsilon$. Here Z and $-$Y denote the positive z-axis and the negative y-axis of the ICRF, respectively C is the ecliptic pole of date, and P and $\bar{\mathrm{P}}$ are the true and mean equator of date, respectively.
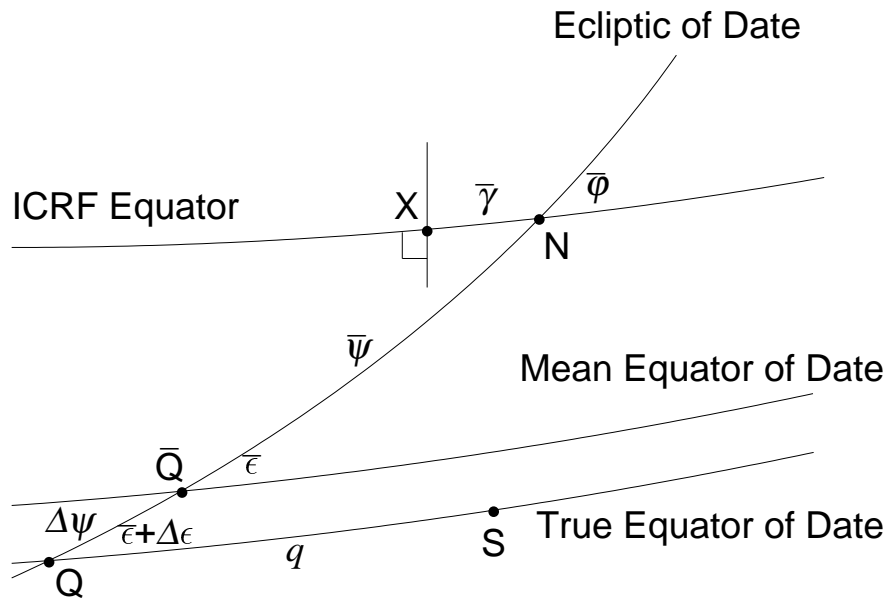
Figure 3. Equinox diagram of new precession angles: Same as Figure 2 but shown in the equinox region. Here X is the x-axis of the ICRF, N is the node of the ecliptic of date with respect to the ICRF equator, Q and $\bar{\text{Q}}$ are the true and mean equinox of date, and S is the CEO.

Now let us determine the luni-solar precession; $\bar{\psi}$ and $\bar{\epsilon}$. We adopt Williams' precession angles η_A and ε_A as the approximation of $\bar{\psi}$ and $\bar{\epsilon}$, respectively. Then, we obtain their corrections as linear functions of time. In determining the corrections, we remove the short periodic variations in the celestial pole offsets in the VLBI observation by choosing a recent nutation theory SF2001 (Shirai and Fukushima 2001). The final results are

$$\bar{\psi} = -(0.043\ 04 \pm 0.000\ 03) + (5\ 038.478\ 12 \pm 0.000\ 20)\ t$$

$$+1.558\ 35\ t^2, \tag{8}$$

$$\bar{\epsilon} = +(84\ 381.406\ 21 \pm 0.000\ 01) - (46.834\ 60 \pm 0.000\ 08)\ t$$

$$-0.000\ 17\ t^2 + 0.002\ 00\ t^3, \tag{9}$$

where we did not attach uncertainties for the parts we assumed. By using the formula thus determined, the residuals in Figure 1 are reduced significantly as shown in Figure 4, where the result for the longitude is omitted because it is similar. Note that all these determinations are in the inertial sense argued in Standish (1981). As natural by-products of these new formulae, the classic precession quantities referred to the mean equator and equinox at J2000.0 are listed in Table 1. As another by-product, we derived the mean celestial pole offset at J2000.0 as $\bar{X}_0 = -(17.12 \pm 0.01)$ mas and $\bar{Y}_0 = -(5.06 \pm 0.02)$ mas. Also we estimated the speed of general precession in longitude at J2000.0 as $p = (5028.7955 \pm 0.0003)''$/Julian century, and the dynamical flattening of the Earth as $H_d = (3.2737804 \pm 0.0000003) \times 10^{-3}$.

Residual after Polynomial Fitting: $\delta\bar{\epsilon}_\mathrm{I}$
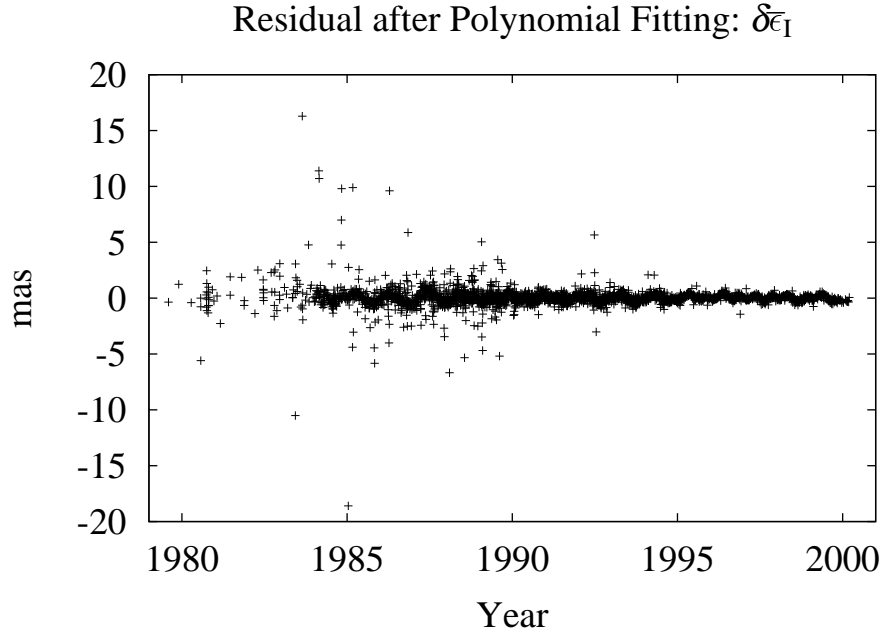
Figure 4. Residual in Celestial Pole Offsets in Obliquity. The result for longitude is similar.

Table 1. Classic Precession Quantities

	1	t	t^2	t^3	t^4
s_A	0.000000	+4.197822	+0.193978	−0.000101	0.000000
c_A	0.000000	−46.812649	+0.048332	−0.000009	0.000000
π_A	0.000000	+47.000488	−0.030813	+0.000415	0.000000
Π_A	+629552.994279	−866.828322	−0.125443	+0.004678	+0.000013
p_A	0.000000	+5028.795766	+1.105390	−0.000022	0.000000
ψ_A	0.000000	+5038.478143	−1.079165	−0.001107	+0.000129
ω_A	+84381.406210	−0.021951	+0.053941	−0.007196	+0.000002
χ_A	0.000000	+10.553205	−2.381552	−0.001064	+0.000141
ϵ_A	+ 84381.406210	−46.834600	−0.000170	+0.002000	0.000000
ζ_A	+2.259114	+2305.805899	+0.244304	+0.017785	+0.000009
z_A	−2.259114	+2306.354618	+1.147240	+0.018372	−0.000019
θ_A	0.000000	+2004.190570	−0.429514	−0.041779	−0.000003

Listed are the polynomial coefficients of the classic precession quantities derived from our determination of new precession angles. Here $s_\mathrm{A} \equiv \sin\pi_\mathrm{A}\sin\Pi_\mathrm{A}$ and $c_\mathrm{A} \equiv \sin\pi_\mathrm{A}\cos\Pi_\mathrm{A}$. Units are arc seconds and t is the time since J2000.0 measured in Julian centuries. All these quantities are referred not to the ICRF but to the mean equator and equinox at J2000.0. Some higher order terms are omitted, and the number of digits is trimmed so that the table is fitted to the page length. For complete expressions and comparison with the existing determinations, the reader may refer to the original paper (Fukushima 2003).

References

Fukushima, T. 2003, AJ, 126, 494.
Harada, W., and Fukushima, T. 2003, submitted to AJ.
Lieske, J. H., Lederle, T., Fricke, W., and Morando, B. 1977, A&A, 58, 1.
Mathews, P.M., Herring, T.A., and Buffet, B.A. 2002, J. Geophys. Res., 107, B4,
        10.1029/2001JB000390.
Seidelmann, P. K. 1982, Cele. Mech., 27, 79.
Shirai, T., and Fukushima, T. 2001, AJ, 121, 3270.
Standish, Jr., E. M. 1981, A&A, 101, L17.
Standish, Jr., E. M. 1982, A&A, 114, 297.
Williams, J. G. 1994, AJ, 108, 711.

ICRS, ITRS, and the IAU Resolutions Concerning Relativity

Mike Soffel & Sergei Klioner

Lohrmann-Observatorium, Institut fur Planetare Geodasie, Technische Universitat Dresden, Mommsenstrasse 13, D-01062 Dresden, Germany

Abstract.
The IAU2000 Resolutions concerning relativity introduce two celestial reference systems, a barycentric one, BCRS with coordinates (t,x), and a geocentric one, GCRS with coordinates (T,X). The two sets of coordinates are related by 4-dimensional space-time transformations. So far the relations of the BCRS and GCRS with the ICRS and ITRS have NOT been discussed. This will be done here. It is argued that the ICRS is a special representation of the BCRS, and the ITRS-coordinates differ from the GCRS ones by a time dependent rotation of spatial coordinates plus possible scale factors. This implies that also the ICRS- and the ITRS- coordinates are related by a generalized Lorentz-transformation.

Earth Orientation Catalogue - An Improved Reference Frame

Jan Vondrák & Cyril Ron

Astronomical Institute, Academy of Sciences of the Czech Republic,
Boční II, 14131 Prague 4, Czech Republic

Abstract.   Optical observations of latitude/universal time variations of nearly five thousand stars (made during the twentieth century at 33 observatories in Earth orientation programmes) are used, in combination with the Hipparcos and Tycho catalogues and their combination with ground-based observations (AR-IHIP), to derive a new improved star catalogue called the Earth Orientation Catalogue (EOC). The first version of the catalogue, EOC-1, based on the observations with instruments observing in local meridian, is now finished. The improved proper motions and/or positions are more convenient for long-term extrapolation of apparent places than those of the original Hipparcos and Tycho Catalogues. The EOC is planned to be used for another new re-analysis of Earth Orientation Parameters based on optical astrometry observations in the 20th century.

1.   Introduction

Solutions of Earth Orientation Parameters (EOP), based on optical observations of latitude and universal time variations were made at the Astronomical Institute, Academy of Sciences of the Czech Republic and Department of Geodesy, Czech Technical University in Prague (Vondrák *et al.* 1998; Vondrák, Ron, & Pešek 2000). All observations made with 47 instruments at 33 observatories in the interval 1899.7-1992.0 were re-calculated to be referred to the Hipparcos Catalogue **HIP** (ESA 1997; Perryman *et al.* 1997) and a unique system of astronomical constants and algorithms. Namely, the IAU 1976 model of precession (Lieske *et al.* 1977) and IAU 1980 model of nutation (Wahr 1981; Seidelmann 1982) were used. These almost 5 million observations were then used in three different solutions, based on more and more data collected, and also using slightly different approaches:

1. Solution OA97 (Vondrák *et al.* 1998), based on observations made with 45 different instruments (48 series) located at 31 observatories. 4.3 million individual observations of latitude/universal time variations were used.

2. Solution OA99 (Vondrák *et al.* 2000), based on observations with 47 instruments (merged into 39 series, with the steps caused by different coordinates of the instruments located at the same observatory removed) at 33 observatories. 4.4 million observations were used.

3. Solution OA00, based on 47 different instruments (merged into 41 series, with slightly different steps in data removed) at 33 observatories. 4.4 million observations were used.
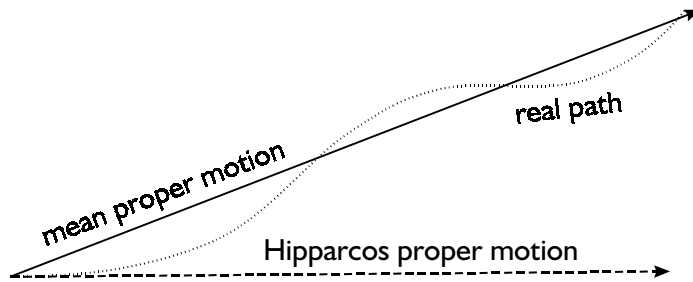
Figure 1.   Path of one of the double star components versus its mean and Hipparcos proper motion

The main differences among these solutions consisted in different approaches to merging the data acquired at the same observatory, and how to treat evident systematic deviations of some Hipparcos stars. As demonstrated in Fig. 1, the main problem is caused by double or multiple stars, with non-linear proper motions. Due to the relatively short Hipparcos mission (less than 4 years), proper motion measured by Hipparcos reflects the instantaneous velocity rather than its mean value needed for long-term extrapolation, even if the amplitude of the periodic component is small.

That is why we were forced to correct from 11% to 20% of the proper motions (and sometimes their mean positions, too, in case that components other than the ones given in Hipparcos Catalogue were observed), before a solution was made, whenever we came upon statistically significant residuals.

Recently new star catalogues (combinations of Hipparcos/Tycho Catalogues with ground-based catalogues) given in the International Celestial Reference System (Ma *et al.* 1998) have appeared, with substantially improved proper motions:

- **TYCHO-2** (Høg *et al.* 2000) containing 2.5 million stars, the combination of Tycho with 144 ground-based catalogues;

- **FK6 I & III** (Wielen *et al.* 1999; Wielen *et al.* 2000) containing 878 basic and 3272 additional fundamental stars, the combination of Hipparcos and FK5 catalogues;

- **GC+HIP** (Wielen *et al.* 2001a) containing 20 thousand stars, the combination of Hipparcos with Boss' General Catalogue;

- **TYC2+HIP** (Wielen *et al.* 2001b) containing 90 thousand stars, the combination of Hipparcos with proper motions from TYCHO-2;

- **ARIHIP** (Wielen et al, 2001c) containing 91 thousand stars, the selection of the "best" stars from the catalogues **FK6, GC+HIP, TYC2+HIP**, and **HIP**.

Wielen *et al.* (1999) introduced the classification of the stars according to their "astrometrical excellence" by assigning a number of asterisks to each star, and

utilized it in their above mentioned catalogues. It goes from *** (highest rank) to no asterisk (lowest rank).

The existence of these catalogues led to the decision of creating a new Earth Orientation Catalogue (EOC), containing only the stars observed in Earth orientation programmes (Vondrák & Ron 2003). The main goal is to set up a new improved reference frame for long-term Earth rotation studies, by using the best catalogues available in combination with the rich observational material obtained from existing Earth orientation programs in the 20th century.

2. The List of Stars in EOC

First we made an inventory of all optical data of Earth orientation programmes available, and found 4422 different objects (stars, photocenters of double stars) observed during 1899.7–1992.0 at 33 observatories. These stars were identified in the catalogues described in the preceding Section, and their catalogue entries (*i.e.*, magnitudes, positions, proper motions, parallaxes and radial velocities, mean epochs and standard errors) were taken over from them, in the following order of importance:

1. **ARIHIP**, from which comes the majority, *i.e.* 2994 stars;

2. **TYCHO 2**, from which come 1250 stars;

3. **HIP**, from which come only 145 stars;

4. local catalogues (*i.e.*, those used by the observatories and often improved from their own observations), from which we took over the remaining 33 stars that could be identified in none of the preceding catalogues.
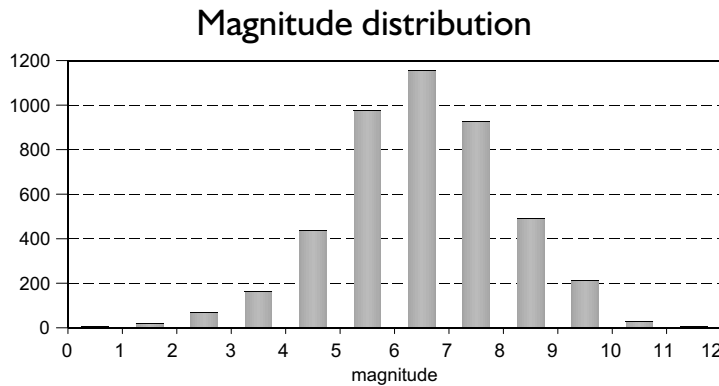
Figure 2. Magnitude distribution of EOC stars

Fig. 2 displays the magnitude distribution, Fig. 3 the statistics of the catalogues from which the stars come. Out of these stars, less than 2000 are classified by Wielen *et al.* as "astrometrically excellent" (*i.e.*, marked with at least one asterisk). Evidently, more than 50% of EOC stars require a thorough inspection and most probably an improvement.

The entries from the above mentioned catalogues form the zero version of the catalogue (**EOC-0**). Star numbers in EOC-0 are assigned as follows:

Original catalogues and 'astrometrical excellency'
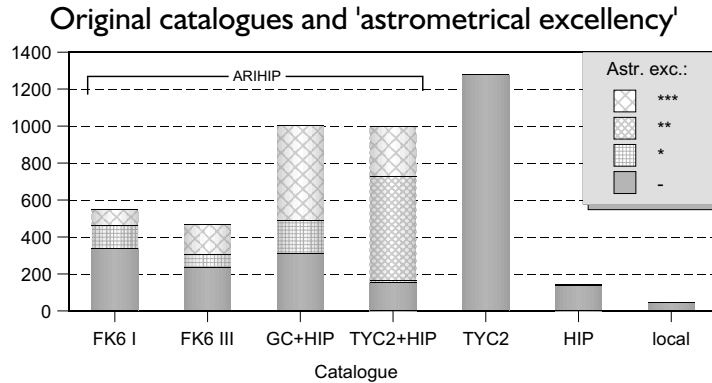
Figure 3. Statistics of where the EOC stars come from, and their 'astrometrical excellency'

- Hipparcos number is used if the star is contained in HIP and is either single or the same entry as given in the original catalogue that was observed.

- Numbers 200001, 200002, ... for the stars that are not contained in Hipparcos Catalogue; there are only 87 such stars (54 being taken over from TYCHO 2 and 33 from local catalogues).

- HIP number + 300000 for the stars that are contained in HIP but are components other than those given as entries in the original input catalogue that was observed. In this case, the displacement of the observed component from the catalogue entry is estimated from the observations; 55 such stars have been found.

It is necessary to add that sometimes different components of a catalogue entry were observed by different instruments. In general, visual instruments are less liable to observe the photocenter instead of a component than photographic or photoelectric instruments; the human eye seems to be still a better detector of light, able to distinguish close objects (about $1 - 2''$ seems to be a limit). In these cases, we keep two different entries in the catalogue, with two different numbers (differing by 300000); the two entries in EOC-0 differ only in position, their proper motions are identical.

3. Further Improvement of EOC

On average, each star was observed in Earth orientation programmes about a thousand times, with the precision of one observation being about 200 mas, usually over a relatively long time interval (decades). It means that the proper motions (and sometimes even positions) can be determined with a precision competing with that of ARIHIP and other similar catalogues. Thus the combination with these input catalogues will surely bring an important improvement. Generally speaking, latitude observations are used to improve declinations, observations of universal time are used to improve right ascensions.

The strategy is to determine the positions of the observed stars with respect to astrometrically excellent stars observed by the same instrument. To this end, we
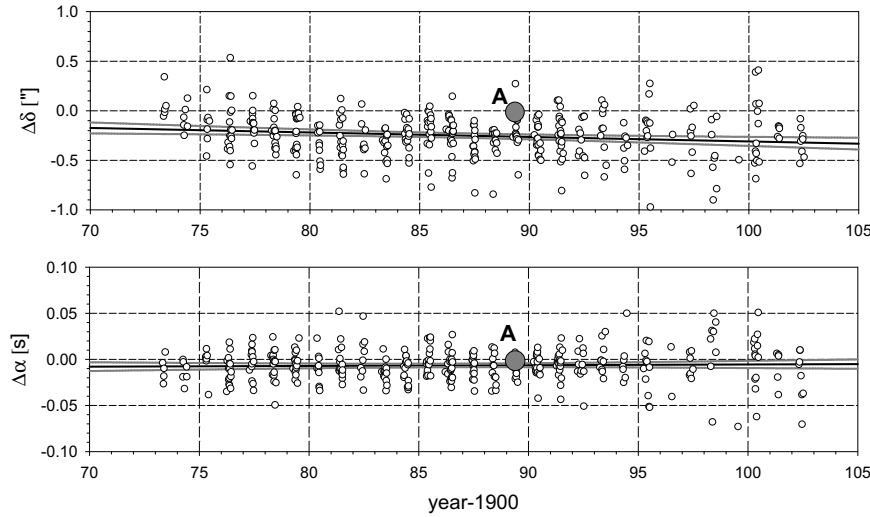
Figure 4.   Example of linear regression: observations with Ondřejov PZT (open circles) of double star 83885; position in Tycho-2 is referred to component A (gray circle), photocenter was observed

- re-compute all available data with the positions and proper motions of EOC-0 (*i.e.*, ARIHIP *etc...*) and the new IAU2000A model of precession-nutation (Mathews, Herring, & Buffet 2002);

- compute the differences of latitude and/or universal time from the mean values of the same night based only on astrometrically excellent stars;

- subject the differences for the same star at different epochs to linear regression;

- check the stars with significant deviations for multiplicity, and estimate the displacement of the reference point (very often photocenter) from the catalogue entry. The corresponding position in EOC-0 is corrected, and the number of the star is increased by 300000.

    An illustrative example of linear regression through observed positions is displayed in Fig. 4. The star with HIP number 83885 is a double star, with its two components 3.45″ apart. Linear regression is depicted as a black line, 95% confidence interval as gray lines. The observations with Ondřejov PZT (open circles) obviously refer to its photocenter, not to the component A (larger gray circle) whose entry is taken from Tycho-2. Consequently, the position in EOC-0 was corrected and the number of the star changed to 383885.

3.1.   Version EOC-1

We have collected the data from 47 instruments of different types, determining latitude and/or universal time, or a mixture of both. They can be divided into four following groups, according to the method of observation that they use:

1. 10 PZTs that observe near local zenith and determine both latitude and universal time:
   2 at Mizusawa, Japan, covering 1959.0-1993.1; 1 at Mount Stromlo, Australia, covering 1957.8-1985.7; 1 at Punta Indio, Argentina, covering 1971.6-1984.5; 1 at Ondřejov, Czech Republic, covering 1973.1-2002.6; 2 at Richmond, Florida, USA, covering 1949.8-1989.4; 3 at Washington DC, USA, covering the interval 1915.8-1992.0;

2. 7 photoelectric transit instruments, observing the transits of stars over the local meridian and determining only universal time:
   1 at Irkutsk, Russia, covering 1979.1-1992.0; 1 at Nikolaev, Ukraine, covering 1974.4-1992.4; 1 at Kharkov, Ukraine, covering 1973.0-1992.0; 3 at Pulkovo, Russia, covering 1959.7-1994.0; 1 at Wuhang, China, covering 1981.9-1987.2;

3. 16 visual zenith telescopes (ZT) and similar instruments (visual zenith tube - VZT, floating zenith telescope - FZT), measuring only latitude:
   7 ZTs at ILS stations (Carloforte, Cincinnati, Gaithersburg, Kitab, Mizusawa, Tschardjui, Ukiah), covering 1899.7-1979.0; 1 ZT at Belgrade, Yugoslavia, covering 1949.0-1986.0; 1 ZT at Blagovestschensk, Russia, covering 1959.0-1992.0; 1 ZT at Irkutsk, Russia, covering 1958.2-1991.0; 1 ZT at Józefoslaw, Poland, covering 1961.8-1996.0; 1 FZT at Mizusawa, Japan, covering 1967.0-1984.8; 2 ZT's at Poltava, Ukraine, covering 1949.7-1990.4; 1 ZT at Pulkovo, Russia, covering 1904.7-1995.0; 1 VZT at Tuorla-Turku, Finland, covering 1963.7-1989.1;

4. 14 equal altitude instruments (Danjon astrolabes - AST, photoelectric astrolabes - PAST, and circumzenithals - CZ) that observe a combination of latitude/universal time:
   1 PAST at Beijing, China, covering 1979.0-1987.8; 1 CZ at Bratislava, Slovakia, covering 1987.0-1991.9; 1 PAST at Grasse, France, covering 1983.2-1992.0; 1 AST at Paris, France, covering 1956.5-1983.0; 1 AST at Pecný, Czech Republic, covering 1970.0-1992.0; 1 CZ at Prague, Czech Republic, covering 1980.2-1992.0; 1 AST at Santiago de Chile, covering 1965.9-1990.9; 2 PAST's at Shaanxi, China, covering 1974.0-1992.0; 1 AST + 1 PAST at Shanghai, China, covering 1962.0-1985.0; 1 AST at Simeiz, Ukraine, covering 1977.0-1991.0; 1 AST at Wuhang, China, covering 1964.0-1986.2; 1 PAST at Yunnan, China, covering 1980.7-1991.3.

The first step in developing the new catalogue, leading to version EOC-1, is to use only the instruments observing in local meridians, *i.e.* the first three groups shown above.

We have obtained the time series of differences (in right ascensions, declinations, or both) between the observed and catalogue position in EOC-0, for each instrument separately. If the same star was observed by several instruments, the corresponding series are merged. In principle, it poses no problem for groups 1 and 2, but the instruments of group 3 observe typically (with only several exceptions, when one or three stars are observed) pairs of stars. For these instruments we thus obtain a mean difference of two declinations, and we face a problem of how to separate these two. We chose to create, from each such series, two new

series (one for each of the two stars) by using the weighting proportional to their squared *rms* error taken from the input catalogue and calculated for the center of the interval covered by observations. In other words, the more precise the original catalogue entry, the smaller the differences in corresponding series and vice versa.

Now the question arises of how to combine a catalogue entry with these series of observations. We create three virtual observations (for the epochs t_1, t_2, t_3) of the same star from the information given in EOC-0: the mean epoch $t_\circ$, *rms* error of the position at this epoch $\sigma_\circ$, and *rms* error of proper motion σ_μ. We chose the solution in which a weighted linear regression made through these three points returns exactly the same values $t_\circ$, $\sigma_\circ$ and σ_μ as given in the input catalogue. Generally, if the central epoch is identified with the one of the input catalogue ($t_2 = t_\circ$) and $t_2 - t_1 = \Delta_1$, $t_3 - t_2 = \Delta_2$, this is achieved by

$$
\begin{aligned}
\sigma_1^2 &= \sigma_\mu^2 \Delta_1 (\Delta_1 + \Delta_2) \\
\sigma_2^2 &= \sigma_\circ^2 \sigma_\mu^2 / (\sigma_\mu^2 - \sigma_\circ^2/\Delta_1\Delta_2) \\
\sigma_3^2 &= \sigma_\mu^2 \Delta_2 (\Delta_1 + \Delta_2).
\end{aligned}
\tag{1}
$$

Choosing an asymmetric distribution of the epochs covering one century, $\Delta_1 = 90$ years, $\Delta_2 = 10$ years, we arrive at

$$
\begin{aligned}
t_1 &= t_\circ - 90, & \sigma_1 &= 94.87\sigma_\mu \\
t_2 &= t_\circ, & \sigma_2 &= \sigma_\circ / \sqrt{1 - (\sigma_\circ/\sigma_\mu)^2/900} \\
t_2 &= t_\circ + 10, & \sigma_3 &= 31.62\sigma_\mu.
\end{aligned}
\tag{2}
$$

The values of σ_i (in mas) are used to compute the weights of the three virtual observations (each of these "observed" values being set to zero) as $p_i = (200/\sigma_i)^2$. They are combined with real observations of the same star whose weights are all equal to 1, under the assumption that their accuracy is 200 mas. The linear regression then yields the corrections to EOC-0 positions and proper motions, to form EOC-1. The comparison of some characteristics of these two catalogues is given in Tab. 1, where median values are displayed. The values of σ are given

Table 1.   Comparison of the catalogues EOC-0 and EOC-1 (σ in mas).

Catalogue	n	Ep_α	σ_α^*	$\sigma_{\mu\alpha}^*$	Ep_δ	σ_δ	$\sigma_{\mu\delta}$
EOC-0	4422	91.25	0.69	0.60	91.26	0.55	0.57
EOC-1	3784	91.18	0.68	0.52	91.10	0.50	0.32

in mas, $\sigma_{\alpha,\mu\alpha}^* = 15\sigma_{\alpha,\mu\alpha} \cos \delta$. The comparison of EOC-0 and EOC-1 shows the improvement brought about by the combination.

4.   Conclusions

At present, only the observations with the instruments observing in local meridians (*i.e.*, PZTs, ZTs and PTIs) are used to form the EOC-1 version of the

new catalogue. It is demonstrated in Tab. 1 that even this preliminary version proves to be more accurate than the input catalogues (ARIHIP, *etc*...). This is true especially for proper motions in declination where the improvement is really substantial, due to very long series of latitude observations. The next step will be to use also the observations with the instruments measuring latitude and universal time by the method of equal altitudes. This problem will be much more complex since the observables (differences in altitude) represent combinations of right ascension and declination differences. We plan to use the EOC catalogue in a new solution of Earth Orientation Parameters in the near future.

References

ESA 1997, The Hipparcos and Tycho Catalogues, ESA SP-1200

Høg, E., Fabricius, C., Makarov, V. V., Urban, S., Corbin, T., Wycoff, G., Bastian, U., Schwekendiek, P., Wicenec, A. 2000, A&A, 355, L27

Lieske, J.H., Lederle, T., Fricke, W. & Morando, B. 1977, A&A, 58, 1

Ma, C., Arias, E. F., Eubanks, T. M., Fey, A. L., Gontier, A.-M., Jacobs, C. S., Sovers, O. J., Archinal, B. A., Charlot, P. 1998, AJ, 116, 516

Mathews, P.M., Herring, T.A. & Buffet, B.A. 2002, J. Geophys. Res., 107 (B4), 10.1029/2001JB000390

Perryman, M. A. C., Lindegren, L., Kovalevsky, J., Høg, E., Bastian, U., Bernacca, P. L., Crz, M., Donati, F., Grenon, M., van Leeuwen, F., van der Marel, H., Mignard, F., Murray, C. A., Le Poole, R. S., Schrijver, H., Turon, C., Arenou, F., Froeschl, M., Petersen, C. S. 1997, A&A, 323, L49

Seidelmann, P.K. 1982, Celestial Mech., 27, 79

Vondrák, J. & Ron, C. 2003, in Journées 2002 Systèmes de Référence Spatio-temporels, ed. N. Capitaine (Observatoire de Paris), 49

Vondrák, J., Pešek, I., Ron, C. & Čepek A. 1998, Publ. Astron. Inst. Acad. Sci. Czech R., 87, 1

Vondrák, J., Ron, C. & Pešek, I. 2000, in ASP Conf. Ser. Vol. 208, Polar motion: Historical and Scientific Problems, Proc. IAU Coll. 178, ed. S. Dick, D.D. McCarthy, & B. Luzum (San Francisco: ASP), 206

Wahr, J.M. 1981, Geophys. J. Roy. Astron. Soc., 64, 705

Wielen, R., Schwan, H., Dettbarn, C., Lenhardt, H., Jahreiss, H., Jährling, R. 1999, Veröff. Astron. Rechen-Inst. Heidelberg No. 35 (Karlsruhe: Kommissions-Verlag G. Braun)

Wielen, R., Schwan, H., Dettbarn, C., Lenhardt, H., Jahreiss, H., Jährling, R., Khalisi, E. 2000, Veröff. Astron. Rechen-Inst. Heidelberg No. 37 (Karlsruhe: Kommissions-Verlag G. Braun)

Wielen, R., Schwan, H., Dettbarn, C., Lenhardt, H., Jahreiss, H., Jährling, R., Khalisi, E. 2001a, Veröff. Astron. Rechen-Inst. Heidelberg No. 38 (Karlsruhe: Kommissions-Verlag G. Braun)

Wielen, R., Schwan, H., Dettbarn, C., Lenhardt, H., Jahreiss, H., Jährling, R., Khalisi, E. 2001b, Veröff. Astron. Rechen-Inst. Heidelberg No. 39 (Karlsruhe: Kommissions-Verlag G. Braun)

Wielen, R., Schwan, H., Dettbarn, C., Lenhardt, H., Jahreiss, H., Jährling, R., Khalisi, E. 2001c, Veröff. Astron. Rechen-Inst. Heidelberg No. 40 (Karlsruhe: Kommissions-Verlag G. Braun)

Astrometry With Large Un-Astrometric Telescopes

Imants Platais

Department of Physics and Astronomy, Johns Hopkins University,
Baltimore, MD 21218

Abstract.
Over the last few decades the number of large telescopes has grown dramatically. These new telescopes were designed to produce sharp images of stars and galaxies and are not necessarily optimized for astrometric measurements. Despite this and some other limitations cutting-edge astrometry can be done with such instruments. Space-based CCD imagers can easily break the 1-mas precision limit, while ground-based telescopes are currently limited to accuracies of 3-5 mas. It is expected that the Large Synoptic Survey Telescope will produce a 15 petabyte imaging database down to $V = 28$ and over 30,000 square degrees of the sky, which opens new horizons for astrometry.

1. Introduction

More than a century ago the invention of the photographic process ushered in a new era in astrometry. The whole sky could be photographed and saved on plates for posterity, which made possible follow-up determinations of positions, proper motions and parallaxes on a massive scale. Most of the existing large star catalogs have their roots in this technology. Besides new wide-field detectors, a new trend in telescope making also started to make headway. While the Yerkes 40-in refractor from 1897 until 1909 was the world's largest functioning telescope, the race for ever-larger apertures was clearly won by reflectors. This trend, however, did not impress astrometrists who continued to cling to the proven refractors and their offshoots – multiple-lens astrographs. At the time, the advantages of refractors were fairly obvious. Only astrographs could deliver an essentially distortion-free field of view over many square degrees on the sky. This had an important practical aspect since the measured cartesian coordinates could be easily translated into the celestial coordinates using a simple linear model tractable by the then-available means of calculation. Although the moderate aperture astrographs have a fairly shallow magnitude floor at about $m_{pg} = 15$, back then that was more than enough for the pressing needs in astrometry.

This order of matters lasted for many decades when in the 1990s astrometrists were caught up with developments in the other fields of astronomy – some welcome and some not so. A considerable challenge was raised by the Hubble Space Telescope (HST) operational needs and capabilities. It was the HST which required a relatively deep and dense all-sky catalog of positions – the Guide Star Catalog (Lasker *et al.* 1990). This catalog was constructed from the measurements of Schmidt telescope plates, considered by astrometrists to be a rather poor choice albeit having no alternative at the time. If one wanted to do astrom-

etry with the HST, the tiny field of view (FOV) and strong distortions in the focal plane made this task quite daunting. However, astrometrists were really caught unprepared when the major companies stopped manufacturing the astronomical photographic plates. As opposed to a photographic plate a single-chip CCD device covers only a tiny fraction of the useful FOV. Unfortunately, the CCD mosaic imagers are too expensive to afford, particularly on small astrometric telescopes. Today's reality is such that astrometry is already an integral part of large imaging projects like the Two Micron All Sky Survey (2MASS) and the Sloan Digital Sky Survey (SDSS) and we should ready ourselves to use the available telescopes to carry out astrometric projects despite the possible limitations that such "un-astrometric" instruments may have. The shift of scientific interests towards the low mass and faint objects in our Galaxy (*e.g.*, cool main sequence dwarfs, brown dwarfs, extrasolar planets, remnants of stars) requires access to large telescopes with apertures over 100 inches. It is therefore instructive to look into the recent progress and difficulties of astrometric work with such telescopes.

2. Telescopes and Imaging Hardware

World-wide to date there are 38 operational imaging telescopes,[1] and several more are under construction, with apertures equal to or exceeding 100 inches. For imaging purposes, most of them have single-CCD-chip devices yielding a typical FOV from $\sim 5' \times 5'$ to $\sim 10' \times 10'$. Only CCD mosaic imagers can deliver a substantially larger FOV without a loss of resolving power (Groom 2000). The entire useful FOV of the 3.6-m Canada-France-Hawaii Telescope, equal to a full square degree, is covered by the MegaPrime camera – the world's largest operational CCD mosaic device of its kind (a 20K×18K array). Of great potential interest to astrometry is also the WIYN 3.5-m telescope One Degree Imager employing 4096 so-called orthogonal transfer CCDs, currently under development (Jacoby *et al.* 2002). This kind of imager offers a low-order adaptive optics capability, which is crucial for short exposures and in high spatial resolution work.

Smaller size CCD mosaic imagers (8K×8K covering $36'$ on a side) are available at the KPNO and CTIO 4-m telescopes. The NOAO CCD Mosaic Imager, has served as "proving ground" to explore the astrometric potential of these devices (Platais *et al.* 2002).

3. Calibrating the CCD Mosaic

A fundamental difference between a photographic plate and a CCD mosaic is that the latter does not have a contiguous light-sensitive area and each CCD chip has its own unique characteristics. Routine flat-fielding takes care of the flux calibration over the entire CCD mosaic but is incapable of characterizing its geometry. In a typical CCD mosaic the buttable CCD chips are attached to a mounting plate in close-packed configuration (gaps smaller than one mm).

---

[1] see WWW at http://www.seds.org/billa/bigeyes.html
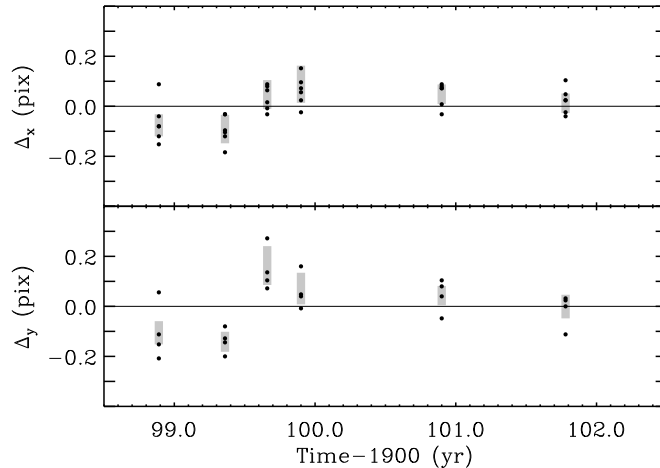
Figure 1.   Deviation of the mean chip-to-chip separation in the NOAO CCD Mosaic Imager as a function of time. The shaded bars indicate a $\pm 1\sigma$ interval around the mean gap location. (Adapted from Platais *et al.* 2002).

Normally the packing fraction *i.e.*, the percentage of a useful CCD mosaic's area, is 90-98%. In order to use the entire CCD mosaic as a single "plate", one has to find the so-called chip constants – position of the chip center and a rotation angle – with respect to a global coordinate system. The most convenient way to obtain these constants is to use an astrometric standard (Platais *et al.* 2002). An extensive monitoring of chip constants over a span of three years indicated that the metric of NOAO CCD Mosaic Imager has experienced a one-time change (Fig. 1) resulting in the gap enlargement. Apparently, astrometric calibrations of CCD mosaics should be performed on a regular basis, particularly if the dewar has been thermally cycled.

Observing relatively bright astrometric standards (V<18) with large-aperture telescopes implies short exposure times to avoid saturated images. This creates a specific problem related to atmospheric noise. During short exposures (less than $\sim$15 s) the correlated motions of stars in atmospheric cells do not entirely randomize and thus leave a semiregular pattern (Fig. 2a). Neglecting that will result in systematic errors in the positions. Without adaptive optics the consequences of this effect can be reduced only by taking multiple exposures and then averaging the positions.

4.   Astrometry with Ground-based Reflectors

In proper-motion work it is assumed that the focal plane of the telescope is geometrically correct, *i.e.* the plate reductions can be limited to a linear model plus tilt terms. By the virtue of optical design the focal planes of long-focus reflectors and multi-lens astrographs normally are flat and geometrically undistorted. However, the focal planes of nearly all large reflectors are distorted, with radial pincushion distortion dominating. To make matters more complicated, the field corrector today could be different from what it is was in the early days – as for the KPNO 4-m telescope. An incomplete third-order polynomial sup-
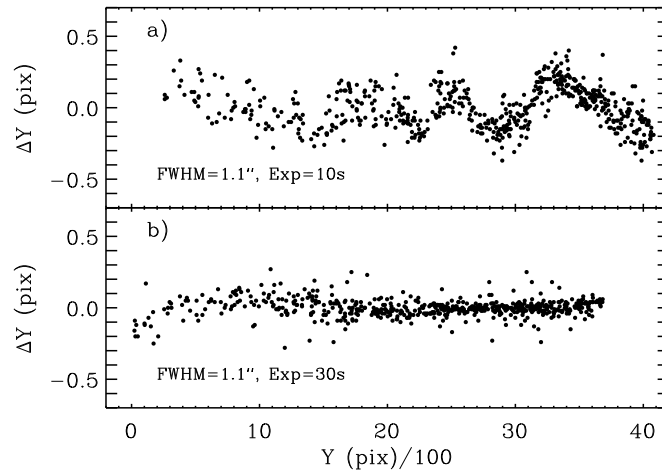
Figure 2. Coordinate differences from two consecutive slightly dithered exposures. If a short exposure time is used, correlated motions due to atmospheric noise persist. (Adapted from Platais *et al.* 2002).

plemented with a fifth-order term is sufficient to fully represent the distorted coordinates in large-telescope focal planes (Platais *et al.* 2002). Another way to tackle the problem of distortions is to pre-correct for it. However, that requires a good knowledge of the optical field angle distortions (OFAD). If the OFAD center is not known, it is necessary to obtain such using the all-sky USNO-B catalog (Monet *et al.* 2003). The high-precision distortion coefficients usually are available in the literature.

With all necessary precautions, the astrometric precision delivered by a large-aperture reflector is impressive. Thus the first-epoch plate material in combination with numerous CCD images, all from the KPNO 4-m telescope, yields a positional precision of 2 mas and the proper motion accuracy as good as 0.15 mas yr^{-1} over a large range of magnitudes (Platais *et al.* 2003). If faint magnitudes ($V>20$) are considered, then there is no alternative to large reflectors, which should be carefully calibrated to reach the precision these telescopes can deliver.

5. Small-field space astrometry with HST

A major impediment in ground-based astrometry is the presence of atmospheric noise in observations. With adaptive optics it can be contained over the range of a few arc-seconds, however, for larger scales we must go outside the atmosphere. The Hubble Space Telescope (HST) is the only imaging telescope currently available for astrometric work in the sub-milli-arc-second regime at faint magnitudes. While the HST interferometric instrumentation is used by astrometrists on a regular basis (*cf.* Benedict *et al.* 2002), direct imaging surprisingly is almost untapped. One may speculate that a small field-of-view, only $\sim2\rlap{.}'5 \times 2\rlap{.}'5$, of the Wide Field Planetary Camera 2 (WFPC2) could be a reason for such ignorance. It is well-known that each of the four WFPC2 cameras yields a significant geometric distortion in the focal plane (Holtzman *et al.* 1995). Only recently the distortion has been documented at the 1-2 mas precision level (Anderson &

OBSERVED SCALE FOR GILLILAND'S OBSERVATIONS
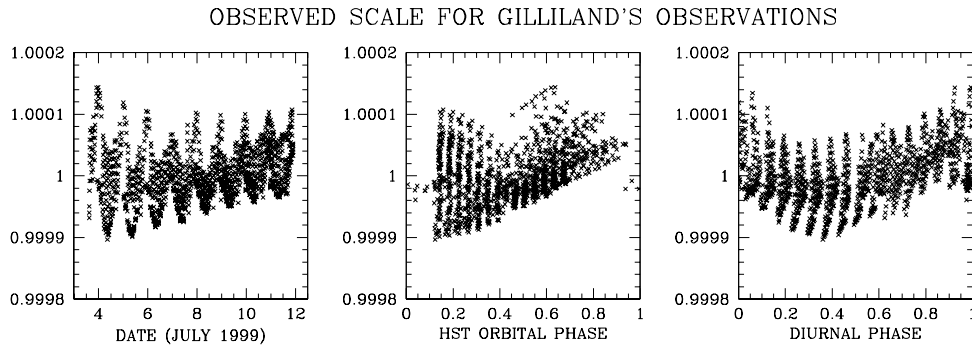
Figure 3.   The scale factors from Gilliland's GO-8267 observations of 47 Tuc as a function of date, HST orbital phase, and diurnal phase. (Adapted from Anderson & King 2003a).

King 2003a) which now allows a 0.5 mas yr^{-1} precision of proper motions to be obtained over just a five-year span (*cf.* Anderson & King 2003b) – equivalent to a $\sim$30 yr time span with a ground-based refractor. Unfortunately, it appears that the WFPC2 chip constants cannot be determined to better than $\sim$0.2 pix due to the intrinsic and unpredictable scatter from frame to frame (Anderson & King 2003a). This confines precision astrometry to each individual chip rather than the whole useful FOV of WFPC2. Thus with small numbers of reference stars, say, a few dozens per CCD chip, the modelling error may be too large to yield precise positions and proper motions. As shown by Anderson & King (2003b), the astrometric performance of the WFPC2 chips is close to ideal in dense stellar environments, such as the cores of globular clusters, having plenty of reference stars.

5.1.   Distortion in WFPC2 and ACS

The studies of distortion by Anderson & King (2003a) and Anderson (2002) highlighted some aspects relevant not only to the HST but also to the future space astrometry missions such as GAIA and AMEX. A very extensive set of observations of the cores of the globular clusters ω Cen and 47 Tuc, analyzed by Anderson & King, is the key element leading us to the present knowledge of the distortion and its characteristics. For example, a contiguous 8-day stare at the core of 47 Tuc reveals a distinct pattern in the changes of the observed plate scales (Fig. 3). Since the scale is variable on the order of up to one part in 10,000, it also causes discernable 1-2% changes in the amount of distortion, which corresponds to $\sim$5 mas at the corner of the Wide Field Camera. The HST is not optimized in terms of insulation pattern and related thermal cycling but it is likely that such an effect in the future space astrometry missions probably will be smaller by 2-3 orders of magnitude. Nonetheless, if we assume a similar amount of distortion to WFPC2, produced by the optics of an astrometric mission, even after much better thermal stabilization it may result in a hefty 50 μas of changes in the distortion. To minimize this effect would require designing such optical systems in which the distortion itself is also minimized.

TABLE CORRECTION FOR X   TABLE CORRECTION FOR Y
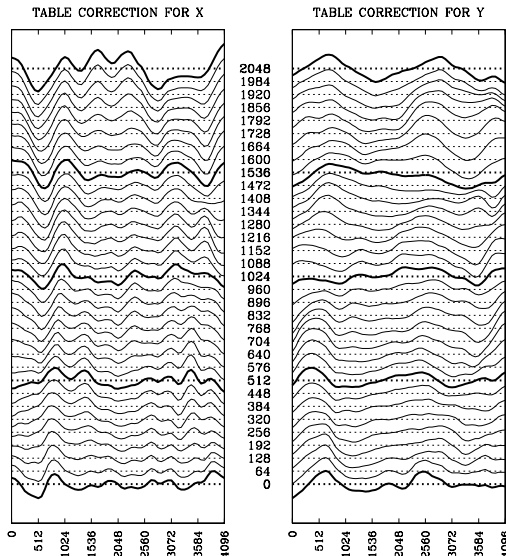
Figure 4.   Graphical presentation of the WFC1 table of corrections. Such corrections usually are not exceeding 0.05 pix and cannot be modelled adequately by a polynomial. (Adapted from Anderson 2002).

A third generation imaging instrument, the Advanced Camera for Surveys (ACS), has the potential to routinely obtain positions with sub-mas precision per exposure (Anderson 2002) as shown for its Wide Field Camera (WFC) having a 50 mas pixel size. This involves two key ingredients: i) a precise Point-Spread Function for the undersampled HST images, ii) accurate modelling of the geometric distortion. Both requirements are, of course, equally valid for the WFPC2 as well. The precision of positions with ACS is so high that a very tiny manufacturing defect on the order of 0.008 pix in each 68th column can be easily detected. Among the various characteristics of the WFC, perhaps one of the most interesting is the high-frequency part of the distortion, as illustrated by Fig. 4. A typical amplitude of such unmodelled distortion is ∼0.05 pix or 2.5 mas, which can be corrected for using a look-up table. The high-frequency part of the distortion is also filter-dependent. The origin of such dependency is not understood but it is clear that at a very high level of precision new effects are appearing, which were earlier hidden in the noise. This is definitely another area where designers of space-grade optics for astrometry should take notice.

6.   Pushing to Fainter Magnitudes – the Case of LSST

Astrometrists have a keen interest in expanding the International Celestial Reference Frame (ICRF) to much fainter magnitudes. One reason for that is a desire to observe objects which are intrinsically faint in optical wavelengths but could be much brighter in other wavelengths, *e.g.* in the radio, which today provide the crucial benchmarks for the ICRF. Although there is no current or planned astrometric survey at magnitudes $V > 20$, one future ground-based project is very appealing from the standpoint of astrometry. The Large Synoptic Survey

Telescope [2] facility offers enormous throughput at a very fast speed of surveying. Capable of reaching 24th magnitude in ten seconds and covering seven square degrees at once, each month the LSST will survey up to 14,000 sq. degrees in several filters. This effort will ultimately lead to a 30,000 sq. degree survey in multiple bandpasses allowing a 10σ limiting magnitude of $V = 28$ to be reached (Tyson 2002). It is not surprising that such an extraordinary survey needs innovative technology – like the chosen Paul 3-mirror optical design and a huge 2.3 Gpix CMOS (or CCD) mosaic. An opto-mechanical system of that complexity and unprecedented configuration has not been tested astrometrically. It may require new approaches similar to the self-calibration implemented by Anderson & King for the HST. Obviously, the short exposures will be adding another layer of complexity as indicated by the KPNO 4-m telescope observations (see Sect. 4). In the context of LSST it is instructive to examine how much the 2MASS positions differ from the now-available high-precision coordinates (Platais *et al.* 2003) in the direction of the open cluster NGC 188 (Fig. 5). Evidently, the 2MASS coordinates are not free from some step-wise looking systematics originating from inadequatedly "pasted" sky tiles. That kind of pattern should and can be eliminated by the appropriate adjustment and thus allow it to reach the intrinsic precision floor provided by the telescope and its detectors.
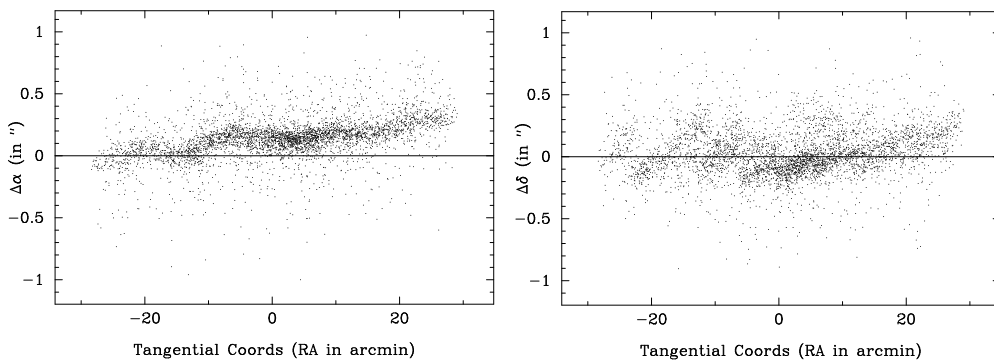
Figure 5.   Differences between the astrometric standard around NGC 188 and the 2MASS catalog as a function of tangential coordinates (right ascension).

7.   Conclusions and Outlook

The few examples presented here show that the future undoubtly belongs to "un-astrometric" telescopes having a segmented detector plane with various degrees of packing fraction. There are two key issues to resolve: 1) to put a mosaic of single detectors onto the global coordinate system; 2) to correct this coordinate

---

[2]see WWW at http://www.lssto.org

system for the focal plane distortion. Both may contain some time-dependent component, hence a strategy must be developed to calibrate it. If after that we wish to put our cartesian coordinates into the International Celestial Reference System, we need appropriate reference stars, which currently is problematic for small fields such as generated by the HST imaging instruments. However, very deep surveys like the one proposed with the LSST consortium can in principle be self-calibrated over a large area of the sky and then anchored to the reference objects of ICRS. That would provide an efficient link between the small-field space-based and the whole sky ground-based astrometry in advance of the upcoming astrometric space missions.

References

Anderson, J. & King, I. R. 2003a PASP, 115, 113

Anderson, J. & King, I. R. 2003b, AJ, 126, 772

Anderson, J. 2002, in The 2002 HST Calibration Workshop, ed. S. Arribas, A. Koekemoer & B. Whitmore, 13

Benedict, G. F. *et al.* 2002, AJ, 124, 1695

Groom, D. E. 2000, Proc. SPIE, 4008, 634

Holtzman, J., *et al.* 1995, PASP, 107, 156

Jacoby, G. H., Tonry, J. L., Burke, B. E., Claver, C. F., Starr, B. M., Saha, A., Luppino, G. A. & Harmer, C. F. W. 2002, Proc. SPIE, 4836, 217

Lasker, B. M., Sturch, C. R., McLean, B. J., Russell, J. L., Jenkner, H. & Shara, M. M. 1990, AJ, 99, 2019

Monet D. G. *et al.* 2003, AJ, 125, 984

Platais, I. *et al.* 2002, AJ, 124, 601

Platais, I., Kozhurina-Platais, V., Mathieu, R. D., Girard, T. M. & van Altena, W. F. 2003, AJ, 126, 2922

Tyson, J. A. 2002, Proc. SPIE, 4836, 10

Status of Space-Based Astrometric Missions

Ralph A. Gaume

U.S. Naval Observatory, 3450 Massachusetts Avenue NW, Washington DC,
20392-5420, USA

Abstract. Since the highly successful Hipparcos space-based astrometry mission (1989-1993), a number of follow-up programs have been proposed to accomplish a wide variety of scientific goals. Due in part to funding pressure and technical challenges, the status of these missions has changed on a near continuous basis (proposal, selection, descope, cancellation, rescope, reproposal). The status, capabilities, operational concepts, and other salient features of the current set of space-based astrometric missions (DIVA, AMEX (SMEX), AMEX (MIDEX), FAME, JASMINE, SIM-PlanetQuest, Gaia, and OBSS) are discussed.

1. Introduction

Compared to ground-based telescopes, astronomical space-based observatories offer distinct advantages while simultaneously presenting numerous additional challenges, including expense; space-based observatories are always more expensive than ground-based telescopes of comparable aperture. In the specific case of astrometry, one major advantage of space is that the accuracy of a space-based observatory is not limited by atmospheric distortion. Also, systematic errors can be reduced compared to ground based observatories owing to the comparatively benign environment of space allowing extremely stable mechanical designs, with residual mechanical changes determined from the utilization of precision metrology systems.

Hipparcos is the world's first, and up to this point only, dedicated space astrometry mission. Owing in part to the great success of the Hipparcos mission, a number of follow-up space astrometry missions have been discussed, planned, proposed, funded, scheduled for launch, rescoped, descoped, and in some cases, cancelled. It is often difficult to keep track of the current status of the various space astrometry missions due in part to the quickly changing nature of the organizational priorities and funding resources of the major national and international space astronomy agencies. This manuscript provides a brief synopsis, Concept of Operation (ConOps), and status of a number of space astrometry missions, beginning with Hipparcos.

2. Hipparcos

• **Synopsis:** First and only dedicated astrometric space mission. Hipparcos was highly successful, despite failure to achieve planned orbit. The great success of Hipparcos has spawned the new generation of space astrometry missions described in this manuscript.
• **Acronym: Hi**gh **P**recision **Par**allax **Co**llecting **S**atellite.
• **Funding Agency: E**uropean **S**pace **A**gency (**ESA**).

- **Launch:** Aug 08, 1989. Operations terminated Aug 15, 1993.
- **ConOps:** Continuous scanning. Two optically combined fields of view.
- **Number of Objects:** 120,000 (Hipparcos), 2.5×10^6 (Tycho-2).
- **Magnitude Range:** 0-12.5 m_v (Hipparcos), 0-12th m_v (Tycho-2).
- **Astrometric Accuracy:** 1 mas @ 9th (Hipparcos), 7 mas @ 9th.
- **Additional Information:** http://astro.estec.esa.nl/Hipparcos

3. FAME

- **Synopsis:** A NASA Medium Explorer (MIDEX) mission. NASA support was withdrawn in January 2002 after completing a preliminary design review, due to uncertainty surrounding detector development, and significant mission cost growth. FAME would have provided a bridge between Hipparcos and higher accuracy missions like Gaia, SIM, and OBSS.
- **Acronym:** **F**ull-sky **A**strometric **M**apping **E**xplorer.
- **Funding Agency:** **N**ational **A**eronautics and **S**pace **A**dministration (**NASA**).
- **Launch:** November 2004 (Planned). Five year mission.
- **ConOps:** Continuous scanning. Two optically combined fields of view.
- **Number of Objects:** 40×10^6 stars.
- **Magnitude Range:** 5-15th m_v.
- **Astrometric Accuracy:** 50 microarcseconds @ 9th magnitude.
- **Additional Information:** http://www.usno.navy.mil/FAME

4. DIVA

- **Synopsis:** A relatively low cost bridge between Hipparcos and higher accuracy missions like Gaia, SIM, and OBSS, DIVA was cancelled in January 2003, due to a moderate funding shortfall. DIVA had progressed through the preliminary design review stage.
- **Acronym:** **D**eutsche **I**nterferometer für **V**ielkanalphotometrie und **A**strometrie.
- **Funding Agency:** **D**eutsches **Z**entrum für **L**uft- und **R**aumfahrt (**DLR**).
- **Launch:** 2006 (Planned). Two year mission.
- **ConOps:** Continuous scanning. Two optically combined fields of view.
- **Number of Objects:** 40×10^6 stars.
- **Magnitude Range:** 5-15th m_v.
- **Astrometric Accuracy:** 200 microarcseconds @ 9th magnitude.
- **Additional Information:** In addition to the sky mapper (astrometric) survey, DIVA was to produce a spectroscopic survey of the brightest 12 million stars and a UV survey of 15 million and 30 million stars at short and longer UV wavelengths, respectively. See: http://www.ari.uni-heidelberg.de/diva/diva.html

Figure 1.   Artists conceptions of the various space astrometry missions. From top left, Hipparcos, DIVA, FAME, second row, AMEX, JASMINE, SIM PlanetQuest, third row, Gaia, OBSS.

5. AMEX (SMEX)

- **Synopsis:** AMEX was a mission proposed to the NASA Small Explorer (SMEX) program. The proposed AMEX program involved an international collaboration, jointly funded by the DLR and NASA. AMEX was primarily based on the DIVA design. A proposal to perform an AMEX concept study was rejected by NASA administrators.
- **Acronym: A**strometric **M**apping **Ex**plorer.
- **Funding Agency:** NASA & DLR.
- **Launch:** 2007 (proposed). Three year mission.
- **ConOps:** Continuous scanning. Two optically combined fields of view.
- **Number of Objects:** 40×10^6 stars.
- **Magnitude Range:** $7\text{-}15^{th}$ m_v.
- **Astrometric Accuracy:** 200 microarcseconds @ 9th magnitude.

6. AMEX (MIDEX)

- **Synopsis:** The U.S. Naval Observatory, in collaboration with NASA-JPL, has continued to develop a more capable version of the DIVA and AMEX (SMEX) mission concept, intended to be proposed to the NASA MIDEX program. Due to changing institutional priorities, in Feb 2004 NASA announced that the next MIDEX proposal opportunity would be significantly delayed. Instrument design, development, and costing activities, along with detector and reduction software development continue.
- **Acronym: A**strometric **M**apping **Ex**plorer.
- **Funding Agency:** NASA (potential).
- **Launch:** 2009 (potential), 5 year mission.
- **ConOps:** Continuous scanning. Two optically combined fields of view.
- **Number of Objects:** more than 40×10^6 stars.
- **Magnitude Range:** 7 to fainter than 15th m_v.
- **Astrometric Accuracy:** approximately 100 microarcseconds @ 9th mag.

7. JASMINE

- **Synopsis:** JASMINE is a Japanese infrared space astrometry satellite, operating at near-IR wavelengths.
- **Acronym: J**apanese **A**strometry **S**atellite **M**ission for **I**nfrared **E**xploration.
- **Launch:** 2013-2015 (potential). Five year mission lifetime.
- **ConOps:** Continuous scanning, galactic plane. Two optically combined fields of view.
- **Number of Objects:** a few 100×10^6.
- **Astrometric Accuracy:** 10 microarcseconds at $m_z = 15.5$ or K=12th.
- **Additional Information:** http://www.jasmine-galaxy.org/

8. SIM PlanetQuest

- **Synopsis:** SIM PlanetQuest is a space-based optical interferometer operating in an earth-trailing orbit. Currently, SIM and Gaia are the only funded space astrometry missions.

- **Acronym: S**pace **I**nterferometer **M**ission.
- **Funding Agency:** NASA.
- **Launch:** 2010 (planned). Five year baseline mission, potential ten year extended mission.
- **ConOps:** SIM PlanetQuest is a pointed mission with predefined targets.
- **Number of Objects:** about 10,000 stars (1,300 grid stars).
- **Magnitude Range:** brighter than (a limiting magnitude of) about 20th.
- **Astrometric Accuracy:** 4 microarcseconds wide angle, 1 microarcsecond narrow angle.
- **Additional Information:** SIM Planetquest is currently in mission development Phase B (Preliminary Design phase). See: http://planetquest.jpl.nasa.gov/SIM

9. Gaia

- **Synopsis:** Gaia is a funded space astrometry mission intended to launch in 2010-2012. Operating at L2, Gaia consists of three instruments which provide astrometric, photometric, and spectroscopic data.
- **Funding Agency:** ESA.
- **Launch:** before 2012 (planned). Five year operation phase.
- **ConOps:** Continuous scanning. Two optically combined fields of view.
- **Number of Objects:** 10^9.
- **Magnitude Range:** 7-20th magnitude.
- **Astrometric Accuracy:** 10 microarcseconds @ 15th m_v.
- **Additional Information:** In addition to astrometry, Gaia will provide 12 band millimagnitide photometry, radial velocity data for brighter stars to an accuracy of a few km/s and spectrophotometry in the visible and near-IR to m_v 17.5. See: http://www.rssd.esa.int/gaia/

10. OBSS

- **Synopsis:** The U.S. Naval Observatory, in collaboration with NASA-JPL, were funded to investigate, study, and develop the OBSS mission as a possible future mission concept within the NASA Astronomical Search for Origins Program. Future funding for OBSS is uncertain, at present.
- **Acronym: O**rigins **B**illions **S**tar **S**urvey.
- **Funding Agency:** NASA.
- **Launch:** next decade (potential).
- **ConOps:** Pointed mission, flexible ConOps.
- **Number of Objects:** 10^9.
- **Magnitude Range:** $\approx 5.5 - 21^{th}$ magnitude, depending on adopted ConOps.
- **Astrometric Accuracy:** Depends on ConOps, but OBSS is capable of obtaining ≈ 8 microarcseconds single epoch astrometric accuracy on a 15th magnitude star in a few hours.
- **Additional Information:** http://www.usno.navy.mil/OBSS

Realization of the inertial frame with GAIA

François Mignard

OCA/CERGA, av. Copernic, F06130 Grasse

Abstract. The ESA astrometry mission GAIA scheduled for launch in mid-2010 will observe thousands of extragalactic sources together with nearly one billion stars. With a target accuracy of 10 μas at $V = 15$ and 50 μas at $V = 18$, this will open a new era in the realization of the primary reference frame. The very principles of this direct realization in the visible are outlined in this paper together with a discussion of modelling problems or intrinsic limitations due to the galactic rotation, source instability or the occurrence of gravitational lensing.

1. Introduction

The adoption of the ICRS on 1 January 1998 was a landmark in the long history of astronomically defined reference frames (Ma *et al.*, 1998) and a noticeable historical break in this field. Starting from Bessel in the last century, the fixed celestial directions were associated with fundamental catalogues of positions and proper motions of stars, resulting from observations attached in various ways to the apparent motion of the Sun. The short-lived FK5 published in 1988 (Fricke *et al.*) was the ultimate representative of this chain of primary reference catalogues, a species now extinct.

The main novelty in the ICRS lies in the adoption of a kinematical system which assumes that the visible Universe does not rotate as a whole, so that the most distant sources have no individual motion relative to each other. As a whole these sources define and materialize a kinematical non-rotating reference system. The extragalactic reference frame is assumed to approximate an inertial frame, defined within the context of General Relativity, through Mach's Principle. In addition to the constraint of lack of transverse motion, the relevant sources should possess minimal intrinsic source structure at the mas level in the region of energy production. Their positional stability has been continuously investigated since, and so far the situation is rather satisfactory (Gontier *et al.*, 2001). There is no best *a priori* method of observation to build the catalogue and the final choice of using radio observations was dictated by the practical possibilities of the 80s. Another choice could be made in the future should the technology permit it.

Today Very Long Baseline Interferometry (VLBI) allows us to have a consistent solution for the positions of extragalactic radiosources to better than 0.5 mas. No major improvement (say by a factor two or three) is expected within the next decade. The primary reference frame (ICRF) consists of a catalogue with the coordinates of the 667 extragalactic radiosources (212 defining sources) derived from several million observations collected over more than fifteen years by a worldwide network. In the visible the subset of best solutions of

the Hipparcos Catalogue (ESA, 1997) was linked to the ICRF to build the optical counterpart (Kovalevsky *et al.*, 1997). It then gives astronomers a nearly direct access to the ICRS and meets most of their needs in this wavelength range. However the quality of the link will deteriorate with time as a result of the limited accuracy of the HIPPARCOS proper motions.

A mission like GAIA will permit a realization of the ICRS more accurate by two or three orders of magnitude from direct observations of the defining sources brighter than magnitude 20 and also by adding in the visible thousands of QSO's recognized from ordinary stars or white dwarfs with the broad- and narrow-band photometry. The sky coverage will be fairly uniform outside a zone of ± 25 degrees centered on the galactic plane. As GAIA will survey the quasars down to an apparent magnitude of 20, there will be plenty of material (about 500 000 from current estimates based on local surveys) to select a small sample, maybe less than 10 000 very clean sources, to construct the primary reference frame directly in the visible, allowing easy access to astronomers.

2.   Introduction: GAIA

GAIA is the European Space Agency mission selected as a Cornerstone 6 within the agency science program. GAIA is a survey satellite designed to provide astrometry, multi-color and multi-epoch photometry and spectroscopy on all objects brighter than $V \approx 20$. (ESA 2000, Perryman *et al.* 2001). GAIA observing principles are similar to those employed so successfully by HIPPARCOS with a scanning satellite observing simultaneously in two widely separated (106 degrees) directions. It will gather detailed positional, kinematical and physical properties of the brightest 1 billion celestial objects in the sky, sampling virtually all kind of stars, moving objects of the solar system and very distant extragalactic sources. Astrometric accuracies of 10 μas at 15th mag. should lead to 20 million stars measured with distance accuracies better than 1%.

In 2002, a new design of the satellite was proposed following a system re-assessment phase, reducing its cost, without changing the scientific performance, at the expense of a slightly longer mission. The selection was confirmed by ESA in June 2002, with a target launch date of mid-2010. The scientific preparation for the mission involves the participation of some 15 working groups sharing responsibility for the simulation, the data processing, the science modelling and the instrument optimization. Extensive simulation programs have been developed feeding all the groups with input data required to test the processing.

Regarding the extragalactic sources, GAIA will contribute significantly to the knowledge of quasars in providing for the first time an all sky flux limited survey to $V = 20$, very difficult to carry out from the ground. The internal autonomous multi-color detection will be very efficient to get rid of the traditional contaminants like the white dwarves, and will permit the selection of a 99.9% star-free sample of QSO's. Simultaneously photometric redshift measurements will be feasible without additional effort for most of the detected sources. At the end one may reasonably expect a census of several hundred thousand quasars at galactic latitudes $|b| > 20° - 25°$. Finally the extensive zero-proper motion survey will provide a direct realization of the quasi-inertial celestial reference frame with a residual rotation less than 0.5 μas yr^{-1} and a space density at

least hundred time larger than that achieved by the radio version of the ICRF. Many more secondary sources (stellar or extragalactic) will also contribute to the access to this frame.

3.   An ICRF with GAIA

As mentioned earlier the choice of the radio technique to materialize the celestial reference system was dictated by practical reasons : there was no other means of observation with the required accuracy to perform the task. GAIA will provide a consistent, nearly all-sky (no observation of extragalactic sources in the galactic plane and its immediate vicinity) rigid sphere of purposely selected QSO's with positional accuracy on each source between 10μas to 150μas at the faint end. Without an additional constraint this quasi-inertial sphere is free to rotate with respect to an idealized inertial frame and its initial orientation has no particular tie with the existing frames. So one must devise a procedure to eliminate the global rotation, discarding during this process the sources showing transverse motions of non-rotational origin. This step will be a very severe test of the underlying principles on which the ICRF concept rests. Obviously the discovery of sources with undisputable and unaccounted for transverse motion will be a result of major cosmological significance.

3.1.   The residual Spin

The spin vector of the GAIA frame with respect to the ICRS will be constrained by imposing that the selected sample of $\sim 10\,000$ extragalactic sources exhibits no overall rotation. One assumes that the intermediate astrometric sphere is rotating relative to the extragalactic sources with the spin vector $\omega_x, \omega_y, \omega_z$ and that the extragalactic sources have no peculiar transverse motion. In this case the observed components of the proper motion are only due to the global spin motion and to random errors.

The observation equations for the components of the spin are then given by

$$\mu_l \cos b \;\; = \;\;\;\; \omega_x \sin b \cos l + \omega_y \sin b \sin l - \omega_z \cos b \tag{1}$$

$$\mu_b \;\; = \;\; -\omega_x \sin l + \omega_y \cos l \tag{2}$$

where the left hand side contains the observed proper motion components. The information contained in a particular source is given by the weighted square of the coefficients of the ω_i, neglecting the off-diagonal terms, always small because the distribution is evenly sampled in longitude. The inverse of the information is proportional to the variance of the spin components. The total available information (Fisher information in statistics) on ω_x, ω_y, ω_z is then given by the diagonal terms of the normal matrix as,

$$\mathcal{I}_{\omega_x} \;\; = \;\; \sum_1^n W_i \left(\sin^2 b_i \, \cos^2 l_i + \sin^2 l_i \right), \tag{3}$$

$$\mathcal{I}_{\omega_y} \;\; = \;\; \sum_1^n W_i \left(\sin^2 b_i \, \sin^2 l_i + \cos^2 l_i \right), \tag{4}$$
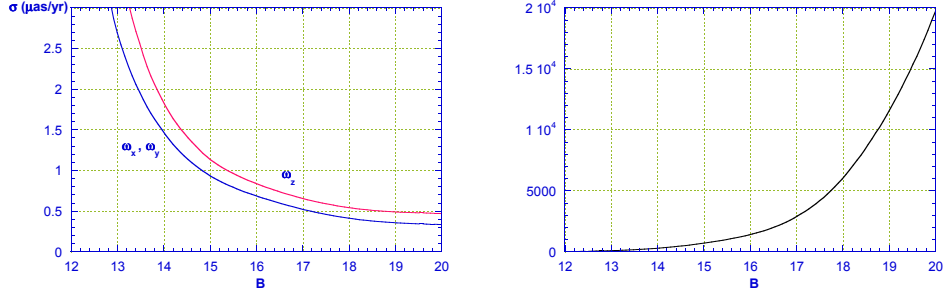
Figure 1.   Left : Precision of the spin rate of the inertial frame determined with GAIA from the observations of the quasars. The precision for a B magnitude is determined when only sources brighter than B are selected. Here galactic coordinates have been used and the random instability has been taken equal to 20 μas yr^{-1}. Though there are many more faint objects than bright ones, the frame is primarily determined with the brightest sources, because of the better astrometric precision. Right : cumulative number of objects brighter than B in the solution .

$$\mathcal{I}_{\omega_z} \quad = \quad \sum_1^n \; W_i \; \cos^2 b_i, \tag{5}$$

where $W_i = 1/\sigma(V_i)^2$ is the weight of the pair of equations for the ith source, computed from the expected performances of GAIA. The information parameter has the advantage over the standard error of being an additive quantity and allows us to assess the relative importance of the observations of bright and faint objects. For a uniform distribution on the celestial sphere one should have $< \sin^2 b >= 1/3$, $< \cos^2 b >= 2/3$, $< \cos^2 l >=< \sin^2 l >= 1/2$. The absence of detected sources in the galactic plane favors the higher latitudes, thus decreasing $< \cos^2 b >$ and leading to a loss of information on ω_z.

3.2.   Results of a simulation

By collecting all Eqs. 1-2 over the extragalactic sources it is possible to determine the ω_i with a weighted least-squares solutions. The sources positions and their magnitude distribution come from the compilation catalogue of Véron-Cetty and the weights have been computed from the expected astrometric accuracy of GAIA. The results plotted in Fig. 1 show that one can end up with a non-rotating frame at the level of 0.5 μas yr^{-1}, provided the source random instability is less than 20 μas. The difference between ω_x, ω_y and ω_z is due to the peculiar space distribution of the sources not observed in the galactic plane (the same will hold with GAIA). It appears that using only the brightest quasars ($\sim B < 18$) will be perfectly sufficient to reach an almost perfect solution.

The random instability of the sources puts a very serious limitation in the ultimate precision of the inertial frame. Extragalactic radiosources display structure on spatial scales from hundreds to one mas with a variety of shape. The variability at radio wavelengths is also correlated to structure change due to relativistic jets. The effect of source structure on position has been studied in radio wavelengths and found to be as large as tens of mas yielding apparent

motion in right ascension. Values of 10 to 30 μas yr^{-1} have been reported. Virtually nothing is known in the visible regarding the $\sim$ mas structure and its time change. However the photometric variability in the optical bands might be an indication that photocentric random motions should not be excluded, in addition to the random microlensing. If relativistic jets seen in radio originated from synchrotron radiation of accelerated charges particles, the same mechanism should be seen in the optical band. Selection of a clean sample will be a difficult, but stringent requirement for the primary realization of the inertial frame. Dirty sources should not be simply dumped in the wastebasket but carefully scrutinized individually or collectively for jet motion (only for nearby AGN's) or structured transverse displacements.

3.3.   Orientation at epoch

While the very notion of a non rotating sphere is defined on physical ground in relation with the concept of inertia, the locations of the pole and of the origin of longitude in the fundamental plane are totally free. The only constraint to apply, as usual in metrology, is the principle of continuity. If the realization of the new standard is better than the previous version, the new system must lie within the uncertainty boxes of the old system. This has been constantly applied in classical metrology for the standard of length and time, and in astronomy during the transition from the FK5 to the ICRF.

Most of the defining sources of the ICRF are bright enough to be observed with GAIA and will be analyzed in the same way as the other extragalactic sources. The three parameters defining this rotation will be obtained by minimizing some merit function, that could be a global least-squares, minimum norm or even by using a very small number of objects regarded as reference beacons. The magnitude distribution of the ICRF defining sources outside the galactic plane in Fig. 2 gives a median magnitude of $B \sim 18$, meaning that the random noise in $\Delta\alpha\cos\delta$ and $\Delta\delta$ will come primarily from the uncertainty in the ICRF positions, typically ~ 0.5 mas. ¿From a simulation using only the defining source brighter than $V = 20$ and with $|b| > 20$ deg, one finds that the zero-point of the VLBI-ICRF and the GAIA-ICRF could differ by no more than ~ 40 μas. Thus there is neither conceptual nor practical difficulty to fix the origin of the GAIA derived ICRF that meets the continuity requirement with the existing frames.

4.   Limitations in the modelling : random microlensing

The basic assumption takes for granted that very distant extragalactic sources have no measurable transverse displacement. This assumption rests on the best VLBI observations on one hand and on a general physical principle tied to the cosmological expansion with QSO's having fixed co-moving coordinates. Nothing valuable can be said today below ~ 50 μas/yr corresponding to 20 years of VLBI positional measurements at ~ 1 mas accuracy. So far no unaccounted break to the principle has been found. If we admit as the most extreme situation that the transverse velocity is comparable in magnitude to the expansion velocity we have $V_t \sim H_0 D$ leading to $\mu_t \sim 10$ μas yr^{-1} thus giving an upper limit for motion of cosmic origin. But other sources are possible and GAIA has an enormous potential to check for transverse displacement on individual sources
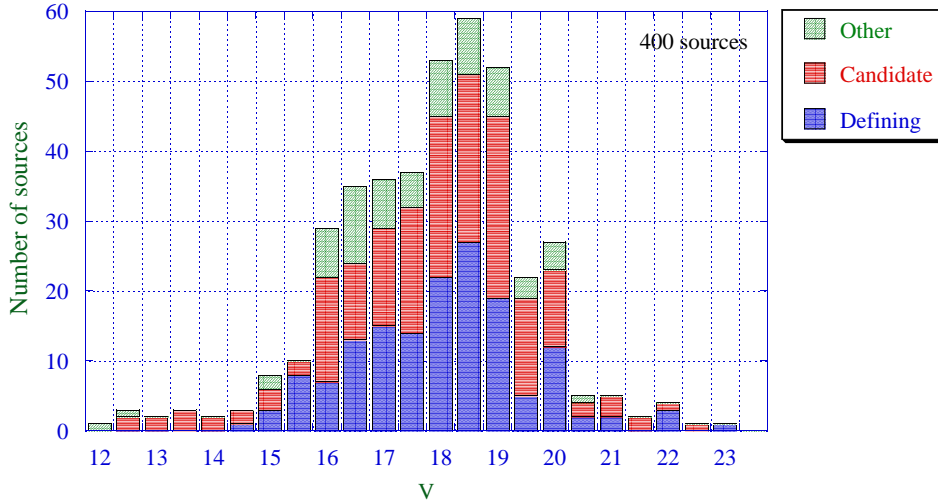
Figure 2.   Distribution over the B magnitude of the ICRF sources outside the the galactic plane ($|b| > 20$ deg) for the three categories of sources. Much of the defining sources are easy targets for GAIA and will be well observed.

and, above all, statistically for systematic motion at the μas yr^{-1} level. A source, well understood, although not yet detected is the so-called *variable galactic aberration* discussed in the GAIA proposal, in Mignard (2002) or in detail by Kovalevsky (2003).

Lensing by stars and galaxies could be one source of transverse motion due to the variable curvature of the lightrays as the lens moves before the observed source. It is a well known fact that the typical magnitude of the deflection by a lens is scaled by the Einstein radius of the lens given by,

$$\theta_E = 1\text{mas} \left(\frac{M}{M_\odot}\right)^{1/2} \left(\frac{10\text{kpc}}{d}\right)^{1/2} \quad \text{for stars} \tag{6}$$

$$\theta_E = 1'' \left(\frac{M}{10^{11}M_\odot}\right)^{1/2} \left(\frac{1\text{Gpc}}{d}\right)^{1/2} \quad \text{for galaxies} \tag{7}$$

So the deflection is in the mas range for microlensing but as large as $1''$ for lensing of extragalactic sources by intervening galaxies. Equations 6-7 referred to a lens with concentrated mass distribution. In the case of a Galaxy the distribution of matter can be much more extended, so that the light ray crosses the galaxy. A better model used the so-called Singular Isothermal Sphere with a constant velocity dispersion and a surface density decreasing as $1/r^2$. This yields a flat rotation curve for the galaxies and a convenient approximate model for a galactic extended halo. In this model it is easy to show that the deflection angle is constant for any ray going through the galaxy and has a value,

$$\alpha = \frac{4\pi\sigma_v^2}{c^2} \approx 1''4 \left(\frac{\sigma_v}{220\text{km/s}}\right)^2 . \tag{8}$$

Therefore, the effect of lensing on the observed direction of QSO's is quite significant and could be the source of spurious transverse motion over a timescale

determined by the motion of the lens. Thus it is important to assess the chance that an extragalactic source is subject to gravitational lensing (we are not concerned here with the problem of multiple images). The probability that a distant QSO comes in near alignment with a closer galaxy is the same as the probability that the light ray goes within θ_E of the center of the galaxy. If n is the number of galaxies per unit volume the fraction of the sky in a layer between distances r and $r + dr$ covered by Einstein disks of angular area $\pi\theta_E^2$ is given by

$$d\tau = nr^2\,\pi\theta_E^2\,dr \tag{9}$$

leading for point mass lenses to the optical depth,

$$\tau = \frac{2\pi}{3}\,\frac{GM}{c^2} nd_s^2, \tag{10}$$

where d_s is the (angular) distance of the source and M the mass of the deflector. To derive(10) one has integrated (9) from the observer to the distant extragalactic source. The expression for the isothermal sphere is different but numerically of the same order of magnitude.

The luminosity function of galaxies is still debated, but redshift surveys indicate that a description with the Schechter function,

$$\Phi(M)dM = \Phi_\star\,\left(\frac{L}{L_\star}\right)^{1+\alpha}\exp(-L/L_\star)\,dM \tag{11}$$

is a fairly good one. From the Las Campanas Survey (Lin *et al.*, 1996) one has $\Phi_\star \approx 0.019h^2$ Mpc^{-3} and $L_\star \approx 8 \times 10^{-9}h^{-2}\,L_\odot$. Integrating over the magnitude this gives a typical density of galaxies $n \sim 0.05$ Mpc^{-3}. We can insert this number in Eq.10 and with $M = 10^{11}M_\odot$, $h = 0.75$ one finds $\tau = 0.01$ at 5 Gpc and 0.04 at 10 Gpc. This means that on the average one quasar out of ten will be lensed by an intervening galaxy.

It is interesting to apply the same formula for microlensing, that is to say the lensing by stars belonging to the Milky Way. By limiting the integration of (9) to the outer boundary of the Galaxy one finds,

$$\tau = 2\pi\,\frac{GM_\star}{c^2}n_\star\Delta_G^2, \tag{12}$$

where $n_\star$ is the stellar density and Δ_G the radius of the Galaxy. With $n_\star \sim 0.05$ pc^{-3} and $\Delta_G \sim 10$ kpc one gets $\tau \approx 10^{-6}$, in agreement with a more refined estimate of Belokurov & Evans (2002). In their paper they also demonstrate from a Monte-Carlo simulation that microlensing is a negligible and unbiased random error in the positional measurements, including that of QSO's.

Therefore microlensing will be a rare event for the QSO's. Nonetheless between 10^3 to 10^4 QSO's positioned by GAIA will be *misplaced* by $\sim 1''$. As long as the images remain unresolved, the shift from the true position is not a major problem if it remains constant. There might be no variation during the ~ 5 years of the mission, but significant variations over 20 or 50 years, which would make these sources poor candidates to become defining sources.

One can estimate the induced transverse motion due to lensing by assuming some kinematical properties for the lenses. A motion of the lens in front of a

QSO of $d\theta$ will cause a motion of the bright image of comparable amplitude (comparable means here within a factor two ; this is easy to show from the lens equation and from the positions of the images). So the spurious proper motion of a lensed QSO is similar to the proper motion of the lens, which 'propagates' its motion to the images. In addition to the cosmic expansion, galaxies have peculiar motions resulting from the gravitational pull exerted by other members of the clusters. The best measured peculiar velocity is that of the Local Group at about 600 km s^{-1}. Taking for the maximum peculiar transverse velocity $V_t \sim 1000$ km s^{-1}, this gives a proper motion of 20 μas yr^{-1} at 10 Mpc and 0.2 μas yr^{-1} at 1 Gpc.

Although the probability of lensing by a galaxy as close as 10 Mpc is tiny, the above figures are just in the range of significance for the realization of the inertial system with GAIA and above all its integrity over several decades. Therefore the perspective of lensed QSO's should not be brushed away although it is not a major concern in the astrometric modelling. The detection during the mission of residual transverse motions, after the system has been brought to rest, will be an indication of possible lensing. Given the large number of sources available for the materialization of the system, it would be no problem to reject these sources from the defining set, but it would be worthwhile to have a ground based follow-up to search for a lens or multiple images.

References

Belokurov, V.A. & Evans N.W., 2002, MNRAS, 341, 649.

ESA 2000, GAIA, Composition, formation and evolution of the Galaxy, ESA-SCI(2000)4.

Fricke W., Schwan H., Lederle T., 1988, The Fifth Fundamental Catalogue, Veroff. Astron. Rechen Inst., 32, Heidelberg.

Gontier, A.-M., Le Bail, K., Feissel, M., Eubanks, T. M., 2001, A&A, 375, 661.

Kovalevsky, J., 2003, A&A, 404, 743.

Kovalevsky J., Lindegren, L., Perryman, M. A. C., Hemenway, P. D., Johnston, K. J., Kislyuk, V. S., Lestrade, J. F., Morrison, L. V., Platais, I., Rser, S., Schilbach, E., Tucholke, H.-J., de Vegt, C., Vondrak, J., Arias, F., Gontier, A. M., Arenou, F., Brosche, P., Florkowski, D. R., Garrington, S. T., Kozhurina-Platais, V., Preston, R. A., Ron, C., Rybka, S. P., Scholz, R.-D., Zacharias, N., A&A, 323 , 620-633 (1997).

Lin, H. ,Kirshner, R. P., Shectman, S. A., Landy, S. D., Oemler, A., Tucker, D. L., Schechter, P. L., 1996, ApJ, 464, 60.

Ma, C. *et al.*, 1998, AJ, 116, 516.

Mignard, F., 2002, in GAIA: A European Project, O. Bienayme & C. Turon, eds., EAS Publ. Ser. 2, 327.

Perryman, M.A.C., de Boer, K. S., Gilmore, G., Høg, E., Lattanzi, M. G., Lindegren, L., Luri, X., Mignard, F., Pace, O., de Zeeuw, P. T., 2001, A&A, 369, 339.

The Hipparcos and Tycho Catalogues, 1996, ESA SP-1200.

Véron-Cetty, M.-P., Véron, P., 2001, A&A, 374, 92.

Astrometric goals of the RadioAstron mission

Vladimir E. Zharov, Igor A. Gerasimov, Konstantin V. Kuimov

Sternberg State Astronomical Institute, 13, Universitetskij prospect,
119992 Moscow Russia

Aleksander E. Rodin & Yury P. Ilyasov

Puschino Radio Astronomy Observatory, 142290 Puschino Russia

Abstract.
The high-apogee elliptical orbit of the RadioAastron international mission will impact precision astrometry at the level of about a microsecond of arc (μas). Its launch could be on March 2006. The RadioAstron program is the next generation of radioastrometry programs. According to the RadioAstron program, initiated by the Astro Space Center of Lebedev Physical Institute of the Russian Academy of Science (supervisor N.S.Kardashev) in collaboration with other institutes of Russia and abroad, the satellite SPECTR carrying a 10-meter radio telescope will be launched in an orbit with eccentricity $e = 0.853$. The apogee distance will be 350 000 km. It is planned that the VLBI observations will be conducted with the largest ground based radio telescopes. The period of revolution of the satellite will be about 9.5 days, and observation time during one revolution can be about 9 days. Observations can be made at P, L, C and K bands with bandwidth 32 MHz. For the shortest wavelength, 1.35 cm, and baseline of about 350 000 km, resolving power of the order of 8 μas can be achieved. It is planned to solve both astrophysical and astrometry problems during a total expected lifetime of the satellite of three years. The main astrometric goal of the mission is the realization of a new International Celestial Reference Frame based on measurements of the coordinates of ~ 100 defining sources with microarcsecond accuracy. Observations of some pulsars using space-ground interferometers and by the timing technique will allow us to connect kinematical and dynamical systems with unprecedented accuracy. Coordinates of ground radio telescopes will be determined with respect to the geocenter.

1. Introduction

The IERS Celestial and Terrestrial Reference Systems (ICRS and ITRS) are the bases for solution of different tasks in different fields of science. The ICRS is realized by the IERS Celestial Reference Frame (ICRF) defined by the J2000.0 equatorial coordinates of 212 defining extragalactic radio sources determined from VLBI observations and distributed all over the sky (Ma *et al.* 1998). Approximately 400 other sources were added to densify the celestial sphere. The precent accuracy of the positions of these sources is 250 μas.

Realizations of the ITRS are called the IERS Terrestrial Reference Frame (ITRF) and consist of lists of coordinates and velocities for selected IERS sites (McCarthy and Petit 2003). Regular VLBI observations are used to maintain

the ICRF and to tie the ICRF to the major reference frames such as the ITRF, the HIPPARCOS optical reference frame, and the dynamical frames realized by the JPL ephemerides of the solar system bodies.

Ground-based observation precision will remain limited because of the atmosphere. In order to solve many astrophysical problems such as the cosmic distance scale, motions of radio sources, and search for dark matter, 10-μas precision or better is required. This goal cannot be reached from the Earth and only space astrometry missions can help to solve these astrophysical problems.

The success of Hipparcos (ESA 1997) has triggered several projects (FAME, DIVA, SIM, GAIA) of astrometric satellites to observe more stars with better accuracies. Hipparcos improved the accuracy of global astrometric measurements from 50 to 1 milliarcsecond (mas). Global astrometric accuracy of 50 to 4 μas is the aim of future FAME, DIVA, SIM, GAIA missions.

In order to increase accuracy of the radio astrometry observations it is necessary to place one radio telescope in space and use it in conjunction with ground based antennas. VLBI baselines are limited to about 10 000 km and this limits the accuracy and the resolving power. There is only one way to increase the baseline: to fly the radio telescope to space. The first program called VSOP (VLBI Space Observatory program) was begun in February 1997 when the first satellite with a telescope, called HALCA, was launched (Kobayashi *et al.* 1998). The instrument on board is an 8-meter dish radio telescope on a highly elliptical 6-hour orbit with an apogee height of 21 000 km. The baselines of ground-space VLBI can reach 25 000 km. It can observe at 1.6, 5, and 23 GHz with a resolving power of the order of 500 to 80 μas.

2. RadioAstron mission

The RadioAstron project is an international collaborative mission to launch a free flying satellite carrying a 10-meter radio telescope in elliptical orbit around the Earth. The aim of the mission is to use the space telescope to conduct VLBI observations in conjunction with the global ground VLBI network in order to obtain images, coordinates and evolution of angular structure of different radio emitting objects in the Universe with extraordinarily high angular resolution. The orbit of the RadioAstron satellite will have an apogee in the range up to 350 000 km. Space ground VLBI measurements with this orbit will provide morphological and coordinate information on galactic and extragalactic radio sources with fringe size up to 8 μas at the shortest wavelength, 1.35 cm.

The RadioAstron mission uses the satellite SPECTR, which is under development by Lavochkin Association Aviation and Space Agency. It is a standard module to be used in several other scientific missions. The total mass of the scientific payload is about 2500 kg, of which the unfolding parabolic 10-m radio astronomy antenna's mass is about 1500 kg, and the scientific package holding the receivers, power supply, synthesizers, control units, frequency standards and data transmission radio system is near 900 kg. The mass of the whole system (satellite and scientific payload)to be carried into orbit by the "PROTON" launcher is about 5000 kg. The expected lifetime of the satellite is three years.

The space radio telescope antenna consists of a deployable parabolic reflector (10-m diameter) which is made of 27 carbon fiber petals and central solid

portion (3-m in diameter). The radio telescope has a focus to diameter ratio $F/D = 0.43$ and overall RMS surface accuracy of 0.7 mm.

Observations can be made at P(0.327 GHz), L(1.665 GHz), C(4.830 GHz) and K(22.220 GHz) frequencies with a bandwidth of 32 MHz in each. The fringe spacings for the largest baseline for all RadioAstron bands are equal to 540, 106, 37 and 8 μas, respectively. Because of the low sensitivity of the 10-m antenna, only large ground telescopes will be useful for obtaining scientific data for most observations with RadioAstron.

There are many constraints for observations with RadioAstron. They are concerned with the attitude control system of the spacecraft, satellite visibility from tracking stations, and limits on the satellite autonomous operations during the orbit. Among the operational constraints, the most important is the number of programmed slews per orbit and the need to observe no less than three defining quasars before each observational session for precise reconstruction of the orbit.

It is planned to investigate both astrophysical and astrometry problems such as:

1. study of radio galaxies, quasars, black holes, neutron stars with very high angular resolution;

2. structure and dynamics of megamaser regions in other galaxies; structure and dynamics of maser radio sources in regions of star formation;

3. turbulent structure of interstellar medium through the scintillations of compact radio sources;

4. cosmological evolution of compact extragalactic radio sources; determination of fundamental cosmological parameters and study of gravitational lenses and the nature of hidden mass;

5. precise astrometry on the level of several microarcseconds, determinations of the distances to pulsars as well as evaluations of their velocities by the measurements of parallax and proper motion;

6. link of kinematical and dynamical celestial reference frames;

7. measurements of secular aberration (motion of the solar system in the galaxy);

8. direct measurements of distances using spherical wave fronts;

9. direct measurements of coordinates of the ground-based telescopes in the ITRS.

3.   Prospects for astrometry

Sensitivity of the ground-space interferometer for unresolved sources is of the order of 30 mJy if the signal-noise ratio (S/N) is equal to 10. This estimate was calculated for the Kalyazin (Russia) – RadioAstron baseline. These telescopes have respectively diameters equal to 64 and 10 m, system temperatures equal to 40 K and 60 K, and effective areas of 1700 m^2 and 40 m^2.

It is planned to observe ~ 100 defining sources with fluxes greater then 1 Jy. Then the S/N will be 30 or more and the uncertainty of the time delay of one observation of the quasar will be ~ 300 ps. It will be necessary to observe no less than three defining quasars before each observational session for precise reconstruction of the orbit. Later these observations of quasars will be used to improve their coordinates. If each of the quasars will be observed more than 100 times we can expect that the uncertainty of the coordinates will be of the order of 10 μas. The list of the defining sources that will be used for reconstruction of orbits and for improvement of the ICRF is shown in Table 1.

Table 1.   Physical characteristics of radio sources

IERS Designation	Type[a]	Redshift	Flux (Jy)[b]		Spectral index	V
			6 cm	15 cm		
0014+813	Q	3.387	0.55	1.00	-0.2	16.5
0133+476	Q	0.859	3.26	2.10	0.5	19.0
0235+164	L	0.940	2.79	2.00	0.6	15.5
0440-003	Q	0.844	2.39	3.53*	-0.2	19.2
0537-286	Q	3.104	1.23	1.00	0.5	20.0
0637-752	G	0.654	6.19	4.51*	-0.1	15.8
0804+499	Q	1.433	2.07	1.30	0.5	18.9
0821+394	Q	1.216	0.99	1.90	-0.2	18.5
0834-201	Q	2.752	3.42	3.30	-0.3	19.4
0955+476	Q	1.873	0.74	1.10	0.1	18.7
1143-245	Q	1.950	1.49	1.10	-0.2	18.0
1308+326	Q	0.997	1.59	1.57*		15.2
1442+101	Q	3.535	1.15	2.01	-0.6	17.8
1538+149	L	0.605	1.95	1.50		17.3
1619-680	Q	1.354	1.81	1.79*		18.0
1725+044	G	0.293	1.21	0.84	0.8	17.0
1743+173	Q	1.702	0.94	0.90	0.1	19.5
1830+285	Q	0.594	1.07	1.30		17.2
1842+681	Q	0.475	0.81	1.20	-0.4	17.9
1954-388	Q	0.630	2.02	1.00		17.1
2029+121	L	1.215	1.29	1.10	0.7	20.3
2037+511	Q	1.687	3.79	5.00		21.0
2113+293	Q	1.514	1.45	1.12		19.5
2145+067	Q	0.999	4.41	3.10	0.5	16.5
2319+272	Q	1.253	1.07	1.10		19.0
2326-477	Q	1.306	2.06	2.40*		16.8

[a]Type of Object: Q = quasar, G = galaxy, L = BL Lac
[b]Asterisk indicates that the reported value is the flux at 11 cm.

An important part of the astrometry program is the observation of pulsars. Sensitivity of the ground-space interferometer is enough to observe ~ 10 pulsars

such as B0329+54, B0833-45, B1641-45 and other with fluxes > 30 mJy (in L-band).

If distances of pulsars or other galactic sources are less then 5 kpc, then straight distance measurements will be possible; the interferometer will be sensitive to the phase difference between plane and spherical wavefronts. It easy to show that correction for the time delay for the spherical wavefront is equal to

$$\Delta\tau = \frac{1}{2c|\mathbf{R}_S|}\Big(|\mathbf{r}_2|^2 - |\mathbf{r}_1|^2\Big),$$

where $|\mathbf{R}_S|$ is distance from the geocenter to pulsar, $|\mathbf{r}_1|, |\mathbf{r}_2|$ are the geocentric dictances of the ground and space telescopes, and c is the velocity of light.

If the uncertainty of the time delay measurement is 1 pc then this correction has to be taken into account for

$$\Delta\tau > 10^{-12},$$

or if $R_S < 5000$ pc for baselines of order $300\,000$ km.

Unfortunately for high frequencies the fluxes of pulsars are weak. The list of pulsars that can be observed during the RadioAstron mission is shown in Table 2. The flux is calculated for 1.6 GHz. Pulsar B1937+21 was added to study the giant pulses. It is expected that coordinates of pulsars will be measured with an uncertainty of ~ 0.1 mas (Table 3).

Table 2.   Pulsars, observed with S/N$\geq$ 10.

Designation	Flux (mJy)	S/N	Period (sec)
B0329+54	140	118	0.714518663
J0437-4715	64	52	0.005757451
B0736-40	57	46	0.374918710
B0833-45	790	640	0.089308556
B0950+08	60	49	0.253065068
B1451-68	57	46	0.263376778
B1556-44	34	23	0.257055723
B1641-45	220	180	0.455059775
B1749-28	26	21	0.562557857
B1929+10	34	23	0.226517821
B1933+16	35	24	0.358736248
B1937+21	11	8	0.001557806
B2020+28	32	22	0.343401720

We expect to tie the ICRF to the dynamical frame DE405 with the same uncertainty. At present, the rotation angles between these systems are known with milliarcsecond accuracy (Table 4). The rotation angles A_1, A_2, A_3 are calculated from analyses of Satellite Laser Ranging (SLR) and VLBI data and from pulsar VLBI and pulsar timing.

Table 3.   Uncertainty δ of position of the pulsars calculated on the the basis
of S/N ratio, and the possibility of the measurement of the parallax

Designation	S/N	δ (mas),	Distance (kpc)	Parallax
B0329+54	118	0.015	1.43	+
J0437-4715	52	0.034	0.14	+
B0736-40	46	0.038	11.03	-
B0833-45	640	0.003	0.5	+
B0950+08	49	0.036	0.12	+
B1451-68	46	0.038	0.45	+
B1556-44	23	0.076	1.63	+
B1641-45	180	0.010	5.3	+
B1749-28	21	0.085	1.53	+
B1929+10	23	0.075	0.17	+
B1933+16	24	0.073	7.94	-
B1937+21	8	0.225	3.6	-
B2020+28	22	0.080	1.3	+

Table 4.   Relative orientation between DE200 and ICRF

Angles	Finger & Folkner 1992	Folkner *et al.* 1994	Rodin & Sekido 2001
A_1	1 ± 3	-2 ± 2	-4 ± 2
A_2	-10 ± 3	-12 ± 3	-13 ± 2
A_3	-4 ± 5	-6 ± 3	-17 ± 6

Another astrometric goal of the RadioAstron mission is the measurement of the variable part of secular aberration due to the solar system motion around the center of mass of the galaxy. The total effect is equal to $V/c \approx 2.5'$, where $V \approx 220$ km/s is the velocity of the Sun. In galactic coordinates b, l the aberration effect can be written as (Zharov 2002)

$$\Delta l \cos b = k \cos b_0 \sin(l - l_0), \tag{1}$$
$$\Delta b = k[\sin b \cos b_0 \cos(l - l_0) - \cos b \sin b_0], \tag{2}$$

where $k = -V/c$, and b_0, l_0 are the apex coordinates. If $b_0 = 0°, l_0 = 90°$ then the constant part of secular aberration is

$$\Delta l \cos b = -k \cos l, \tag{3}$$
$$\Delta b = k \sin b \sin l, \tag{4}$$

but this effect cannot be observable and corresponds to the constant displacement of the coordinates of the quasars. If we assume that motion of the Sun around the center of the galaxy is circular, then a yearly variation of direction of the apex is $dl_0/dt = n$, where $n = 2\pi/T \approx 2.6 \cdot 10^{-8}$ y^{-1} is the mean motion of the solar system, $T = 240 \cdot 10^6$ years being the period of revolution. The variable yearly part of secular aberration is

$$\delta(\Delta l \cos b) = -kn \sin l, \tag{5}$$
$$\delta(\Delta b) = +kn \sin b \cos l. \tag{6}$$

The coefficient kn is ~ 4 μas. Maximum variation of galactic longitude l will be for the quasars with coordinates $b \approx 0°$, $l \approx \pm 90°$. Maximum variation of galactic latitude b will be for the quasars with coordinates $b \approx \pm 90°$ and $l \approx 0°$ or $180°$. Measurements of arcs between quasars that are in these regions are planned during the RadioAstron mission.

4. Conclusion

The capabilities of future space astrometry missions are very promising. Extending the accuracy of VLBI measurements gives us the possibility to investigate both astrophysical and astrometric problems such as the generation of precise fundamental celestial reference frames, links of kinematical and dynamical celestial reference frames, measurement of the position of ground radio telescopes in the terrestrial reference frame, pulsar parallax and proper motion measurements, tests of General Relativity, and measurement of secular aberration of the defining sources.

References

ESA, 1997, *The Hipparcos and Tycho Catalogues*, ESA Publication SP-1200, 17 volumes.

Kobayashi, H., Wajima, W., Murata, Y., Hirabayashi, H., Kameno, S., Kawaguchi, N., Inoue, M., Murphy, D. W., 1998, in *Radio emission from galactic and extragalactic compact sources*, J.A. Zensus, G.B. Taylor and J.M. Wrobel (eds), IAU Colloquium 164, Astron. Soc. Pacific. Conf. Series**144**, 11-15.

McCarthy, D. D., Petit, G., 2004, IERS Conventions 2003, IERS Technical Note 32.

Ma, C., Arias, E.F., Eubanks, T.M. Fey, A. L., Gontier, A.-M., Jacobs, C. S., Sovers, O. J., Archinal, B. A., Charlot, P., 1998, AJ, 116, 516.

Finger & Folkner 1992, TDA Progr. Rep. 42-109, JPL, CA.

Folkner *et al.* 1994, A&A, 287, 279.

Rodin & Sekido 2001, AP-RASC Conf. Digest, Chuo Univ., Tokyo, p.388.

Zharov V.E., 2002, *Spherical Astronomy* (in Russian).

Misleading Proper Motions of Galactic Objects at the Microarcsecond Level

Jean Kovalevsky

Observatoire de la Cote d'Azur, Avenue Copernic, 06130 Grasse, France

Abstract.

At the microarcsecond (μas) observational level of accuracy foreseen by the GAIA program, the effects of the curvature of stellar orbits around the center of the galaxy cannot be neglected. The curvature of the solar system barycentric motion induces a time dependent component of the aberration, which reaches, in some regions of the sky, 4 μas per year. In the case of stars, it is combined with a similar effect due to the curvature of the galactocentric orbit of the star, which may reach 600 μas per year for a star situated at 50 parsecs from the center of the galaxy, and much larger closer to it. The formulae permitting us to compute these apparent proper motions are given together with the maps describing this effect within the galaxy. They disappear if one uses a galactocentric rather than a barycentric reference frame. The advantages and difficulties of this frame are discussed.

Relating the Dynamical Reference Frame and the Ephemerides to the ICRF

E. M. Standish

CalTech/Jet Propulsion Laboratory; 301-150; Pasadena, CA 91109

Abstract. In the past, the motions of solar system bodies were used to establish a non-rotating "inertial" reference system, often referred to as "the dynamical reference frame". With the establishment of the ICRF, the use of a dynamical reference frame has become obsolete in this context.

Planetary ephemerides, on the other hand, continue to play vital roles in a number of other applications, such as spacecraft navigation, mission design, *etc.* For present-day ephemerides, the accuracies of the inner planet positions are 1 km or less in all coordinates, including the orientation of the system onto the ICRF. Certain quantities are much better known over specific time intervals (*e.g.*, Earth-Mars distance over the past few decades, throughout which it has been accurately measured). The outer planet positions are significantly less well-known, being established during the present era by CCD observations to about 0.″05 or so, but quickly deteriorating for decades away from the present.

1. Introduction

In the past, the dynamical nature of the solar system ephemerides was used to establish an inertial reference frame. Now, however, since the ICRF is assumed to be inertially founded (at least to presently observable accuracy), and thereby automatically provides an inertial reference system for astronomy, the use of a dynamical reference frame, *per se*, has become obsolete. The ephemerides themselves, however, still provide a major element in the navigation of spacecraft, mission design, scientific studies, observation prediction and reduction, determination of specific astronomical constants, *etc.*

This paper briefly discusses the former use of the "dynamical reference frame", the recent orientation of the ephemerides onto the ICRF and the advantages therein, the various uses made of the ephemerides, and finally gives some estimates to the accuracies of the ephemerides themselves.

2. Former Use of a Dynamical Reference System

Formerly, the fundamental reference system of positional astronomy was provided by the series of "FK" ("Fundamentalkatalog") stellar catalogues, where the motions of the stars are subject to a number of systematic errors such as precession, star-streaming, galactic rotation, cluster proper motions, *etc.* Each of these effects is correlated to some extent with a general rotation of the reference system, and as such, it used to be necessary to anchor the system to inertial space using the motions of the Moon and planets.

In order to visualize how a dynamical system can determine an inertial frame, one may perhaps think of a single unaccelerated body. If, as measured from an observing platform, the body does not appear to move in a straight line with constant velocity, then the platform is not inertial; it is rotating or being accelerated somehow. Similarly, if the body is moving in an approximately elliptical orbit, in an inertial frame the ellipse cannot show rotation that is unaccounted for. In both cases, as well as in the actual general case, accurate measurements do not allow an unmodeled rotation of the reference system.

Now, with the advent of the ICRF, the planetary ephemeris is no longer needed to remove any rotation from the reference system. For the reference frame of the ephemerides, the whole inner planetary system is automatically adjusted onto the ICRF by fitting to VLBI observations of spacecraft in the vicinity of a planet. With an accurate planetocentric spacecraft ephemeris, the measurement relates the planet's position to the catalogue sources.

3.   Orientations of the Ephemerides

In the past, the 1950-based ephemerides of JPL have been aligned onto the FK4 reference frame by means of the series of meridian circle (transit) observations of the planets. Starting with DE200, the ephemerides were aligned onto their own mean equator and dynamical equinox of J2000 (see Standish, 1982). Starting with DE400, the ephemerides have been oriented onto the ICRF (formerly, the "IERS reference frame") by means of the VLBI observations included in the adjustments. In this context, the choice of the ICRF is advantageous for a number of reasons:

- The ICRF is now the standard reference frame in astronomy.

- The timing and polar motion information used for the orientation of the Earth are now referred to the ICRF.

- The ICRF is accessible. In fact, the ephemerides are now fit to a number of VLBI observations which were referenced to the ICRF (formerly, the IERS reference frame). Among all of the ephemeris observations which are explicitly given in a celestial reference system, these ICRF-based ones are the most accurate.

- The ICRF is stable; future improvements to the coordinates are to be done so that no net rotational displacement is introduced. Measurements over extended periods of time, used for the ephemerides, will therefore remain consistent with each other.

- The ICRF may be considered inertial to a high degree of accuracy. It is true that the sources do show some time-varying structure; however, these will be even further diminished in the future with extended modeling and with observations at smaller wavelengths where the structures are less pronounced.

4.   Uses of the Ephemeris

Though the concept of a dynamical reference frame is now obsolete, the justification for continued ephemeris refinement and production continues.

- Spacecraft navigation: a) the saving of fuel with fewer and smaller mid-course maneuvers, and b) the mere possibility of aero-braking upon immediate arrival at Mars - without first going into orbit.

- Mission planning: "Feasibility of particular mission concepts".

- Predictions and reductions of astronomical measurements: observational accuracy is often increased with improved *a priori* knowledge; in fact, some observations are not even possible without an accurate ephemeris.

- Background force model for the computation of small body orbits: asteroids, comets., *etc.*

- Determination of astronomical constants: the length of the AU, planetary masses, gravity fields, *etc.*

- Testing of relativity, alternative gravitational theories, gravity waves, $\dot{G}$, *etc.*

- Analyses of historical records.

5.   Accuracies of Present-Day Ephemerides

While modern observations (radar ranging, spacecraft ranging, and VLBI) are able to accurately pinpoint certain ephemeris quantities at the times of the observations, uncertainties in the ephemerides arise when the ephemerides are propagated over time, due to the impossibility of being able to model exactly all the forces relevant to the ephemerides. Foremost among these are the perturbations from many asteroids whose masses are not well-known, but which are large enough to significantly influence the motions of Earth and Mars.

A recently-submitted paper (Standish, 2003) presents estimates of the accuracies of modern-day ephemerides. Comparisons of older ephemerides with the more recent ones give good indications of the errors in the older versions. Present errors still exist, due mainly to the asteroids, as discussed by Williams (1984) and by Standish and Fienga (2002).

For a quick rule-of-thumb, the following is a guideline: during the present decade or so, relative distances and angles between the inner solar system bodies are accurate to a few hundred meters; even better for certain quantities, such as geocentric ranges and heliocentric Earth-planet angles. The orientation of this system onto the outside reference frame, the ICRF, is accomplished by the inclusion of VLBI observations of a number of spacecraft in orbit around Venus and Mars. The residuals show a scatter of less than $0.''001$; assuming no systematic error, the orientation of the whole inner system must then be accurate to the sub-milliarcsecond level.

For the outer planets, modern CCD measurements now show single (presumably *random*) errors of about $0.''1$, so that present-day plane-of-sky positions

(directions) are determined to a few hundredths of an arcsecond during the present epoch. The mean motions, or, equivalently, the heliocentric distances, depend upon the less accurate observations extending backward over the past century. Errors for these amount to a sizable fraction of an arcsecond per century. Assuming a mean motion uncertainty of $0.''5/\text{cty}$ the derived distance uncertainties would be $25km$, $100km$, and $650km$ for Jupiter, Saturn, and Uranus, respectively; uncertainties in the eccentricities can double these numbers. For Neptune and Pluto, which haven't been observed over a full period (with the impersonal micrometer, introduced in 1911), the uncertainties away from the present few decades can be several thousand kilometers.

6.   Future JPL Ephemerides

JPL will continue to provide planetary and lunar ephemerides to the astronomical community, as it has over the past 30 years. The JPL ephemerides will continue to be based upon our best knowledge of physics, using the PPN formalism of relativity, with the equations of motion correct and complete through order 1/c**2. The independent variable of the equations will continue to be "T_{eph}", a relativistic coordinate time, rigorously equivalent to the IAU's newly-defined quantity, TCB, but having the added benefit that $|T_{eph} - TT| < 2$ milliseconds of time.

References

Standish, E.M. 1982, "Orientation of the JPL Ephemerides, DE200/LE200, to the Dynamical Equinox of J2000", A&A, 114, 297-302.

Standish, E.M. 2004, "An approximation to the errors in the planetary ephemerides of the Astronomical Almanac", A&A, 417, 1165-1171.

Standish, E.M. and Fienga, A.G. 2002, "Accuracy limit of modern ephemerides imposed by the uncertainties in asteroid masses", A&A, 384, 322-328.

Williams, J.G. 1984, "Determining Asteroid Masses from Perturbations on Mars", Icarus, 57, 1-13.

The ICRS and the IERS Information System

Wolfgang R. Dick, Bernd Richter, & Wolfgang Schwegmann

IERS Central Bureau, BKG, Richard-Strauss-Allee 11, 60598 Frankfurt am Main, Germany

Abstract. This paper discusses the role of the International Earth Rotation and Reference Systems Service (IERS) for the International Celestial Reference System (ICRS) with emphasis on the IERS Information System, consisting of data, publications, documentation, and other information in printed and online form. Plans for a new database-driven information system are outlined.

1. Introduction

The IERS was established as the International Earth Rotation Service in 1987 by the International Astronomical Union and the International Union of Geodesy and Geophysics, and it began operation on 1 January 1988. As of 1 January 2001 the IERS has a new structure, and in 2003 it was renamed the International Earth Rotation and Reference Systems Service. The primary objective of the IERS is to serve the astronomical, geodetic and geophysical communities by providing the following:

• The International Celestial Reference System (ICRS) and its realization, the International Celestial Reference Frame (ICRF).

• The International Terrestrial Reference System (ITRS) and its realization, the International Terrestrial Reference Frame (ITRF).

• Earth orientation parameters required to study Earth orientation variations and to transform between the ICRF and the ITRF.

• Geophysical data to interpret time/space variations in the ICRF, ITRF or Earth orientation parameters, and model such variations.

• Standards, constants and models (*i.e.*, conventions) encouraging international adherence.

As one of the Product Centers of the IERS, the ICRS Center is responsible for the maintenance of the ICRS and the ICRF, in close cooperation with the International VLBI Service for Geodesy and Astrometry (IVS) which serves as one of the IERS Technique Centers. The Convention Center releases the IERS conventional models, constants and standards. The IERS Central Bureau is responsible for the management of the IERS, including the edition of publications and reports and the maintenance of documentation. Also the Analysis Coordinator and some of the Combination Centers are involved in ICRS issues.

2. The ICRS and the IERS Information System

The IERS Information System comprises

• publications (IERS Annual Reports, IERS Technical Notes, IERS Messages), available online and in printed form,

• IERS Bulletins and other products (data files) available by e-mail and from different ftp and Web servers,

• documentation and meta information published on the Web servers of the IERS components and at the central server <www.iers.org> maintained by the Central Bureau.

The ICRS is well represented in this IERS Information System:

• The ICRS and the ICRF, their documentation as well as auxiliary information are available online at the Web pages of the ICRS Center (for links see <www.iers.org/iers/products>).

• The ICRS/ICRF is documented in an IERS Technical Note (Ma & Feissel 1997). A new Technical Note on the ICRS is in preparation. Additional papers on the ICRS/ICRF by members of the ICRS Center and the IVS have been published in journals and conference proceedings.

• The models, constants and other standards to be used for the ICRS are given in the IERS Conventions. The latest version (McCarthy 1996) will soon be replaced by a new one, which is already available in its nearly final state (see <www.iers.org/iers/products/conv>). The IERS Conventions contain also a short documentation of the ICRS/ICRF itself.

• The IAU 2000 Resolutions, which are to a large extent related to the ICRS, and their implementation were discussed in an IERS Workshop, the Proceedings of which were published as an IERS Technical Note (Capitaine *et al.* 2002), online version at <www.iers.org/iers/publications/tn/tn29>.

• The ICRS Center and the IVS report on their activities in the IERS Annual Reports. For the latest report see Dick & Richter (2003), the last three reports are also available online at <www.iers.org/iers/publications/reports>.

• The IVS as one of IERS Technique Centers (see <www.iers.org/iers/tc/ivs/>) maintains its own information system including Web sites and publications. It provides also updates to the ICRF produced by individual IVS Analysis Centers (see <ivscc.gsfc.nasa.gov/service/cddis-products-crf.html>).

• Rapid and short information from the IERS is distributed through IERS Messages (see <www.iers.org/iers/publications/messages>), some of which concern also the ICRS.

• The central IERS Web site <www.iers.org> provides general information on the IVS and the ICRS Center, as well as meta information on IERS products including the ICRS and the ICRF. In the future, this meta information will be organized in the form of a database, giving also direct access to the IERS products.

3.   The new IERS Information and Database System

The goal of the planned IERS Information and Database System is to coordinate the data and information flow between the IERS components (mainly Technique Centers, Product Centers, and Combination Centers) and to give users an easier access to IERS products and publications. For this, all relevant data and products of the IERS will be archived at a central place to guarantee their long-term availability. At the same time the consistency and timeliness of the contents of the information system as well as easy access will be guaranteed by managing the information in a database. Also the metadata of all products and publications will be modeled in the database to allow the users to search for specific data or topics with respect to space, time and content.

Presently, the user of IERS products (including the ICRS/ICRF) has to navigate through various Web pages on different servers where he is able to download the data in the provided (fixed) format that is not unique for all the data. To link related data to each other the user has to take care about the various formats. In addition to the product information, the central IERS Web site <www.iers.org> contains information about IERS publications, IERS structure and components as well as news and general information on Earth rotation and reference frames. Currently, all this product information is stored in static Web pages, and the same information can be found in different places. Thus, it is tedious to keep the information consistent and up to date without redundancy.

The new system will manage its contents dynamically, *i.e.* all time dependent information as well as information that appears within multiple pages will be retrieved from a database. Additionally, the new system will allow more flexible navigation through the metadata related to the IERS products. The metadata will be kept in a database while the products are going to be stored in a file archive system.

In order to be able to link related data the heterogeneous formats of the products have to be transformed into a common format. The eXtensible Markup Language (XML) is going to be used for this (Bray *et al.* 2000). The usage of XML not only allows us to link related data but also to easily exchange data and to present them in different ways like Web pages, pdf, *etc.* For presentations, only server-side technologies will be used, so that the user needs no special programs or browser plug-ins. All components of the new system will be based on open source software. The information system will be run on an Apache Web Server, while the open source relational database management system PostgreSQL or MySQL is going to be used to store the metadata. The Web interface to access and browse this information can be realized by using scripting languages like PHP or JavaScript. The proposed concept has been proven by test applications.

The first step when building a database-driven Web site is to build the database tables to model the information to be represented. This is currently in progress for the metadata of the IERS products. These are based on a list compiled by the working group of the IERS Analysis Coordinator. It describes all IERS products by the same keywords. This list with metadata on the products has been translated into new product information Web pages by the Central Bureau (see <www.iers.org/iers/products>, example in Fig. 1).
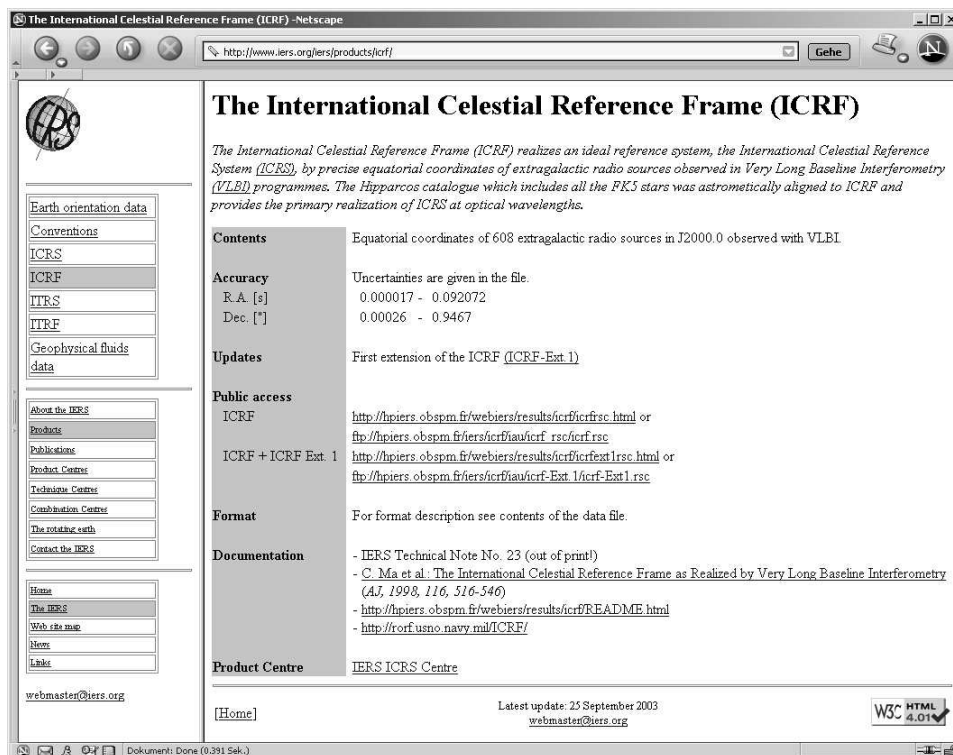
Figure 1.   Web page with metadata on the ICRF.

For more details on the new system, see Richter *et al.* (2003).

References

Bray, T., Paoli, J., Sperberg-McQueen, C. M., & Maler, E. 2000, Extensible Markup Language (XML) 1.0 (Second Edition), W3C Recommendation (http://www.w3.org/TR/REC-xml).

Capitaine, N., Gambis, D., McCarthy, D. D., Petit, G., Ray, J., Richter, B., Rothacher, M., Standish, E. M., & Vondrak, J., eds. 2002, Proceedings of the IERS Workshop on the Implementation of the New IAU Resolutions (IERS Tech. Note 29) (Frankfurt a. M.: BKG).

Dick, W. R., & Richter, B., eds. 2003, IERS Annual Report 2002 (Frankfurt a. M.: BKG).

Ma, C., & Feissel, M., eds. 1997, Definition and Realization of the International Celestial Reference System by VLBI Astrometry of Extragalactic Objects (IERS Tech. Note 23) (Paris: Obs. Paris).

McCarthy, D. D., ed. 1996, IERS Conventions (1996) (IERS Tech. Note 21) (Paris: Obs. Paris).

Richter, B., Schwegmann, W., & Dick, W. R. 2003, in Proceedings of the IUGG Symposium G07 "IGGOS", Sapporo 2003, J. of Geodynamics, in print.

ICRS — ITRS connection consistent with IAU (2000) Resolutions

Irina Kumkova

Institute of Applied Astronomy RAS, 10, Kutuzov emb, St.Petersburg, 191186 RUSSIA

Michael Stepashkin

Saint-Petersburg Institute for Informatics and Automatics RAS

Abstract.   Algorithms for direct and reverse relativistic four-dimensional transformation of barycentric and geocentric celestial reference coordinate systems (BCRS and GCRS) according to IAU Resolution B1(2000) are developed. Transformation between BCRS and GCRS is considered as a part of a general process of linking the International Celestial Reference System to the International Terrestrial Reference System, provided by the International Earth Rotation Service.

1.   Introduction

VLBI development resulted in the significant improvement of observational positional accuracy. Since the early 1980s the precision of the observations has reached 1-2 milliarcseconds and later sub-milliarcseconds. The sub-milliarcsecond-level and the microarcsecond-level of precision anticipated for future observational systems demands improved models at all levels of analysis. These improved models require us to take into account corrections for the General Theory of Relativity in data processing. That is why in 1990 at IAU Colloquium 127 (IAU, 1991), IAU recommendations for reference frames and time scales were formulated in the framework of General Relativity for the first time. It is necessary to mention that, in practice, relativistic corrections in celestial mechanics and in astrometry were investigated and applied earlier. The main technique of such an investigation has been Post-Newtonian barycentric (refering to the Solar System) equations of motion of celestial bodies and light propagation. However in 1991 affirmation of IAU recommendations as Resolution A4 (1991) at the 21st General Assembly (GA) of the IAU and later as Resolution 2 of the IUGG (1991) provided the foundation for the qualitative change of the role of General Relativity for ephemerides. At present according to IAU Resolutions two main coordinate systems exist for practical use. These are ICRS, International Celestial Reference System and ITRS, International Terrestrial Reference System. (Siedelmann and Kovalevsky, 2002). The time scales of the ICRS and ITRS should be respectively TCB (Barycentric Coordinate Time) and TCG (Geocentric Coordinate Time). These scales should be considered as part of a four-dimensional relativistic coordinate system, connected by four-dimensional relativistic transformations with an additional three-dimensional rotation of the

space axes of coordinates. It is necessary to mention that IAU Resolution A4 (1991) has not been realized to its full extent because ICRS and ITRS were used as Newtonian three-dimensional space coordinate systems. Moreover TDB, Barcentric Dynamical Time and Terrestrial Time are used instead of TCB and TCG correspondingly.

To solve the majority of astronomical tasks it is sufficient to have only the ICRS, ITRS and their practical realizations ICRF and ITRF. However to connect ICRF and ITRF it is necessary to introduce one more local geocentric system with the same time scale, TCG, that ITRS has, and with the same direction of space axes, that ICRS has. Such a system is introduced by IAU Resolution 1.3 (2000), and it is an intermediate system between BCRS, Barycentric Celestial Reference System, identified with ICRS, and ITRS and has the title of GCRS, Geocentric Celestial Reference System.

Astronomical practice requires transformations between the BCRS and ITRS in both directions. The direct transformation $BCRS->ITRS$ is necessary in the case of observations in the ITRS. At present it is used implicitly in the analysis of radio interferometric observations. The time delay in TCB is transferred to TCG with further reduction to the scale of proper time of one of the observational stations, while the barycentric baseline vector, in the sense of a difference between space BCRS coordinates of two stations, is transferred to a geocentric baseline vector, in the sense of a difference between space ITRS coordinates of observational stations. Such transformations should become routine procedures in processing high precision astrometric observations in the future development of space astrometry for space projects such as SIM, GAIA and AMEX

The reverse transformation $ITRS->BCRS$, is necessary to describe the observational procedures in the BCRS, such as in the present Lunar Laser Ranging (LLR) data processing. The transformation between BCRS and ITRS goes in two stages. In the first stage the BCRS is connected by relativistic four-dimensionl space-time transformations to the GCRS — a geocentric system, kinematically non-rotating with respect to BCRS. In the second stage the GCRS is connected to the ITRS by a Newtonian three-dimensional transformation. The latter is specified by the IERS documents following IAU Resolutions B1.3, B1.6, B1.7, B1.8.

The present work aims to develop techniques for the practical use of $BCRS \rightarrow GCRS$ and $GCRS \rightarrow BCRS$ transformations (Brumberg and Groten, 2001) in astrometry. We will follow IAU specified realizations of BCRS and GCRS with TCB and TCG, correspondingly. Problems resulting from the need to introduce scale factors due to the use of TDB and TT instead of TCB and TCG, are considered in Brumberg and Groten (2001). We did not consider the $GCRS->ITRS$ transformation in the paper.

2.   Computation Technique

To carry out calculations to transform from BCRS to GCRS and reverse it is necessary to know the Earth's velocity vector, Solar System bodies'potential *etc.* These have been obtained by means of the software ERA (Krasinsky and Vasiliev, 1996).

Note that in IAU Resolution B1 (2000), equation (2.1) is given with an accuracy of the order of c^{-4} for the transformation of time scales, although the accuracy for coordinate transformations is determined by values of order c^{-2}, (IAU, 2001; see also comments in Brumberg and Groten, 2001).

Calculations have been carried out for two objects: a hypothetical one located at a distance of 1 a.u. from the barycenter of the Solar System, and for a source in a geostationary satellite orbit. It is known that the orbit of a geostationary satellite is located in the plane of the Earth's equator, and its radius is equal to 42164 m. That's why for calculations we took a point in a geostationary orbit with coordinates (42164,0,0) at an epoch in TCG in the GCRS.

2.1. Algorithm to transform from BCRS to GCRS (direct transformation)

Except for functions of time, mentioned above, for direct transformation it is necessary to know the function $A = A(t)$ — the relativistic time equation, calculated by integration in numerical as well as analytical form. It is necessary to mention that A(t) is determined by its derivation to the accuracy of an additive arbitrary constant, to be determined from supplementary conditions. The constant for the function A(t) has been considered in detail in (Guinot, 2000), and has been calculated following Fairhead and Bretagnon (1990).

2.2. Algorithm to transform from GCRS to BCRS (reverse transformation)

The reverse transformation is constructed by means of similar tables of values as mentioned above depending on the argument in TCG (In the limit of Post-Newtonian accuracy it does not require any additional calculations). Additional calculations (compared to the direct transformation) will be needed only in the case of the determination the Earth's motion as a function of TCG. After the table values have been calculated, source coordinates at that epoch in the BCRS are determined by reverse transformation (Brumberg and Groten, 2001)

3.   Results

As was mentioned above, to check the proposed technique we carried out calculations following the suggested schemes of direct and reverse transformations in two ways (numerical and analytical) for an object, located in a geostationary orbit and a hypothetical object, located at the distance of 1 a.u. from the barycenter of the Solar System. To control the accuracy of the transformations, four-dimensional coordinates were used as initial data for the reverse transformation. The reverse transformation resulted in four-dimensional coordinates of the source in the BCRS. The comparison of the obtained values and initial numbers characterizes the accuracy of the calculations. The analysis of the calculations shows that the accuracy that was initially fixed has been obtained. For both sources the time transformation is less than 10^{-9}, and for the coordinate transformation, the relative error is less then $2.5 \cdot 10^{-8}$.

4. Conclusions

The results show that calculated coordinates using the suggested techniques do not differ from set values at the level of the required precision (Post-Newtonian approach taking into account terms of order c^{-2}). Thus, the precision level of the task is reached. Consequently the proposed numerical realization to transform from BCRS to GCRS and from GCRS to BCRS can be applied to the analysis of radio interferometric observations of high precision and to process Laser Lunar Ranging (LLR) data. However it is necessary to take into account the fact that, despite IAU recommendations, TDB (but not TCB) and TT (but not TCG) can be scales of coordinate time in the BCRS and in the GCRS, respectively. It will require introduction of special scale factors (Brumberg and Groten, 2001), but the principal algorithm will be the same one. The algorithm illustrates the practical application of new IAU Resolutions to the problem of connections between Celestial and Terrestrial coordinate systems based on General Relativity.

References

Brumberg V. A. and Groten E, 2001. A&A, 367, 1070–1077.

Fairhead L. and Bretagnon P., 1990. A&A, 229, 240–247.

Guinot B. In: J2000, "A fundamental epoch for origins of reference systems and astronomical models," Proc. of Journees 2000 (ed. N.Capitaine), pp. 209–213, Obs. de Paris.

IAU, 1991. Proceedings of the 127th Colloquium of the International Astronomical Union. Reference Systems. Observatory Washington, D.C., 1991.

IAU, 2001. IAU Information Bull. 88, 28–40 (Erata: ibid., 89, 4, 2001).

Krasinsky G. A. and Vasiliev M. V., 1996. In: Proceeding of IAU Colloquium 165, Poznan, Poland, July 1-5, pp.239–244.

Siedelmann P. K. and Kovalevsky J. 2002, A&A, 392, 341-351.

THE FUTURE DEVELOPMENT OF GROUND-BASED ASTROMETRY

Magda Stavinschi

Astronomical Institute of the Romanian Academy, Str. Cutitul de Argint 5, RO-040558 Bucharest, Romania, E-mail: magda@aira.astro.ro

Jean Kovalevsky

Observatoire de la Côte d'Azur - CERGA, av. Copernic, F-06130 Grasse, France, E-mail: Jean.Kovalevsky@obs-azur.fr

Abstract. The Working Group (WG) on The Future Development of Ground-based Astrometry was created following the decision of Division 1 at its XXIVth IAU General Assembly of the International Astronomical Union (IAU) at Manchester. During the three years it was chaired by M. Stavinschi (Romania) and Jean Kovalevsky (France). The members are Daffydd Wyn Evans (UK), Carlos Lopez (Argentina), Dan Pascu (USA), Antonio Pugliano (Italy), Manuel Sanchez (Spain), Ramakhrisna Teixeira (Brazil), and Arthur Upgren (USA).

1. Activities of the Working Group

The first action taken by the Working Group was to identify the existing small astrometric instruments. A questionnaire was distributed among observatories, and we received 30 descriptions of instruments in 12 different countries. Many of them are working in some programs, but others are now closed. The conclusion was that there are many instruments that could be used efficiently, if adequate programs were to be proposed. They are described in the Working Group web site: http://www.astro.ro/wg.html

The next step was to gather interested people to discuss possible programs to be undertaken with those or similar instruments. The first meeting took place in 2001 in Munich during JENAM, as a joint discussion on European Astronomy with Small Telescopes. A report was published in the EAS Newsletter, issue 22, December, 2001.

Then, during the "Journées 2002: Systèmes de référence spatio-temporels" in Bucharest, a second half-day meeting was organized. The report will be published in the proceedings of the meeting by Observatoire de Paris.

In 2002, a call was made to the community to contact us to propose cooperative programs using small or medium-sized telescopes for some defined scientific objective. The proposals received are presented below.

2. Instrumentation

Clearly, the traditional astrometric instruments, such as meridian circles, astro-labes or astrographs, performing as they did twenty years ago cannot compete with results obtained with space astrometry for the position of celestial objects, or with VLBI or GPS for the rotation of the Earth. They must be upgraded so they can still play a role in astronomy. The Working Group has identified several possibilities.

1) **CCD mosaics.** Systems with 4096 x 4096 pixels are now available and the read-out capabilities have improved considerably. In addition, the scan mode allows increasing the field of view, at least in one direction. Cheap and easy to install, with a very high sensitivity, they are the closest to the perfect detector in astronomy.

2) It is now possible, with small and medium size telescopes to reach the diffraction limit in resolution. **Speckle interferometry** is currently being in-stalled at the focus of some telescopes. It involves recording speckle patterns on a CCD and combining several hundred images and to reconstruct a perfect im-age by a computer. One needs a fast computer to compute the autocorrelation function. Speckle interferometry is particularly suited to observe close binary stars.

3) **Photometers** are easy to install at the focus of a telescope and can be used for many programs. Small telescopes are sufficient and it would be a good to dedicate it to single or, better, multichannel photometry. In addition to astrometric applications (eclipses, occultations, eclipsing binaries), there are plenty of possible programs of monitoring variable stars.

4) One can also mention the **solar astrolabe** used to observe the variations of the solar diameter, but it is rather expensive and difficult to build.

3. Conditions for Earth-based programs

The principal condition is that, whenever space astrometry can potentially achieve results where ground-based astrometry cannot compete, such programs should not be undertaken. But, space astrometry missions have their own limi-tations.

- **They are not flexible:** observations are either constrained by a scanning law (GAIA) or by overall programming (SIM or HST);

- **They are not designed for monitoring:** it is not possible to get long sequences of observations of a single body;

- **They have a limited lifetime:** many astronomical features must be observed either indefinitely, or at least a longer time;

- **They often need preliminary data:** for instance, ephemerides of minor planets or predictions of magnitudes of irregular variables.

4. Cooperative projects sponsored by the Working Group

In response to the call for cooperative astrometric programs using ground-based small or medium-size instruments, the Working Group received five proposals.

Some of them are new, and some were already operational, but sought support in order to enlarge participation.

1- Mutual phenomena of Jupiter and Saturn satellites (PHEMU - PHESAT)

Jean-Eudes Arlot, IMCCE, Paris Observatory

Using the opportunity of the transit of the Sun and the Earth through the equatorial plane of Jupiter and Saturn, observations of mutual occultations or eclipses with CCDs provide relative positions of these satellites with a high astrometric accuracy. They are used to improve the models describing their motion.

2- Ground-based monitoring of astrometric binaries (GMAB)

George Gontcharov, Pulkovo Observatory

About a hundred astrometric binary candidates have been discovered by Hipparcos. They should have periods of 10-50 years. Additional observation from the ground must be made in order to determine their periods and other orbital elements and reveal photocentric orbits that will allow us to determine the masses of the components.

3- Dedicated astrometric network for the follow-up of GAIA

William Thuillot, IMCCE, Paris Observatory

The objective of the network is to observe on alerts to get CCD images of targets in order to confirm their detection and follow their evolution. The network should be planned now with tests of acquisition of images of test targets and the development of the processing of the images. Preliminary programs of observations may be organized, for instance on minor planets or comets.

4- Optical counterparts of radio sources

Gennady Pinigin, Nikolaev Observatory, Ukraine

The link between the International Celestial Reference Frame (ICRF) and the optical realizations like the Hipparcos catalogue is a major problem to which ground-based astrometry can bring valuable contributions using CCD observations.

5- Variation of the solar diameter

Alexandre Humberto Andrei, National Observatory, Rio de Janeiro

The solar diameter has periodic and irregular variations that are not well understood. In particular, they may be partly caused by atmospheric effects depending on the geographical position of the observatory. It is therefore necessary to have several well distributed solar astrolabes. A close technical cooperation among stations has proven to be highly desirable.

5. Other possible objectives for ground-based astrometry

There are many other scientifically sound objectives that could be assigned to ground-based instruments. Some need coordinated observations, some may be made as a single observatory program. Examples:

Solar system:

- Observation of minor planet positions for the determination of the masses of perturbing bodies

- Observations of Earth-cruisers, for which one needs to update frequently the orbits frequently

- Bulk observations of newly discovered objects in order to get good orbits for recognition purposes

- Observation of small planetary satellites using a mask technique to dim the luminosity of the planet

Stars and stellar systems:

- Observation of close binaries by speckle interferometry. The large number of these objects and the potential for determining stellar masses call for more instruments devoted to speckle interferometry.

- Determination of stellar diameters by speckle interferometry or using occultations by the Moon.

- Photometry of variable stars, in particular eclipsing binaries, which permits stellar mass determination.

- Recognition of stars and determination of their proper motions in highly crowded fields badly conditioned for space astrometry.

The WG was approved for another three years.

Astrometric Measurements of Radio Sources Optical Counterparts. OATo Campaign: Some Final Results

B. Bucciarelli, M.T. Crosta, M.G. Lattanzi, G. Massone, R. Morbidelli

Astronomical Observatory of Torino, I-10025

W. Jin, Z. Tang[1]

Astronomical Observatory of Shanghai, 200030 China

G. Deiana, A. Poma, S. Uras

Astronomical Observatory of Cagliari, I-09012

Abstract.   We present photographically determined positions of a sub-set of 20 radio sources from a larger sample collected by OATo during a dedicated campaign, as described in this paper. Targets are from the list of extra-galactic objects adopted by the IAU for the realization and maintenance of the ICRF. The results obtained so far are in agreement with the VLBI-determined radio positions at an accuracy level of better than 100 microarcseconds.

1.   Introduction

A campaign for the determination of precise optical positions of some 87 ICRF radio sources by photographic observations was carried out by the Astronomical Observatory of Torino (OATo) during approximately 7 years, starting in 1987. The complete data archive, consisting of about 400 plates, has been digitized using the Torino-Cagliari Measuring Machine (TO.CA.M.M.), whose stability has shown to be better than $1\mu m$. Some preliminary results on the astrometric quality of these data can be found in Chiumiento *et al.* (1990), Del Bo' *et al.* (2000), Lattanzi *et al.* (2001). During the last year, the data reduction procedures have been revised to take full advantage of the high-quality reference catalogues recently made available, and all the digitized images are consistently being re-calibrated. In this paper we briefly outline the program and present the positions of a sample of 20 targets.

2.   The program

Our QSO targets were originally chosen among the list proposed by the Working Group formed at IAU Coll. 48 "Modern Astrometry", under the auspices of former IAU Commission 24, as compact sources displaying both radio and optical

---

[1]Visiting Scientist at OATo, Oct 2002-May 2003

counterparts, and therefore suitable for establishing a radio/optical extragalactic reference frame (Argue *et al.* 1984). Since the beginning of the OATo campaign the properties of the WGRF catalogue have been extensively studied, and the characterization of each radio source entirely derived from VLBI data analysis (Ma and Feissel 1997). Owing to the faintness of most optical counterparts of extragalactic radio sources and to the stellar density of the suitable reference catalogues available at the time this program was begun - mainly the Carlsberg Meridian Catalogues 4, 5 and 6 (CAMC 1989, 1991, 1992) -, a multi-step approach was adopted to derive the QSOs' positions in a consistent reference frame. In particular, 10- to 20-minute exposures taken at the 38-cm MORAIS Photographic Refractor of Torino Observatory, with a useful field of 1.5 x 1.5 degrees, to determine the position of anonymous stars, which were then used to reduce the smaller ($\sim$ 30-arcminute field), deeper plates (30- to 90-min exposures) of the OATo's 105-cm REOSC Astrometric Reflector. Additional plates were taken at the ESO La Silla GPO 39-cm Astrograph, the long-focus Ritchey-Chretien 152-cm reflector of Loiano Observatory, University of Bologna, and, at a later stage, the ING JKT 0.9-meter Cassegrain telescope at La Palma. Blue plate emulsions, type 103a-O and IIa-O and IIIa-J were always used. This choice was justified by the chromatic aberration of the MORAIS optics being a minimum in the blue spectral region.

3. Plate Digitization

All plates have been digitized with the Torino-Cagliari measuring machine TO.CA.M.M., an original Ascorecord which has been fully automated, its basic mechanical and optical structure being maintained (Del Bo' *et al.* 2000). The scans are carried out in "pointed mode", *i.e.*, a list of stellar coordinates taken from the GSC-I (Lasker *et al.* 1990) is used to drive the plate holder to the chosen x, y position by two synchronous motors and the stellar image is centered in the CCD field. At this point the optical rulers are read and a CCD exposure is taken and stored as a FITS file. Extensive tests performed on some of these plates have demontrated a scanning stability of 1 microarcsecond or even better.

4. Plate Reductions

The reference catalogues used for the present work are the CAMC-11 (Carlsberg Meridan Catalogues 1999) and Tycho-2 (Høg *et al.* 2000); Special purpose equatorial catalogues like CAMC-12 (Carlsberg Meridian Catalogues 2002) and the ACRS (Stone *et al.* 1999), to check for the presence of undetected small scale systematics and/or magnitude effects were also used. We plan to incorporate the new Carlsberg Meridian Circle Catalogue and UCAC releases (CAMC-13 and UCAC-2) in our reductions before publishing the complete set of QSO positions.

For each telescope we tested the significance of non-linear terms up to a full 3rd order polynomial - also including a pure and coma-like magnitude term - which could originate from sky modelling, optical field distortion, plate misalignment, guiding errors and residual aberrations. The solution was carried out using un-weighted ordinary least squares and all the formal errors were obtained from the computation of the covariance matrix and the application of rigorous

error propagation formulae. Moreover, the procedure was iterated after elimination of reference stars with residuals larger than 2.6 times the sigma of unit weight of the ξ and η fits, independently.

5.   Results and Conclusions

The following results for 20 radio sources are representative of the quality of our entire sample. Table 1 contains the derived optical positions and relative errors, having performed a direct link to the Tycho-2 and CAMC-11 catalogues, independently. The VLBI coordinates of each object as given by IERS are also listed for comparison. From a preliminary analysis of this small sample, our coordinates are in good agreement with the VLBI ones within the stated errors. We plan to attempt a statistical analysis of the differences between the optical and radio positions when we will have reduced the complete dataset.

References

Argue A.N., de Vegt, C., Elsmore, B., Fanselow, J., Harrington, R., Hemenway, P., Johnston, K. J., Kuhr, H., Kumkova, I., Niell, A. E., Walter, H., Witzel, A., 1984, A&A, 130, 191.

Carlsberg Meridian Catalogues, La Palma, Numbers 1-11, 1999, Copenhagen Univ. Obs., Royal Greenwich Obs., Real Inst. y Obs. de la Armada en San Fernando.

Carlsberg Meridian Catalogue, La Palma, Number 12, 2002, Copenhagen Univ. Obs., Royal Greenwich Obs., Real Inst. y Obs. de la Armada en San Fernando.

Chiumiento, G., Lanteri, L., Lattanzi, G., Massone, G. 1991, Internal Precision in CCD Astrometry of QSO Optical Counterparts, IAU Coll 127, 14-20 October 1990.

Del Bo', M., Deiana, G.L., Lattanzi, M.G., Massone, G., Poma, A., Porcu, F., Salvati, F.,Uras, S., The TOCCAM Project, Proceedings of the IAU coll. 178, Dick S., McCarthy D. & Luzum B. eds., ASP Conference series vol. 208, 2000.

Høg, E., Fabricius, C., Makarov, V.V., Urban, S, Corbin, T., Wycoff, G., Bastian, U., Schwekendiek, P. and Wicenec, A., 2000, A& A 352.2, L19-L22.

Lasker, B., Sturch, C., McLean, B., Russel, J., Jenkner, H., and Shara, M. 1990, A.J. 99, 2019.

Lattanzi M.G., Massone G., Poma A., Uras S., Journées 200: Systèmes de référence spatio-temporels, Paris 18-20 September 2000; edited by N. Capitaine, Paris: Observatoire de Paris, ISBN 2-901057-45-4, 2001, p. 33 - 36.

Ma C. and Feissel M. eds. 1997, Definition and Realization of the International Celestial Reference System by VLBI Astrometry of Extragalactic Objects, IERS Technical Note 2.

Stone, R.C., Pier, J.R., and Monet, D.G., 1999, A.J., 118, 2488.

Table 1.   Results for 20 radio sources. For each target the ICRS designation and J2000 equatorial coordinates are listed, followed by the CAMC-11 and Tycho-2 derived positions and formal errors.

QSO-ID	RA	IERS	CAMC11/ TYCHO2		DEC	IERS	CAMC11/ TYCHO2	
0112-017	1h 15m	17.0999s	17.1043	(0.103)	-1d 27'	4.577"	4.567	(0.106)
			17.1095	(0.107)			4.557	(0.107)
0333+321	3h 36m	30.1076s	30.1058	(0.068)	32d 18'	29.342"	29.431	(0.068)
			30.1084	(0.070)			29.409	(0.070)
0716+714	7h 21m	53.4484s	53.4341	(0.064)	71d 20'	36.363"	36.306	(0.064)
			53.4340	(0.064)			36.250	(0.064)
0735+178	7h 38m	7.3937s	7.4037	(0.070)	17d 42'	18.998"	18.890	(0.073)
			7.4049	(0.068)			18.851	(0.068)
0736+017	7h 39m	18.0338s	18.0377	(0.096)	1d 37'	4.618"	4.721	(0.104)
			18.0369	(0.100)			4.719	(0.100)
0836+710	8h 41m	24.3652s	24.3882	(0.056)	70d 53'	42.173"	42.268	(0.060)
			24.3956	(0.069)			42.159	(0.056)
0839+187	8h 42m	5.0941s	5.1096	(0.080)	18d 35'	40.990"	41.030	(0.079)
			5.1064	(0.074)			40.963	(0.073)
0851+202	8h 54m	48.8749s	48.8839	(0.056)	20d 6'	30.640"	30.567	(0.056)
			48.8832	(0.054)			30.579	(0.054)
0954+658	9h 58m	47.2451s	47.2758	(0.082)	65d 33'	54.818"	54.828	(0.081)
			47.2754	(0.072)			54.881	(0.072)
1039+811	10h 44m	23.0625s	23.0839	(0.133)	80d 54'	39.443"	39.317	(0.131)
			23.0480	(0.135)			39.347	(0.135)
1252+119	12h 54m	38.2556s	38.2591	(0.128)	11d 41'	5.895"	5.838	(0.128)
			38.2546	(0.132)			5.863	(0.125)
1253-055	12h 56m	11.1665s	11.1736	(0.062)	-5d 47'	21.524"	21.576	(0.062)
			11.1747	(0.065)			21.560	(0.056)
1328+307	13h 31m	8.2881s	8.3169	(0.155)	30d 30'	32.959"	33.027	(0.143)
			8.3082	(0.054)			32.996	(0.051)
1611+343	16h 13m	41.0642s	41.0608	(0.284)	32d 12'	47.909"	47.905	(0.214)
			41.0714	(0.216)			47.938	(0.180)
1633+382	16h 35m	15.4929s	15.5459	(0.105)	38d 8'	4.500"	4.647	(0.098)
			15.5179	(0.168)			4.968	(0.161)
1652+398	16h 53m	52.2166s	52.2186	(0.078)	39d 45'	36.608"	36.613	(0.078)
			52.2214	(0.078)			36.573	(0.079)
1749+096	17h 51m	32.8185s	32.8038	(0.723)	9d 39'	0.728"	0.723	(0.161)
			32.8111	(0.164)			0.676	(0.163)
1803+784	18h 0m	45.6839s	45.6933	(0.117)	78d 28'	4.018"	4.055	(0.117)
			45.6855	(0.117)			4.067	(0.118)
1928+738	19h 27m	48.4952s	48.5256	(0.083)	73d 58'	1.570"	1.476	(0.086)
			48.4981	(0.076)			1.445	(0.075)
2200+420	22h 2m	43.2913s	43.3089	(0.085)	42d 16'	39.980"	39.892	(0.087)
			43.2946	(0.083)			39.892	(0.083)

REFERENCE FRAMES AND GROUND-BASED ASTROMETRY

Magda Stavinschi

Astronomical Institute of the Romanian Academy, Str. Cutitul de Argint 5, RO-040558 Bucharest, Romania, E-mail: magda@aira.astro.ro

Abstract. We analyze the contributions of ground-based astrometry to the extension of the optical reference frame to faint stars in crowded fields, production of input catalogues for future space projects, re-observing existing catalogues for proper motion determination, linking optical and radio reference frames, positions of radiosource optical counterparts, stellar catalogues, *etc.* It is one of the tasks of the Working Group (WG) for The Future Development of Ground-Based Astrometry.

1. HIPPARCOS Catalogue

The link between the ICRF and the Hipparcos catalogue was not straightforward. It could be achieved only through a variety of techniques. Some practical applications of the Hipparcos catalogue as an ICRF optical counterpart are limited by its low density of stars, about 118 000 objects distributed all over the sky and typically brighter than V = 10.0. It provides the best reference available to test objects with $8.0 \leq V \leq 13.0$. The IAU noted in 2000 that the Hipparcos frame will depart from ICRF due to the uncertainties in proper motion (pm). The observations and the study of the positions of optical counterparts of ICRF radio sources provide a powerful tool for the detection and removal of systematic errors in a stellar catalog as well the estimation of its external accuracy. This method is limited by the precision of the optical counterpart observations and by the density of available ICRF sources in the sky. Maintenance and extension of the extragalactic reference frame and Hipparcos reference frame are clearly missions of ground-based astrometry, as well as the links between various reference frames.

2. Why ground-based astrometry?

As space astrometry missions are optimized for the determination of positions, pm, and parallaxes of stars, there is no sense to have ground-based programs to obtain these parameters. Only specialized telescopes which could observe very faint stars could still be used, and even in this case the Hipparcos accuracy is very difficult to reach. There is however an exception: in very densely crowded fields, the GAIA images will overlap, and will not be separated properly. It is necessary to carry out ground-based observations for objects such as low-luminosity stars (M dwarfs, white dwarfs and brown dwarf candidates), and the optical counterparts of extragalactic radio sources as both are too faint to

observe by satellite, as well as multiple stars with periods longer than the limited life of satellite. An improved double star catalogue is required.

3.   Optical and radio regions

A useful contribution of ground-based astrometry could be the establishment of the link between the optical stars and the radioastronomical coordinate system. A good network for observing the extragalactic/optical sources and intermediate reference stars could still improve the reference frame.

Such a program was CONFOR - Connection of Frames in Optical and Radio regions. It was undertaken for the determination of relative orientation and errors of radioastronomical and optical coordinate systems. The extension of the inertial frame ICRF to the optical domain is a worldwide astrometric task. The optical reference frame, which will continue to be widely used for optical observations, navigation and guidance will require subsequent observations at the accuracy level of HIPPARCOS, or better. The IAU Commission 8 WG "The Future Development of the Ground-Based Astrometry" could help with a large densification project.

4.   Densification

Densification is the area where the most significant advances took place during the last three years. The observational programs with CCDs involve small-field observations of faint stars, so generally there will not be measurable bright stars in the field, and fainter stars must be used as reference stars. Thus, there is an urgent need to accurately densify the optical reference frame to fainter stars. A CCD survey of the sky to magnitude 15 or 16 could densify the HIPPARCOS catalog at about the 30 mas accuracy level.

Tycho 2 has about 2 500 000 stars, with an uncertainty of 10 mas for magnitudes less than 9 and 100 mas for M = 12. In spite of the quality of Tycho-2 catalogue, we need more. For all sky catalogues, the Tycho-2 Catalogue, utilizing re-reduced Tycho star mapped data from the Hipparcos satellite and over 140 ground-based observational catalogues for the computation of pm, was released by Copenhagen University Observatory and the U.S. Naval Observatory in February, 2000. So, the accessibility to the ICRS has to be improved in the optical domain by enlarging the number of good positions and proper motions based on the Tycho-2 catalogue, for regions of the sky around extragalactic radio sources.

5.   New astrometric compilations

Regions containing pre-main sequence (PMS) stars in Chamaeleon, Lupus and Upper Scorpius-Ophiuchus are also helpful. For instance, the Valinhos Meridian Circle Catalogue VMCC, as well as other new astrometric compilations can be important steps towards a quality enhancement of the Tycho-2 catalogue, mainly for those new objects with $V \geq 10.0$. This catalog contains 41 721 stars brighter than $V \sim 16.0$ observed at least 3 times with the Valinhos Meridian Circle.

For magnitudes ranging from V = 8.0 to 14.0 the internal average positional precision is 40 mas (Camargo *et al.* 2000).

6.   Photographic plates

A straightforward method to determine the ICRF-Hipparcos link is to observe the optical counterparts of compact radio-sources, using plates from Schmidt telescopes or from the prime focus of large telescopes. The catalogues combining the old photographic plates or the earlier catalogues with the current observations have been released to improve proper motions.

Maintenance and extension of the Hipparcos catalogue with plates taken with different refractors is required. Jin reported on such a program with the 3435 plates taken with the 40-cm refractor at Shanghai, beginning with observations taken in 1901. These plates belong to 764 different sky areas and contain 10,000 Hipparcos stars. The position and proper motions for 54 stars, including 16 Hipparcos stars, whose mean standard errors in RA and Dec are 0.70 and 0.59 mas/yr in pm and 10.5 and 7.5 mas in position, were obtained with respect to ACT reference catalogue by using 15 plates in two areas (Wang *et al.* 2000). The plate archive could be a very good help for this.

7.   Differences between catalogues

The systematic difference of the FK5 pm system compared with that of Hipparcos, analyzed via the PPM and ACRS catalogues was determined at Shannxi. The global rotation of pm between the PPM and Hipparcos and between the ACRS and Hipparcos shows a large offset compared with the correction of the precession constant. It could be the internal nonrigid feature of the FK5 pm system and the low accuracy of the alignment of PPM to the system of the FK5 (Zhu 1999, 2000.)

8.   ICRF extension

The most serious difficulty to achieve the ICRF extension is the availability of first epoch positions, when proper motion measurements are involved. There is also the need for accurate relationships among the reference frames in different wavelengths.

References

Camargo, J.I.B., Teixeira, R., Benevides-Soares, P., Ducourant, C., 2001, A&A, 375, 308.
Wang, J. J., Chen, L., Wu, Z. Y., Gupta, A. C., Geffert, M., AA Suppl Ser., 142, 373.
Zhu Zi 1999, AJ, 117, 1103.
Zhu Zi 2000, AJ 112, 1103.

Coupling between the Earth's rotation rate and precession-nutation

Sébastien Lambert

SYRTE - UMR8630/CNRS, Observatoire de Paris, 61 avenue de l'Observatoire, 75014 Paris, France

Abstract.   For different Earth models, we computed the effects of variations in the Earth's rotation rate on precession-nutation. In the case of a refined model with elastic mantle and decoupled liquid core, we found a major contribution of -136.56 μas and 6.18 μas on the 18.6-year nutation respectively in longitude and in obliquity, and a decrease of -3222.80 μas/century in the precession rate in longitude.

1.   Introduction

In the framework of the implementation of the IAU2000A precession-nutation model, it is necessary to compute all the effects with amplitudes of the order of tenths of microarcseconds. Variations in the Earth's rotation rate due to zonal tides are well known. They have been detected in observations (Hefty & Capitaine 1990) and models are provided (Yoder *et al.* 1980; McCarthy 1996; Defraigne & Smits 1999). However, in the dynamical equations of Earth rotation, the coupling between the axial component of the instantaneous vector of rotation and its equatorial component, giving rise to nutations, is generally neglected and therefore the effects of this coupling are not considered. In this study, we compute the coupling between the effects of zonal tides in the Earth's rotation rate and precession-nutation for different Earth models.

2.   Dynamical equations of the Earth rotation

We consider the Earth as an ellipsoidal body with small irregularities in its figure. In a rotating frame in which the axes are oriented towards the Earth's mean axes of inertia, the angular momentum conservation law is

$$\frac{\mathrm{d}\vec{H}}{\mathrm{d}t} + \vec{\omega} \times \vec{H} = \vec{\Gamma}, \tag{1}$$

where $\vec{H}$ is given by the product of the inertia tensor with the instantaneous vector of rotation of the Earth $\vec{\omega} = \Omega(m_1, m_2, 1 + m_3)$. $\vec{\Gamma}$ is the tidal torque expressed in the terrestrial frame. The equatorial part is derived from the sectoral part of the lunisolar potential ϕ (Sasao *et al.* 1980):

$$\Gamma = -i\Omega^2(C - A)\phi e^{-i\Phi}, \tag{2}$$

where C and A are the axial and equatorial moments of inertia of the Earth, Φ is the Earth rotation angle. ϕ depends on the right ascension α and declination δ of the perturbing body:

$$\phi = \frac{3K^2\mu}{\Omega^2 r^3}\sin\delta\cos\delta(\cos\alpha + i\sin\alpha), \qquad (3)$$

where K^2 is the geocentric gravitational constant, μ is the ratio between the mass of the disturbing body and the mass of the Earth and r is its geocentric distance. This leads to the Euler-Liouville equation:

$$\dot{m} - i\sigma_r(1+m_3)m + \frac{\dot{c}+i\Omega c}{A} = \frac{\Gamma}{A\Omega} = -i\sigma_r\phi e^{-i\Phi}, \qquad (4)$$

in which $c = c_{13} + ic_{33}$ is the non-diagonal element of the inertia tensor. $\sigma_r = \Omega(C-A)/A$ is the Euler frequency depending on the dynamical ellipticity $H_d = (C-A)/C$. For a rigid Earth with an ellipsoidal shape, Equation (4) becomes

$$\dot{m} - i\sigma_r(1+m_3)m = \frac{\Gamma}{A\Omega} = -i\sigma_r\phi e^{-i\Phi}. \qquad (5)$$

If we consider a more refined Earth model, the increment of inertia c is related to the rotation vector, to the potential and to the inertia moments (Sasao *et al.* 1980). Therefore, for an elastic Earth, the Euler frequency σ_r is modified by the factor $1 - \kappa\Omega/\sigma_r \simeq 0.68$ where κ is the secular Love number. The addition of a decoupled liquid core brings the factor to $(A/A_m)(1 - \kappa\Omega/\sigma_r) \simeq 0.77$ where A_m is the equatorial mean moment of inertia of the mantle. These factors act as scale factors for the resonance frequency and, following Equation (4), as scale factors for the excitation amplitudes in the right member.

3.   Variations of the dynamical ellipticity and rotation rate

Considering that the trace of the inertia tensor is constant (Melchior 1978), and letting $\delta(2A + C) = 0$, we have

$$\delta H_d = \delta\left(\frac{C-A}{C}\right) = \frac{3}{2}\frac{\delta C}{C}, \qquad (6)$$

Variations in H_d induce variations in the length of day (LOD) and in the axial component of the instantaneous vector of rotation of the whole Earth:

$$\frac{\delta C}{C} = \frac{\delta LOD_z}{\overline{LOD}} = -m_{3,z} \qquad (7)$$

where the subscript z denotes that these variations come from zonal tides. We adopt the model from Defraigne & Smits (1999) established for an Earth model with a decoupled core and an inelastic mantle, and ocean effects included using a transfer function computed by Mathews *et al.* (2002).

4. Coupling effects

In the dynamical equations of Earth rotation (4), both H_d and m_3 appear. Three kinds of coupling are noted:

(**A**) the torque is proportional to H_d (see Equation (4). It can be shown that this is the major effect.

(**B**) the left hand side of Equation (4) contains the product $m \times m_3$. It can be shown that this coupling gives corrections below the microarcsecond level.

(**C**) the quantity m_3 is present in the sidereal rotation angle Φ to transform the torque expressions from the fixed reference frame to the rotating reference frame (rotation of $-\Phi$, Equation (2)) and to transform the rotation vector coordinates m into the nutation angles, according to Euler's kinematical relationships (rotation of $+\Phi$). These two rotations in opposite sense compensate themselves.

We have computed the effects of the variations in the Earth rotation rate on the nutation angles by introducing variations as listed in (A), (B) and (C) above and solving the dynamical Equation (4) for different Earth models. One can see that the addition of an elastic mantle and a decoupled core should modify the amplitudes from the same factors which affect the resonance frequency. The factor is 0.68 for an elastic mantle and 0.77 for an Earth with an elastic mantle and a liquid core.

Table 1.   Effects of zonal tides on nutation angles (μas). RE: rigid Earth; EM: elastic mantle; EM+FC: elastic mantle and liquid core.

l	l'	F	D	Ω		$\Delta\psi$		$\Delta\epsilon$	
						sin	cos	sin	cos
0	0	0	0	1	RE	-179.27	-2.05	-0.17	8.42
					EM	-125.42	-1.42	-0.12	7.72
					EM+FC	-136.56	-1.59	-0.12	6.18
0	0	2	-2	2	RE	-3.65	0.03	0.00	0.00
					EM	-2.52	0.02	0.00	0.00
					EM+FC	-2.88	0.03	0.00	0.00
0	0	0	0	2	RE	-3.00	-0.06	-0.03	1.94
					EM	-2.01	-0.04	-0.02	1.30
					EM+FC	-2.33	-0.04	-0.02	1.48
l	l'	F	D	Ω		$t \times \cos$			
0	0	0	0	0	RE	-4197.73			
					EM	-2823.61			
					EM+FC	-3222.80			

5. Discussion and conclusion

Several recent studies have evaluated the effects of variations on the Earth's rotation rate on precession and nutations. Souchay & Folgueira (1999) used the Hamiltonian formulation to compute the nutations, for a basic Earth model (elastic homogeneous body). It involves the total potential energy which is

proportional to H_d. They found a contribution of -168 μas to the 18.6-year term in longitude and 9 μas to the 18.6-year term in obliquity and other smaller contributions. However, the contribution to the precession rate is not discussed.

Bretagnon (2000) made non-rigid nutation series by applying the transfer function MHB2000 (Mathews *et al.* 2002) to the SMART97 rigid nutation series. Given that MHB2000 does not take into account the variations in the Earth's rotation rate, these effects were added to the third component of the Earth's rotation vector and the Euler's angles were recomputed from Euler's kinematical relationships. This method gave rise to an 18.6-year term in obliquity whose amplitude is 712 μas. Actually, according to the explanation (C), this term is compensated by taking into account the variations of the rotation rate in the dynamical equations and should not be considered. Moreover, this term does not contain the effects of (A).

Mathews *et al.* (2002) investigated a refined Earth model (elastic mantle and decoupled liquid core) to evaluate the influence of the second order terms due to tidal variations in the dynamical equations. Contributions of -98 μas and -29 μas are found to the 18.6-year term respectively in longitude and in obliquity and a correction of about -21 mas/c on the precession in longitude.

In our study, we recomputed the zonal tides effects on nutation using the Hamiltonian theory. We found the same values as Souchay & Folgueira (1999) and an additional correction of -4278.5 μas/c to the precession rate in longitude. To validate these results, we solved Equation (4) for different Earth models with the variations in the rotation rate taking into account the effects listed in (A), (B) and (C). (See Table 1.) For an elastic Earth with a decoupled liquid core, we concluded that the coupling changed the 18.6-year nutation term by -136.56 μas in longitude and 6.18 μas in obliquity. Other contributions are about a few μas. The correction to the precession rate in longitude is -3222.80 μas/c.

References

Bretagnon, P. 2000, in Journées Systèmes de Référence Spatio-Temporels Proc., ed. N. Capitaine, Observatoire de Paris, 177.

Defraigne, P., & Smits, I., 1999, Geophys. J. Int., 139, 563.

Hefty, J., & Capitaine, N., 1990, Geophys. J. Int., 103, 219.

Mathews, P. M., Herring, T. A., & Buffett, B. A., 2002, J. Geophys. Res., 107, B4, 10.1029/2001JB000390.

McCarthy, D. D. 1996, IERS Conventions, IERS Technical Note 21.

Melchior, P., 1978, *The Tides of the Planet Earth*, Pergamon Press.

Sasao, T., Okubo, S., & Saito, M., 1980, in IAU Symposium 78, eds. E. P. Federov, M. L. Smith, & P. L. Bender (Hingham, Mass.: Reidel), 165.

Souchay, J., & Folgueira, M., 1999, Earth, Moon and Planets, 81, 201.

Yoder, C. F., Williams, J. G., & Parke, M. E., 1981, J. Geophys. Res., 86, 881.

ICRF Densification Via HIPPARCOS-2MASS Cross-Identification

Goran Damljanović

Astronomical Observatory, Volgina 7, 11160 Belgrade, Serbia and Montenegro

Jean Souchay

Observatoire de Paris, DANOF, 61, avenue de l'observatoire, 75 014 Paris, France

Abstract. We developed a cross-identification programme of stars of any two catalogues, and applied it to the HIPPARCOS-2MASS catalogues. We found 37 940 common stars, after selecting a rejection criterion, that we set to a 3σ value. The procedure was more than 68.5% successful. There were 117 955 HIPPARCOS stars, and 162 195 232 2MASS Second Incremental Data Release ($\sim 47\%$ of the sky) in our basic selection. Then, we calculated a preliminary systematic error ($\sim 0''.10$) of differences $\Delta\alpha$ and $\Delta\delta$ of common stars, included it in the programme, and the cross-identification was nearly 80% successful.

1. Introduction

The mean density of stars of the HIgh Precision PARallax COllecting Satellite (HIPPARCOS) Catalogue (ESA 1997) is <3 stars/sq.deg. The magnitude is mostly $7 < V < 9$. The density is not sufficient to ensure a suitable astrometric reduction for observations carried out in small fields with CCD detectors (for the reductions of observations of fainter stars), and the magnitude is far too restricting nowadays when searching for reference stars for astrometric calibration. It is necessary to produce large stellar catalogues with fainter visible/infrared sources and linked to the ICRF (International Celestial Reference Frame). There are various recent catalogues which should help the densification of the ICRF, at optical wavelengths and at other ones including the Tycho-2 Catalogue, the USNO CCD Astrograph Catalogue (UCAC), the Two Micron All Sky Survey (2MASS), the Deep Near Infrared Survey of the Southern Sky (DENIS), *etc.*

Since 1997, HIPPARCOS is considered the primary optical counterpart of the ICRF. After a decision of the IAU General Assembly in Kyoto, 1997, the ICRF was adopted as the realization of the ICRS (International Celestial Reference System) from the beginning of 1998. It is based on a catalogue of 608 compact radio sources (Ma *et al.* 1998) which are determined with an internal precision of 0.3 to 0.5 marcsec. It has been updated recently by the ICRF-Ext.1, which includes 59 new sources (IERS Annual Report 1999).

2. HIPPARCOS and 2MASS Catalogues

HIPPARCOS is the optical frame with roughly 110 000 stars brighter than magnitude 12, and gives for each object, among a very large number of parameters, the position with an accuracy of the order of 1 marcsec at 1991.25 (the epoch of the catalogue), and the proper motions in $\mu_\alpha \cos \delta$ and μ_δ with a standard error of about 1 marcsec/yr. The positions and proper motions of stars are the bases of the optical frame HCRF (Hipparcos Celestial Reference Frame).

2MASS is based on two highly automated 1.3-m telescopes (with observing facilities at Mt. Hopkins, Arizona and Cerro Tololo, Chile), equipped with a three channel camera to observe the sky simultaneously at J (1.25 μm), H (1.65 μm) and K_S (2.17 μm). The 2MASS Second Incremental Data Release (Cutri *et al.* 2001) includes a Point Source Catalogue (PSC), with positions and photometry for 162 213 354 sources, an Extended Source Catalogue (XSC) with positions and photometry for 585 056 objects and an Atlas of Images (1 897 017 FITS images). The 2MASS telescopes map the sky with overlapping strips (tiles) by using a freeze-frame scanning technique. They are operated by the Smithsonian Astrophysical Observatory (SAO) and the National Optical Astronomy Observatories (NOAO). The PSC of 2MASS has been divided onto 49 right ascension segments, $0^h \leq \alpha < 24^h$, ordered by increasing δ within each segment. The data cover 19 681 square degrees, or about 47% of the sky. The PSC consists of brightness data in three survey bands and positions, without proper motions. The magnitude limits are: 15.8 for J band, 15.1 for H, and 14.3 for K_S. The positions are accurate to $< 0''\!.2$, and α and δ are given in the J2000 system. (Each star has its epoch of observation). The positions of the 2MASS sources are correlated with the ACT (Urban *et al.* 1998) or USNO-A optical catalogues. Note that positional associations do not mean identifications between the infrared and optical sources. The positions of 2MASS objects are tied to the ICRS via the ACT Reference Catalogue. Some positional solutions may have random walks as much as $1''\!.0$ from the ICRS frame. The ACT catalogue has 988 758 stars to about $V = 11$ and with positional error $< 0''\!.03$. The tiles with few or poorly distributed reference stars have poor astrometric solutions and bigger discrepancies from the reference frame. About 77% of the PSC objects have $|b| < 20°$. (The majority of point sources are concentrated towards the galactic plane.) Concerning the possible sources of 2MASS positions errors, we mention the relative sparsity of ACT reference stars near the galactic poles, and problems of observations/reductions near the galactic center and near tile ends.

2.1. The Cross-Identification of HIPPARCOS and 2MASS

The cross-identification programme is based on the rejection criterion, that we set to a 3σ value. We make the 2MASS PSC positions comparison with respect to the positions given by the HIPPARCOS. We did separately the cross-identification in each of 49 segments adopted for 2MASS. The identification was considered as effective when the HIPPARCOS star could be coupled to only one 2MASS star within a 3σ vicinity in both coordinates (α and δ). We tested our method inside a very small part of the sky including a few HIPPARCOS stars, just to check the quality of our results. We ran our detection algorithm within

the 49 above mentioned 2MASS segments. Some stars were without enough data and we removed them before beginning the final cross-identification procedure. Therefore 18 122 stars, which represent about 0.01% of the 2MASS PSC were removed from the catalogue. In a similar way, 263 stars were removed from HIPPARCOS (about 0.22%), because of the absence of proper motion data. Finally, we had 117 955 HIPPARCOS stars.

For each star, we calculated the standard deviation σ in α and in δ respectively σ_α and σ_δ, by using HIPPARCOS and 2MASS data. The calculated value of σ_α (and σ_δ) depends on itsparts, $\sigma_\alpha^2 = \sigma_{\alpha 1}^2 + \sigma_{\alpha 2}^2 + \sigma_{\alpha 3}^2$ (and $\sigma_\delta^2 = \sigma_{\delta 1}^2 + \sigma_{\delta 2}^2 + \sigma_{\delta 3}^2$). The values $\sigma_{\alpha 1}$ and $\sigma_{\delta 1}$ are based on the standard errors of the HIPPARCOS positions, and calculated by using the HIPPARCOS data. The values $\sigma_{\alpha 2}$ and $\sigma_{\delta 2}$ are based on the differences in the observational epochs between HIPPARCOS and 2MASS (both catalogues data) and the errors of proper motions $\mu_\alpha \cos \delta$ and μ_δ (from the HIPPARCOS data). The values $\sigma_{\alpha 3}$ and $\sigma_{\delta 3}$ are based on the position error ellipse, and calculated by using the 2MASS data. The position error ellipse 2MASS data have: major axis ($2a$), minor axis ($2b$), and position angle (β). It was necessary that $\sigma_{\alpha 1}$ and $\sigma_{\alpha 3}$ ($\sigma_{\delta 1}$ and $\sigma_{\delta 3}$) are consistent with each other, and because of it, we calculated the values of the standard error ellipse in the α direction and in the δ one.

The epoch of HIPPARCOS observations is 1991.25, but each star of the 2MASS PSC has its own epoch of observation, and it is necessary to take into account the standard error for the proper motions by using the values of $\mu_\alpha \cos \delta = \mu_{\alpha *}$, μ_δ and the epoch differences t (in years). Therefore, the positions in both catalogues are consistent with the J2000.0 epoch. Before carrying out the cross-identification procedure we took into account the changes of the HIPPARCOS coordinates α_H and δ_H due to the epoch differences t (in years) by using the HIPPARCOS proper motions $\mu_{\alpha *}$ and μ_δ, $\alpha_{Hipp} = \alpha_H + \mu_{\alpha *} t / \cos \delta$ and $\delta_{Hipp} = \delta_H + \mu_\delta t$, where α_{Hipp} and δ_{Hipp} are at the epoch of the 2MASS observations. Then, we did the cross-identification of HIPPARCOS-2MASS, and our procedure identified the common star if its position satisfies $\alpha_{Hipp} - \alpha_{2MASS} = \Delta \alpha < 3\sigma_\alpha$ and $\delta_{Hipp} - \delta_{2MASS} = \Delta \delta < 3\sigma_\delta$.

Following this principle we found 37 940 common stars, which represents about 32.2% of the 117 955 HIPPARCOS stars in our basic selection. Because of the fact that the 2MASS Second Incremental Data Release covers about 47% of the sky, this means that our cross-identification procedure is more than 68.5% successful. At present, one of the reasons for $100\% - 68.5\% = 31.5\%$ cases is the systematic part of σ_α (and σ_δ) which we did not know at the beginning of our cross-identification procedure. If we suppose that the the systematic error between HIPPARCOS and 2MASS coordinates is less than $0''\!.1$ (in agreement with our preliminary investigations about the systematic discrepancies of HIPPARCOS-2MASS coordinates), and put it into our cross-identification programme, we can reach near 80 % of thecommon stars. Another reason is that the 2MASS Second Incremental Data Release covers 47% of the sky. Some of the stars are not present in both catalogues, but only in one of them. We removed 18122 stars from the 2MASS PSC and 263 stars from the HIPPARCOS because these stars were without enough data for our programme.

Only two unsuccessful cross-identifications (of 37 940 common stars) have been found. Each of the HIPPARCOS stars H16658 and H85045 can be asso-

ciated with two 2MASS ones. In the HIPPARCOS Catalogue, the star H16658 is noted as a single star, but the star H85045 is noted as a double star (WDS17229+1628, J1248 AB). From our results, both H16658 and H85045 are close double stars, or maybe the star H16658 is not double, but there is another one with close coordinates.

3. Conclusions

The results of the cross-identification of HIPPARCOS-2MASS stars are presented using our programme based on the 3σ criterion. Only two unsuccessful cases of 37 940 detected common stars have been found. We conclude that these two cases are close double stars or just near each other on the sphere. Our investigation is in agreement with similar actions relating to efforts to link big stellar catalogues (the visible and infrared ones) to the ICRF.

References

Cutri, R. M., Skrutskie, M. F., Van Dyk, S., Chester, T., Evans, T., Fowler, J., Gizis, J., Howard, E., Huchra, J., Jarrett, T., Kopan, E. L., Kirkpatrick, J. D., Light, R. M., Marsh, K. A., McCallon, H., Schneider, S., Stiening, R., Sykes, M., Weinberg, M., Wheaton, W. A., Wheelock, S. 2001, Explanatory Supplement to the 2MASS Second Incremental Data Release, University of Massachusetts and the Infrared Processing and Analysis Center/California Institute of Technology, NASA and NSF.

ESA 1997, The Hipparcos and Tycho Catalogues, ESA SP - 1200.

International Earth Rotation Service (IERS) 1999, Annual Report 1999, Observatoire de Paris.

Ma, C., Arias, E. F., Eubanks, T. M., Fey, A. L., Gontier, A.-M., Jacobs, C. S., Sovers, O. J., Archinal, B. A., Charlot, P., 1998, AJ, 116, 516.

Urban, S. E., Corbin, T. E., Wycoff, G. L. 1998, AJ, 115, 2161.

Extending the ICRF to Higher Radio Frequencies - First Imaging Results

A. L. Fey, D. A. Boboltz

U.S. Naval Observatory - 3450 Massachusetts Avenue NW, Washington DC, 20392-5420, USA

P. Charlot

Observatoire Aquitain des Sciences de l'Univers - CNRS/UMR 5804, BP 89, 33270 Floirac, France

E. B. Fomalont

National Radio Astronomy Observatory - 520 Edgemont Road, Charlottesville, Virginia 22903–2475, USA

G. E. Lanyi, L. D. Zhang

Jet Propulsion Laboratory - California Institute of Technology, 4800 Oak Grove Drive, Pasadena, CA 91109-8099, USA

and the K-Q VLBI Survey Collaboration

Abstract.
We present first imaging results and preliminary source structure analysis of 108 extragalactic objects observed using the Very Long Baseline Array (VLBA) at 24 GHz and 43 GHz as part of a joint NASA, USNO, NRAO and Bordeaux Observatory program to extend the ICRF to higher radio frequencies.

1. Introduction

At the XXIII General Assembly of the International Astronomical Union (IAU) held on 20 August 1997 in Kyoto, Japan, the International Celestial Reference Frame (ICRF) (Ma *et al.* 1998) was adopted as the fundamental celestial reference frame. As a consequence, the definitions of the axes of the celestial reference system are no longer related to the equator or the ecliptic but have been superseded by the defining coordinates of the ICRF. The ICRF is currently defined by the radio positions of 212 extragalactic objects obtained using the technique of Very Long Baseline Interferometry (VLBI) at frequencies of 2.3 and 8.4 GHz over the past 20+ years.

Because the positions in the ICRF now form the underlying basis for all astrometry, subsequent IAU resolutions have encouraged the astrometric community to extend the ICRF to other wavelengths.

We present first imaging results and preliminary source structure analysis of 108 extragalactic objects observed using the Very Long Baseline Array (VLBA)

at 24 GHz and 43 GHz as part of a joint NASA, USNO, NRAO and Bordeaux Observatory program to extend the ICRF to higher radio frequencies. The long term goals of this program are:

- to develop higher frequency reference frames for improved deep space navigation,

- to extend the VLBA calibrator catalog at 24 and 43 GHz,

- to provide the benefit of the ICRF catalog to new applications at these higher frequencies, and

- to study intrinsic source structure at 24 and 43 GHz with the goal of improving the astrometric accuracy.

In this paper, we concentrate on the latter goal of evaluating the intrinsic structure of the observed ICRF sources. A description of the astrometric analysis can be found in Jacobs *et al.* (2003).

2.   Source Selection and Observations

Extragalactic sources were selected for observation with the VLBA at 24 and 43 GHz based on the following criteria:

- ICRF source

- "Structure Index[1]" of 1 or 2 at both 2.3 and 8.4 GHz

- High quality in VLA Calibrator list

- Estimated $S_{\nu=32\mathrm{GHz}} \geq 1$ Jy

    - extrapolated from 8.4 GHz flux density
    - spectral index from VLA Calibrator list

The same set of 65 sources was observed on both 2002 May 15 and 2002 Aug 25. Forty-three additional sources, together with 24 overlap sources from the first two epochs, were observed on 2002 Dec 26.

All selected sources were successfully observed at both 24 GHz and 43 GHz and images were produced.

3.   Imaging Results

Contour plots of the final self–calibrated images at 24 and 43 GHz for 108 extragalactic sources can be obtained from the USNO Radio Reference Frame Image Database:

- `http://www.usno.navy.mil/RRFID/`

---

[1]Structure Index is defined by Fey & Charlot (1997) as an estimate of the contribution of intrinsic source structure to the measured group delay used for astrometric VLBI. The "Structure Index" ranges from a value of 1 for the least contribution (best astrometric sources) to a value of 4 for the most contribution (worst astrometric sources).

4.   Analysis Results

- Gaussian component models fitted to the images show that the sources are generally more compact as one goes from the ICRF frequency of 8.4 GHz to 24 GHz. This result suggests that reference frames defined at these higher frequencies will be less susceptible to the effects of intrinsic structure than the ICRF.

- The sources appear to be no more compact at 43 GHz than at 24 GHz. This result suggests that we may be partially resolving the core for some sources at 43 GHz.

- The "Structure Index" (see Fey & Charlot 1997) was calculated for all 65 sources observed on 2002 May 15 at both 24 GHz and 43 GHz. The calculated "Structure Index" suggests that the observed sources may be better astrometrically at the higher frequencies.

References

Fey, A. L. & Charlot, P. 1997, ApJS, 111, 95.

Jacobs, C. *et al.* 2003, presented at "Future Directions in High Resolution Astronomy: A Celebration of the 10th Anniversary of the VLBA" held June 8-12, 2003, in Socorro, New Mexico, USA, to be published in the ASP Conference Series.

Ma, C., Arias, E. F., Eubanks, T. M., Fey, A. L., Gontier, A.-M., Jacobs, C. S., Sovers, O. J., Archinal, B. A., Charlot, P., 1998, AJ, 116, 516.

JAPAN ASTROMETRY SATELLITE MISSION
—JASMINE PROJECT—

Taihei Yano, Naoteru Gouda, Yukiyasu Kobayashi, Takuji Tsujimoto
Yukitoshi Kan-ya

National Astronomical Observatory, Mitaka, Tokyo 181-8588, Japan

Yoshiyuki Yamada

Graduate School of Science, Kyoto University, Sakyo-ku, Kyoto
606-8502, Japan

Hiroshi Araki, Seiichi Tazawa, Kazuyoshi Asari, Seiitsu Tsuruta, Hideo
Hanada, Nobuyuki Kawano

National Astronomical Observatory, Mizusawa, Iwate 023-0861, Japan

Abstract.
JASMINE is the name of a Japanese infrared (z-band: 0.9μm, or K-band: 2.2μm) scanning astrometric satellite, planned to be launched between 2013 and 2015. The main objective of JASMINE is to study the fundamental structure and evolution of the disk and the bulge components of the Milky Way Galaxy. A further important objective is to investigate stellar physics. In order to accomplish the objective, JASMINE will measure parallaxes, positions and proper motions with a precision of 10 microarcsec (μas) at z = 15.5mag or K = 12mag.

1. Overview of JASMINE

The primary goal of JASMINE (Japan Astrometry Satellite Mission for INfrared Exploration) is the measurement of the trigonometric parallaxes, positions, and proper motions of about a few hundred million stars in order to study the fundamental structure and evolution of the disk and the bulge components of the Milky Way Galaxy. Overall design of JASMINE is shown in Figure 1 (the left side).

The accuracy of the measurement is 10 microarcsec at z = 15.5 mag or K = 12 mag. JASMINE is planned to be launched in around 2013. The spacecraft will be placed in a L2 point of the Sun-Earth system using the H-II A rocket JAXA (Japan Aerospace Exploration Agency) in Japan. The rotational axis is $3.5°$ away from the galactic pole, rotating with a 3.7-hour period which precesses around the galactic pole direction every 28.6 days. Accordingly, JASMINE will scan the restricted regions around the galactic plane and sweep repeatedly. The mission life time is 5 years. The above parameters are summarized in Table 1.
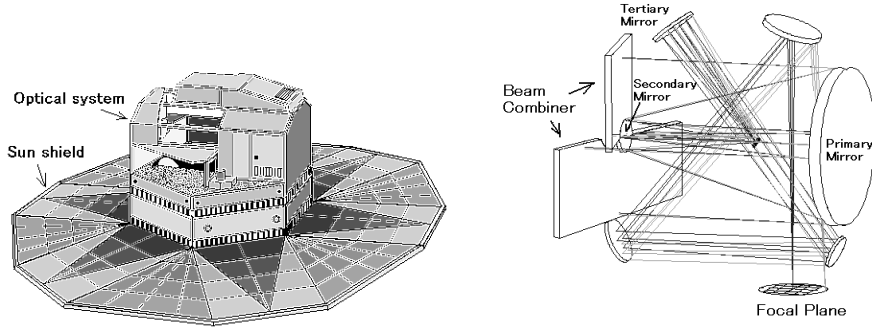
Figure 1.   Overview of JASMINE and its optics

Mission Time	5yr
Rotation Period	3.7h
Precession Period	28.6days
Rotation Axis	around the Galactic Pole
Launcher	H-II A
Orbit	L2 point of the Earth-Sun system

Table 1.   Summary of the mission.

1.1.   Optics

In order to accomplish measurements of astrometric parameters with high accuracy, optics with a long focal length and a wide focal plane are required. In 1977, Korsch proposed a three-mirror system with a long focal length and a wide focal plane. However, the center of the field is totally vignetted because of the folding mirror. Therefore we consider the improved Korsch system in which the center of the field is not vignetted. The schematic of the optics is shown in Figure 1 (the right side). Finally we obtain the diffraction limited optical design with small distortion.

Optics design	Korsch System (3mirrors)
Aperture size	2.0m
Focal length	66.7m
pixel size	15μm
pixel on sky	46.4mas
Array size	6cm$\times$3cm
Pixels per detector	4096$\times$2048
Number of detectors	162 (9$\times$18)

Table 2.   Summary of the instrument parameters

The aperture size of the optics is 2.0m, and its focal length, f,is 66.7m in order to accomplish $f\lambda/Dw = 2$, where λ, D, and w are the wavelength, the aperture size, and pixel size, respectively. The size of the detector for z-band is

6 cm×3 cm with 4096×2048 pixels. The pixel size is 15 μm which corresponds to 46.4 milliarcsec (mas) on sky. These parameters are summarized in Table 2.

2. Centroiding Experiment

Measuring the centroiding of stars is one of the most important problems for astrometry. We examined the accuracy of the centroid of stars. We obtain the relative distance of stars with an accuracy of 1/300 pixel, which is almost ideal. Our experimental method is shown below.

2.1. Algorithm

Here, we show the algorithm used in this experiment. First, we pick up two stars in a star field image to measure the distance. Second, we seek the pixel in which the number of photons is a maximum in each star. Then we pick up 5×5 pixels around the two pixels. Only this information is used to measure the distance between the two stars. Third, we calculate the photon-weighted mean of each star by the following equation.

$$\left(\begin{array}{c} x_c \\ y_c \end{array} \right) = \frac{1}{\sum_i \sum_j N_{ij}} \left(\begin{array}{c} \sum_i \sum_j N_{ij} i \\ \sum_i \sum_j N_{ij} j \end{array} \right)$$

where, N_{ij} is the number of photons at the position (i,j).

The photon-weighted means (x_c, y_c) derived by the above equation are different from the real positions (x_a, y_a). Here, we assume that the difference between the photon-weighted mean and the real position is proportional to the deviation of the photon-weighted mean from the center of the pixel.

$$x_a - x_c = k x_c \tag{1}$$

where, k is a coefficient. This assumption is originally from FAME. However, we note that the coefficients k have different values for two stars in general. Then we treat k as different values in this paper although the FAME team treats k as one parameter. We calculate parameters k by using the least-squares method. Then we obtain the real position x_a.

We define the positions of star1 and star2 as x_{a1} and x_{a2}, respectively.

$$x_{ai} = x_{ci} + k i x_{ci} \quad (i = 1, 2), \tag{2}$$

where, x_c is the photon-weighting mean of a star. Here we define a function I as

$$\begin{array}{rcl} I & = & 0 (x_{c2} > x_{c1}), \\ I & = & 1 (x_{c2} < x_{c1}). \end{array} \tag{3}$$

The relative distance of two stars $|\delta x_a|$ is

$$\begin{array}{rcl} |\delta x_a| & = & x_{a2} - x_{a1} + I, \\ & \equiv & \alpha \Delta + \beta x_{c1} + I, \end{array} \tag{4}$$

where, $\alpha = (1 + k2)$, $\beta = (k2 - k1)$, $\gamma = -|\delta x_a|$, and $\Delta = (x_{c2} - x_{c1})$.

We would like to obtain values of parameters, k1 and k2, in which the following equation is satisfied with smallest error. In other words, we use a least-squares method. So, we define S as $S = \sum(\alpha\Delta + \beta x_{c1} + \gamma + I)^2$. The derivative of S by each parameter is set equal to zero, that is, $\frac{\partial S}{\partial \alpha} = 0$, $\frac{\partial S}{\partial \beta} = 0$, and $\frac{\partial S}{\partial \gamma} = 0$ are satisfied. Then we obtain the equations of parameters, α, β, and γ.

$$\begin{pmatrix} \sum \Delta^2 & \sum \Delta x_{c1} & \sum \Delta \\ \sum \Delta x_{c1} & \sum x_{c1}^2 & \sum x_{c1} \\ \sum \Delta & \sum x_{c1} & \sum 1 \end{pmatrix} \begin{pmatrix} \alpha \\ \beta \\ \gamma \end{pmatrix} = -\begin{pmatrix} \sum \Delta I \\ \sum x_{c1} I \\ \sum I \end{pmatrix}.$$

Accordingly, we obtain the positions of stars.

2.2. Experimental Results

We have taken twenty image frames by sliding the CCD array. The results are shown in Figure 2. The horizontal axis indicates the photon-weighted mean of star1. The vertical axis indicates the distance between two stars. Here, we note that the integer part of the distance is eliminated. Accordingly, the distance has a value between 0 and 1. The squares show only the separations between photon-weighted means of two stars, (that is, no correction is performed). On the other hand, the diamonds are the estimated distances between two stars determined by by using the algorithm. The estimated distances (the diamonds) are shown again in the right side of Figure 2. The distance can be estimated with a variance of about 1/300 pixel.
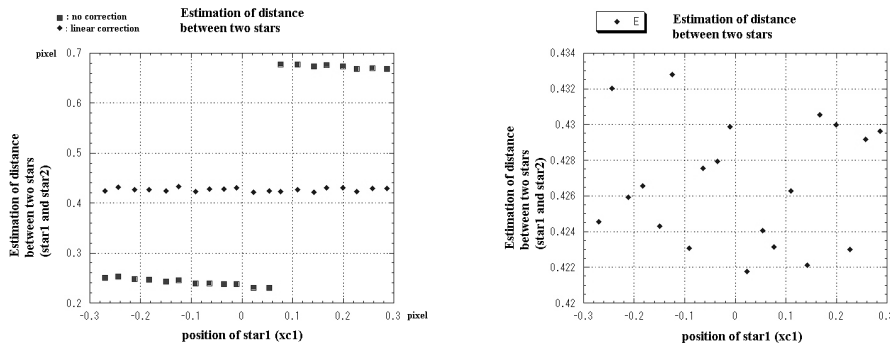

Figure 2.   Relative distance between two stars against the position of star 1.

References

Triebes, K., Gilliam, L., Harris, F., Hilby, T., Horner, S., Monet, D., Perkins, P., and Vassar, R. 1999, American Astronomical Society, 195th AAS Meeting, #88.02; Bulletin of the American Astronomical Society, Vol. 31, p. 1505.

The USNO Extragalactic Reference Frame Link Program

Marion I. Zacharias

USRA, 1101 17th St. NW, Suite 1004, Washington DC, and USNO

Norbert Zacharias, & Theodore J. Rafferty

U.S. Naval Observatory, 3450 Mass. Ave. NW, Washington DC, 20392

Abstract. The objective of this project is to improve the link between the radio and optical reference frames over the initial Hipparcos effort. The alignment of the radio-optical systems is important for absolute proper motions and source identification across the wavelength spectrum. There are 717 ICRF+extensions radio sources. The U.S. Naval Observatory (USNO) extragalactic reference frame link program includes all applicable ($\approx$ 600) sources with optical counterparts. Furthermore, USNO is involved in the extragalactic link of the Space Interferometry Mission (SIM) and plans for a new astrometric, ground-based, 1-meter class telescope.

1. Current Program

USNO is involved in an extragalactic link program since the 1980's (Zacharias *et al.* 1999). In 1998 a new program started for an all-sky astrometric survey that links Hipparcos and Tycho stars to the defining, optically faint sources in a two-step approach, the deep observing and the wide-field observing.

Table 1 summarizes our deep CCD observing. Many International Celestial Reference Frame (ICRF) source counterparts are observed more than once.

Contemporaneous with the NOAO observing runs, wide-field images of ICRF source fields (Table 2) with the USNO Twin Astrograph (Table 3) are taken as part of the USNO CCD Astrograph Catalog (UCAC) project. This allows us to link the optical positions of ICRF sources to the Hipparcos System, utilizing anonymous secondary reference stars in the 12 to 16 mag range, similar to the previous photographic program (de Vegt *et al.* 2001).

The coordinate system of a CCD frame is linked to the available reference stars in that field to within a finite precision. The standard error of this zero-point uncertainty, σ_z, per coordinate is:

$$\sigma_z \;\geq\; \sqrt{\frac{\sigma_{ref}^2 + \sigma_{xyr}^2 + \sigma_{atm}^2}{n_r - p}},$$

with σ_{ref} being the average error of a reference star catalog position, σ_{xyr} the error of the CCD x,y position of a reference star, σ_{atm} the contribution from the turbulence in the atmosphere, n_r the number of reference stars used in the CCD frame, and p the number of model parameters in the "plate adjustment."

Table 1.   Deep optical imaging observing runs.

ID	telescope		date		nights	sources
n	CTIO	0.9m	Oct	1997	4	15
o	CTIO	0.9m	Dec	1997	5	37
p	CTIO	0.9m	Feb	1998	5	29
q	CTIO	0.9m	Jul	1998	6	46
r	CTIO	0.9m	Aug	1998	6	44
s	CTIO	0.9m	Jan	1999	5	56
t	CTIO	0.9m	Mar	1999	5	56
u	CTIO	0.9m	Jun	1999	4	61
v	CTIO	0.9m	Sep	1999	6	52
w	CTIO	0.9m	Dec	1999	5	57
x	CTIO	0.9m	Mar	2000	4	77
y	CTIO	0.9m	Jun	2000	5	51
z	CTIO	0.9m	Sep	2000	5	77
a	CTIO	0.9m	Jan	2001	5	39
b	KPNO	2.1m	Jun	2001	5	42
A	KPNO	0.9m	Nov	2001	3	1
B	KPN0	0.9m	Jan	2002	4	18
C	KPNO	0.9m	May	2002	7	42
D	KPNO	0.9m	Jun	2002	4	28
E	KPNO	0.9m	Sep	2002	5	40
F	KPNO	0.9m	Dec	2002	3	18
G	KPNO	0.9m	May	2003	8	53

Table 2.   Observing of ICRF source fields at the USNO astrograph.

observing dates	Jan 1998 to June 2003
number of detected sources	≈ 600
number of frames for ICRF	14,653
number of frames rejected	about 20 %
exposure times	30 and 150 sec
average number of frames per run and source	8 - 16
control of systematic errors plus observe	observe on both sides of pier calibration fields frequently
wide-field imaging	within 2 weeks of NOAO runs

Table 3.   The USNO Twin Astrograph and camera.

clear aperture	206	mm
focal length	2057	mm
number of lens elements	5	
corrected for bandpass	550–710	nm
usable flat field of view	≈ 9	degree
active guiding with	ST4 at visual lens	
number of pixels	4095 x 4095	
field of view	61 x 61	arcmin
pixel size	9.0	μm
pixel scale	0.9	"/pixel
spectral bandpass used	579–642	nm
limiting magnitude	≈ 16.0	2 min.

The above is the minimal error, neglecting linear and higher order terms from the error propagation in the "plate adjustment" model. There are 2 steps:

1. from Tycho2 stars to astrograph CCD frames,

2. from secondary reference stars (astrograph) to deep CCD frames.

The errors σ_{xyr} and σ_{atm} can be reduced by taking multiple exposures. Systematic errors usually limit the averaged σ_{xyr} values for many frames. Error estimates are given in Table 4. Units are milliarcseconds (mas).

Table 4.   The USNO Twin Astrograph and camera.

	step 1		step 2	
	single frame	avr. 9 frames	single frame	avr. 4 frames
σ_{ref}	40	40	10	10
σ_{xyr}	15	10	10	5
σ_{atm}	45	15	20	10
$n_r - p$	40	40	60	60
σ_z	10	7	3	2

The total error per optical position of an ICRF counterpart is:

$$\sigma_{tot} \geq \sqrt{\sigma_{z1}^2 + \sigma_{z2}^2 + \sigma_{xyS}^2}$$

with σ_{z1}, σ_{z2} being the average σ_z for step 1 and 2, respectively, and $\sigma_{xyS} = 3$ to 30 mas for a centroiding error of ICRF source images averaged over all deep CCD frames. The expected total error of an optical position will be in the range of 8 to 30 mas. Using 400 "good" ICRF optical counterparts, an error of the (optical−radio) frame tie of less than 1 mas is expected, a significant improvement over the current Hipparcos Celestial Reference Frame (HCRF) to ICRF formal alignment error of about 2.5 mas at a mean epoch near 2001.

This is an ongoing project. As of August 2003, 94% of the sky has been observed by the astrograph and all sky coverage is expected by May 2004. Observing of ICRF optical counterparts is continuing in parallel (Assafin *et al.* 2003).

2.   SIM activity

The NASA Space Interferometry Mission (SIM) is scheduled for launch around 2010. For the SIM key science project *Astrophysics of reference frame tie objects* (K. Johnston as PI), USNO has started on the preparatory science work. Targets include extragalactic sources as well as compact radio stars. The goal is the selection of the most suitable candidates as well as the investigation of the optical, astrometric stability of a selected number of sources. For these purposes a pilot monitoring project began in Fall 2002 at the 1.55-m Strand telescope at the Naval Observatory Flagstaff Station for about a dozen representative sources (Zacharias 2003).

3.   URAT

A design study has been performed for the USNO Robotic Astrometric Telescope (URAT) of about 0.9-meter aperture with a $3°$ field of view, enabling a global sky survey to be observed in two years. The goal is an extension of the reference frame at the 10 mas level to 15 to 18 mag stars, with about 30 mas accuracy at a limiting magnitude of about 20. URAT also could observe directly the ICRF counterparts and tie to the ICRF. There will be an option to observe selected bright stars, giving direct access to the HCRF. More details can be found at de Vegt *et al.* (2003), and Zacharias (2002).

References

Assafin,M., Zacharias, N., Rafferty, T. J., Zacharias, M. I., da Silva Neto, D. N., Andrei, A. H., Vieira Martins, R., 2003, AJ, 125, 2728.

de Vegt,C., Hindsley, R., Zacharias, N., Winter, L., 2001, AJ, 121, 2815.

de Vegt,C., Laux,U., Zacharas, N., 2003, in "Small Telescopes in the New Millenium", ed. T.Oswalt, Kluwer Acad. Publ. p. 255.

UCAC2 available on CD-ROM, send request to *nz@usno.navy.mil*
      see also http://ad.usno.navy.mil/ucac.

Zacharias,N., Zacharias, M. I., Hall, D. M., Johnston, K. J., de Vegt, C., Winter, L., 1999, AJ, 118, 2511.

Zacharias,N. 2002, Proc. SPIE 4836, eds. T.A.Tyson & S.Wolff, 279.

Zacharias,N. 2003, in Astronomy in Latin America, Second Meeting on Astrometry in Latin America and Third Brazilian Meeting on Fundamental Astronomy, eds. R. Teixeira, N.V. Leister, V.A.F. Martin, P. Benevides-Soares, ADeLA Publications Series, vol. 1, p.123-130.

Testing the Hipparcos/ICRF Link Using Radio Stars

D. A. Boboltz, A. L. Fey, K. J. Johnston, N. Zacharias & R. A. Gaume

U.S. Naval Observatory, 3450 Massachusetts Avenue NW, Washington DC, 20392-5420, USA

Abstract. We have undertaken an effort to verify and improve the radio/optical frame link through connected element interferometer astrometry of radio stars. In our first epoch, we observed 19 radio stars using the Very Large Array in A-configuration plus the Pie Town Very Long Baseline Array antenna (VLA+PT). Differences in right ascension and declination were computed between our VLA+PT data and the Hipparcos positions updated to our epoch (2000.94). A weighted least-squares fit to the position differences was performed and the three rotation angles between the radio and optical frames were determined. We found that the two frames are aligned to within the formal errors of approximately 3 milliarcseconds per axis. Presented here are the results of this work and the plans for future work.

1. Introduction

The current version of the International Celestial Reference Frame (ICRF) is defined by the positions of 212 extragalactic objects derived from Very Long Baseline Interferometry (VLBI) observations (Ma *et al.* 1998). This is currently the International Astronomical Union (IAU) sanctioned fundamental astronomical reference frame. At optical wavelengths, the Hipparcos catalog (Perryman *et al.* 1997) now serves as the primary realization of the extragalactic frame. The link between the Hipparcos catalog and the ICRF was accomplished through a variety of ground-based and space-based efforts (Kovalevsky *et al.* 1997) with the highest weight given to VLBI observations of 12 radio stars by Lestrade *et al.* (1999). The standard error of the alignment was estimated to be 0.6 mas at epoch 1991.25, with an estimated error in the system rotation of 0.25 mas yr^{-1} per axis. Thus at the epoch of our observations (2000.94) the alignment of the Hipparcos frame and the ICRF had a formal error of approximately 2.5 mas. Due to errors in the proper motions, the random position errors of individual Hipparcos stars increased from $\sim$1 mas in 1991 to $\sim$10 mas at the time of our observations.

2. Observational Results

We used the VLA+PT configuration to determine astrometric positions of 19 radio stars in the International Celestial Reference Frame (ICRF) (Boboltz *et al.* 2003). The 3.6-cm radio wavelength positions of these stars were directly linked to the positions of distant quasars through phase-referencing observations. The positions of the ICRF quasars are known to 0.25 mas, thus providing an absolute
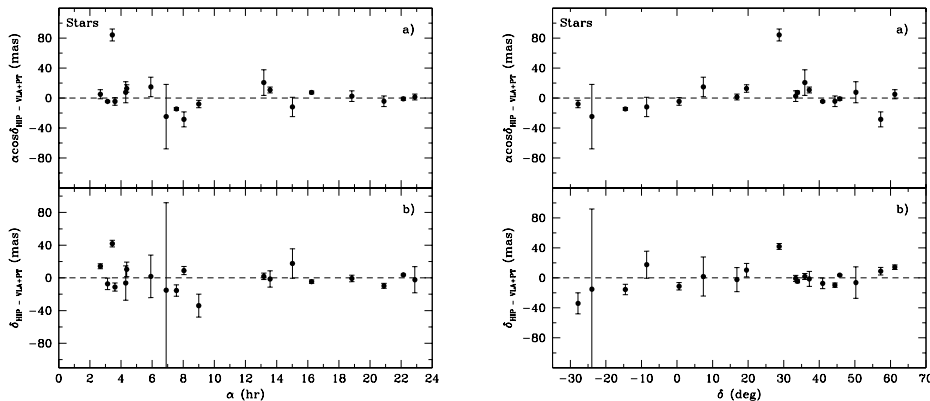
192

Figure 1.   Differences between the Hipparcos positions updated to the epoch of our observations, and our VLA+PT measured positions as a function of source right ascension α (left panel) and source declination δ (right panel) for the 19 radio stars observed. Differences in $\alpha \cos \delta$ are plotted in (a) and differences in declination are plotted in (b) for both the left and right panels. Error bars are from our VLA+PT measurements.

reference at the angular resolution of our VLA+PT observations ($\sim$150 mas). Average values for the errors in our derived positions for all sources were 13 mas and 16 mas in $\alpha \cos \delta$ and δ respectively, with accuracies approaching 1–2 mas for some of the stars observed. Differences between the ICRF positions of the 38 quasars, and those measured from our observations showed no systematic offsets, with mean values of -0.3 mas in $\alpha \cos \delta$ and -1.0 mas in δ. Standard deviations of the quasar position differences of 17 mas and 11 mas in $\alpha \cos \delta$ and δ respectively, are consistent with the mean position errors determined for the stars.

We also compared the positions of the 19 stars as derived from our VLA+PT observations with the corresponding Hipparcos positions updated to the epoch of our observations, Julian Day 2451889. Figure 1 plots the position differences for the radio stars as a function of source right ascension (left panel) and as a function of source declination (right panel). Error bars are those derived from our VLA+PT observations. In Figure 1, it is apparent that roughly half of the positions derived from our VLA+PT data do not agree with the Hipparcos positions to within the uncertainties in our measurements.

3.   Testing the Radio/Optical Frame Link

Position differences ($\Delta \alpha \cos \delta, \Delta \delta$) in the optical (Hipparcos) minus radio (our VLA+PT observations) were calculated for 18 of the 19 stars observed at our 2000.94 epoch. The star UX Ari was excluded because of its nature as a triple system as verified by our VLA data (see Boboltz *et al.* 2003). In a weighted least-squares adjustment, the 3 rotation angles between the optical and radio frames were determined (see Table 1) from these data. For the radio positions,

we used the errors reported in Table 2 of Boboltz *et al.* (2003). For the optical positions we used the Hipparcos errors at epoch (1991.25) updated to our epoch using the Hipparcos proper motion errors. Our analysis indicates insignificant alignment rotations of less than 1 mas with a formal error of $\sim$3 mas per axis. The reduced χ^2 for the alignment is $\approx$1.0, confirming the error estimates for the input data.

Table 1.   Radio/Optical Frame Alignment.

Axis	Rotation (mas)	Formal Error (mas)
x	−0.23	2.89
y	−1.87	3.19
z	2.26	2.82

Our radio-star results provide a critical check on the Hipparcos-to-ICRF alignment and confirm that the Hipparcos frame is indeed inertial at the expected level. Similarly, in a pilot investigation, 172 extragalactic sources were used to compare the ICRF/optical frames (Assafin *et al.* 2003). This program yielded similar results with no significant system rotations found and formal errors on the 3 mas level. However, systematic errors in the preliminary, wide-field, optical data of $\sim$10 mas were reported. For determining possible radio/optical frame differences, the use of radio stars is currently more competitive because the accurate Hipparcos data can be utilized directly.

4.   Future Work

The program to verify and update the link between the Hipparcos frame and the ICRF via radio stars is a continuing effort. Observations using the Multi-Element Radio Linked Interferometer Network (MERLIN) of 15 radio stars were taken in October, 2001. The data from the 11 stars detected have been analyzed, and the 6-cm positions have been determined to an accuracy of $\sim$5 mas. This data will be combined with observations reported in Boboltz *et al.* (2003) and Johnston, de Vegt & Gaume (2003) to update the proper motions and the radio/optical frame link (Fey *et al.* in preparation). In addition, second epoch VLA+PT observations were recorded in June 2003. A total of 50 radio stars were observed over 48 hours, and reduction of the data is ongoing. Finally, an additional epoch, consisting of 48 hours of MERLIN time, will be observed in the fourth quarter of 2003. These additional VLA+PT and MERLIN observations will also be combined with all previous observations to determine accurate positions and proper motions for $\sim$50 radio stars which can then be used for linking the ICRF to the Hipparcos and future optical reference frames.

References

Assafin, M., Zacharias, N., Rafferty, T. J., Zacharias, M. I., da Silva Neto, D. N., Andrei, A. H., & Vieira Martins, R. 2003, AJ, 125, 2728.

Boboltz, D. A., Fey, A. L., Johnston, K. J., Claussen, M. J., de Vegt, C., Zacharias, N., & Gaume, R. A. 2003, AJ, 126, 484.

Johnston, K. J., de Vegt, C., & Gaume, R. A. 2003, AJ, 125, 3252.

Kovalevsky, J., Lindegren, L., Perryman, M.A.C., Hemenway, P.D., Johnston, K.J., Kislyuk, V.S., Lestrade, J.F., Morrison, L.V., Platais, I., Röser, S., Schilbach, E., Tucholke, H.-J., deVegt, C., Vondrak, J., Arias, F., Gontier, A.M.,Arenou, F., Brosche, P., Florkowski, D.R., Garrington, S.T., Kozhurina-Platais, V., Preston, R.A., Ron, C., Rybka, S.P., Scholz, R.-D., Zacharias, N., 1997, A&A, 323, 620.

Lestrade, J.-F, Preston, R. A., Jones, D.L., Phillips, R. B., Rogers, A. E. E., Titus, M. A., Rioja, M. J., & Gabuzda, D. C. 1999, A&A, 344, 1014.

Ma, C., Arias, E.F., Eubanks, T.M., Fey, A.L., Gontier, A.-M., Jacobs, C.S., Sovers, O.J., Archinal, B.A., Charlot, P., 1998, AJ, 116, 516.

Perryman M. A. C., Lindegren, L., Kovalevsky, J., Høg, E., Bastian, U., Bernacca, P.L., Crézé, M., Donati, F., Grenon, M., vanLeeuwen, F., vanderMarel, H., Mignard, F., Murray, C.A., LePoole, .S., Schrijver, H., Turon, C., Arenou, F., Froeschlé, M., Petersen,C.S., 1997, A&A, 323, L49.

Another Look at Non-Rotating Origins

George H. Kaplan

U.S. Naval Observatory, 3450 Massachusetts Ave. NW, Washington
DC, 20392-5420

Abstract. Two "non-rotating origins" were defined by the IAU in 2000 for the measurement of Earth rotation: the Celestial Ephemeris Origin (CEO) in the ICRS and the Terrestrial Ephemeris Origin (TEO) in the ITRS. Universal Time (UT1) is now defined by an expression based on the angle θ between the CEO and TEO. Many previous papers, *e.g.*, Capitaine, Guinot, & McCarthy (2000), developed the position of the CEO in terms of a quantity s, the difference between two arcs on the celestial sphere. A similar quantity s' was defined for the TEO.

As an alternative, a simple vector differential equation for the position of a non-rotating origin on its reference sphere is presented here. The equation can be easily numerically integrated to high precision. This scheme directly yields the unit vector of the CEO in the ICRS, or that of the TEO in the ITRS, as a function of time. This simplifies the derivation of the main transformation matrix between the ITRF and the ICRS. The directness of the development may have pedagogical and practical advantages for the vast majority of astronomers who are unfamiliar with the history of this topic.

IAU resolution B1.8 from the 2000 General Assembly, which establishes the Celestial Ephemeris Origin (CEO) and the Terrestrial Ephemeris Origin (TEO), and redefines UT1 in terms of the angle θ between them, has not received wide publicity within the general astronomical community. Among those who are aware of it, probably few appreciate its basis or implications. The CEO and TEO are specific examples of the concept of a "non-rotating origin" (NRO), first described by Guinot (1979). The concept itself is quite simple, but the mathematical details of its practical implementation, as usually presented (*e.g.*, Capitaine et al. 2000), may discourage non-specialists. This paper describes an alternative mathematical development, which is precise enough for practical computations, but avoids some of the untidy aspects of an analytical approach based on spherical trigonometry. In the space allotted here, only an outline of the scheme can be presented.

A non-rotating origin can be most simply described as a point on the moving equator whose instantaneous motion is always orthogonal to the equator. If $\mathbf{n}(t)$ is a unit vector toward the instantaneous pole and $\mathbf{x}(t)$ is a unit vector toward an instantaneous non-rotating origin, a simple geometric construction based on this definition yields the following differential equation:

$$\dot{\mathbf{x}}(t) = -\Big(\mathbf{x}(t) \cdot \dot{\mathbf{n}}(t) \Big)\, \mathbf{n}(t). \tag{1}$$

That is, if we have a model for the motion of the pole, $\mathbf{n}(t)$, the path of the non-rotating origin is described by $\mathbf{x}(\mathbf{t})$, once an initial point on the equator, $\mathbf{x}(t_0)$, is chosen. Conceptually and practically, it is simple to integrate this

equation, using, for example, a standard 4th-order Runge-Kutta integrator. For the motions of the real Earth, fixed step sizes of order 0.5 day work quite well, and the integration is quite robust. Since this is really a one-dimensional problem carried out in three dimensions, two constraints can be applied at each step: $|\mathbf{x}| = 1$ and $\mathbf{x} \cdot \mathbf{n} = 0$.

By numerically integrating this equation, we obtain a time series of unit vectors, $\mathbf{x}(t)$. Depending on our model of the motion of the pole, $\mathbf{n}(t)$, these vectors point toward either the celestial or terrestrial non-rotating origin. That is, the vectors define the directions of either the CEO in the ICRS or the TEO in the ITRS. If we are working in the celestial frame and the CEO is the non-rotating origin of interest, the model of the pole's motion is:

$$\mathbf{n}(t) = \mathbf{F} \, \mathbf{P}^{\mathrm{T}}(t) \, \mathbf{N}^{\mathrm{T}}(t) \begin{pmatrix} 0 \\ 0 \\ 1 \end{pmatrix} \tag{2}$$

where $\mathbf{F}$, $\mathbf{P}$, and $\mathbf{N}$ are the standard matrices for frame bias, precession, and nutation, respectively. The transpose symbols on the precession and nutation matrices indicate that they transform vectors from time t to J2000.0. The frame bias matrix transforms vectors from the dynamical system to the ICRS.

Once the integration is completed, the main part of the ITRS-to-ICRS transformation (which converts a terrestrial vector to the equivalent celestial vector) can be simply expressed, for any epoch t_i, in terms of the components of three unit vectors: $\mathbf{x}(t_i)$, $\mathbf{n}(t_i)$, and $\mathbf{y}(t_i) = \mathbf{n}(t_i) \times \mathbf{x}(t_i)$. These three vectors have components expressed with respect to the ICRS axes and define the orthonormal basis for what has been called the "intermediate" coordinate system. This system has the celestial pole in the z-direction and the CEO in the x-direction, with the instantaneous equator as the xy-plane. The transformation matrix that takes a vector from the intermediate system to the ICRS is simply:

$$\mathbf{C} = \begin{pmatrix} \mathbf{x} \, \mathbf{y} \, \mathbf{n} \end{pmatrix} = \begin{pmatrix} x_1 & y_1 & n_1 \\ x_2 & y_2 & n_2 \\ x_3 & y_3 & n_3 \end{pmatrix} \tag{3}$$

But to apply this matrix, we must first get the terrestrial vector into the intermediate system. A vector in the ITRS, after correction for polar motion, is transformed to the intermediate system by a simple rotation through the angle θ, which is a linear function of UT1 (the expression is specified in IAU resolution B1.8 of 2000). So the complete transformation from the ITRS to the ICRS is

$$\mathbf{r}_c = \mathbf{C} \, \mathbf{R}_3(-\theta) \, \mathbf{W}' \, \mathbf{r}_t, \tag{4}$$

where $\mathbf{r}_t$ is a vector in the ITRS, $\mathbf{r}_c$ is the corresponding vector in the ICRS, $\mathbf{W}'$ is the polar motion matrix, and $\mathbf{R}_3$ represents a simple rotation about the z-axis. (See Chapter 5 of the IERS Conventions (2003) for the expression for θ and the form of $\mathbf{W}'$, there referred to as $\mathbf{W}(t)$.)

This approach also provides a very simple equation for apparent sidereal time. Greenwich apparent sidereal time (GAST) is simply the Greenwich hour angle (GHA) of the true equinox of date. Using the form of eq. (2), the direction
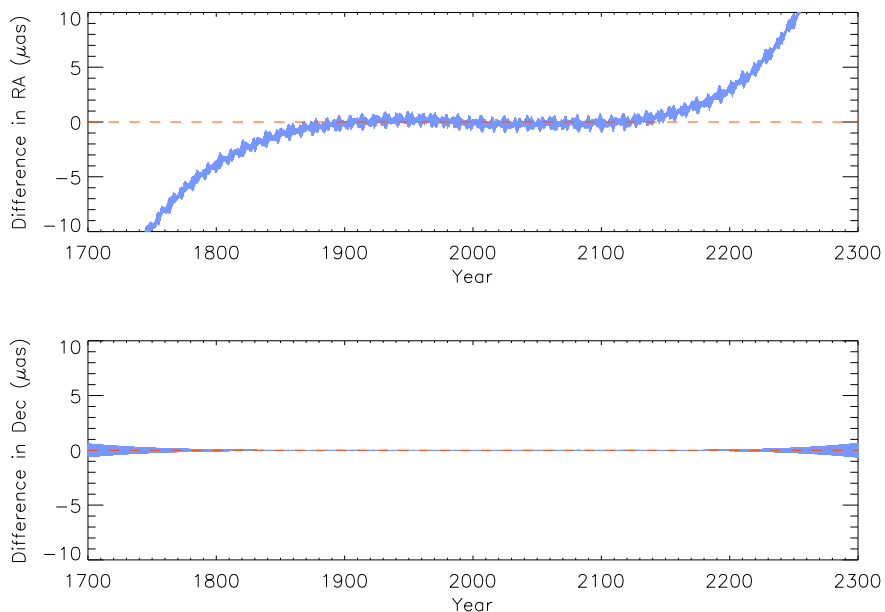
Figure 1.   Differences in results of ITRS-to-ICRS transformation methods: CEO-based minus equinox-based. A numerical integration of the CEO position in the ICRS was used for the CEO-based method.

of the true equinox in the ICRS is given by

$$\boldsymbol{\Upsilon}(t) = \mathbf{F}\,\mathbf{P}^{\mathrm{T}}(t)\,\mathbf{N}^{\mathrm{T}}(t)\,\begin{pmatrix} 1 \\ 0 \\ 0 \end{pmatrix} \tag{5}$$

and its direction in the intermediate system must be $(\,\boldsymbol{\Upsilon}\cdot\mathbf{x}, \boldsymbol{\Upsilon}\cdot\mathbf{y},\,0\,)$. If we define the Greenwich meridian to be the plane that passes through the TEO and the poles, then Greenwich apparent sidereal time is just

$$\mathrm{GAST} = \mathrm{GHA}\,\boldsymbol{\Upsilon} = \theta - \arctan\left(\frac{\boldsymbol{\Upsilon}\cdot\mathbf{y}}{\boldsymbol{\Upsilon}\cdot\mathbf{x}}\right) \tag{6}$$

since θ is the angle between the TEO and the CEO, and the latter defines the direction $\mathbf{x}$.

Does this whole approach work in practice? If so, its results must match those given by a conventional equinox-based development. Figure 1 shows the differences in the results of CEO-based and equinox-based methods of performing the ITRS-to-ICRS transformation on a vector in the equatorial plane. For these computations, the numerical integration of the CEO position was based on the motion of the pole defined by the IAU 2000A precession-nutation model, as given in the IERS Conventions (2003). The new IERS formula for sidereal time (including all the "complementary terms") was used in the equinox-based (conventional) transformation. The initial CEO position used in the integration was adjusted so that the difference between the two methods was zero at 2003.0.
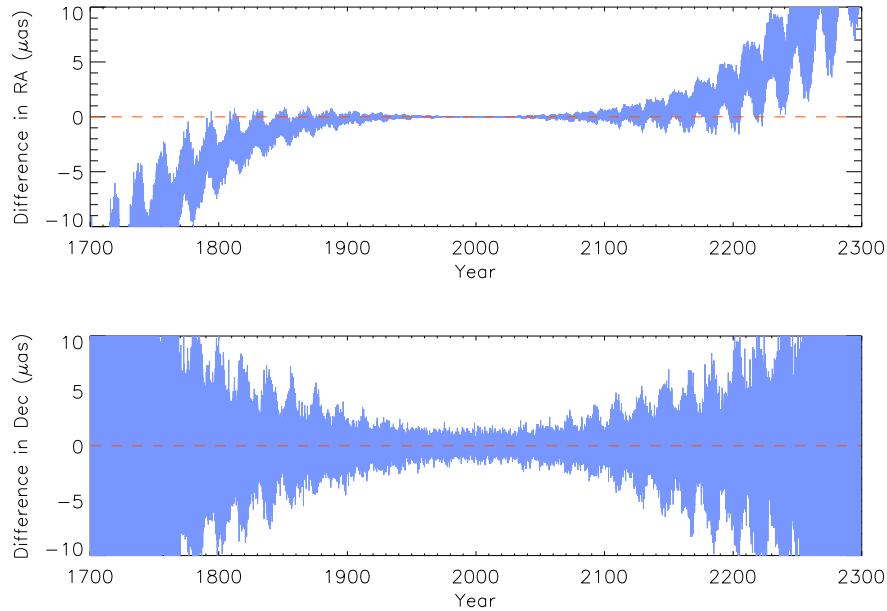
Figure 2.   Same as Fig. 1, except that IERS algorithms based on analytic series were used for the CEO-based method.

(The ICRS right ascension of the CEO at J2000.0 turned out to be $0\rlap{.}{''}002012$.) Polar motion and ΔT were assumed zero throughout. The figure shows that the two transformation schemes match to within a few microarcseconds from 1800–2200, with some divergence outside of that time frame. A similar comparison of the two kinds of sidereal time formulas yields differences that are identical by eye to the top plot of Fig. 1. The same systematic pattern (with some additional numerical noise) is seen in Fig. 2, which shows the same kind of ITRS-to-ICRS transformation comparison, but using only IERS algorithms throughout. Therefore, the CEO integration approach described here seems to be at least as precise as that provided by the IERS.

The CEO integration development and results will be described in more detail in Kaplan (2004).

References

Capitaine, N., Guinot, B., & McCarthy, D. D. 2000, A&A, 355, 398.

Guinot, B. 1979, in IAU Symp. 82, Time and the Earth's Rotation, ed. D. D. McCarthy & J. D. H. Pilkington (Dordrecht: Reidel), 7.

IERS Conventions (2003), http://maia.usno.navy.mil/conv2000.html.

Kaplan, G. 2004, in preparation.

IDV Sources as ICRF Sources: Viability and Benefits

Roopesh Ojha

Australia Telescope National Facility, CSIRO, PO Box 76, Epping,
NSW 1710, Australia

Alan L. Fey

U.S. Naval Observatory, 3450 Massachusetts Ave. NW, Washington
DC, 20392-5420

David L. Jauncey

Australia Telescope National Facility, CSIRO, PO Box 76, Epping,
NSW 1710, Australia

Kenneth J. Johnston

U.S. Naval Observatory, 3450 Massachusetts Ave. NW, Washington
DC, 20392-5420

James E. Lovell & Lucyna Kedziora-Chudczer

Australia Telescope National Facility, CSIRO, PO Box 76, Epping,
NSW 1710, Australia

Abstract. Radio sources that exhibit rapid variability in their light curves, as a result of radio wave propagation through turbulent electron density fluctuations in the interstellar medium, appear to be the most compact sources in the sky. In particular, the most variable weak sources, might be the most point-like and, thus, some of the best candidates for densification of the International Celestial Reference Frame (ICRF) and consequent improvement in its accuracy. Further, the advent of the Mk IV/V VLBI system will make use of weaker sources easier. We will discuss the viability of this idea and state the benefits that might flow from this approach.

1. Introduction: The International Celestial Reference Frame

Very Long Baseline Interferometry (VLBI) observations of selected strong compact extragalactic radio sources have been used to define and maintain a radio reference frame with sub-mas precision. This ICRF was adopted as the fundamental celestial reference frame at the XXIII General Assembly of the International Astronomical Union (IAU) held on 20th August 1997 in Kyoto, Japan (Ma *et al.* 1998). The ICRF is currently defined by the radio positions of 212 extragalactic objects obtained using the technique of VLBI at radio frequencies of 2.3 and 8.4 GHz over the past 20+ years.

2. ICRF: Current Limitations & Future Improvement

The ICRF is currently limited by (a) Deficit of defining sources, particularly in the Southern Hemisphere, (b) Sources having variable core-jet structure which causes position variations (can in principle be corrected) and (c) The fact that the ICRF is composed mostly of brighter (> 0.2 Jy at 8.4 GHz) sources many of which suffer from structure problems.

Thus, future improvement will involve: (a) Increasing the number of defining sources and (b) Incorporating sources that have little or no structure (presumably leading to increased position stability). IDV/ISS sources may be the answer!

3. What are IDV/ISS Sources ?

Intra Day Variable (IDV) sources are flat-spectrum extragalactic sources which show amplitude variations at centimeter wavelengths. Variation timescales are typically less than a day. Interstellar Scintillation (ISS) is the principal cause of this IDV.

4. VLBA Observations of IDV Sources

We used the VLBA to make 8.4 GHz snapshot images of a sample of Low Flux Density Scintillating (LFDS) sources (flux ≈ 0.1 Jy) from the MASIV 5 GHz VLA survey for scintillating extragalactic sources (Lovell *et al.* 2003). VLBA images at 8.4 GHz of 18 High Flux Density Scintillating (HFDS) sources (flux ≈ 1 Jy) and 40 High Flux Density Non-scintillating (HFDN) sources were obtained from the USNO Radio Reference Frame Image Database (RRFID). First results from imaging 38 sources are presented here and two typical images are shown in Figure 1.

5. What is the Milliarcsecond Scale Structure of Scintillating Sources ?

The Lovell *et al.* (2003) VLA survey results showed an increase in both the fraction of scintillators and in their amplitude of variability, with decreasing flux. This raised the possibility that the milliarcsecond structures of scintillators may differ from non-scintillators. Our VLBI observations address the following questions: (1) Are there any morphological differences, at mas scales, between scintillating and non-scintillating sources? and (2) Are there any morphological differences, at mas scales, between high flux density, ≈ 1 Jy, and low flux density, ≈ 0.1 Jy, scintillating sources?

6. Results of Analysis

In order to obtain a quantitative classification of the sources based on their milliarcsecond scale structure, we calculated a "Core Fraction" which we define as the ratio of correlated flux density on the longest VLBA baseline (≈ 250 Mλ) to the correlated flux density on the shortest baseline.
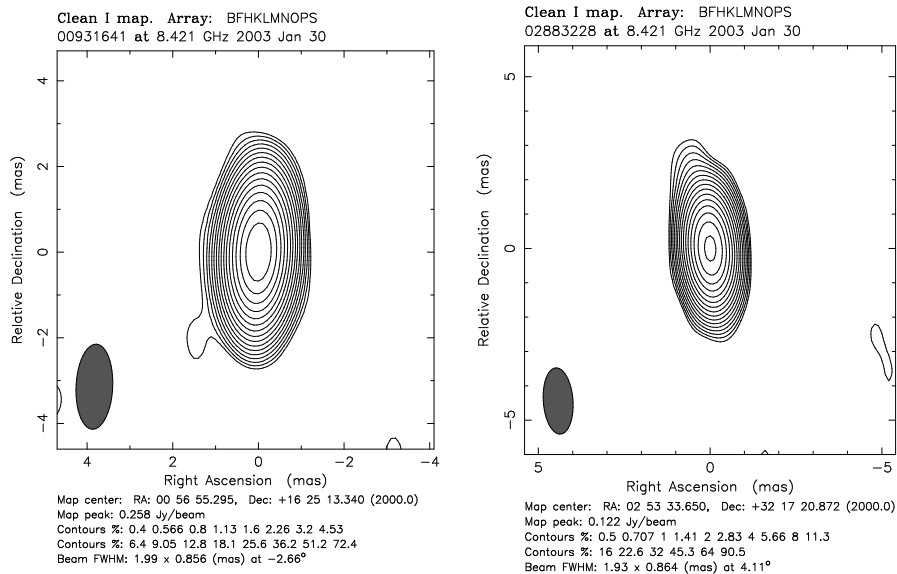
Figure 1.   Two typical VLBA images of LFDS sources. Contours are in $\sqrt{2}$ steps starting at 3σ.

Calculation of the mean and standard deviations of the Core Fractions for the three samples yields: (1) No significant difference between LFDS and HFDS sources (difference $= 1.5\sigma$) and (2) Significant difference between HFDN sources and both LFDS and HFDS sources (difference $= 6.4\sigma$ and 3.3σ respectively). A limitation at the moment is the small number (18) of known HFDS sources. These results are summarized in Fig 2.

7.   Summary of VLBA results

Scintillating sources have different mas scale morphologies from non-scintillating sources. They have a higher fraction of their total flux in an unresolved (< 1 mas) core. Amongst the HFDS sources, it would appear that only the core components scintillate. Low and high flux density scintillating sources do not, on average, have different morphologies (Note: The HFDS sample is small, 18 sources at present).

8.   Implications for Improvement of the ICRF

Results of our analysis show that scintillating sources have proved to be some of the most compact sources. This may make the LFDS sample ideal reference sources for the next generation (Mk IV/V) astrometry and geodesy reference frames. The increased sensitivity of Mk IV/V VLBI will probably be required to observe the generally weaker IDV sources. While the compact morphology of IDV sources suggests their use as ICRF sources, their position stability will need
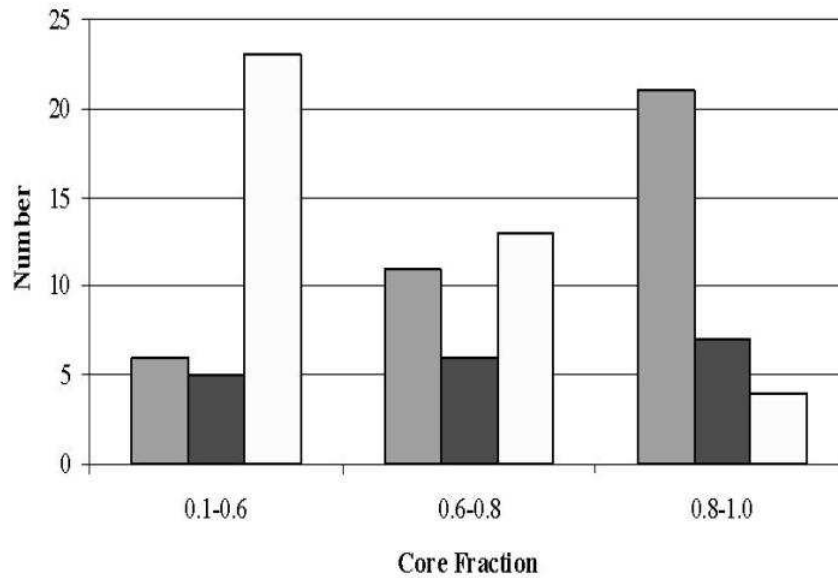
Figure 2. Histogram illustrating distribution of core fraction for the three samples. Grey, black and white columns represent LFDS, HFDS and HFDN sources respectively.

to be established. The 18 HFDS sources are ICRF sources and may provide a good test of the positional stability of IDV sources in general. This is the subject of future work. As VLBI assumes that sources do not change over the period of observation, the amplitude variability of IDV sources may introduce spurious structure into the images.

References

Ma C., Erias, E. F., Eubanks, T. M., Fey, A. L., Gontier, A. -M., Jacobs, C. S., Sovers, O. J., Archinal, B. A. & Charlot, P. 1998, AJ, 116, 516

Lovell, J. E., Jauncey, D. L., Bignall, H. E., Kedziora-Chudczer, L., Macquart, J. -P., Rickett, B. J. & Tzioumis, A. K. 2003, AJ, 126, 1699.

USNO/ATNF Astrometry and Imaging of Southern Hemisphere ICRF Sources

Roopesh Ojha, David L. Jauncey

Australia Telescope National Facility, CSIRO, PO Box 76, Epping, NSW 1710, Australia

Alan L. Fey, Kenneth J. Johnston

U.S. Naval Observatory, 3450 Massachusetts Ave. NW, Washington DC, 20392-5420

Richard G. Dodson, Simon D. Ellingsen, Peter M. McCulloch

University of Tasmania, Hobart, Australia

George D. Nicolson, Jonathan F. H. Quick

Hartebeesthoek Radio Astronomy Observatory, Krugersdorp, South Africa

John E. Reynolds, Anastasios K. Tzioumis & Warwick E. Wilson

Australia Telescope National Facility, CSIRO, PO Box 76, Epping, NSW 1710, Australia

Abstract. The USNO and the ATNF are collaborating in a continuing VLBI research program in Southern Hemisphere source imaging and astrometry. The goals of this program are twofold: to image all southern hemisphere ICRF sources at least twice for structure monitoring and to search for new astrometric sources for densification of the ICRF. All 184 existing ICRF sources south of -20 degrees, have been observed for imaging at least once. Imaging and a second epoch of observations are underway. In order to identify new extragalactic radio sources to be added to the ICRF, survey observations of selected ATCA calibrator sources have been interspersed among the imaging observations. These survey observations have, to date, identified a total of 29 possible astrometric targets. Dedicated astrometric VLBI experiments have been scheduled to determine accurate positions for these sources.

1. Project Goals

We wish to image ICRF sources at 8.4 GHz in order to obtain source structure information at least at two epochs for variability monitoring. We also wish to estimate the effect of structure on astrometric positions.

We wish to increase ICRF source density in order to better define the reference frame, provide more sources for phase referencing and to provide a strong tie between the hemispheres through overlap of common sources
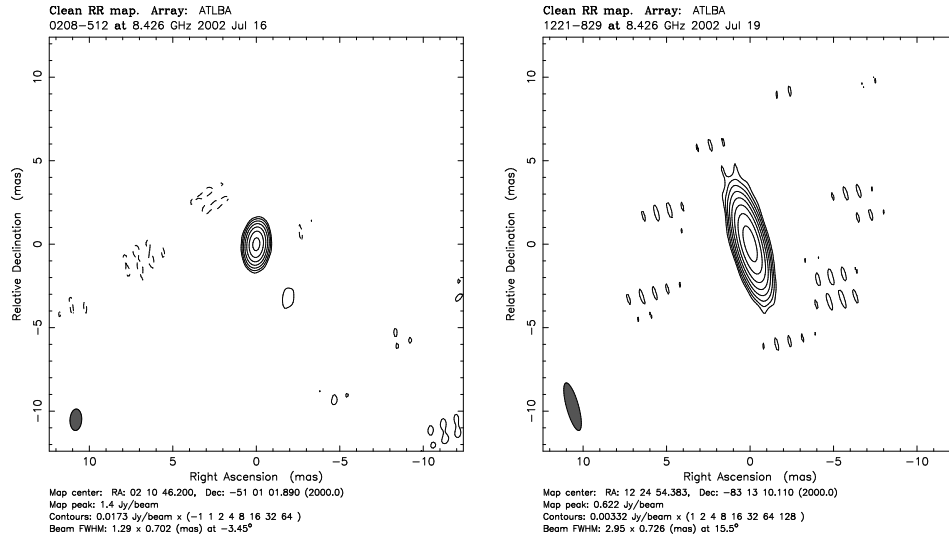
Figure 1.   Example Images: The Good

2.   Observing Parameters

For our imaging observations the telescopes used are those of the Australian Long Baseline Array (which comprises six antennas at Narrabri and one each at Parkes, Mopra, Hobart and Ceduna) augmented by the telescopes at Hartebeesthoek, Kashima and Kokee. We observe at a frequency of 8.4 GHz only and the recording mode is S2. The data are correlated at the ATNF Correlator, Marsfield, NSW.

For our astrometry observations the telescopes used are those at Hartebeesthoek, Hobart, Kashima, Kokee and Parkes. The observations are made at simultaneous 8.4 and 2.3 GHz frequencies and the recording mode used is Mk IIIA. The data are correlated at the Washington correlator, USNO, Washington DC.

3.   Observational Status: Imaging

The first epoch of observations is complete with all 184 ICRF sources south of −20 degrees declination observed. The data has all been correlated and calibrated and about a third of it has been imaged. Approximately half the sources show extended structure with about 10% showing double structure (unsuitable for ICRF). The second epoch of observations is in progress. Figures 1, 2 and 3 show examples of different morphologies seen in this survey.

4.   Observational Status: Astrometry

To date survey observations of 108 sources have been completed. 29 new candidate sources have been identified and positions for 15 of these sources were obtained (10 with sub-mas precision). An additional 12 far south sources were
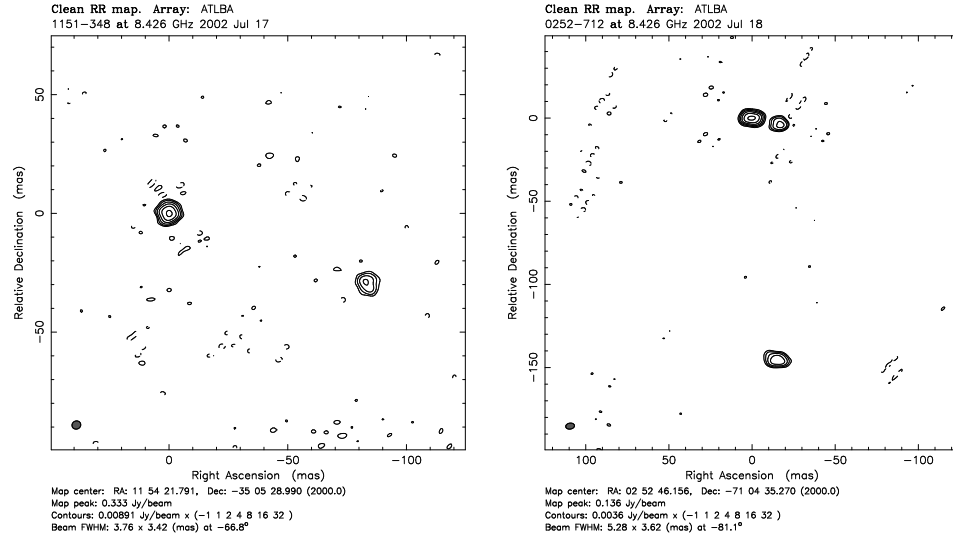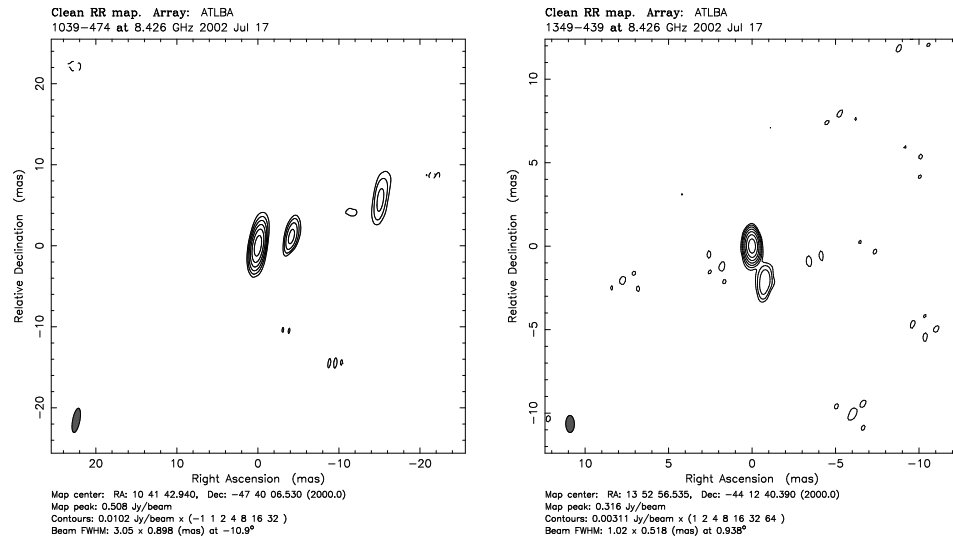
Figure 2.   Example Images: The Bad

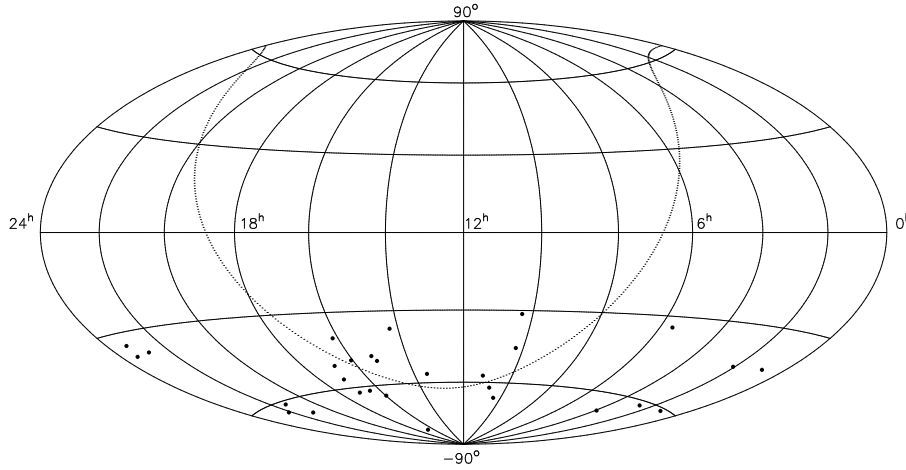Figure 3.   Example Images: The Ugly

Figure 4.   Distribution of 29 new Southern Astrometric Sources

observed and are awaiting correlation. A second survey of 50 sources is under-
way. Note that these sources are all south of declination −30 degrees. Fig 4
shows the distribution of the 29 new southern astrometry sources.

5.   Science from the Imaging Survey

Apart from improving the astrometic accuracy of the ICRF, the imaging survey
will enable study of a flux limited complete sample and of the properties of well-
defined sub-samples *e.g.* EGRET sources, GPS/CSS sources and comparisons
between well defined sub-samples *e.g.* BL Lac objects and quasars. Further
it will allow investigation of misalignment between mas and arcsec jets, proper
motion, as well as both static and variable, polarization properties.

Relativistic satellite attitude: joining local and global reference frames for the realization of space-born astrometric catalogues

Donato Bini †, Beatrice Bucciarelli ‡, Maria T. Crosta ‡, Fernando de Felice$^+$, Mario G. Lattanzi‡, and Alberto Vecchiato‡

†*Istitute "M. Picone", C.N.R., and I.C.R.A., Rome, Italy*
‡*Turin Astronomical Observatory, Pino Torinese, Turin, Italy*
$^+$*Department of Physics, University of Padova, Padova, Italy*

Abstract. The definition of the satellite rest frame plays a fundamental role in the relativistic treatment of space observations. We find a mathematical representation of this frame which is an analytical solution accurate to $(v/c)^3$ and corresponds to the expected attitude of the astrometric satellite Gaia. We named this frame *attitude frame* since it takes into account the satellite's actual orbital motion and attitude law, both computed in global BCRS coordinates. Moreover, we show that the running time on-board of Gaia is compatible with IAU resolution B1.5 (2000).

1. Introduction

New space technologies allow for astrometric accuracies of ~ 1 microarcsecond (μas) in the determination of stellar positions (de Boer *et al.* 2000). As a consequence of this high accuracy, the analysis of the space astrometric data requires methods fully developed in a general relativistic context. This means that future stellar catalogues need to be based on a new relativistic rendition of the astrometric parameters, the latter derived from the solution of the observation equations linking the astrometric observables to the astrometric unknowns (*i.e.* parallax and proper motion). In order to exploit these equations as boundary data essential for the reconstruction of the light trajectory connecting the satellite to an emitting star (de Felice *et al.* 2003a; Kopeikin & Mashhoon 2002; Kopeikin & Gwinn 2000; Klioner 2003; Bini & de Felice 2003), the expression of any physical observation made within the satellite also requires a determination of its rest frame consistently with the precepts of general relativity. We call this *attitude frame*, *i.e.* a comoving frame consisting of a *clock* and a *spatial* triad of orthonormal axes that provides a local Cartesian reference system, adapted to the satellite composite motion. Here, we specify the attitude frame for Gaia (de Boer *et al.* 2000), the new global astrometry mission of ESA, approved for launch not later than 2012, with a possible window in 2010. In what follows Latin indices run from 1 to 3, Greek indices run from 0 to 3.

2. Mathematical preliminaries for the astrometric set-up

The mathematical quantity which defines a rest-frame of a given observer (the satellite in our case) is a *tetrad adapted to that observer*, namely a set of four unitary mutually orthogonal four-vectors $\lambda_{\hat{\alpha}}$ one of which, namely $\lambda_{\hat{0}}$, is the observer's four-velocity and describes the space-time history of the observer in a given space-time. The other $\lambda_{\hat{a}}$ form a spatial triad of space-like vectors, defined up to a spatial rotation. Since there are infinitely many possible *spaces* to be fixed within a satellite, our task is to identify unambiguously those which correspond to the actual satellite attitude. In the case of Gaia, the background space-time geometry felt is that of the Solar System which can be assumed as the only source of gravity; moreover it generates a weak gravitational field so we shall retain only terms of first order in the gravitational constant G and consider these terms only up to the order of $(v/c)^3 \sim 0.1$ μas, where v is the average velocity within the Solar System for which we have gravitational balance. The space-time geometry is

then given by $g_{\alpha\beta} = \eta_{\alpha\beta} + h_{\alpha\beta} + O(h^2)$, where $O(h^2)$ denotes non linear terms in h, the coordinates are $x^0 = t, x^1 = x, x^2 = y, x^3 = z$, the origin being fixed at the barycenter of the Solar System, $\eta_{\alpha\beta}$ is the Minkowskian metric. The choice of the metric is compatible with IAU resolution B1.3 (2000), which identifies a *global* Barycentric Celestial Reference System (BCRS) by three mutually orthogonal axes centered at the barycenter of the Solar System (B) and pointing to distant cosmic sources chosen so to assure that the system is kinematically non rotating. The coordinate axes then define a Cartesian-like coordinate system (x, y, z) and we assume that a space-like hypersurface exists everywhere with equation $t(x, y, z)$ =constant. The function t is chosen as coordinate time. In de Felice *et al.* (2003b) we illustrate how one can make the choice of the coordinate time not arbitrary. Hence, together with the set (x, y, z), it provides a coordinate representation of the space-time and fixes the space-time metric. At any space-time point there exists an observer **u** which is at rest with respect to the BCRS and whose world line is parallel to the local coordinate time axis. Actually, it belongs to a congruence of curves everywhere proportional to a time-like Killing vector field (de Felice *et al.* 2003a). Assume first that this observer is located at the origin of the BCRS, then this system can be locally identified by a spatial triad of unitary and orthonormal vectors (Bini & de Felice 2003). In this case the proper time of **u** is the barycentric proper time. This frame will be termed *local BCRS* and its proper time varies as a function of the position (de Felice *et al.* 2003b).

3. The attitude frame

Gaia is expected to orbit the Sun-Earth System in the outer Lagrangian point $L2$ (de Boer *et al.* 2000). Moreover, the satellite rotates about its x axis which forms a fixed angle α with the Sun direction; the spin axis then precesses about the Sun direction (Lindegren 2001; Mignard 2001). Therefore, we need to fix the direction to the Sun as seen from within the satellite rest frame. Let us fix the satellite's trajectory as the time-like, unitary four-vector $\mathbf{u}'$ $(u'^\alpha u'_\alpha = -1)$. With respect to the local BCRS defined at each point of the satellite's trajectory, the Sun direction is fixed by rotating the triad $\{\lambda_{\hat{a}}\}$ by an angle ϕ_s around $\lambda_{\hat{3}}$ and then by an angle θ_s around the vector image of $\lambda_{\hat{2}}$ under the ϕ_s rotation (see Figure 1). Thus we have the new triad adapted to the observer u:

$$\lambda^{(s)}{}_{\hat{a}} = \mathcal{R}_2(\theta_s)\mathcal{R}_3(\phi_s)\lambda_{\hat{a}}, \tag{1}$$

where $\mathcal{R}_i$ $(i = 1, 2, 3)$ are rotation matrices. From (**??**), it is easy to deduce the explicit expressions of the new triad components relative to the BCRS (Bini, Crosta, & de Felice 2003).

In order to identify a tetrad frame which is adapted to the satellite world-line and whose spatial triad is consistent with the satellite attitude, we boost the vectors of the triad $\{\lambda_{\hat{a}}^{(s)}\}$ to the satellite rest frame and obtain the following boosted triad (Jantzen, Carini, & Bini 1992):

$$\lambda_{\hat{a}}^{(bs)\alpha} = P(u')^\alpha_\sigma \left[\lambda_{\hat{a}}^{(s)\sigma} - \frac{\gamma}{\gamma + 1}\nu^\sigma \left(\nu^\rho \lambda_{\rho\hat{a}}^{(s)} \right) \right]_{\hat{a}=1,2,3}, \tag{2}$$

where $P(u')^\alpha_\sigma = \delta^\alpha_\sigma + u'^\alpha u'_\sigma$ is the operator which projects in the rest frame of $\mathbf{u}'$, ν^α is the relative spatial velocity of $\mathbf{u}'$ with respect to the local observer $\mathbf{u}$, and γ is the Lorentz factor. The vector $\lambda_{\hat{1}}^{(bs)}$ identifies the direction to the Sun as seen by the satellite itself. The other vectors of the boosted triad are related to $\lambda_{\hat{1}}^{(bs)}$ by the simple relations:

$$\cos\theta_s \lambda_{\hat{2}}^{(bs)} = \frac{d}{d\phi_s}\lambda_{\hat{1}}^{(bs)} \quad \lambda_{\hat{3}}^{(bs)} = \frac{d}{d\theta_s}\lambda_{\hat{1}}^{(bs)}. \tag{3}$$

The tetrad $\{\lambda_{\hat{0}}^{(bs)} \equiv \mathbf{u}', \lambda_{\hat{a}}^{(bs)}\}$ will be referred to as the *Sun-locked frame*. The explicit expressions of the components of these vectors relative to the BCRS are reported in
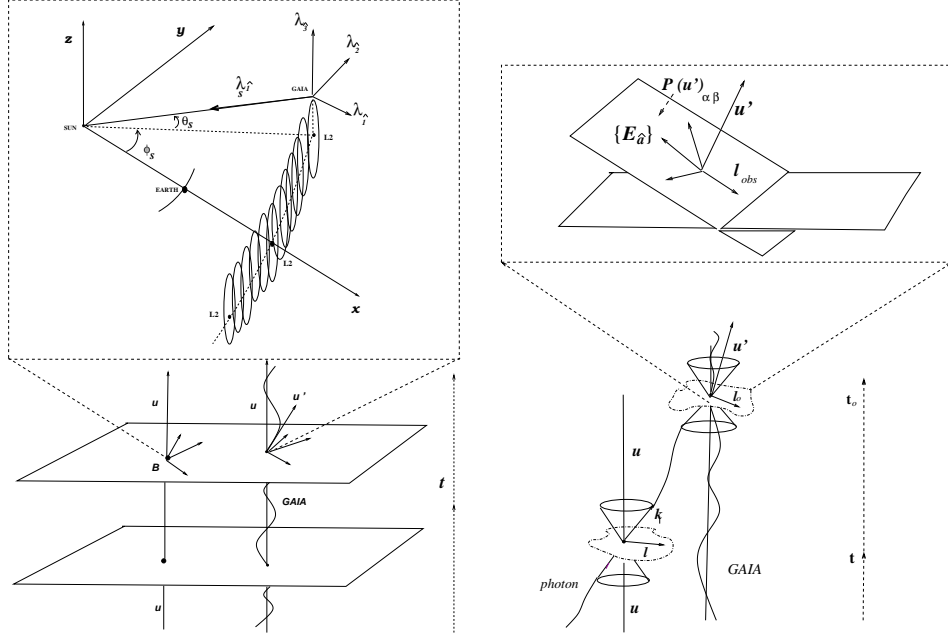
Figure 1.   The spatial triad $\lambda_{\hat{a}}$ is co-moving with the barycentric observer **u** (**B**= barycenter) defined at the Gaia center-of-mass at each point along its Lissajous orbit about L2. The $\lambda_{\hat{1}}^{(s)}$ identifies the instantaneous Sun direction with respect to **u** (on the left). The Sun direction as seen on-board will be obtained by boosting the vector $\lambda_{\hat{1}}^{(s)}$ to the satellite motion. The Gaia's attitude triad $E_{\hat{a}}$ is defined in the satellite Lorentz boosted rest frame (on the right).

Bini *et al.* (2003). Finally, to deduce the Gaia attitude frame, which is our main goal, we have to make the following final steps: i) rotate the Sun-locked triad by an angle $\omega_p t$ about the vector $\lambda_{\hat{1}}^{(bs)}$ which constantly points to the Sun (ω_p is the angular velocity of precession); ii) rotate the resulting triad by a fixed angle α about the image of the vector $\lambda_{\hat{2}}^{(bs)}$ under rotation i); iii) rotate the triad obtained after step ii) by an angle $\omega_r t$ about the image of the vector $\lambda_{\hat{1}}^{(bs)}$ under the previous two rotations (ω_r is the angular velocity of the satellite spin). The triad resulting from these three steps will be the satellite *attitude triad*; this is given by:

$$\mathbf{E}_{\hat{a}} = \mathcal{R}_1(\omega_r t)\mathcal{R}_2(\alpha)\mathcal{R}_1(\omega_p t)\lambda_{\hat{a}}^{(bs)} \qquad \hat{a} = 1,\, 2,\, 3. \tag{4}$$

Again, the full expressions of the triad vectors $\mathbf{E}_{\hat{a}}$ are given in Bini *et al.* (2003). These vectors enter the formulas for the *astrometric observable* defined as the angles that the incoming light ray k^α forms with the axes of the spatial attitude triad in the rest frame of the satellite (de Felice & Clark 1990), *i.e.*:

$$\cos\psi_{(E_{\hat{a}},\ell)} \equiv \mathbf{e}_{\hat{a}} = \frac{P(u')_{\alpha\beta}k^\alpha \mathbf{E}_{\hat{a}}^\beta}{(P(u')_{\alpha\beta}k^\alpha k^\beta)^{1/2}}, \tag{5}$$

where no sum is meant over $\hat{a}$, and ℓ is the local line of sight, given by $\ell^\rho = P(u)^\rho{}_\sigma k^\sigma$.

4. The clock on board

The general relativistic formula which relates the time interval between two events is given in de Felice & Clark (1990) as $dT = -(1/c) g_{\alpha\beta} u^\alpha dx^\beta$. We refer to dT as the interval of proper time of an observer on board. If we adopt the IAU metric for $g_{\alpha\beta}$ and since the satellite is a physical observer $(u'_\alpha u'^\alpha = -1)$, the expansion for u'^0 in powers of c^{-1} allow us to obtain the formula which ties the running of time of the clock on board to that of the clock at the origin of the BCRS (up to the order of c^{-4}).

$$
dT_s \approx dt - c^{-2}\left[\left(\frac{v^2}{2} + w(\mathbf{x},t)\right) + v^i dr^i\right] + c^{-4}\left[\left(\frac{w^2(\mathbf{x},t)}{2} - \frac{v^4}{8} - \frac{3v^2 w(\mathbf{x},t)}{2}\right.\right.
$$
$$
\left.\left. + 4w^i(\mathbf{x},t)v^i\right) dt + 4w^i(\mathbf{x},t)dr^i - \left(3w(\mathbf{x},t) + \frac{v^2}{2}\right)v^i dr^i\right],
$$

where $r^i = x^i - x^i_s$. It is easy to check that if we make a first-order Taylor expansion about the satellite center $\mathbf{x}_s$ of the potential and the vector potential, we obtain the same relations as those described in IAU resolution B1.5 (Second Recommendation).

5. Conclusion

In this poster we have synthesized how to relate attitude frame quantities to local BCRS components consistently with the requirements of general relativity. This will provide an essential *ingredient* needed to solve the boundary problem at any observation event, in a form suitable to be implemented in a computer code for space-born astrometric data reduction under development (de Felice et al. 2003b), *i.e.* for the determination of location and state of motion of celestial sources.

References

Bini, D., & de Felice, F. 2003, Class. Quantum Grav., 20, 2251.

Bini D., Crosta, M.T., & de Felice, F. 2003, Class. Quantum Grav., in press.

de Boer, K.S., Gilmore, G., Høg, E., Lattanzi, M.G., Lindegren, L., Luri, X., Mignard, F., & de Zeeuw, P.T. 2000, ESA-SCI (2000)4.

de Felice, F. & Clark, C.J.S. 1990, Relativity on curved Manifolds, Cambridge University Press.

de Felice, F., Crosta, M.T., Vecchiato, A., Bucciarelli, B., & Lattanzi, M.G. 2003a, submitted to Phys.Rev.D.

de Felice, F., Vecchiato, A., Crosta, M.T.,Bucciarelli, B., & Lattanzi, M.G. 2003b, in preparation.

Jantzen, R.T., Carini, P., & Bini, D. 1992, Annals of Physics, 215, 1.

Klioner, S. 2003,AJ, 125, 1580.

Kopeikin, S.& Gwinn, C. 2000 IAU Col. 180, Towards Models and Constants for Submicrosecond Astrometry, ed. K.J. Johnston, D. McCarthy, B.J. Luzum & G. H. Kaplan (Washington DC: U.S. Naval Observatory), 303.

Kopeikin, S.M. & Mashhoon, B. 2002, Phys.Rev.D, 65, 064025.

Lindegren, L. 2001, SAG-LL-35 (Gaia Project technical note).

Mignard, F. 2001, GAIA-FM-010 (Gaia Project technical note).